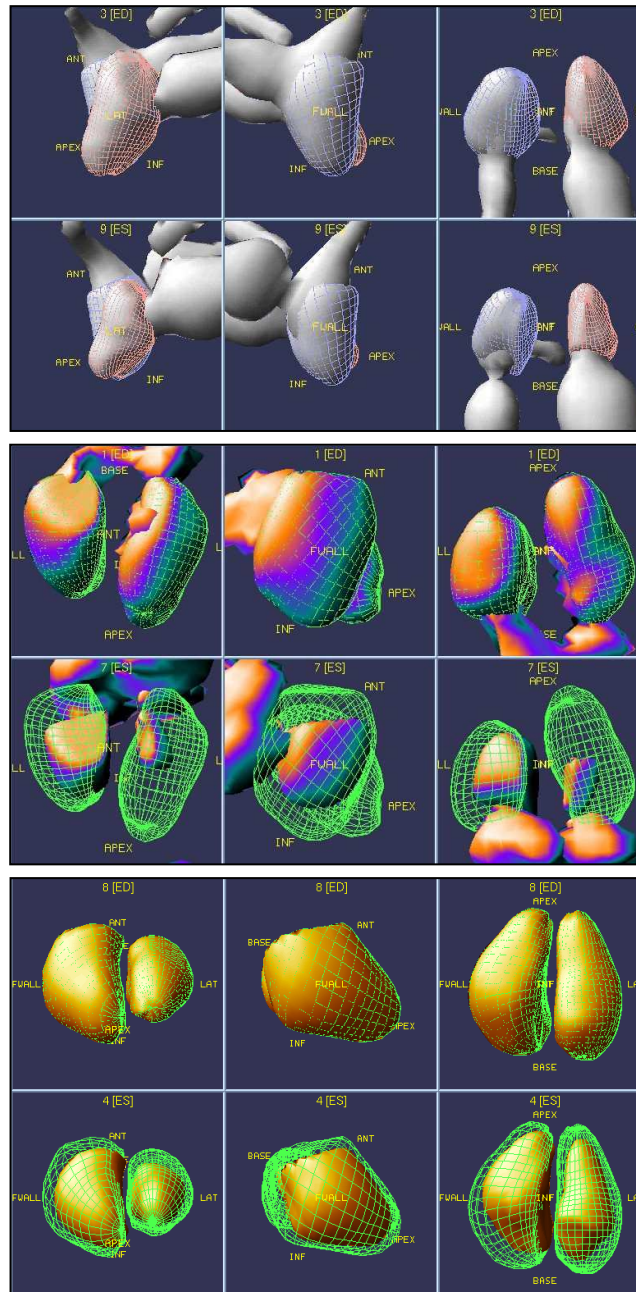


Evaluation of Cardiac Volumes by New Scintigraphic Techniques



Pieter De Bondt



Ghent University
Faculty of Medicine and Health Sciences
Division of Nuclear Medicine

Evaluation of Cardiac Volumes by New Scintigraphic Techniques

**Evaluatie van cardiale volumes door nieuwe scintigrafische
technieken**

Pieter De Bondt

Thesis submitted in fulfilment of the requirements for the degree of
doctor in medical sciences

2005

Promotors:

Prof. Dr. R.A. Dierckx

Prof. Dr. J. De Sutter

Photo on cover page:

Tomographic radionuclide study in a three-dimensional model from a dynamic heart phantom (upper picture), a cat (middle picture) and a normal volunteer (lower picture).

ISBN 9077972021

Division of Nuclear Medicine

Ghent University Hospital

De Pintelaan 185

B-9000 Ghent

Belgium

Printing: Drukkerij Reproduct, Voskenslaan 205, 9000 Gent

© 2005 Pieter De Bondt

Promotors:

Prof. Dr. R. A. Dierckx **Nuclear Medicine, Ghent University**
Prof. Dr. J. De Sutter **Cardiology, Ghent University**

Guidance commission:

Prof. Dr. R. A. Dierckx **Nuclear Medicine, Ghent University**
Prof. Dr. T. Gillebert **Cardiology, Ghent University**
Prof. Dr. J. De Sutter **Cardiology, Ghent University**
Dr Ir. F. Jacobs **Nuclear Medicine, Ghent University**
Prof. Dr. C. Van de Wiele **Nuclear Medicine, Ghent University**

Examination commission:

Prof. Dr. C. De Wagter **Department of Radiotherapy and Nuclear Medicine,
Ghent University**
Prof. Dr. P. Verdonck **Hydraulics Laboratory, Ghent University**
Prof. Dr. T. Gillebert **Cardiology, Ghent University**
Prof. Dr. P. Franken **Nuclear Medicine, Free University Brussels**
Prof. Dr. W. Wijns **Cardiology, OLV Hospital Aalst**
Prof. Dr. M. De Roo (emeritus) **Nuclear Medicine, Catholic University Leuven**
Prof. Dr. B.L. Van Eck-Smit **Nuclear Medicine, AZ Amsterdam, The Netherlands**

Dean of the Faculty of Medicine:

Prof. Dr. Jean-Louis Pannier

Table of contents

Table of contents	7
Introduction and outline of the thesis	11
Part 1: Gated Myocardial Perfusion SPECT	21
Chapter 1: Age- and gender-specific differences in left ventricular cardiac function and volumes determined by gated SPECT	21
Eur J Nucl Med. 2001 May;28(5):620-4.	21
Summary	22
Introduction	23
Materials and methods	23
Results	24
Discussion	27
Conclusion	29
References	30
Part 2: Gated Bloodpool SPECT, phantom experiments	35
Chapter 2: Validation of planar and tomographic radionuclide ventriculography by a dynamic ventricular phantom	35
Nucl Med Commun. 2003 Jul;24(7):771-7.	35
Summary	36
Introduction	36
Materials and methods	37
Results	41
Discussion	45
Conclusion	47
References	48
Chapter 3: Accuracy of commercial available processing algorithms for planar radionuclide ventriculography using a dynamic left ventricular phantom	51
Nucl Med Commun. 2004 Dec;25(12):1197-202.	51
Summary	52
Introduction	52
Materials and methods	53
Results	55
Discussion	59
Conclusion	60
References	62
Chapter 4: Validation of Gated Blood Pool SPECT cardiac measurements tested using a biventricular dynamic physical phantom	65
J Nucl Med. 2003 Jun;44(6):967-72.	65
Summary	66
Introduction	66
Materials and methods	67
Results	72
Discussion	76
Conclusion	78
References	79

Chapter 5: Accuracy of four different algorithms for the analysis of tomographic radionuclide ventriculography using a physical dynamic four-chamber cardiac phantom	81
J Nucl Med. 2005 Jan;46(1):165-71.	81
Summary	82
Introduction	82
Materials and methods	83
Results	87
Discussion	93
Conclusion	94
References	96
Part 3: Gated Bloodpool SPECT, human experiments	99
Chapter 6: Model dependence of gated blood pool SPECT ventricular function measurements	99
J Nucl Cardiol. 2004 May-Jun;11(3):282-92.	99
Summary	100
Introduction	100
Materials and Methods	101
Results	107
Discussion	119
Conclusion	121
References	123
Chapter 7: Agreement between four available algorithms to evaluate global systolic left and right ventricular function from tomographic radionuclide ventriculography and comparison with planar imaging.	127
Nucl Med Commun. 2005 Apr;26(4):351-9.	127
Summary	128
Introduction	128
Materials and Methods	129
Results	130
Discussion	146
Conclusion	150
References	151
Chapter 8: Comparison of “QUBE” and “4D-MSPECT” tomographic radionuclide ventriculography calculations to magnetic resonance imaging	155
Submitted to J Nucl Med	155
Summary	156
Introduction	157
Materials and Methods	157
Results	160
Discussion	170
Conclusion	173
References	174
Chapter 9: Normal values for left and right ventricular ejection fraction and volumes from tomographic radionuclide ventriculography	177
Submitted to Nucl Med Commun	177
Summary	178
Introduction	179
Materials and methods	179
Results	180
Discussion	183

Conclusion	194
References	196
General Discussion	199
Conclusion	213
Besluit	215
Dankwoord	216

Introduction and outline of the thesis

Nuclear Medicine

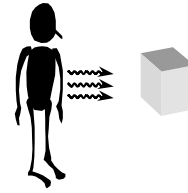
Diagnostic nuclear medicine is a specialized area that uses small amounts of radioactive substances to examine organ function. The substance or molecule that is being used is called the tracer or radiopharmaceutical, this is a pharmaceutical connected to an isotope. This isotope is unstable and emits gamma-rays. Mostly Technetium99m (Tc99m) is used because of its favorable physical characteristics.

The pharmaceutical is especially designed to go to a specific place in the body where there could be a disease or abnormality. Several studies had been carried out so that the particular radiopharmaceutical is going to a well-known organ. The “bone”-agent (Tc99m -MDP) is a calcium analogue which is after injection being incorporated into the bone on spots where there is bone-formation. The image you get from “outside” the patient is not a skeleton but an image of metabolic function of the bone. As a consequence, you don’t see a fracture, you see the new bone formation around the fracture. The “cardiac”-agent (Tc99m -Sestamibi or Tc99m -Tetrofosmin) is being hold in a special part of the myocardial cell (mitochondria). When this is done, two things are certain: the molecule is being carried to the heart :the blood vessel (coronary) was patent, and the myocardial cell lives (no infarct).

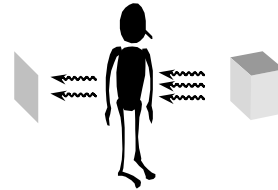
The radioactive part of the radiopharmaceutical emits radiation into the detector, called the gamma-camera. Here is the main difference with radiology, where the patient receives some external x-rays, absorbs some, while the remaining part is captured (usually) on the other side of the patient. In nuclear medicine, the patient radiates always while the camera doesn’t. (Figure 1) The same is true for the therapy conditions in nuclear medicine where the therapeutic dose (much higher than in diagnostic procedures) is being brought as close as possible to the “target” organ, this can be the thyroid in benign hyperthyroidism (Graves) or bone in skeletal metastases.

Diagnosis

Nuclear Medicine:
functional imaging



Radiology:
(mostly) anatomical imaging



Therapy

Nuclear Medicine is working with open and
internal radioactive sources
the patient “radiates” himself



Radiotherapy is working with external radioactive sources
the “machine” radiates the patient

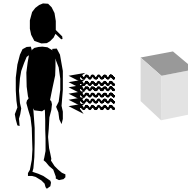


Figure 1

There are several types of gamma-camera’s, small or large and single-, double- or triple headed. One head of the camera consists of a flat screen that is placed as close as possible to the patient. When the head of the camera is not moving, you get a planar acquisition or 2-dimensional image of the tracer distribution of that part of the body that is been studied. For the bone scan, there was soon some interest to scan dynamically from head to toe, the so called whole body scans, and the head of the camera starts at one side of the body and moves slowly to the other side, so that the full body could be displayed. Sometimes dynamic physiologic processes are scanned, e.g. vascularisation of hand or foot, excretion of kidneys, or transit and emptying of stomach. The head of the camera is then placed over the ROI and together with the 2-dimensional tracer distribution, time is acquired and images are repeated after a certain predefined period. These are dynamic scans that are mainly carried out if some

organ functions seem too slow, e.g. a slower gastric emptying in a patient with diabetes.

Nuclear Cardiology

During decennia, a lot of attention went to imaging of the heart. Mainly two separate techniques were used, or the myocardial left ventricular (LV) wall or the myocardial cavity (blood pool or ventriculography) are studied.

With limited spatial resolution, it was clear that mostly LV wall was studied when examining myocardial wall, since the right ventricular (RV) wall has smaller wall thickness, too small to have accurate measurements with conventional nuclear imaging techniques. During the first years, LV wall perfusion was studied in a planar mode, but later a three-dimensional technique was developed (so called SPECT technique). The radiopharmaceutical is brought to the heart through (open) cardiac blood vessels and being trapped in the (living) myocardial cells. Therefore, this technique is mainly used to study LV perfusion and/or metabolism. The cardiac PET technique was also developed, with the advantage of smaller spatial resolution, but with the disadvantage of requiring a dedicated PET camera, with high cost and limited availability of camera and radiopharmaceutical.

The technique of studying the myocardial cavity is done by preventing the radiopharmaceutical to leave the blood vessels, and to make dynamic (or gated) scans of the cardiac chambers. The scan is dynamic because together with the blood pool activity, the ECG-signal of the patient is captured, in order to evaluate the kinetic information of the heart during one or several heart beats. The most important measurement from these type of scans is the LV ejection fraction, being the portion of blood pumped to the systemic circulation from the LV. The blood pool scan or ventriculography is mostly executed in the planar mode, so called planar ventriculography (PRV), with the gamma-camera positioned before the chest of the patient (anterior) with an angulation to the left side, to obtain an ideal separation of LV with other cardiac structures, e.g. RV and atrial cavities.

Cardiac function studied in nuclear cardiology: why?

The clinical relevance of measurements of cardiac function cannot be overemphasized. Based on scientific and clinical observations, measures of ventricular function provide information for most of the most critical diagnostic and therapeutic decisions. The LV has been most extensively studied because of its involvement in common disorders

such as hypertension or ischemic heart disease. Any dysfunction of the left side of the heart is mostly clinically obvious by some consequences in the systemic circulation. However, an increasing amount of data is available concerning right ventricular (RV) function in several disorders including pulmonary heart disease, congenital heart disease, valvular disorders and inferior myocardial infarction [1].

Several methods are available to assess cardiac chamber function and include echocardiography, computed tomography, magnetic resonance imaging and radionuclide techniques with blood pool activity (ventriculography) and with myocardial activity (perfusion or viability). These various methods are based on different physical principles and contain complementary information. Each of them is characterized by some strengths and some pitfalls. It will therefore not be easy to find an accurate “one-stop-shop” examination in cardiology [2] to cover all these items of clinical interest and to “scan” the heart in one single examination for perfusion, function, anatomy, valve status, pressure information, systolic and diastolic function,...

The most innovative change in nuclear cardiology recently is the extensive validation and use of gated myocardial perfusion SPECT to examine perfusion and function in one examination. Together with observation of perfusion defects and its reversibility, evaluation of global and regional LV function is more and more done. By adding the “gated” modality to the SPECT-imaging technique, not only supplementary information was added to the description of the images, also the accuracy in differentiating a real perfusion defect, due to a coronary lesion, or an attenuation artifact was significantly increased.

Planar ventriculography (PRV) is since long the gold standard for LVEF determination, although clinical use of this technique declined due to the success of echocardiography. Where the latter produces more parameters of LV function, morphology and information of valvular status, the interest in PRV is only for the determination of LVEF. If we have now the possibility to get three-dimensional information of the heart function in a satisfactory resolution (in space and time) without supplementary radiation of the patient and we have some quantitative results of LV and RV function, even if the latter is still investigational, I think it is worth to combine the SPECT technique with radionuclide ventriculography, tomographic radionuclide ventriculography (TRV). While the slower computer systems and smaller disk space was long an argument not to perform this technique, in most departments, this is not the case nowadays. Even a visual evaluation of the gated reconstructed

slices (visual inspection of the “three-dimensional beating heart”) of a ventriculography study can learn a lot more of global and even regional kinetic information of LV and RV, when the observer is experienced with the technique.

Old against new methods to process TRV

Fischmann reported in 1989 [3] : “Gated blood pool tomography: a technology whose time has come”. When he would mean that the technique of taking three-dimensional images of the radionuclide ventriculography is possible and useful, this is correct to my opinion. But more than 15 years later this technique isn’t used in clinical daily practice, and I think there are several reasons for this. First workstations in the early years were not fast enough and had not enough memory to process and store these images. Second, automatic software to process TRV is only available recently. For years until the publication of the first automatic algorithm [4] several attempts were made to process TRV, and (nearly) none of them became widespread and popular. In the years after the first paper of TRV from Moore [5] , TRV was acquired and reconstructed into short-axis, long-axis and four-chamber-view planes for visual evaluation [6]. They studied 15 patients with atrial septal defect or myocardial infarction and they could clearly demonstrate the superiority of TRV in assessing regional asynergy and dilatation of ventricles and atria. From then, several own manual techniques were used by different authors [7; 8] but it was clear that this time-consuming way of analysis, could never become popular. Other methods of analysis used several slices which are summed after reconstruction to make one thick slice along the ventricular cavities [9; 10; 11] or “dual gated tomograms” where 2 SPECT scans are acquired, one at end-diastole and one end-systole [12; 13]. Others tried to map fourier phase analysis from TRV short axis slices onto a two-dimensional polar map [14], onto several slices of a reconstructed TRV [15] or onto a three-dimensional reconstructed skeleton of the bloodpool activity [16; 17]. More and more, the idea became accepted that for optimal analysis of TRV of LV and RV, only a three-dimensional technique could give accurate results [18; 19] but it was only when automated three-dimensional were developed [4; 20; 21; 22], the interest in TRV and the number of published papers increased. Only, it was strange that many of these programs were distributed before a full validation, not only for LVEF, but also for LV and even more important RV end-diastolic and systolic volumes.

So now we have some software programs available, but they seem to be undervalidated.

Outline of the thesis

This thesis is focused on research on gated perfusion SPECT (GSPECT) and TRV, with two main questions: what are normal values for LV and RV function from GSPECT and TRV and what about validation of the technique and processing of TRV?

In **chapter 1** normal values for LV ejection fraction (EF) and LV end-diastolic volume (EDV) and end-systolic volume (ESV) were calculated in a population with low pre-test likelihood for coronary artery disease (CAD). We looked for age- and gender-dependent differences.

From chapter 2 to chapter 9 we did research on TRV. We validated first TRV by different dynamic heart phantoms (part 2) before we tested TRV further in human experiments (part 3).

In **chapter 2** we developed a dynamic LV phantom because we wanted to know if it was possible to acquire planar and tomographic ventriculography scans from a dynamic volume, and to correctly measure volumes and ejection fractions from this volume. We looked for differences between planar and tomographic calculations. Moreover, with a special technique of (manually) calculating volumes from SPECT scans, region growing, we tried to identify the optimal cut-off when calculating volumes.

During **chapter 3** we used this phantom further to compare 10 commercially available software programs to process PRV and to calculate LVEF. When this would be possible, we had not only an interesting scientific tool for ventriculography studies, we would have possibility to use this LV phantom in software audits and quality assurance procedures.

In **chapter 4** we developed a dynamic biventricular heart phantom, with a LV and RV attached to each other. This would be a better resemblance of the real situation with respect to the normal proportion from LV to RV. We wanted to know if TRV was possible to correctly separate LV from RV. The ellipsoidal shape of LV and the more triangular shape of RV were taken into account. Septal thickening was also provided since the space between LV and RV was not active (radioactivity is kept in the ventricles) and the LV “mass” is kept constant (space was filled with gel). In contrast to the first LV model, we tried an active filling and emptying through the ventricles (instead of passive filling and emptying through surrounding fluid alterations like the first model). We used here to process the images the software BP-SPECT [22] .

Next step was the development of a four-chamber dynamic cardiac model in **chapter 5**. After simulation between both ventricles, attention went to a correct separation of ventricles from atria, for LV as well as RV. We used the four most used software programs nowadays to process TRV, QBS from the Cedars Sinai group, Los Angeles, USA [4], QUBE from the Free University of Brussels, Belgium [20], 4D-MSPECT from the University of Michigan, USA [21] and BP-SPECT, the software developed at the Columbia University, New York, USA [22].

From part 3 we started to test the different softwares in patients and volunteers. **Chapter 6** was carried out in cooperation with the Division of Nuclear Medicine, Northwestern Hospital, Chicago, USA and the Division of Cardiology, Columbia University, New York, USA. Differences in modeling between QBS [4] and BP-SPECT [22] was tested in 422 patients, 31 normal subjects and 16 phantom experiments. In 21 patients, comparison with MRI could be made. The difference between a count-based method (BP-SPECT) was compared with a geometry-based method (QBS).

We compared LVEF from the four mentioned software programs to process TRV with PRV in 166 patients in **chapter 7**. Furthermore, ventricular volumes from TRV (QBS, QUBE and 4D-MSPECT) were compared with those from BP-SPECT, the latter being the only method so long with a validation of ventricular volumes with MRI [22; 23].

Since MRI is nowadays the standard for ventricular volumes validation, we had the opportunity to match TRV data from 28 patients from Columbia University with MRI data, with all four programs to process TRV in **chapter 8**.

Finally, we set up in **chapter 9** a prospective database of normal subjects of 51 persons (29 men and 22 women) to provide normal values for LV and RV EF, EDV and ESV from TRV, processed with the available software algorithms. It was further interesting to study the gender differences in LV and RV function, and compare these findings with the GSPECT results from chapter 1.

References

1. Redington, A. N. Right ventricular function. *Cardiol.Clin.* 20[3], 341-9, v. 2002.
2. Wijns, W. The diagnosis of coronary artery disease: in search of a "one-stop shop"? *J.Nucl.Med.* 46[6], 904-905. 2005.
3. Fischman, A. J., Moore, R. H., Gill, J. B., and Strauss, H. W. Gated blood pool tomography: a technology whose time has come. *Semin.Nucl Med* 19[1], 13-21. 1989.
4. Van Kriekinge, S. D., Berman, D. S., and Germano, G. Automatic quantification of left ventricular ejection fraction from gated blood pool SPECT. *J.Nucl.Cardiol.* 6[5], 498-506. 1999.
5. Moore, M. L., Murphy, P. H., and Burdine, J. A. ECG-gated emission computed tomography of the cardiac blood pool. *Radiology* 134[1], 233-235. 1980.
6. Tamaki, N., Mukai, T., Ishii, Y., Yonekura, Y., Yamamoto, K., Kadota, K., Kambara, H., Kawai, C., and Torizuka, K. Multiaxial tomography of heart chambers by gated blood-pool emission computed tomography using a rotating gamma camera. *Radiology* 147[2], 547-554. 1983.
7. Chevalier, P., Bontemps, L., Fatemi, M., Velon, S., Bonnefoy, E., Kirkorian, G., Itti, R., and Touboul, P. Gated blood-pool SPECT evaluation of changes after radiofrequency catheter ablation of accessory pathways: evidence for persistent ventricular preexcitation despite successful therapy. *J Am.Coll.Cardiol.* 34[6], 1839-1846. 15-11-1999.
8. Naruse, H., Fujisue, R., Ohyanagi, M., Todo, Y., Tateishi, J., Kawamoto, H., Tanimoto, M., Iwasaki, T., and Fukuchi, M. [Right ventricular ejection and regional wall motion evaluated by cardiac blood pool emission computed tomography]. *J.Cardiol.* 17[3], 577-585. 1987.
9. Casset-Senon, D., Philippe, L., Babuty, D., Eder, V., Fauchier, L., Fauchier, J. P., Pottier, J. M., and Cosnay, P. Diagnosis of arrhythmogenic right ventricular cardiomyopathy by fourier analysis of gated blood pool single-photon emission tomography. *Am.J Cardiol.* 82[11], 1399-1404. 1-12-1998.
10. Canclini, S., Terzi, A., Rossini, P., Vignati, A., La Canna, G., Magri, G. C., Pizzocaro, C., and Giubbini, R. Gated blood pool tomography for the evaluation

- of global and regional left ventricular function in comparison to planar techniques and echocardiography. *Ital.Heart J* 2[1], 42-48. 2001.
11. Bartlett, M. L., Srinivasan, G., Barker, W. C., Kitsiou, A. N., Dilsizian, V., and Bacharach, S. L. Left ventricular ejection fraction: comparison of results from planar and SPECT gated blood-pool studies. *J Nucl Med* 37[11], 1795-1799. 1996.
 12. Ohtake, T., Nishikawa, J., Machida, K., Momose, T., Masuo, M., Serizawa, T., Yoshizumi, M., Yamaoki, K., Toyama, H., Murata, H., and . Evaluation of regurgitant fraction of the left ventricle by gated cardiac blood-pool scanning using SPECT. *J.Nucl.Med.* 28[1], 19-24. 1987.
 13. Underwood, S. R., Walton, S., Ell, P. J., Jarritt, P. H., Emanuel, R. W., and Swanton, R. H. Gated blood-pool emission tomography: a new technique for the investigation of cardiac structure and function. *Eur.J.Nucl.Med.* 10[7-8], 332-337. 1985.
 14. Neumann, D. R., Go, R. T., Myers, B. A., MacIntyre, W. J., Chen, E. Q., and Cook, S. A. Parametric phase display for biventricular function from gated cardiac blood pool single-photon emission tomography. *Eur.J Nucl Med* 20[11], 1108-1111. 1993.
 15. Nakajima, K., Bunko, H., Tada, A., Tonami, N., Hisada, K., Misaki, T., and Iwa, T. Nuclear tomographic phase analysis: localization of accessory conduction pathway in patients with Wolff-Parkinson-White syndrome. *Am.Heart J* 109[4], 809-815. 1985.
 16. Mate, E., Mester, J., Csernay, L., Kuba, A., Madani, S., and Makay, A. Three-dimensional presentation of the Fourier amplitude and phase: a fast display method for gated cardiac blood-pool SPECT. *J Nucl Med* 33[3], 458-462. 1992.
 17. Botvinick, E. H., O'Connell, J. W., Kadkade, P. P., Glickman, S. L., Dae, M. W., Cohen, T. J., Abbott, J., and Krishnan, R. Potential added value of three-dimensional reconstruction and display of single photon emission computed tomographic gated blood pool images. *J Nucl Cardiol.* 5[3], 245-255. 1998.
 18. Groch, M. W., Marshall, R. C., Erwin, W. D., Schippers, D. J., Barnett, C. A., and Leidholdt, E. M., Jr. Quantitative gated blood pool SPECT for the assessment of coronary artery disease at rest. *J.Nucl.Cardiol.* 5[6], 567-573. 1998.

19. Mariano-Goulart, D., Collet, H., Kotzki, P. O., Zanca, M., and Rossi, M. Semi-automatic segmentation of gated blood pool emission tomographic images by watersheds: application to the determination of right and left ejection fractions. *Eur.J.Nucl.Med.* 25[9], 1300-1307. 1998.
20. Vanhove, C., Franken, P. R., Defrise, M., Momen, A., Everaert, H., and Bossuyt, A. Automatic determination of left ventricular ejection fraction from gated blood-pool tomography. *J.Nucl.Med.* 42[3], 401-407. 2001.
21. Ficaro, E. P., Quaife, R. F., Kritzman, J. N., and Corbett, J. R. Validation of a New Fully Automatic Algorithm for Quantification of Gated Blood Pool SPECT: Correlations with Planar Gated Blood Pool and Perfusion SPECT. *J.Nucl.Med.* 5, 97P. 2002.
22. Nichols, K., Saouaf, R., Ababneh, A. A., Barst, R. J., Rosenbaum, M. S., Groch, M. W., Shoyeb, A. H., and Bergmann, S. R. Validation of SPECT equilibrium radionuclide angiographic right ventricular parameters by cardiac magnetic resonance imaging. *J.Nucl.Cardiol.* 9[2], 153-160. 2002.
23. Nichols, K., Humayun, N., De Bondt, P., Vandenberghe, S., Akinboboye, O. O., and Bergmann, S. R. Model dependence of gated blood pool SPECT ventricular function measurements. *J Nucl Cardiol.* 11[3], 282-292. 2004.

Part 1: Gated Myocardial Perfusion SPECT

CHAPTER 1:

AGE- AND GENDER-SPECIFIC DIFFERENCES IN LEFT VENTRICULAR CARDIAC FUNCTION AND VOLUMES DETERMINED BY GATED SPECT

Pieter De Bondt ^{1,4} , Christophe Van de Wiele ¹ , Johan De Sutter ² , Frederic De Winter ¹ , Guy De Backer ^{2,3} , Rudi Andre Dierckx ¹

¹ Division of Nuclear Medicine, Ghent University Hospital, Ghent, Belgium

² Department of Cardiology, Ghent University Hospital, Ghent, Belgium

³ Department of Cardiac Rehabilitation, Ghent University Hospital, Ghent, Belgium

⁴ Department of Nuclear Medicine, Antwerp University Hospital, Edegem, Belgium

Eur J Nucl Med. 2001 May;28(5):620-4.

SUMMARY

The aim of this study was to determine normative volumetric data and ejection fraction values derived from gated myocardial single-photon emission tomography (SPECT) using the commercially available software algorithm QGS (quantitative gated SPECT). From a prospective database of 876 consecutive patients who were referred for a 2-day stress-rest technetium-99m tetrofosmin (925 MBq) gated SPECT study, 102 patients (43 men, 59 women) with a low (<10%) pre-test likelihood of coronary disease were included (mean age 57.6 years). For stress imaging, a bicycle protocol was used in 79 of the patients and a dipyridamole protocol in 23. Left ventricular ejection fraction (LVEF) and end-diastolic and -systolic volumes (EDV and ESV) were calculated by QGS. EDV and ESV were corrected for body surface area, indicated by EDVi and ESVi. To allow comparison with previous reports using other imaging modalities, men and women were divided into three age groups (<45 years, ≥45 years but <65 years and ≥65 years). Men showed significantly higher EDVi and ESVi values throughout and lower LVEF values when compared with women in the subgroup ≥65 years ($P<0.05$, ANOVA). Significant negative and positive correlations were found between age and EDVi and ESVi values for both women and men and between LVEF and age in women ($P=0.01$). LVEF values at bicycle stress were significantly higher than at rest ($P=0.000$, paired *t* test), which was the result of a significant decrease in ESV ($P=0.003$), a phenomenon which did not occur following dipyridamole stress ($P=0.409$). The data presented suggest that LVEF and EDVi and ESVi as assessed by QGS are strongly gender- specific. Although the physiological significance of these results is uncertain and needs further study, these findings demonstrate that the evaluation of cardiac function and volumes of patients by means of QGS should consider age- and gender-matched normative values.

INTRODUCTION

Reduced left ventricular (LV) function is a potent predictor of cardiac events in patients with coronary or valvular heart disease, symptomatic heart failure and hypertension [24; 25; 26]. Estimation of left ventricular ejection fraction (LVEF) and end-diastolic and end-systolic volumes (EDV and ESV) from gated single-photon emission tomography (SPECT) myocardial perfusion images has recently become possible through the development of several software algorithms [27; 28; 29; 30; 31; 32; 33; 34]. The most widespread method, quantitative gated SPECT, or QGS, developed at Cedars Sinai, is an automatic algorithm operating in three-dimensional space, based on asymmetric Gaussian fitting of count profiles across the myocardium and identification of endo- and epicardial surfaces. Currently however, the extent to which age, gender and type of stress test per se influence measures of LV function as estimated by QGS, independent of clinically apparent cardiovascular disease, is largely unknown. Therefore, this study set out to determine normative volumetric data and ejection fraction values using QGS for comparison of individual patients and for follow-up of global cardiac function.

MATERIALS AND METHODS

Between November 1998 and May 1999, we prospectively studied 876 consecutive patients referred to our stress laboratory for a 2- day stress-rest technetium-99m tetrofosmin gated SPECT study. From among this group, 102 normotensive patients with a pretest likelihood for coronary heart disease <10% and normal stress and rest perfusion images as determined by two experienced readers (P.D.B. and C.V.D.W.) were included in the study. None of the patients suffered from diabetes or presented with left or right bundle branch block or atrial fibrillation. Additionally none of the patients had a pacemaker. There were 43 men and 59 women, and their mean age was 57.6 years. Men and women were divided into three age groups to allow comparison with previous reports using other imaging modalities for the assessment of normative cardiac functional parameters and to serve as reference values in routine clinical practice: men and women aged under 45 years of age, men and women older than 45 but younger than 65 years of age and men and women above 65 years of age.

99m Tc-tetrofosmin gated SPECT

99m Tc-tetrofosmin injections (925 MBq) were performed following overnight fasting during peak exercise of a bicycle protocol (number of patients (n) = 79) or intravenous pharmacological coronary vasodilatation with dipyridamole (0.142 mg/kg per minute infused over 4 min, n=23) and under resting conditions the day after. Data acquisition started at least 30 min following tracer injection in the supine position using a triple-headed gamma camera equipped with low-energy high-resolution collimators (Prism 3000, Marconi, Cleveland, Ohio). Imaging was performed over 360° (120 sectors of 3°), with a total imaging time of 21 min. Data were stored in a 64x64 bit matrix. Acquisitions were gated for eight frames per cardiac cycle with a beat acceptance window set at 20% of the average R-R interval, calculated prior to image acquisition. Images were reconstructed using a low-pass filter with an order of 5.0 and a cut-off of 0.21. Attenuation correction, background subtraction and beat rejection were not performed. The resulting transaxial image sets were reoriented into short-axis sets to which the automatic QGS algorithm was applied.

Statistical analysis

Data are expressed as mean±1 standard deviation. Comparisons between rest and exercise values were performed using Student's t-test for paired or unpaired observations. Equality of variance was assessed by Levene's test. Pearson's correlation coefficient was used for statistical analysis of relationships between myocardial function and age. Analysis of variance was performed to identify differences between groups of individuals. A value of $P < 0.05$ was considered statistically significant.

RESULTS

The values for volumes (with and without correction for body surface area) and ejection fraction at rest, as well as anthropometric patient data, are listed in Table 1.

Variable	Overall group (n=102)	Men (n=43)	Women (n=59)
Age (years)	57.6 ± 12.4	56.0 ± 13.0	58.8 ± 11.9
BMI (g/m ²)	27.2 ± 5.2	27.5 ± 5.6	27.0 ± 4.9
BSA	1.8 ± 0.2	2.0 ± 0.2	1.7 ± 0.2
EF (%)	62.8 ± 8.7	58.9 ± 6.2	65.6 ± 9.2
EDV (mL)	88.1 ± 28.0	105.5 ± 25.1	75.4 ± 22.7
ESV (mL)	34.4 ± 16.4	44.3 ± 14.4	27.3 ± 14.0
EDVi (mL/m ²)	47.5 ± 13.3	53.8 ± 13.6	43.0 ± 11.1
ESVi (mL/m ²)	18.5 ± 8.3	22.6 ± 7.9	15.5 ± 7.3

Table 1

Demographic and anthropometric findings at rest

(BMI, Body mass index; BSA, body surface area; EF, ejection fraction; EDV, end-diastolic volume; ESV, end-systolic volume; EDVi, end-diastolic volume index; ESVi, end-systolic volume index)

Significant differences between men and women were found for all volumetric parameters in all age groups and for EF only in the subgroup ≥65 years of age. When normalised to body surface area (data indicated by EDVi and ESVi), differences in volumes between the genders and in EF in the subgroup ≥65 years were still evident, with the exception of the EDVi in the age group <45 years of age. Men showed significantly higher volume values throughout and lower EF values when compared to women in the subgroup ≥65 years. Within-gender differences in EF or volumetric parameters between the different age groups were found only in women of the ≥65 year age group, who had significantly higher EF values and significantly lower EDV and ESV values (Table 2).

Variable	Age					
	< 45 years		45 - < 65 years		≥ 65 years	
	Men (n=6)	Women (n=8)	Men (n=25)	Women (n=29)	Men (n=12)	Women (n=22)
Age (years)	36.3 ± 10.1	37.6 ± 5.5	53.2 ± 5.1	56.2 ± 6.1	71.8 ± 6.4	69.9 ± 4.9
BMI (g/m ²)	26.2 ± 5.8	26.7 ± 4.3	29.0 ± 6.2	27.8 ± 5.7	25.2 ± 3.3	26.0 ± 4.0
BSA	2.0 ± 0.2	1.7 ± 0.1	2.0 ± 0.2	1.8 ± 0.2	1.9 ± 0.1	1.7 ± 0.1
EF (%)	55.5 ± 5.2	57.5 ± 7.8	59.2 ± 6.0	63.8 ± 8.6	60.1 ± 6.9 ^o	70.9 ± 7.7*
EDV (mL)	129.7 ± 25.8 ^o	85.6 ± 13.3	104.0 ± 23.3 ^o	82.9 ± 26.3	96.6 ± 22.6 ^o	61.9 ± 11.6*
ESV (mL)	58.3 ± 15.1 ^o	37.3 ± 11.7	43.4 ± 13.0 ^o	31.2 ± 15.0	39.0 ± 13.4 ^o	18.4 ± 7.1*
EDVi (mL/m ²)	67.0 ± 17.8	49.4 ± 8.9	52.0 ± 12.4 ^o	45.5 ± 12.7	51.1 ± 10.9 ^o	37.3 ± 6.6
ESVi (mL/m ²)	30.5 ± 10.1 ^o	21.8 ± 6.7	21.6 ± 6.9 ^o	17.0 ± 7.5	20.6 ± 7.0 ^o	11.2 ± 4.4*

Table 2

Myocardial functional parameters assessed by QGS, by age and gender

*P<0.05, ANOVA, within one gender ^oP<0.05, ANOVA, between genders

(BMI, Body mass index; BSA, body surface area; EF, ejection fraction; EDV, end-diastolic volume; ESV, end-systolic volume; EDVi, end-diastolic volume index; ESVi, end-systolic volume index)

On the other hand, significant negative and positive correlations were found between age and EDVi and ESVi values for both women and men and between EF values and age in women (Table 3).

Variable	Correlation coefficient (p-value)		
	All (n=102)	Men (n=43)	Women (n=59)
EF (%)	0.42 (0.000)	0.18 (NS)	0.55 (0.000)
EDV (mL)	-0.45 (0.000)	-0.46 (0.002)	-0.46 (0.000)
ESV (mL)	-0.49 (0.000)	-0.45 (0.003)	-0.55 (0.000)
EDVi (mL/m ²)	-0.41 (0.000)	-0.39 (0.010)	-0.42 (0.001)
ESVi (mL/m ²)	-0.48 (0.000)	-0.40 (0.009)	-0.54 (0.000)

Table 3

Gender-specific relation of rest LV volumes and EF to age

(EF = ejection fraction, EDV = end-diastolic volume, ESV = end-systolic volume, EDVi = end-diastolic volume index, ESVi = end-systolic volume index, NS = not significant)

Overall, EF values following stress were significantly higher than those obtained at rest: $64.7\% \pm 8.6\%$ at stress versus $62.8\% \pm 8.7\%$ at rest ($P=0.03$). When subdivided according to type of stress testing, a significant difference between EF at rest versus stress was found following bicycle stress testing ($62.0\% \pm 8.0\%$ at rest versus $64.7\% \pm 7.8\%$ following stress, $P=0.000$) but not following pharmacological stress testing ($64.5\% \pm 10.7\%$ at rest versus $64.4\% \pm 11.2\%$ following stress, $P=0.478$). The increase in EF following bicycle test when compared to dipyridamole stress testing was the result of a significant decrease in ESV following bicycle stress (36.2 ± 18.9 mL at rest versus 33.15 ± 17.9 mL following stress, $P=0.003$) which did not occur following dipyridamole stress (24.8 ± 13.4 mL at rest versus 29.5 ± 14.1 mL following stress, $P=0.409$).

DISCUSSION

Comparison with other non-invasive imaging modalities

Age- and gender-specific differences in myocardial function have been previously reported using echocardiography [35; 36; 37; 38; 39; 40] and magnetic resonance imaging (MRI) [41; 42; 43; 44; 45; 46; 47; 48; 49]. Most of these studies have been limited to a small number of patients and have included individuals with a younger mean age, on average ± 30 years, than that of patients with cardiac disease. Mean values for EF, EDV and ESV at rest in these series range, respectively, from 62.1%–69.9%, 108–130 mL and 35–49.3 mL using MRI and from 58.1%–60%, 95–112 mL and 35–38.6 mL using echocardiography. Whereas results for EF in the present series are comparable (mean 62.3%; SD 8.7%) to those previously reported, values obtained for EDV and ESV were lower, at 88.1 mL (SD 27.9 mL) and 34.4 mL (SD 16.4 mL), respectively. Although the higher mean age in our series may have been at least partly responsible for the lower EDV and ESV values found, methodological problems should also be considered. As shown by Nakajima et al. using a mathematical digital phantom, the limited resolution of the gamma camera may result in underestimation of the LV volume by 15% for a volume of 101 mL, 25% for a volume of 52 mL and 50% for a volume of 37 mL [50]. Also, count subtraction with varying LV cavity background activity may be insufficient to correct for spill-over from systolic counts from opposing myocardial walls into one another and into the LV cavity in smaller hearts, thus contributing to LV underestimation at systole [51]. Comparable differences in volumes

and in EF as measured by MRI, echocardiography and radionuclide angiography were recently reported by Bellenger et al. [52]. On the basis of these and our own findings, it may be concluded that volumetric myocardial values and EF values assessed by different imaging modalities, including SPECT and QGS, are not clinically interchangeable.

Gender-related differences

In terms of gender-specific differences, significantly higher EDV and significantly lower EF values, the latter limited to the subgroup ≥ 65 years old, were found in men compared to women. Normalisation to body surface area (BSA) did not eliminate these differences. These findings are in contrast to those obtained by Sandstede et al. [49] and Lorenz et al. [41]. Sandstede et al., using cine MRI with breathholding, found that following normalisation to BSA, significant differences between men and women in LV volumes were eliminated. Lorenz et al., using cine MRI in a series of 75 patients, also found gender independence for EF when corrected for BSA. Possibly, the non-linear underestimation of myocardial volumes using gated SPECT as suggested by Nakajima et al., with increasing underestimation at smaller volumes, may have resulted in over-reduction of EDVi and ESVi in women when compared to men [50].

Age-related differences

Data on age-related differences in EF and EDV and ESV are conflicting. Whereas De Simone et al. demonstrated an increase in LV chamber size in older women [39], Merino et al. found no differences in EDV, ESV or EF in two groups of volunteers aged 22 ± 1 and 70 ± 4 years [40]. On the other hand, Sandstede et al. showed a significant decrease in systolic and diastolic LV volumes with increasing age. In this series, however, EF values remained nearly unchanged [39]. Comparable results were obtained by Slotwiner et al., who found a slight but significant increase in LVEF and a decrease in chamber size with age in a large series of 464 clinically normal adults aged 16–88 years [53]. Gender differences in this series were, however, not directly assessed. Instead, these authors used partial correlation coefficients, accounting for gender. From their data it is nevertheless unclear how this dichotomous variable was incorporated in the statistical analysis. In the present series, using analysis of variance, age-related differences were only noted in the group of women aged ≥ 65 years, who showed significantly lower EDV and ESV and significantly higher EF values. On the other hand, using correlation analysis, significant negative and positive correlations were found between age and EDV and ESV for both women and men and

between EF values and age in women, in agreement with the findings reported by Slotwiner et al. and Sandstede et al. [49]. Thus, the absence of an age-related significant difference in the three groups of men and in the groups of women below 65 years of age may have been the result of the relatively small number of patients per group, not allowing a significant difference to emerge.

Effect of stress type on functional parameters

In keeping with previous findings of Kumita et al. [54], bicycle testing resulted in a significant increase in EF and a significant reduction in ESV due to an increase in cardiac inotropism. Lack of this effect during dipyridamole stress explains why no significant difference in EF was found at rest and following dipyridamole administration.

Study limitations

Due to ethical considerations, coronary angiography could not be performed to confirm the absence of significant coronary artery disease. Also, the effect of true obesity on EF and volume calculation could not be assessed owing to the limited number of patients with a body mass index (BMI) >30.

CONCLUSION

In summary, using QGS, we observed significant changes in both chamber volumes and EF with increasing age. Furthermore, volumes and EF as assessed by QGS seem strongly gender-specific. Although the physiological significance of these results is uncertain and needs further study, the findings demonstrate that the evaluation of cardiac function and volumes of patients by means of gated SPECT and QGS should consider age- and gender-matched normative values.

REFERENCES

1. Mock MB, Ringquist I, Fisher LD, Davis KB, Chaitman RB, Kouchoukos NT, Kaiser GC, Alderman E, Ryan TJ, Russel RO, Jmulin S, Fray D, Killip TI. Survival of medically treated patients in the coronary artery surgery study (CASS) registry. *Circulation* 1982; 66: 562-571.
2. Koren MJ, Devereux RB, Casale PN, Savage DD, Laragh JH. Relation of left ventricular mass and geometry to morbidity and mortality in uncomplicated essential hypertension. *Ann Intern Med* 1991; 114: 345-352.
3. De Simone G, Devereux RB, Casale PN, Savage DD, Laragh JH. Midwall LV mechanics : an independent predictor of cardiovascular risk. *Circulation* 1996; 93:259-265.
4. Grucker G, Florentz P, Oswald T, Chambron J. Myocardial gated tomoscintigraphy with Tc-99m-methoxyisobutyl-isonitrile (MIBI): regional and temporal activity curve analysis. *Nuc Med Commun* 1989; 10: 723-732.
5. DePuey EG, Nichols K, Dobrinsky C. Left ventricular ejection fraction assessed from gated myocardial perfusion SPECT. *J Nucl Med* 1993; 34: 1871-1876.
6. Germano G, Kiat K, Kavanagh PB et al. Automatic quantification of ejection fraction from gated myocardial perfusion SPECT. *J Nucl Med* 1995; 36: 2138-2147.
7. Faber TL, Akers MS, Peshock RM, Corbett JR. Three-dimensional motion and perfusion quantitation in gated single-photon emission computed tomograms. *J Nucl Med* 1991; 32: 2311-2317.
8. Villanueva-Meyer J, Mena I, Narahara KA. Simultaneous assessment of left ventricular wall motion and ventricular perfusion with technetium-99m-methoxy isobutyl isonitrile at stress and rest in patients with angina: comparison with thallium-201 SPECT. *J Nucl Med* 1990; 31: 457-463.
9. Williams KA, Taillon La. Left ventricular function in patients with coronary artery disease assessed by gated tomographic myocardial perfusion imaging. *J Am Coll Cariol* 1996; 27: 173-181.

10. DePuey EG, Rozanski A. Using gated technetium-99m-sestamibi SPECT to characterize fixed perfusion defects as infarct or artifact. *J Nucl Med* 1995; 36: 952-955.
11. Germano G, Berman DS. On the accuracy and reproducibility of quantitative gated myocardial SPECT (editorial). *J Nucl Med* 1999: 810-813.
12. Wahr DW, Wang YS, Schiller NB. Left ventricular volumes determined by two-dimensional echocardiography in a normal adult population. *J Am Coll Cardiol* 1983; 1: 863-868
13. Feigenbaum H. Appendix. In *Echocardiography*, Ed. Feigenbaum H, Lea & Febiger, Pennsylvania, USA, 1993; p670.
14. Gardin JM, Siscovick D, Anton-Culver H, Lynch JC, Smith VE, Klopfenstein HS, Bommer WJ, Fried L, O'Leary D, Manolio TA. Sex, age and disease after echocardiographic left ventricular mass and systolic function in three living elderly (the cardiovascular health study). *Circulation* 1995; 91: 1739-1748.
15. Pearson AC, Gudipati CV, Labovitz AJ. Effects of aging on left ventricular structure and function. *Am Heart J* 1991; 121: 871-875.
16. Dannenberg AL, Levy D, Garisson RJ. Impact of age on echocardiographic LVM in a healthy population (the Framingham study). *Am J Cardiol* 1989; 64: 1066-1068.
17. De Simone G, Devereux RB, Roman MJ, Ganau A, Chien S, Alderman MH, Atlas S, Laragh JH. Gender differences in left ventricular anatomy, blood viscosity and volume regulatory hormones in normal adults. *Am J Cardiol* 1991; 68: 1704-1708.
18. Merino A, Alegria E, Castello R, Martinez-caro D. Influence of age on LV contractility. *Am J Cardiol* 1988; 62: 1103-1108.
19. Lorenz CH, Walker ES, Morgan VL, Klein SS, Graham TP Jr. Normal human right and left ventricular mass, systolic function, and gender differences by cine magnetic resonance imaging. *J Card Magn Reson* 1999; 1: 7-21.
20. Sakuma H, Globits S, Bourne MW, Shimakawa A, Foo TK, Higgins CB. Improved reproducibility in measuring LV volumes and mass using multicoil breath-hold cine MR imaging. *J Magn Reson Imaging* 1996; 1: 124-127.

21. Rominger MB, Bachmann GF, Geuer M, Puzik M, Boedeker RH, Ricken WW, Rau WS. Accuracy of right and left ventricular heart volume and left-ventricular muscle mass determination by cine MRI and breath-hold technique. *Fortschr Roentgenstr* 1999; 170: 54-60.
22. Dulce MC, Mostbeck GH, Firse KK, Caputo GR, Higgins CB. Quantification of the left ventricular volumes and function with cine MRI imaging: comparison of geometric models with three-dimensional data. *Radiology* 1993; 188: 371-376.
23. Matsuoka H, Hamada M, Honda T, Kobayashi T, Suzuki M, Ohtani T, Takezaki M, Abe M, Fujiwara Y, Sumimoto T et al. Measurement of cardiac chamber volumes by cine magnetic resonance imaging. *Angiology* 1993; 44: 321-327.
24. Katz J, Whang J, Boxt LM, Barst RJ. Estimation of right ventricular mass in normal subjects and in patients with pulmonary hypertension by nuclear magnetic resonance imaging. *J Am Coll Cardiol* 1993; 21: 1475-1481.
25. Pitton MB, Just M, Grebe P, Kreitner KF, Erbel R, Thelen M. Errors during MRT measurements of left ventricular volumes using a multi-slice technique. *Fortschr Roentgenstr* 1992; 157: 447-451.
26. Semelka RC, Tomei E, Wagner S, Mayo J, Kondo C, Suzuki JI, Caputo GR, Higgins CB. Normal left ventricular dimensions and function: interstudy reproducibility of measurements with cine MR imaging. *Radiology* 1990; 174: 763-768.
27. Sandstede J, Lipke C, Beer M, Hofmann S, Pabst T, Kenn W, Neubauer S, Hahn D. Age- and gender-specific differences in left and right ventricular cardiac function and mass determined by cine magnetic resonance imaging. *Eur Radiology* 2000; 10: 438-442.
28. Nakajima K, Taki J, Higuchi T, Kawano M, Taniguchi M, Maruhashi K, Sakazume S, Tonami N. Gated SPECT quantification of small hearts: mathematical simulation and clinical application. *Eur J Nucl Med* 2000; 27(9):1372-1379.
29. Nichols K, Tamis J, DePuey G, Mieres J, Malhotra S, Rozanski A. Relationship of gated SPECT ventricular function parameters to angiographic measurements. *J Nucl Cardiol* 1998; 5: 295-303.
30. Bellenger NG, Burgess MI, Ray SG, Lahiri A, Coats AJS, Cleland JGF, Pennell DJ. Comparison of left ventricular ejection fraction and volumes in heart failure

by echocardiography, radionuclide ventriculography and cardiovascular magnetic resonance. *Eur Heart J* 2000, 21: 1387-1396.

31. Slotwiner DJ, Devereux RB, Schwartz JE, Pickering TG, Desimone G, Ganau A, Saba PS, Roman MJ. Relation of age to left ventricular function in clinically normal adults. *Am J Cardiol* 1998; 82: 621-626

Part 2: Gated Bloodpool SPECT, phantom experiments

CHAPTER 2:

**VALIDATION OF PLANAR AND
TOMOGRAPHIC RADIONUCLIDE
VENTRICULOGRAPHY BY A DYNAMIC
VENTRICULAR PHANTOM**

Pieter De Bondt¹, Stijn Vandenberghe², Stefaan De Mey², Patrick Segers², Olivier De Winter¹, Johan De Sutter³, Christophe Van de Wiele¹, Pascal Verdonck², Rudi Andre Dierckx¹

¹ Division of Nuclear Medicine, Ghent University Hospital,

² Hydraulics Laboratory, Ghent University,

³ Department of Cardiology, Ghent University Hospital, Ghent, Belgium De Pintelaan
185, 9000 Ghent, Belgium

Nucl Med Commun. 2003 Jul;24(7):771-7.

SUMMARY

While there is growing interest in the automatic processing of tomographic radionuclide ventriculography (TRV) studies, the validation of these programs is mainly limited to a comparison of TRV results with data from planar radionuclide ventriculography (PRV) or gated perfusion single photon emission computed tomography (SPECT). The aim of the study was, therefore, to use a dynamic physical cardiac phantom for the validation of ejection fraction (EF) and volumes from PRV and TRV studies. A new dynamic left ventricular phantom was constructed and used to acquire 21 acquisitions in the planar and tomographic mode. The directly measured volumes and ejection fractions of the phantom during the acquisitions were considered as the gold standard for comparison with TRV and PRV. Ejection fractions were calculated from PRV by background-corrected end-diastolic and end-systolic frames. Volumes and ejection fractions were calculated from TRV by region growing with different lower thresholds to search for the optimal threshold. EF from PRV correlated significantly with the real EF ($r=0.94$, $p=0.00$). The optimal threshold value for volume calculation from TRV in 336 cases was 50% ($r=0.98$, $p=0.00$) yielding the best slope after linear regression. When considering these calculated end-diastolic and end-systolic volumes, EF highly correlates ($r=0.99$, $p=0.00$) with the real EF, and this correlation was significantly ($p=0.04$) higher compared to EF from PRV. Our experiments prove that EF measured from TRV yields more accurate results compared with PRV in dynamic cardiac phantom studies.

INTRODUCTION

Planar radionuclide ventriculography (PRV) is a well validated, widely used, straightforward and highly reproducible technique for the assessment of left ventricular ejection fraction [1]. Nevertheless, this technique suffers from the fact that two-dimensional (2D) compressions of three-dimensional data are used and important structures in planar acquired cardiac images may be hidden or masked by objects in front of or behind them, introducing uncertainties in ejection fraction (EF) calculation. To resolve the limitations associated to this 2D technique, several automatic or semi-automatic methods have been developed that allow assessment of volumes (and hence left ventricular cardiac function) from tomographic radionuclide

ventriculography (TRV) data [2-4]. When compared to PRV, these techniques provide a more accurate separation of the cardiac chambers leading to supplementary information on biventricular volumes, wall motion and regional ejection fraction [5]. In general, the clinical usefulness of these algorithms has been established through direct comparison with data derived from PRV, but most of these algorithms have never been validated against a dynamic cardiac phantom [3,4]. Although cardiac phantom studies oversimplify cardiac anatomy and should not be considered as clinically gold standards, they have the advantage of absolute control over variables and accurate knowledge of the parameters under study. This study reports on the validation of PRV and TRV for measuring left ventricular volume and ejection fraction by using a newly developed dynamic physical cardiac phantom.

MATERIALS AND METHODS

Phantom description

A Plexiglas reservoir (the atrium) was connected to an ellipsoidal model ventricle, made from silicone rubber and surrounded by a fluid-filled tank (Figure 1-2). Ventricular filling and emptying was achieved by means of a piston pump that withdraws/adds water from/into the water tank yielding a sinusoidal filling and emptying pattern. Pump rate was controlled such that a constant heart rate of about 65 beats/min was obtained (mean 64.7, range 62 – 68).

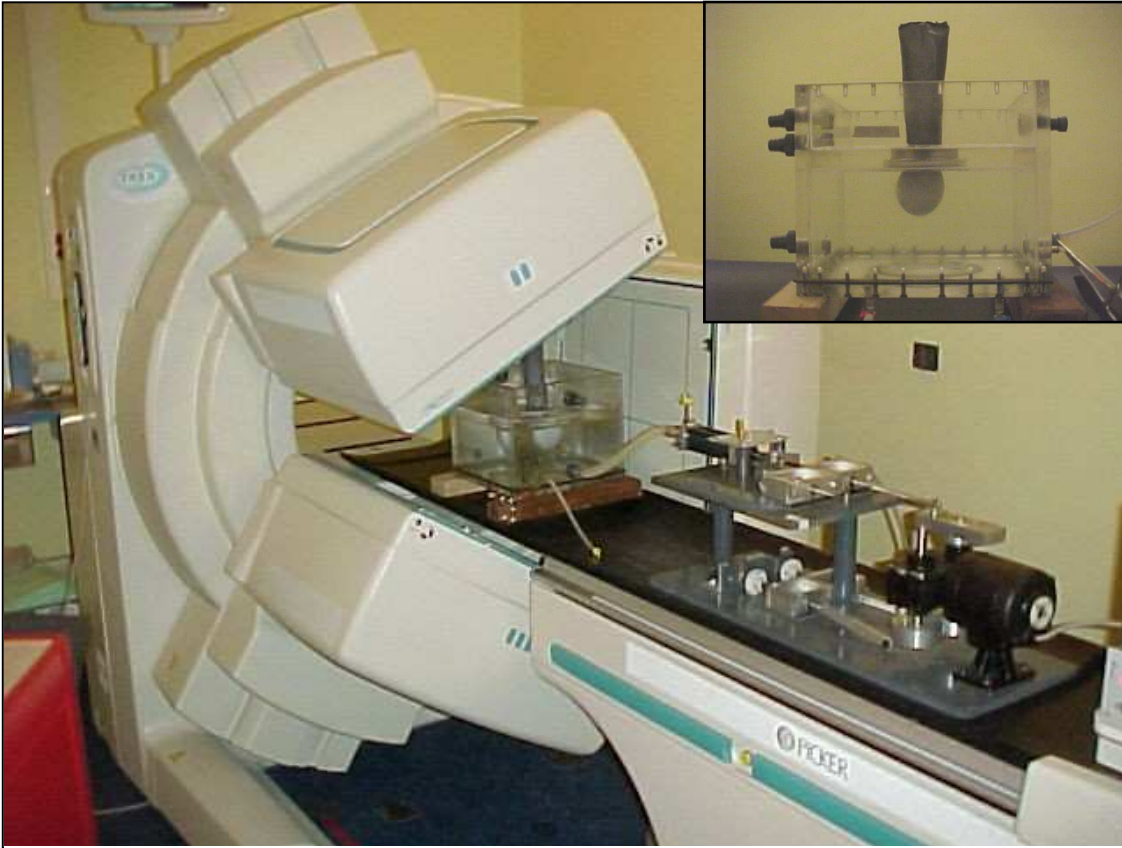


Figure 1

The phantom in the reservoir (upper right corner) positioned on a three-headed gamma camera (IRIX, Marconi-Phillips, Cleveland Ohio).

An electrical contact generated a voltage peak when the piston pump reached its outmost position (end-diastolic volume of ventricular cavity) to simulate the patient's ECG-trigger. Stroke volumes were adjusted by changing the stroke length of the plunger of the piston pump. The ventricular end-diastolic volume was changed by altering the volume of water in the surrounding tank.

True volumes were determined by measuring the contents of the phantom in end-diastolic (ED) and end-systolic (ES) position. To calculate the volumes in the frames other than ED and ES, the following formula (1) was applied:

$$(1) \quad y = \frac{(EDV - ESV)}{2} \times \cos\left(\frac{2 \times \pi \times fr}{nfr}\right) + EDV - \frac{(EDV - ESV)}{2}$$

with y = actual volume, fr = frame number and nfr = total number of frames (16)

Thus obtained volumes were used as the gold standard.

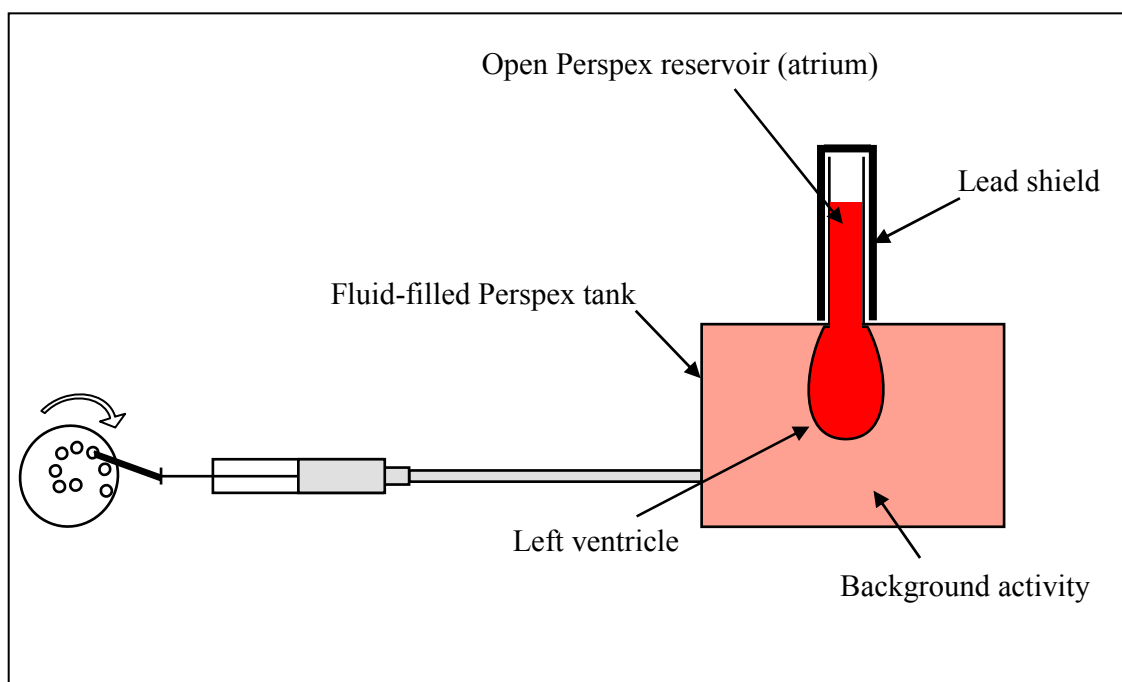


Figure 2
Design of the phantom-setup

Data acquisition

Atrium and ventricle were filled with Tc99m with a concentration varying between 10 and 14 mCi/l, the background varied from 0.3 to 2 mCi/l. Twenty-one different raw data sets were acquired for PRV and TRV covering a wide range of ventricular end-diastolic volumes (27 – 290 mL, mean 122 mL) and stroke volumes (22 – 59 mL, mean 42 mL) in order to obtain a wide range of EF (7 – 66 %, mean 35%).

Planar imaging

PRV data were acquired over a 5 minute period, in 16 electrocardiographic gated frames, 64 x 64 matrix, zoom 1.333 (pixel size 7 mm) and with a beat acceptance window at 20 % of the average R-R interval calculated just before the acquisition was started. One projection was obtained with 1 head of a three-headed gamma camera (IRIX, Marconi-Phillips, Cleveland Ohio). The low energy high resolution collimator was positioned perpendicular to the surface of the phantom, in order to obtain a

projection view of a long vertical axis of the ventricle. FWHM (Full width at half-maximum) at 10 cm distance of the camera used is 7.6 mm. Counts/pixel in all summed frames varied in the left ventricle from 2236 to 9990 (mean 5769) and in the background from 415 to 3965 (mean 1796). In each frame, counts were calculated in the LV volume with a lower threshold of 50%. A rectangular region was drawn outside the LV to calculate the background activity/pixel and this correction was applied to the LV counts. The frame with the highest counts corresponded with the ED frame, those with the lowest counts, the ES one. EF was calculated with the formula (2):

$$(2) \quad EF = \frac{(EDcounts - EScounts)}{EDcounts} \times 100$$

Tomographic imaging

TRV data were acquired using the same camera, equipped with the same collimators. Parameters of acquisition were as follows: 360° step-and-shoot rotation, 40 stops per head, 30 seconds per stop, 64 x 64 matrix, zoom 1.422 (pixel size 6.5 mm), 16 time frames and with a beat acceptance window at 20 % of the average R-R interval. The projection data were reconstructed by filtered backprojection using a Butterworth filter (cutoff frequency: 0.5 cycles/cm; order: 5). Transverse slices of every time frame were used as input for the MultiModality software (Nuclear Diagnostics, Hermes version 3.6, 1999). In total 336 transverse reconstructed studies were used to calculate volumes applying region growing (RG) on reconstructed slices. This method delineates three dimensional (3D) volumes using a threshold without an edge weight. A seeding point was positioned in the voxel containing the maximum counts in the ventricle. Different growing limits (46%, 48%, 50%, 52%, 54%) were applied in order to define the optimal threshold. After detection of the optimal threshold, ED volume and ES volume were defined for each study and EF was calculated using the above mentioned formula, with ED and ES volumes (V) in stead of counts.

Statistical Analysis

Correlations between calculated and true values were expressed as the Pearson coefficient for the volume data (n=336) and Spearman rank coefficient for the EF data (n=21). Variability about the regression line was expressed as the standard error of the estimate (SEE). The significance of the differences between various thresholds used was determined by analysis of variance using Bonferroni correction. Bland-Altman analysis of differences versus means of paired values was used to search for trends and

systematic errors. Statistical significance was defined as $p < 0.05$.

RESULTS

Results of volume calculation are shown in Table 1 and expressed by linear regression and Bland-Altman analysis for the different thresholds.

	Linear regression				Bland-Altman analysis	
	Equation	SEE	r	p	Mean difference (RG – actual)	Standard deviation of difference
RG 46	$y = 0.79 + 1.07 x$	0.79	1.00	0.00	9.41	7.27
RG 48	$y = -0.81 + 1.04 x$	0.76	1.00	0.00	4.14	6.29
RG 50	$y = -2.33 + 1.01 x$	0.75	1.00	0.00	-1.12	5.73
RG 52	$y = -3.57 + 0.98 x$	0.71	1.00	0.00	-6.09	5.66
RG 54	$y = -4.65 + 0.95 x$	0.71	0.99	0.00	-11.15	6.21

Table 1
(SEE = standard error of the estimate)

An excellent correlation was found for all chosen thresholds (46%, 48%, 50%, 52% and 54%) and differences between the volumes obtained by various thresholds were not statistically significant. However, as the 50% threshold yielded the best slope after linear regression and the smallest mean percentage error as determined by Bland-Altman analysis, this value was defined as the optimal threshold (Figure 3.).

A highly significant correlation was found between the calculated PRV EF and the real EF ($r=0.94$, $p=0.00$; Figure 3.) as well as between TRV EF and actual EF ($r=0.99$, $p=0.00$; Figure 4.). The correlation was significantly higher for TRV compared to PRV ($p=0.04$). Bland-Altman analyses of differences versus mean calculated EF and actual EF demonstrated no significant trends or biases (Figure 3 and 4).

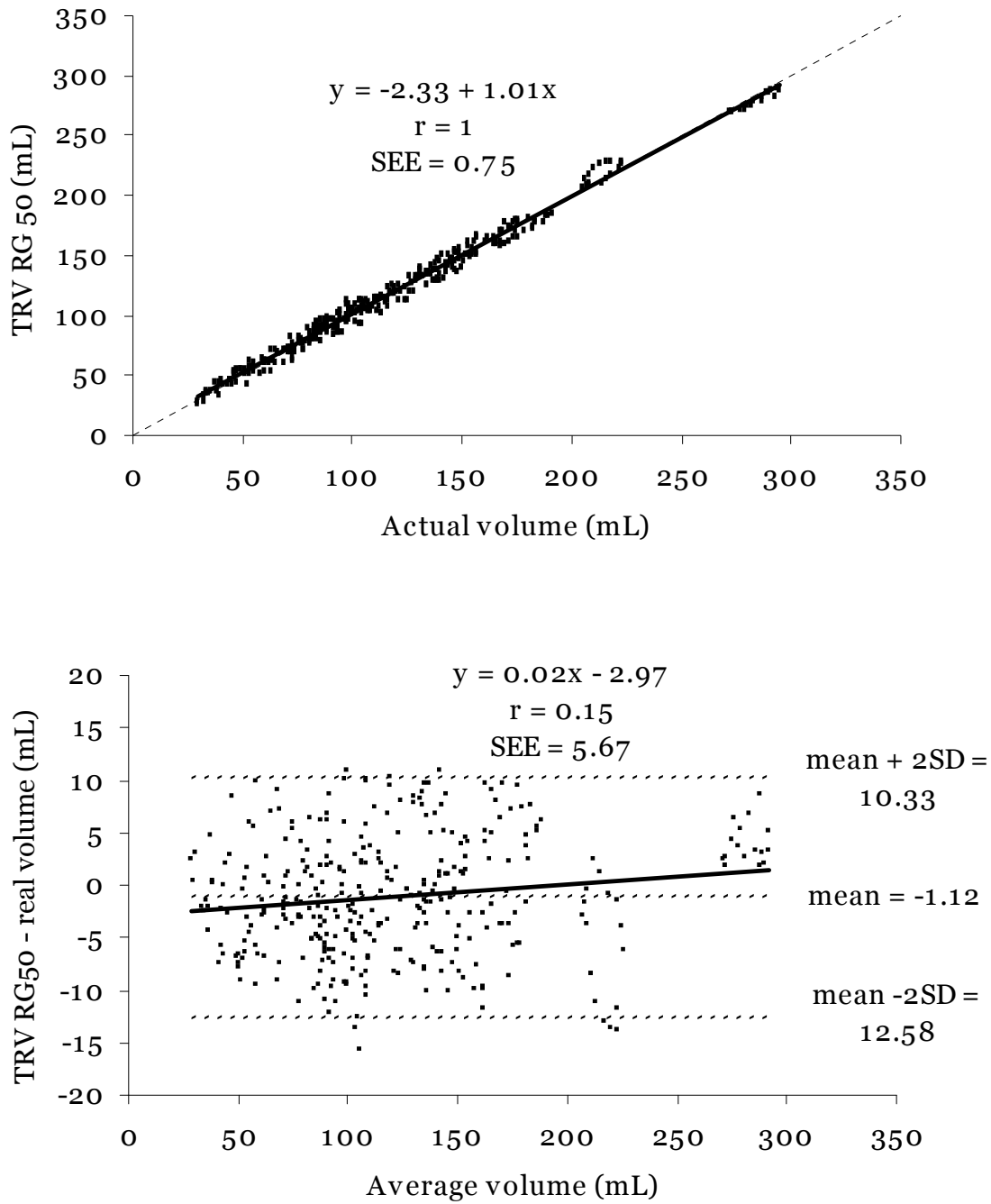


Figure 3
 Linear regression (A) and Bland-Altman (B) analysis for volume determination with a threshold of 50% (TRV RG50) against the real volumes.

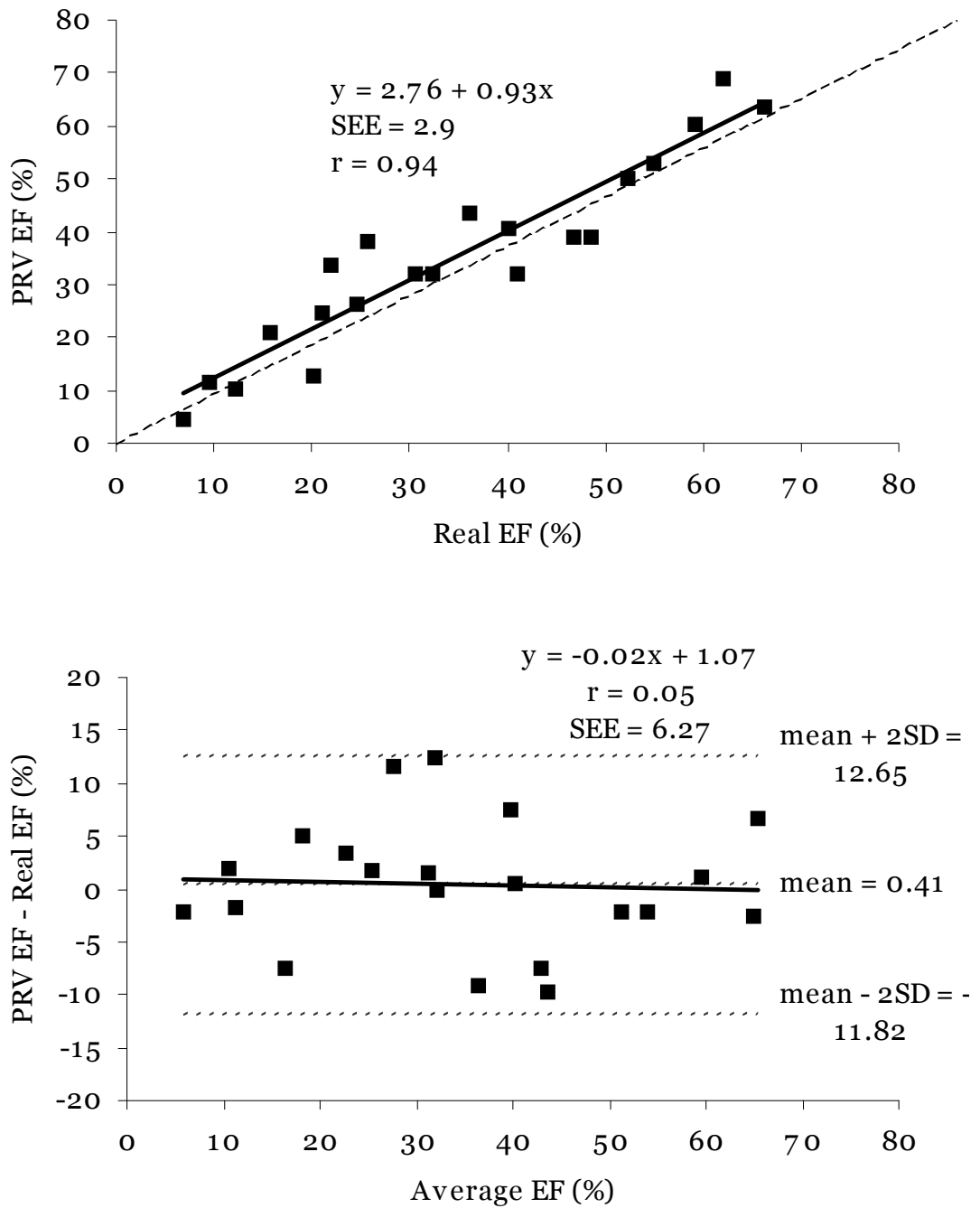


Figure 4
 Linear regression (A) and Bland-Altman (B) analysis for EF calculations with PRV against the real EF

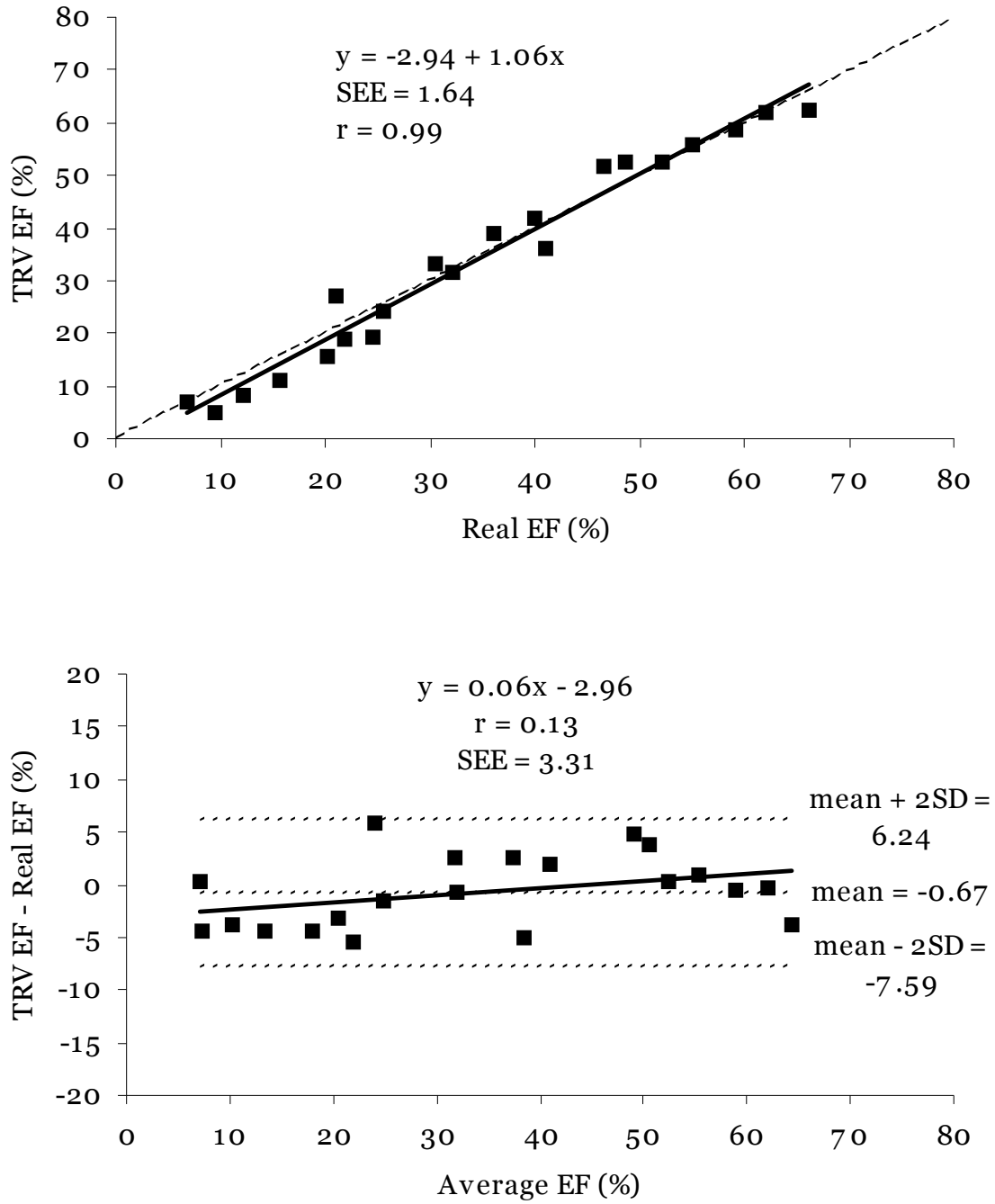


Figure 5
 Linear regression (A) and Bland-Altman (B) analysis for EF calculations with TRV against the real EF

The most common criterion used to define a volume with SPECT (as is also the case in the study presented) is a count threshold or the inclusion of all voxels within a selected percentage of the maximum counts as being within the volume. A number of factors is known to influence the accuracy of estimation of volumes when adopting this methodology. The most influential factors are the source size relative to the system spatial resolution and the source shape. As shown by King et al. [6], the use of a 50% threshold to determine the location of the edge along the axis of cylindrical and spherical sources leads to a systematic and progressive underestimation of the source volume for diameter/FWHM ratios smaller than 6 which is more important for sphere shaped volumes than for cylindrical ones. Once the ratio decreases below 2.0 the edge starts to move back out and eventually the volume is overestimated as the ratio decreases further. In contrast, for bar shaped sources, the estimated location of the edge is essentially equal to the actual location of the edge until the width of the object has decreased below 2 times the FWHM. In the presented data series, the smallest volume included was 27 mL, corresponding to a diameter of approximately 36 mm. Taking into account the system spatial resolution of 7.6 mm, this results in a minimal ratio of 4.7, with the vast majority of volumes included in this study exceeding a ratio of 6.0. Furthermore, the ellipsoidal shape of the phantom ventricle approximates more closely cylindrical than spherical shapes, thus further reducing the degree of underestimation.

DISCUSSION

The optimal threshold of 50% defined in the presented data series is in agreement with previous data obtained by Tauxe et al. [7] using seven ellipsoidal static phantoms ($y = 1.96 + 0.979 x$, $r=0.997$) with increasing volumes (range : 53 – 5047 mL), despite the fact that in our study “low-count” reconstructed slices were used originating from gated tomographic data. The robustness of this value - despite the presence of surrounding activity and the inclusion of attenuation and scatter within the phantom - suggests that the latter factors are of minor importance when compared to the shape and size of the volume relative to the system spatial resolution. Although the use of a number of thresholds (as suggested by Faber et al. [8]) may theoretically provide overall more accurate results, particularly for smaller volumes, this procedure is impractical and difficult to implement in routine clinical practice.

We used a Butterworth filter with the characteristics based on recent guidelines [9]

and publications [3,4]. As the filter choice defines the edge, it will codefine the optimal threshold value to be used for region growing. In this regard, restoration filters (e.g. Wiener filter) or smoothing filters (e.g. Hann or Hamming filters), require lower threshold values as confirmed by Chin et al. [10] and Front et al. [11]. Chin et al. placed a static cardiac phantom with a fixed volume in a torso phantom, reconstructed the projection data with a Wiener filter and found an optimal threshold of 37%. Front et al. used a Hanning filter and found a threshold of 43% to be optimal for volume calculation from SPECT, with a regression line given as $y = -3.2 + 1.061 x$ ($r = 0.99$).

To the best of our knowledge, dynamic cardiac phantom experiments for radionuclide ventriculography have only been described twice by Pretorius et al. [12] and Simon et al. [13]. Only the latter group used a real physical dynamic cardiac phantom for the evaluation of ventricular volumes. They, unfortunately, performed only planar acquisitions. Pretorius et al. validated ventricular volume calculations from TRV with a mathematical cardiac torso phantom (MCAT). The correlation for 360° projection data of the left ventricle without attenuation correction varied between 0.967 and 0.984, and the SEE values varied between 5.44 and 9.78. However, using their mathematical model and a count-based method, they found significant overestimations for ESV. Simon et al. adopted the technique described by Links et al. [14] for volume determination taking into account the counts from a “blood” sample, radioactive decay, background and attenuation. When comparing different imaging distances (9 cm vs. 5 cm), the accuracy of volume determinations declined with increasing distance, resulting in a systematic underestimation of true volumes ($y = 15.25 + 0.88x$; SEE = 3.38 at 9 cm). A similar progressive underestimation of true volumes with increasing distance was described by Fearnow et al. using a single hollow acrylic sphere filled with aqueous ^{99m}Tc in a elliptical torso phantom and ascribed to excessive background subtraction. Due to the physical limitation of our phantom which was placed in a tank and the property of a tomographic acquisition, the imaging distance in our study was about 20 cm. The excellent results that we obtained despite this remote distance suggests that background correction is of less influence when deriving volumes from TRV.

Study limitations

No scatter and attenuation correction was applied during the reconstruction of our phantom studies. The phantom could not be placed in a torso phantom because of physical limitations. Although these corrections could theoretically have a significant

impact on the volume-calculations this was not supported by the excellent results obtained. No asymmetric ventricles (similar to the right ventricle) or respiratory motion was applied in this experiment. Our model offers potential for this, but the aim of the current study was to validate the volume calculation from a simplified ventricular volume as a first step, and now we can further develop a multiple cardiac chamber model, with more realistic shaped cardiac and mediastinal structures.

CONCLUSION

To the best of our knowledge, this is the first study to use a physical dynamic ventricular model for validation of PRV and TRV studies. Both techniques yielded good results for EF calculation, with more accurate results for TRV compared to PRV, and also for volume measurements. This model may serve as standard to study the influence of parameters included in commercially available algorithms to process TRV. Future experiments will include a right and left ventricle with a realistic geometry, the use of a volume-curve generator and the incorporation of the model in a torso phantom.

Acknowledgements

Stijn Vandenberghe and Stefaan De Mey are recipients of a specialization grant of the IWT (Flemish institutie for the promotion of Institute for the Promotion of Innovation by Science and Technology in Flanders). Patrick Segers is funded by a post-doc grant by the fund for scientific research Flanders, Belgium (FWO-Vlaanderen).

REFERENCES

1. Wackers FJ, Berger HJ, Johnstone DE, et al. Multiple gated cardiac blood pool imaging for left ventricular ejection fraction: validation of the technique and assessment of variability. *Am J Cardiol.* 1979;43:1159-1166.
2. Mariano-Goulart D, Collet H, Kotzki PO, Zanca M, Rossi M. Semi-automatic segmentation of gated blood pool emission tomographic images by watersheds: application to the determination of right and left ejection fractions. *Eur J Nucl Med.* 1998;25:1300-1307.
3. Vanhove C, Franken PR, Defrise M, Momen A, Everaert H, Bossuyt A. Automatic determination of left ventricular ejection fraction from gated blood-pool tomography. *J Nucl Med.* 2001;42:401-407.
4. Van Kriekinge SD, Berman DS, Germano G. Automatic quantification of left ventricular ejection fraction from gated blood pool SPECT. *J Nucl Cardiol.* 1999; 6:498-506.
5. Corbett JR, Jansen DE, Lewis SE, et al. Tomographic gated blood pool radionuclide ventriculography: analysis of wall motion and left ventricular volumes in patients with coronary artery disease. *J Am Coll Cardiol.* 1985;6:349-358.
6. King MA, Long DT, Brill AB. SPECT volume quantitation: influence of spatial resolution, source size and shape, and voxel size. *Med Phys.* 1991;18:1016-1024.
7. Tauxe WN, Soussaline F, Todd-Pokropek A, et al. Determination of organ volume by single-photon emission tomography. *J Nucl Med.* 1982;23:984-987.
8. Faber TL, Akers MS, Peshock RM, Corbett JR. Three-dimensional motion and perfusion quantification in gated single-photon emission computed tomograms. *J Nucl Med.* 1991;32:2311-2317.
9. Updated imaging guidelines for nuclear cardiology procedures, part 1. *J Nucl Cardiol.* 2001;8:G5-G58
10. Chin BB, Bloomgarden DC, Xia W, et al. Right and left ventricular volume and ejection fraction by tomographic gated blood-pool scintigraphy. *J Nucl Med.* 1997;38:942-948.

11. Front D, Ioselevsky G, Frenkel A, et al. In vivo quantitation using SPECT of radiopharmaceutical uptake by human meningiomas . Radiology. 1987;164:93-96.
12. Pretorius PH, Xia W, King MA, Tsui BM, Pan TS, Villegas BJ. Evaluation of right and left ventricular volume and ejection fraction using a mathematical cardiac torso phantom. J Nucl Med. 1997;38:1528-1535.
13. Simon TR, Walker BS, Matthiesen S, et al. A realistic dynamic cardiac phantom for evaluating radionuclide ventriculography: description and initial studies with the left ventricular chamber. J Nucl Med. 1989;30:542-547.
14. Links JM, Becker LC, Shindlecker JG, et al. Measurement of absolute left ventricular volume from gated blood pool studies. Circulation. 1982;65:82-91.

CHAPTER 3:

ACCURACY OF COMMERCIAL AVAILABLE PROCESSING ALGORITHMS FOR PLANAR RADIONUCLIDE VENTRICULOGRAPHY USING A DYNAMIC LEFT VENTRICULAR PHANTOM

Pieter De Bondt¹, Olivier De Winter¹, Stijn Vandenberghe², Frederic Vandevijver¹,
Patrick Segers², Art Bleukx³, Hampshire Ham¹, Pascal Verdonck², Rudi Andre Dierckx¹

¹ Division of Nuclear Medicine, Ghent University Hospital,

² Hydraulics Laboratory, Ghent University, Ghent, Belgium De Pintelaan 185, 9000
Ghent, Belgium,

³ Department of Civil Engineering, K.U. Leuven, Belgium

Nucl Med Commun. 2004 Dec;25(12):1197-202.

SUMMARY

Automatic and semi-automatic algorithms to calculate ejection fraction (EF) from planar radionuclide ventriculography (PRV) are being used for years in nuclear medicine. Validation of these algorithms is scarce and often performed on outdated versions of the software. Nevertheless, clinical trials where PRV is being used as the golden standard for EF are numerous. Because of the importance attributed to the EF calculated by these programs, the accuracy of the resulting EF was assessed with a dynamic left ventricular physical phantom. A dynamic left ventricular phantom was used to simulate 21 combinations of various ejection fractions (7 – 66 %) and end-diastolic volumes (27 – 290 mL). For each combination, a planar radionuclide ventriculography was acquired, converted to an interfile format and transferred into processing stations with 10 different contemporarily-available commercial algorithms. The golden standard was the “real” EF of the phantom, derived from the exact volume of the ventricle in end-diastolic and end-systolic position. Correlation and Bland-Altman analysis was performed between the real EF and the calculated EF. The correlation for all data was excellent ($r = 0.98$), the mean difference was very acceptable (0.98 %). Nevertheless, Bland-Altman analysis showed a significant trend in the difference between real and calculated EF, with a growing underestimation for higher ranges of EF, due to an overestimation of background in larger volumes compared to smaller ones. EF from PRV, calculated with commercially available algorithms correlates closely to the real EF of a dynamic left ventricular phantom. This phantom can be used in the development and validation of algorithms of PRV studies, in software audits and in quality assurance procedures.

INTRODUCTION

Planar radionuclide ventriculography (PRV) is well established and since years generally accepted as the golden standard for the calculation of left ventricular ejection fraction (EF) [1,2]. The technique is simple, robust and easy to perform. Nearly all manufacturers of nuclear medicine equipment provide workstations with available processing software for PRV. Most of these programs provide some references about the methods used to calculate EF, but information about the development and the clinical validation of the algorithm is mostly limited or absent.

Therefore, the aim of this study is to investigate the general accuracy of ten such commercially available programs for the calculation of LVEF with a dynamic ventricular phantom.

MATERIALS AND METHODS

Dynamic phantom

The development of the phantom used for this study was previously described [3]. In short, a thin-walled ellipsoidal silicone ventricle was suspended in a water-filled Perspex tank and contraction and relaxation were simulated by adding and withdrawing water from the tank with a piston pump. Twenty-one acquisitions were performed, covering a wide range of ventricular end-diastolic volumes (27 – 290 mL, mean 122 mL) and stroke volumes (22 – 59 mL, mean 42 mL) in order to obtain a wide range of EF (7 – 66 %, mean 35%). Atrium and ventricle were filled with a solution of Tc99m pertechnetate in water, with a concentration varying between 10 and 14 mCi/l, the background varied from 0.3 to 2 mCi/l. An electrical contact generated a voltage peak when the piston pump reached its outmost position (end-diastolic volume of ventricular cavity) to simulate the patient's ECG-trigger.

Data acquisition

PRV data were acquired over a 5 minute period, in 16 electrocardiographic gated frames, 64 x 64 matrix, zoom 1.333 (pixel size 7 mm) and with a beat acceptance window at 20 % of the average R-R interval calculated just before the acquisition was started. An acquisition was obtained with 1 head of a three-headed gamma camera (IRIX, Marconi-Phillips, Cleveland Ohio). The low energy high-resolution collimator was positioned perpendicular to the surface of the phantom, in order to obtain a projection view of a long vertical axis of the ventricle.

Name	Workstation/ Company	Address	Version	Type of background ROI definition and correction	Ref.
(a) Multi-Gated Analysis	Odyssey/Philps Medical Systems	Best, The Netherlands	march 2001	FBS, CDBS and CDDA	yes
(b) Gated Heart Analysis (FUGA)	Hermes/Nuclear Diagnostics	Hägersten, Sweden	june 2000	FBS and CDBC	yes
(c) Gated Blood Pool (GBP)	Vision/ GE Medical Systems	Milwaukee, USA	march 2000	FBS	yes
(d) Gated Bloodpool	Icon/ Siemens	Munich, Germany	NA	NA	NA
(e) Gated Bloodpool	Toshiba Medical Systems	Zoetermeer, The Netherlands	Version 5.3	FBS: Between 3 and 6 o'clock, 2 pixels wide and 2 pixel from diastolic ROI	NA
(f) EF Analysis Protocol	eNTEGRA/ GE Medical Systems	Milwaukee, USA	may 2000	FBS: Between 1 and 6 o'clock, 4 pixels wide and 1 pixel from systolic ROI	no
(g) Gated Bloodpool	Mirage / Segami Corporation	Paris, France	v 5	NA	no
(h) Ejection Fraction (Planar)	NuQuest/ Alphanuclear	Buenos Aires, Argentina	2.0	FBS: manually drawn ROI outside LV at end diastole	no
(i) Heart Gated	Windows/ Medicimaging	Ljubljana, Slovenia	2002, v 1.0	FBS: manually drawn ROI outside LV	NA
(j) xt_erna	Vision/ GE Medical Systems	Milwaukee, USA	NA	FBS: manually or automatically drawn ROI outside LV at end diastole	NA

Table 1

(NA: not available; FBS: Fixed Background Subtraction; CDBS: Cycle-Dependent Background Subtraction: correction of non-ventricular counts, being pulled into the space that is occupied by the left ventricle during contraction (Wall Motion Region); CDDA: Cycle-Dependent Diskinetic Addition: correction for ventricular counts in end-systole, being outside the ROI drawn for end-diastole

Processing

The acquisitions were converted to an interfile format and stored digitally. The programs that were used in this study are designated a to e and are summarised in table 1.

The first three programs (a,b,c) were available on-site. Programs (d) and (e) were

available in resp. the Department of Nuclear Medicine, Algemeen Ziekenhuis Zusters van Barmhartigheid, Ronse, Belgium and in the Department of Nuclear Medicine, Breda, The Netherlands. The other programs (f-j) were obtained from the manufacturer. All acquisitions, on-site as well as off-site, were processed blindly, without knowledge of the real EF and all scans were first processed without operator interference (automatic algorithm). If the automatic option failed to detect the correct end-diastolic and end-systolic region, there was a manual intervention based on the amplitude and phase image. Misplacement of the left ventricular ROI was mostly due to an inclusion of the left atrium into the ROI. In all cases, defining a new centre in the left ventricle was enough to let the program define a new and correct region of interest (ROI). All results were sent back to Ghent University, where the statistical analysis was performed.

Statistical Analysis

χ^2 analysis was used to test whether data were normally distributed. Results were reported as mean values \pm 1 standard deviation (SD). Correlations between calculated and true (measured) values were expressed as the Pearson coefficient. Variability about the regression line was expressed as the standard error of the estimate (SEE). Bland-Altman analysis of differences versus means of paired values was used to search for trends and systematic errors. Statistical significance was defined as $p < 0.05$.

RESULTS

All values of EF were normally distributed. For all data (Figure 1.), an excellent correlation was calculated ($r = 0.98$), the mean difference was very acceptable (0.98 %) and a significant trend was seen in the Bland-Altman analysis with a growing underestimation for the calculated EF for higher EF. Calculated EF correlated highly with true values for all algorithms (from $r = 0.95$ till $r = 0.99$) (Figure 2.). With the exception of algorithm b, all regressions showed a significant slope < 1 . In Bland-Altman analysis (Figure 3.), only the slopes of algorithms c, g, and j differed significantly from 0, showing a trend for these algorithms to underestimate higher EF's.

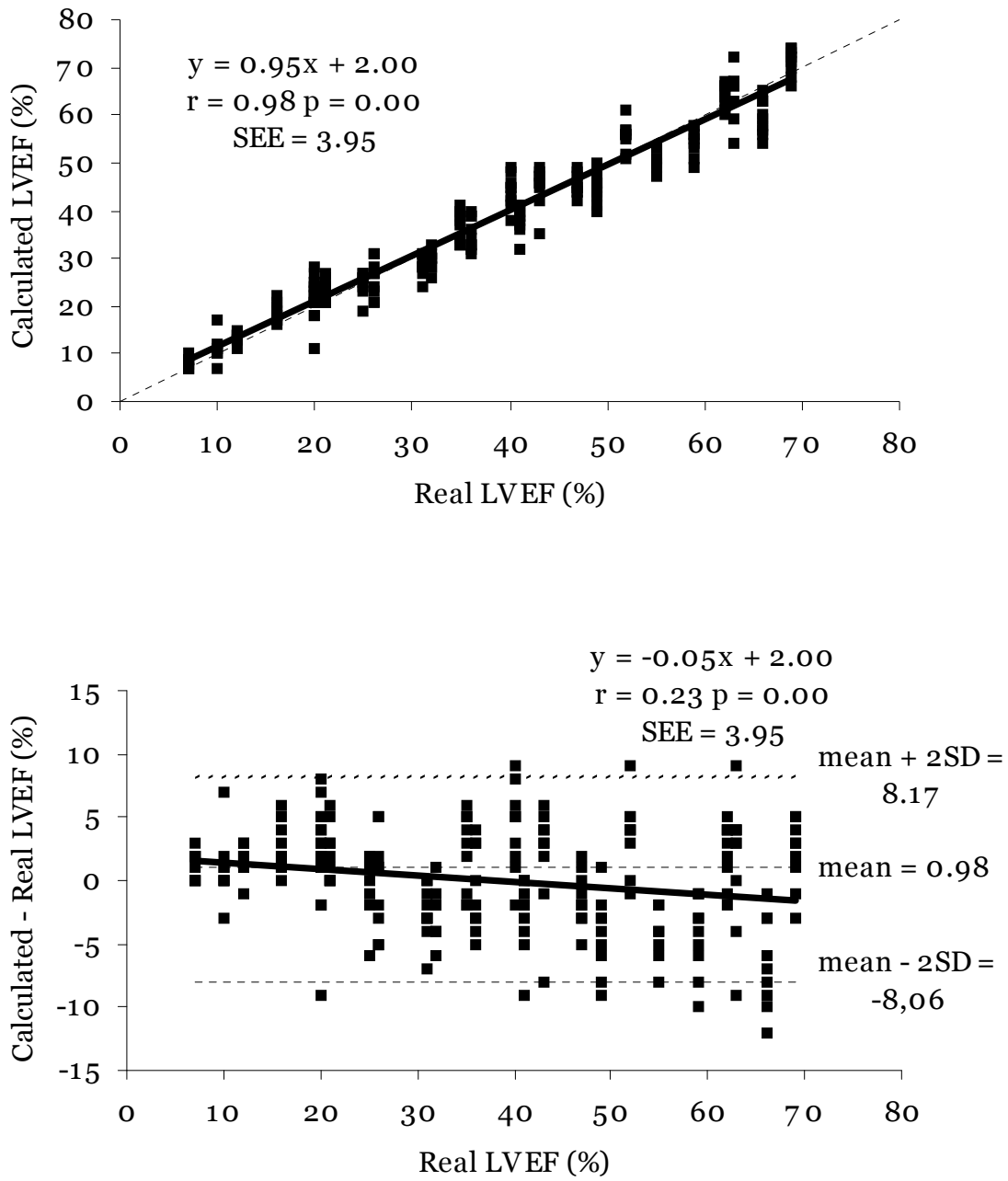


Figure 1

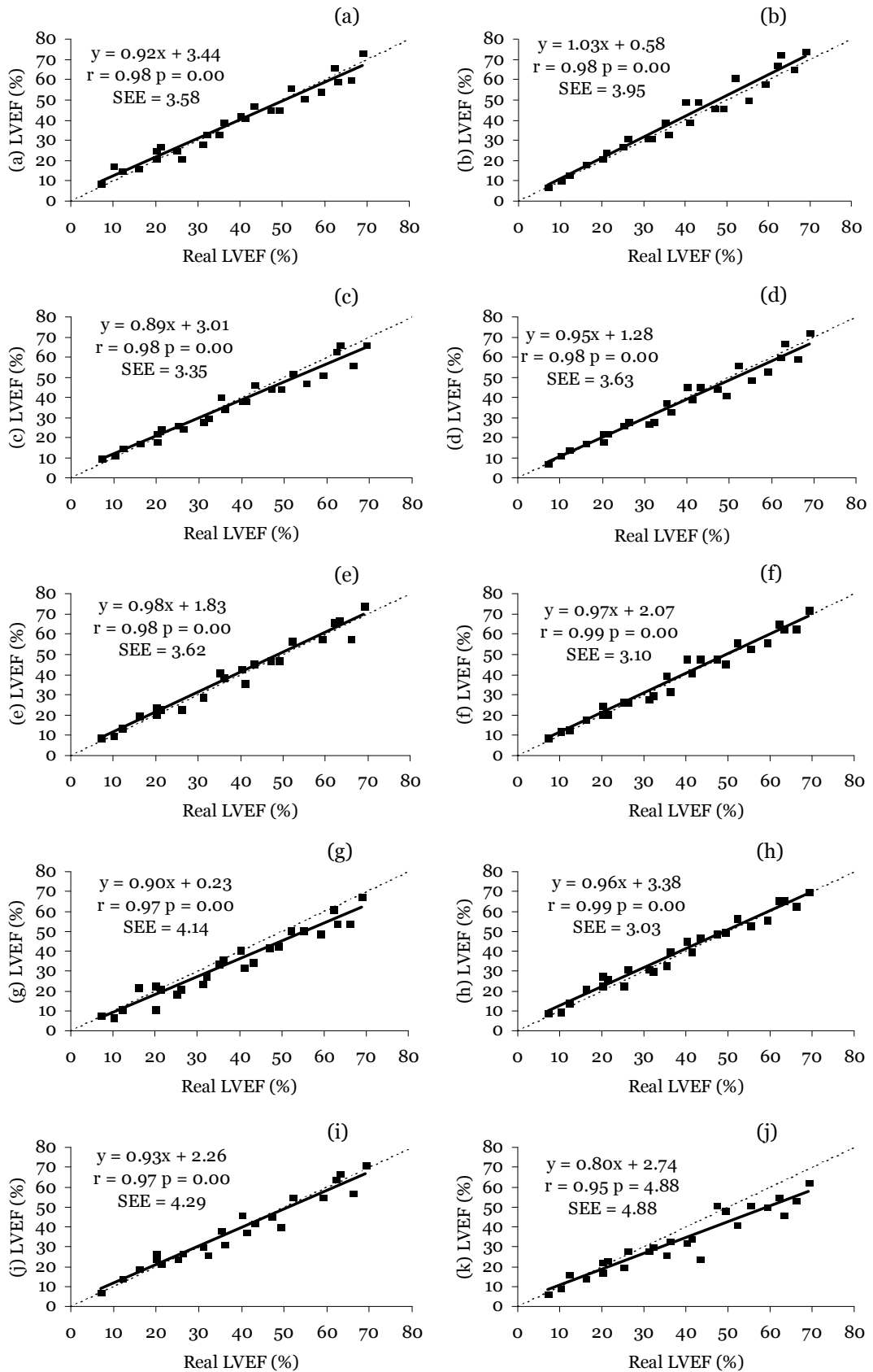


Figure 2

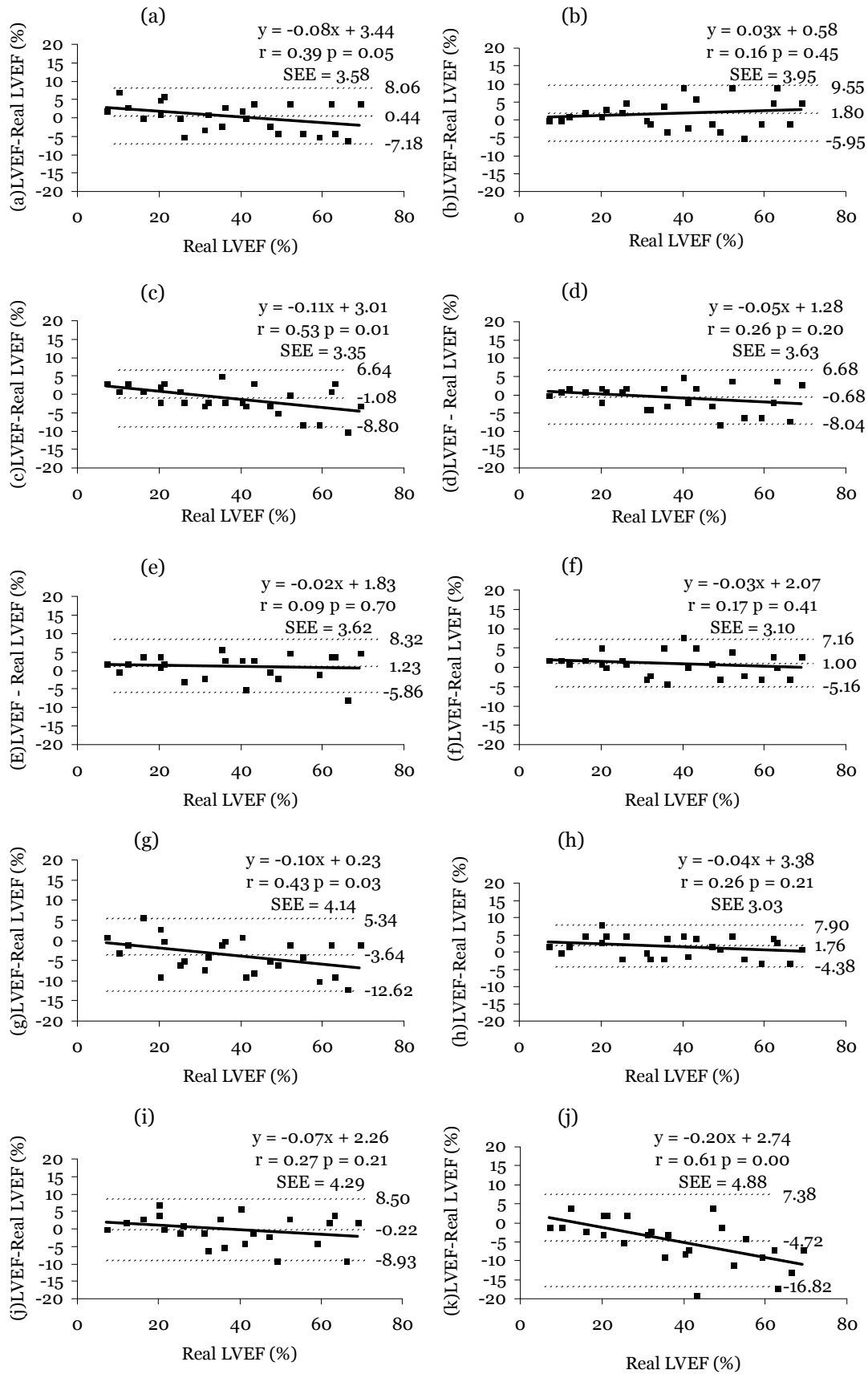


Figure 3

DISCUSSION

From the early 1970s, PRV has been extensively studied and validated. The first reports compared scintigraphic and radiographic EF [4,5]. Correlation coefficients were found from 0.72 to 0.95. As the technique got more and more automated, PRV became the golden standard for measuring global left ventricular function. The first paper, dating back from 1985, gave an overview of different commercial computer programs for analysis of PRV. Reiber et al. compared 8 algorithms, and did a correlation study with contrast angiography for 5 algorithms [6]. Over the years, processing algorithms have not changed substantially, but they have been adapted and modified to newer and faster computer systems. The validation of these programs was not of primary importance to the manufacturers, and their results were incontestably accepted. Moreover, the result of PRV is these days even used to validate EF calculated from gated myocardial perfusion SPECT and gated blood pool SPECT. A phantom validation, mathematical or physical, of the available software is often suggested in literature, but only rarely done, which explains the primary aim of this particular study.

The best correlation for all algorithms is seen in the lower range of EF, which is of higher clinical importance than the higher range of EF. The larger variation and higher underestimation in determining EF in the higher range is in our opinion due to the high degree of absorption in the wall of the Perspex tank. Because the absorption coefficient of Perspex is much higher compared to the mixture of muscle, bone, fat, and skin, the attenuation of photons in our experiment is higher than in the human body. Without absorption correction, LV volume values were underestimated by a factor of 3.6 on average [7]. Another reason for underestimating higher ejection fractions is due to the oversubtraction of background [8]. Using larger volumes usually attained high ejection fractions. The amount of background anterior and posterior to the left ventricle in our model is inversely proportional to the volume of the ventricle. By using a constant background, larger volumes are oversubtracted compared to smaller ones.

The type of background correction was available in eight of ten algorithms (table 1.). Most of the algorithms use a fixed background, automatically or manually drawn, mostly a few pixels wide and between 3 and 6 o'clock away from the end-diastolic

region of interest (ROI). Other types of background correction were seen in algorithm (a) and (b), particularly a correction for non-ventricular counts, being pulled into the ventricular ROI (CDBS: Cycle-Dependent Background Subtraction) and a correction for ventricular counts being pushed outside the ventricular ROI during contraction (CDDA: Cycle-Dependent Dyskinetic Addition). Although being appropriate in some clinical situations, these different types of background correction can't be the cause of the different trends, which are seen for the different algorithms.

A limitation of the dynamic cardiac phantom used in this study is the absence of the right heart and the left atrium. The background activity was constant in all directions from the left ventricle. Consequently, only an estimation of the global accuracy to correctly identify the end-diastolic and end-systolic region and to calculate EF with the available programs could be assessed.

CONCLUSION

EF from planar radionuclide ventriculography, calculated with commercially available algorithms correlates closely to the real EF of a dynamic left ventricular phantom. This dynamic left ventricular phantom can help to develop algorithms to calculate EF from planar radionuclide ventriculography studies. Furthermore, these data can also be used in quality assurance procedures and to analyse interobserver and interdepartmental variability, like being performed during software audits.

Acknowledgements

Stijn Vandenberghe is a recipient of a specialization grant of the Flemish Institute for the Promotion of Innovation by Science and Technology in Flanders (IWT-993171).

I thank Dr. Carlos De Sadeleer, who made it possible to use the software of his department (d). I am very grateful to Nico Mijnders, Physicist at the Dept of Nuclear Medicine, Amphia Hospital, Breda, The Netherlands and André Dobbeleir, Physicist at the Department of Nuclear Medicine, Middelheim Hospital, Antwerp, Belgium, who performed the processing of resp. software's (e) and (g). I thank the people of GE Medical Systems, who were so kind to process the phantom data with their program (f). I want to thank Dr. Liliana L. Bouso from Alfanuclear (h), Buenos Aires, Argentina and Dr. Valentin Fidler, Medical Physicist, chief scientist in Xlab, Ljubljana Technology Park, Slovenia from Medicimaging (i), for making it possible to test their software with our phantom data. I thank all companies who gave their active and

passive support to finalize this study.

REFERENCES

1. Wackers F. J., Berger H. J., Johnstone D. E., Goldman L., Reduto L. A., Langou R. A., Gottschalk A., and Zaret B. L. Multiple Gated Cardiac Blood Pool Imaging for Left Ventricular Ejection Fraction: Validation of the Technique and Assessment of Variability. *Am.J.Cardiol.* 1979;43(6):1159-66.
2. Strauss H. W., Zaret B. L., Hurley P. J., Natarajan T. K., and Pitt B. A Scintiphotographic Method for Measuring Left Ventricular Ejection Fraction in Man Without Cardiac Catheterization. *Am.J.Cardiol.* 1971;28(5):575-80.
3. De Bondt P., Vandenberghe S., De Mey S., Segers P., De Winter O., De Sutter J., Van De Wiele C., Verdonck P., and Dierckx R. A. Validation of Planar and Tomographic Radionuclide Ventriculography by a Dynamic Ventricular Phantom. *Nucl.Med.Comm.* 2003;24(7):771-7.
4. Dehmer G. J., Lewis S. E., Hillis L. D., Twieg D., Falkoff M., Parkey R. W., and Willerson J. T. Nongeometric Determination of Left Ventricular Volumes From Equilibrium Blood Pool Scans. *Am.J.Cardiol.* 1980;45(2):293-300.
5. Rigo P., Alderson P. O., Robertson R. M., Becker L. C., and Wagner H. N., Jr. Measurement of Aortic and Mitral Regurgitation by Gated Cardiac Blood Pool Scans. *Circulation* 1979;60(2):306-12.
6. Reiber J. H. Quantitative Analysis of Left Ventricular Function From Equilibrium Gated Blood Pool Scintigrams: an Overview of Computer Methods. *Eur.J.Nucl.Med.* 1985;10(3-4):97-110.
7. Seiderer M., Bohn I., Buell U., Kleinhans E., and Strauer B. E. Influence of Background and Absorption Correction on Nuclear Quantification of Left Ventricular End-Diastolic Volume. *Br.J.Radiol.* 1983;56(663):183-7.
8. Simon T. R., Walker B. S., Matthiesen S., Miller C., Triebel J. G., Dowdey J. E., and Smitherman T. C. A Realistic Dynamic Cardiac Phantom for Evaluating Radionuclide Ventriculography: Description and Initial Studies With the Left Ventricular Chamber. *J.Nucl.Med.* 1989;30(4):542-7.
9. Germano G., Kiat H., Kavanagh P. B., Moriel M., Mazzanti M., Su H. T., Van Train K. F., and Berman D. S. Automatic Quantification of Ejection Fraction From Gated Myocardial Perfusion SPECT. *J Nucl Med* 1995;36(11):2138-47.

- 10 Faber T. L., Cooke C. D., Folks R. D., Vansant J. P., Nichols K. J., Depuey E. G., Pettigrew R. I., and Garcia E. V. Left Ventricular Function and Perfusion From Gated SPECT Perfusion Images: an Integrated Method. *J Nucl Med* 1999;40(4):650-9.

CHAPTER 4:

VALIDATION OF GATED BLOOD POOL SPECT CARDIAC MEASUREMENTS TESTED USING A BIVENTRICULAR DYNAMIC PHYSICAL PHANTOM

Pieter De Bondt¹, Kenneth Nichols², Stijn Vandenberghe³, Patrick Segers³, Olivier De Winter¹, Christophe Van de Wiele¹, Pascal Verdonck³, Arsalan Shazad², Abu H Shoyeb², Johan De Sutter⁴

¹ Division of Nuclear Medicine, Ghent University Hospital, Ghent, Belgium

² Division of Cardiology, Department of Medicine, Columbia University College of Physicians and Surgeons, New York, NY, USA

³ Hydraulics Laboratory, Ghent University, Ghent, Belgium

⁴ Department of Cardiology, Ghent University Hospital, Ghent, Belgium

J Nucl Med. 2003 Jun;44(6):967-72.

SUMMARY

We have developed a biventricular dynamic physical cardiac phantom to test gated blood pool (GBP) SPECT image processing algorithms. Such phantoms provide absolute values against which to assess accuracy of both right and left computed ventricular volume and ejection fraction (EF) measurements. Two silicon-rubber chambers driven by two piston pumps simulated crescent-shaped right ventricles wrapped partway around ellipsoidal left ventricles. Twenty experiments were performed at Ghent University, for which right and left ventricular true volume and EF ranges were 65-275 mL and 55-165mL, and 7-49% and 12-69%, respectively. Resulting 64x64 simulated GBP-SPECT images acquired at 16 frames per R-R interval were sent to Columbia University, where 2 observers analysed images independently of each other, without knowledge of true values. Algorithms automatically segmented right ventricular activity volumetrically from left ventricular activity. Automated valve planes, mid-ventricular planes and segmentation regions were presented to observers, who accepted these choices or modified them as necessary. One observer repeated measurements > 1 month later without reference to previous determinations. Linear correlation coefficients of the mean of the 3 GBP-SPECT observations versus true values for right and left ventricles were 0.80 and 0.94 for EF and 0.94 and 0.95 for volumes, respectively. Correlations for right and left ventricles were 0.97 and 0.97 for EF and 0.96 and 0.89 for volumes for interobserver agreement, and 0.97 and 0.98 for EF and 0.96 and 0.90 for volumes, respectively, for intraobserver agreement. No trends were detected, though volumes and RVEF were significantly higher than true values. Overall, GBP-SPECT measurements correlated strongly with true values. The phantom evaluated shows considerable promise for helping to guide algorithm developments for improved GBP-SPECT accuracy.

INTRODUCTION

Gated blood pool (GBP) single photon emission computed tomography (SPECT) offers several potential advantages over conventional equilibrium radionuclide angiography (planar-ERNA). It has been shown that GBP-SPECT assesses left ventricular (LV) ejection fraction (EF) more accurately than does planar-ERNA. [1] In addition, separating the ventricles and atria provides supplementary information

regarding biventricular volumes, regional wall motion and regional EF. [2] Several automatic or semi-automatic methods have been developed that allow assessment of LV systolic function from GBP-SPECT data. [2-6]

However, relatively few GBP-SPECT studies have dealt explicitly with validating right ventricular (RV) measurements. [3-7] Yet, RV functional parameters may prove to be clinically quite important, considering that evidence has been mounting that RVEF may be a more sensitive predictor of adverse events than LVEF for some cardiac diseases, including congestive heart failure. [8,9] Nevertheless, there have not yet been any reports published concerning the use of dynamic physical phantoms to evaluate algorithms that compute RV functional parameters. Therefore, we developed a dynamic cardiac biventricular phantom with which to evaluate new image processing algorithms for the calculation of LVEF, RVEF, left ventricular volumes (LVV) and right ventricular volumes (RVV) derived from GBP-SPECT data.

MATERIALS AND METHODS

Phantom Description (Figure 1)

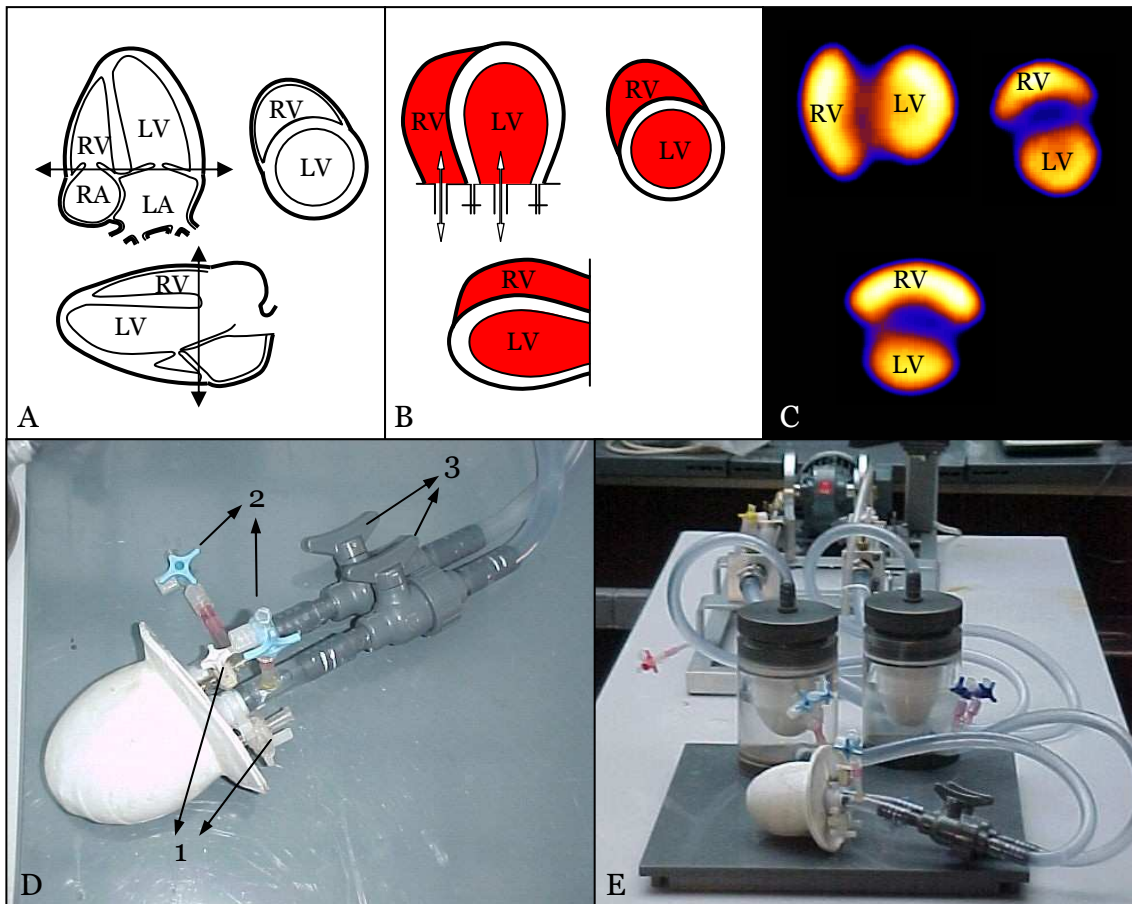


Figure 1

Development and description of the phantom.

A. Ventricles were cut off at the atrioventricular border

B. A single-walled right ventricle was attached to a double-walled left ventricle

C. Horizontal long axis slice (upper left), short axis slice (upper right) and vertical long axis slice (down) of the activity distribution in the phantom.

D. Detail of the biventricular model. Valves 1 are used to fill the septal wall with gel; valves 2 to de-aerate the tubings, to inject the tracer, and to empty the ventricles for volume measurements. Valves 3 are the in- and outgoing tubes to the ventricles.

E. Overview of the experimental model, with the piston pump in the back, the membranes in the middle and the ventricular model at front.

The phantom included two ventricular chambers. The left ventricle consisted of 2 concentric ellipsoids forming inner and outer walls (Figure 1B). The space between the 2 ellipsoids was filled with ultrasound acoustic gel, yielding a varying free wall and septal wall thickness varying between 0.5 and 1.5 cm. The gel is injected into the septal

wall via 2 stopcocks embedded in the latex model. By keeping the injected volume of gel constant between the walls, ventricular wall thickness increased at systole (due to decrease of the ventricular inner volume) and decreased at diastole, thereby approximating systolic wall thickening. A realistic approximation of this situation is necessary for the evaluation of the possibility for the algorithm to separate both ventricles correctly during processing of the images. The relatively thinner (2mm) single-walled crescent-shaped right ventricle was attached to the outer septal LV wall and wrapped partway around the LV. Ventricles were cut off at the atrioventricular border, at the point at which the chambers were supplied by varying amounts of water from connecting plastic tubes to simulate LV and RV filling and emptying. An activity concentration of 10 mCi/L of Tc-99m in water was used in the chambers, with no background activity. Two separate piston pumps were used to supply the water to each ventricle, for which different stroke volume settings for both ventricles produced a wide range of simulated ejection fractions and end-diastolic (ED) volumes. To set the end-diastolic volumes, the piston pump was fixed in its end-diastolic position. Valve 3 in Figure 1D was closed and volume was added/withdrawn to increase or decrease end-diastolic volume. By changing the stroke length of the piston pump, stroke volumes could be controlled. Following each individual experiment, volumes of both ventricles were measured at ED and at end-systole (ES) by suctioning out and measuring the contents of both ventricular chambers. In order to limit the necessary amount of radioactive tracer and not to contaminate the complete circuit, the ventricles were separated from the pump by 2 membranes, encapsulated in a plexiglas housing (Figure 1E).

Data Acquisition, Reconstruction and Reorientation

Twenty experiments were performed at Ghent University, for which RV and LV true volume and EF ranges were 65-275 mL and 55-165mL, and 7-49% and 12-69%, respectively. GBP-SPECT data were acquired using a three-detector gamma camera (IRIX, Marconi-Phillips, Cleveland Ohio) with low energy high-resolution collimators. Parameters of acquisition were as follows: 360° step-and-shoot rotation, 40 stops per head, 30 seconds per stop, 64 x 64 matrix, zoom 1.422 (pixel size 6.5 mm), and 16 time bins per R-R interval, with a beat acceptance window at 20% of the average R-R interval. An R-wave simulator synchronized with the pistons supplied R-wave triggers. Projection data were pre-filtered using a Butterworth filter (cutoff frequency: 0.5 cycles/cm; order: 5) and reconstructed by filtered backprojection using an x-plane ramp filter. Data were then reoriented into gated short axis tomograms. Rectangular

regions of interest, with outside masking, were drawn in the vicinity of simulated ventricles so that only ventricular structures and small portions of connecting tubes were visible. The resulting gated short axis data sets then were copied to a CD-ROM, which was shipped to Columbia University.

GBP-SPECT Algorithms

Processing was performed at Columbia University by two independent observers, who analysed data without reference to each other's results, and who had no knowledge of true phantom values. One observer reprocessed data > 1 month after his initial analyses without reference to his previous computations.

The algorithms used gated short axis tomograms as input data. Algorithms ran automatically, and their first display to the observer was of a simultaneous view of RV volume curves, functional parameters, and computed outlines superimposed on all short axis and horizontal long axis tomographic sections shown as a continuous cine loop. To produce these RV calculations, the programs first identified RV mid-planes by searching for maximum count areas in volumetric regions likely occupied by these chambers. Counts above a 35% threshold of global maximum counts of the entire set of collected data were used to segment the RV from the LV. The same count threshold was used for both the RV and LV. The specific 35% count threshold value was chosen because it had been used successfully in previous studies to derive myocardial surfaces from myocardial perfusion gated SPECT, and from GBP-SPECT. [7,10] Systolic count change images and Fourier phase images were used to estimate ED and ES tricuspid and pulmonary valve planes volumetrically. When presented with phantom data, the algorithms identified the posterior RV wall as the tricuspid valve plane and the anterior RV wall as the pulmonary valve plane. Moving tricuspid and pulmonary valve planes were interpolated from ED and ES valve planes for all other gating intervals. These planes were used to limit, in the posterior direction, the number of short axis slices included in subsequent volume calculations. ED and ES vertical long axis section count profiles were used to define moving pulmonary valve planes, so as to limit maximum heights of short axis outlines.

Observers were free to accept all RV results or to modify intermediate choices. To allow this, observers reviewed identified mid-RV planes, indicated as boxes framing estimated mid-plane locations projected onto simultaneous cines of short axis and vertical long axis projections. ED and ES vertical long axis and ED short axis RV profile estimates were displayed, which observers could accept or redraw as necessary,

until satisfied that generated RV outlines conformed to the visual impression of the size, shape and motion of the RV throughout the heart cycle.

All RV counts were then subtracted from the 3D gated volume of count data, leaving primarily LV counts. These were handled by algorithms similar to those described above for the RV, again using 35% count threshold segmentation criteria. Automatically determined LV outlines superimposed on all short axis and horizontal long axis sections were then shown to an observer as an endless cine loop. As with the RV processing, observers were free to redraw ED and ES vertical long axis and ED short axis LV profiles, until satisfied that outlines conformed to the LV throughout the heart cycle. In general, for both RV and LV processing manual interventions were rarely required for choices of ED or ES frames, but usually needed for VLA outlines for those simulations for which septal curvature was substantial, which was the case for over half of the simulations. Volumes were computed geometrically from the number of 3D voxels corresponding to counts above the 35% count threshold, while EF's were computed from changes in counts summed over all included ventricular voxels. This "hybrid" approach was adopted as it had previously been found to provide optimal accuracy of calculations when compared to correlative MRI studies. [11] These steps were accomplished using platform-independent computer-programming software ("IDL," Research Systems Inc., Boulder, CO) implemented on a commercially available computer system (ICON, Siemens Medical Systems, Chicago, IL).

Statistical Analysis

Chi-square analysis was used to test whether data were normally distributed. Numerical results were reported as mean values ± 1 SD. In comparing algorithmic output to real phantom values, mean computed values were tabulated from three measurements: one each for the two observers, along with the one observer's repeated measurements. In comparing computed volumes to true values, ED and ES volumes were considered together to form LVV and RVV data sets. Correlations between calculated and true values were expressed as the Pearson coefficient. Linear regression equations were calculated for all data pairs. Variability about the regression line was expressed as the standard error of the estimate (SEE). Bland-Altman analysis of differences of paired values versus true values was used to search for trends and systematic errors. The limit of statistical significance was defined as probability $p < 0.05$ for all tests.

RESULTS

Calculation of Volumes

All values of both calculated and real EF and volume values were found to be normally distributed. Calculated ES and ED ventricular volumes of the two observers' three analyses were averaged and correlated highly with real values ($r = 0.95$; $p < 0.0001$, $n = 40$ and $r = 0.93$; $p < 0.0001$, $n = 40$, for left and right ventricle respectively) (Figure 2).

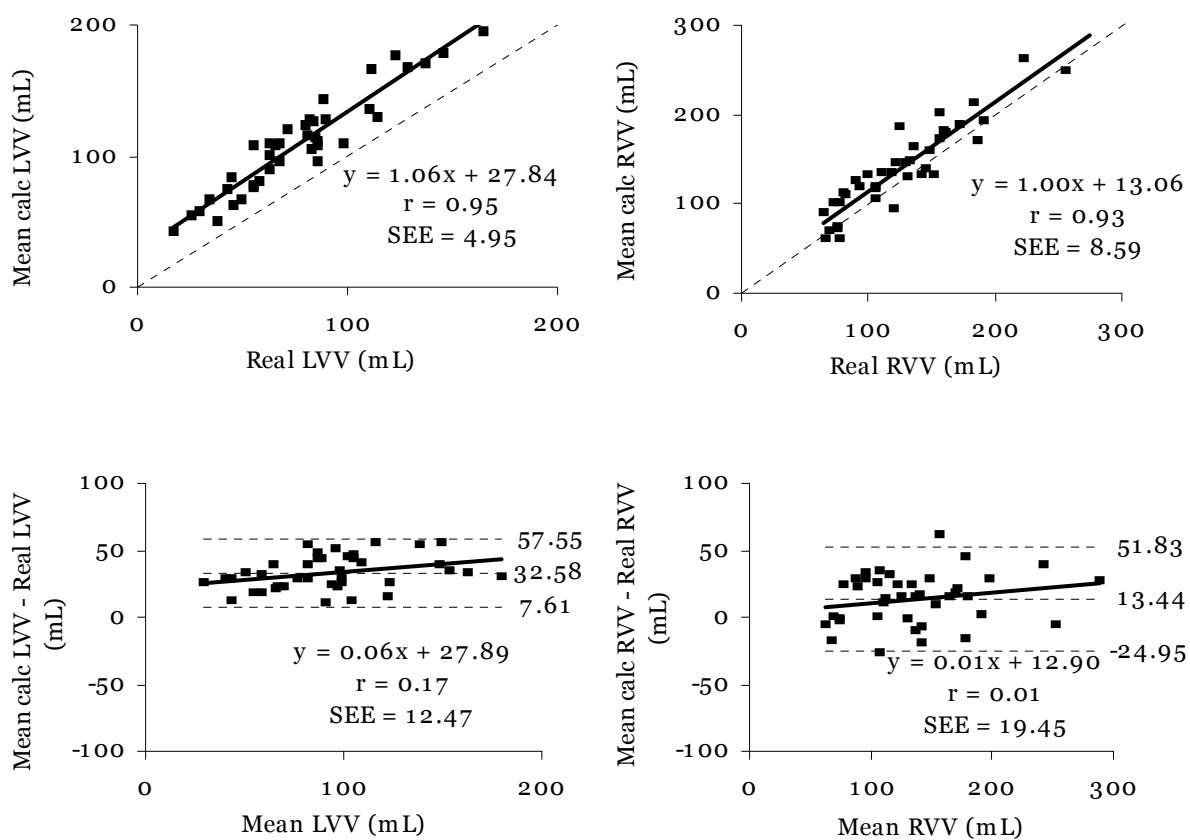


Figure 2

Linear regression and Bland-Altman analysis of mean calculated left and right ventricular volumes (MLVV and MRVV) versus real left and right ventricular volumes (RLVV and RRVV)

Bland-Altman analysis showed that while slopes of trends were not statistically significant for left or right volumes (Figure 2), nonetheless calculated LVV was statistically significantly higher than real LVV, and that calculated RVV was statistically significant higher than real RVV. This was confirmed by paired t-test results for both left volumes ($109 \text{ mL} \pm 38 \text{ mL}$ versus $77 \text{ mL} \pm 34 \text{ mL}$, $p < 0.001$, $n = 40$) and for right volumes ($143 \text{ mL} \pm 54 \text{ mL}$ versus $129 \text{ mL} \pm 50 \text{ mL}$, $p < 0.01$, $n = 40$). Sub-analyses of ED volumes and ES volumes alone, rather than both ED and ES volumes analysed together, yielded essentially the same results.

Calculation of EF

Calculated LVEF and RVEF correlated highly with real values ($r = 0.94$; $p < 0.0001$, $n = 20$ and $r = 0.80$; $p < 0.0001$, $n = 20$, respectively) (Figure 3).

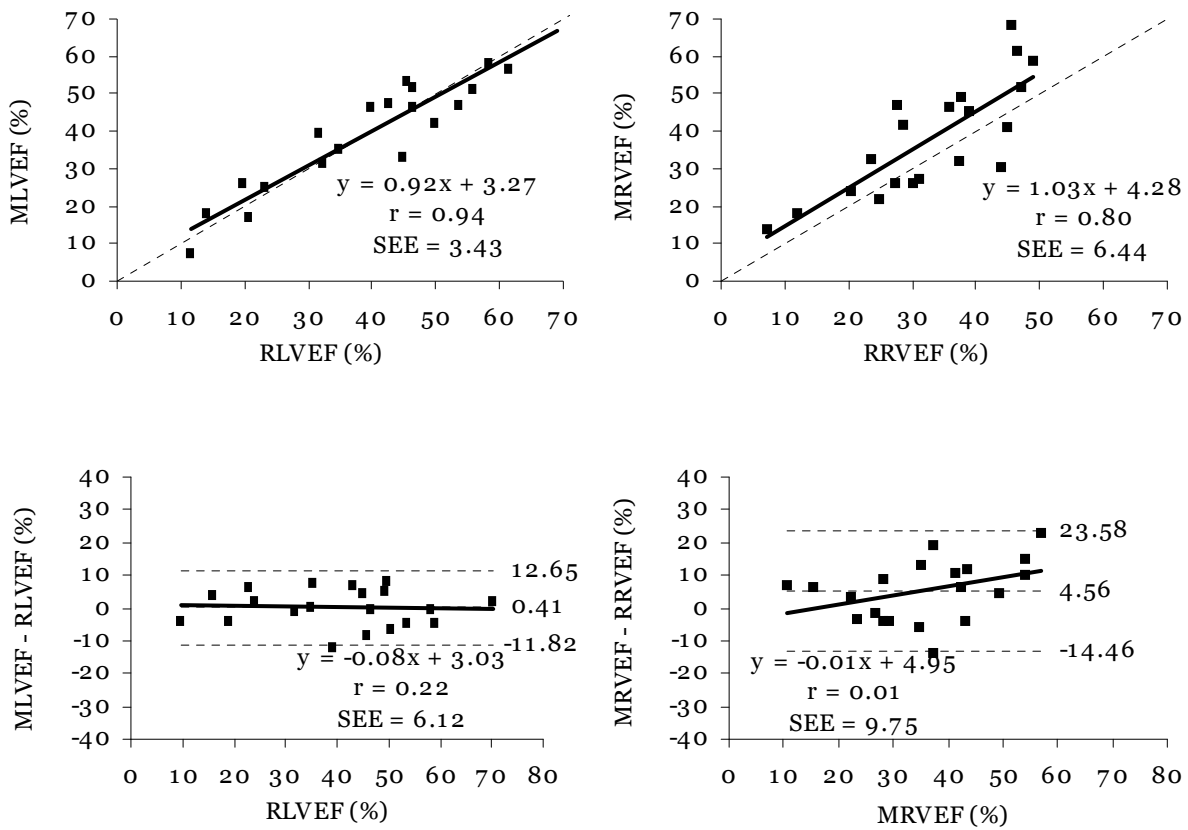


Figure 3
 Linear regression and Bland-Altman analysis of mean calculated left and right ventricular ejection fraction (MLVEF and MRVEF) versus real left and right ventricular ejection fraction (RLVEF and RRVEF)

The difference in strengths of association ($r = 0.80$ for RVEF but $r = 0.94$ for LVEF) was not statistically significant for this sample size ($n = 20$). Bland-Altman analysis showed that slopes of trends were not statistically significant for LVEF or RVEF (Figure 3). However, paired t-test results showed that while calculated LVEF was the same as real LVEF ($40\% \pm 16\%$ versus $40\% \pm 16\%$, $p = \text{NS}$, $n = 20$), calculated RVEF was significantly higher than real RVEF ($38\% \pm 15\%$ versus $33\% \pm 12\%$, $p < 0.0001$, $n = 20$).

Data Processing Reproducibility

Correlations for LV and RV were 0.97 and 0.97 for EF and 0.89 and 0.96 for volumes for interobserver agreement (Figure 4), and 0.98 and 0.97 for EF and 0.90 and 0.96 for volumes for intraobserver agreement (Figure 5). All correlations were statistically

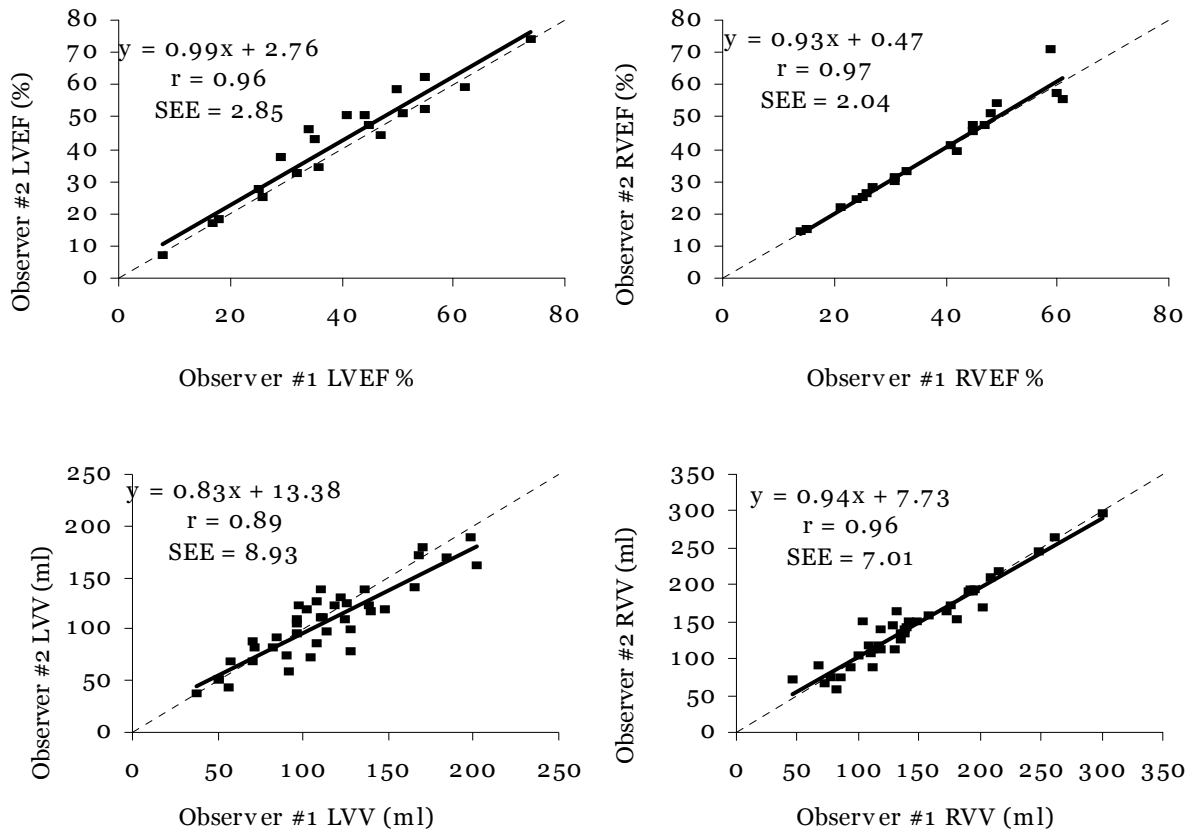


Figure 4

Interobserver variability shown by linear regression of left and right ventricular ejection fraction and volumes measurements of two different observers

significant ($p < 0.0001$). These values were consistent with those found in a previous validation of this algorithm against cardiac magnetic resonance measurements [7].

Sub-analyses of each of the two observers' three measurements were not statistically different from analysis of the means of the three measurements, as expected, given the strengths of associations for interobserver and intraobserver agreement.

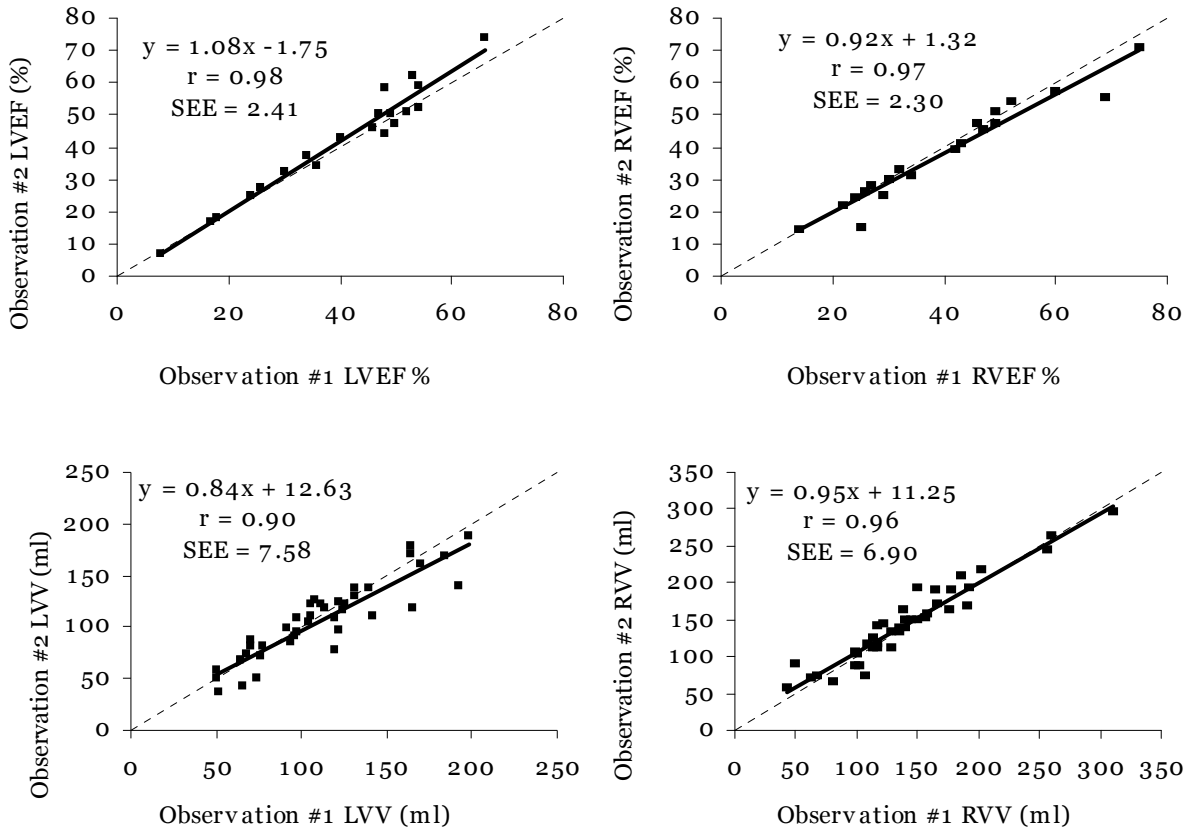


Figure 5

Intraobserver variability shown by linear regression of left and right ventricular ejection fraction and volumes measurements of two observations for the same observer

DISCUSSION

Overall, excellent correlation was obtained between computed versus real values for all measured parameters. However, the 6.4% RVEF SEE errors were larger than the 3.4% LVEF SEE errors. One factor contributing to this difference was that the phantom RV is wrapped around the LV for a greater degree of septal curvature than had been observed previously when applying the algorithms to patient data. Consequently, it was more challenging to the algorithms, and to the observers, to match regions to count thresholds for phantoms with the greatest amount of septal curvature. This may also have contributed to the larger RV volume SEE of 9 mL compared to 5 mL for LV volumes, although the larger range of real volume values (65-275 mL for RV but 55-165mL for LV; Figure 2) undoubtedly contributed to the finding.

Computed volumes were significantly larger than real volume values. This may have

been due in part to the use of the 35% count threshold. Previous experiments by our group with dynamic ventricular phantoms showed that a count threshold of 50% yielded optimally accurate results, when experiments were performed with a variable background activity. [12] It is possible that a threshold of 35% may produce better agreement with MR for patient data, even though a higher threshold produces better agreement with phantom values, considering that the phantom lacked atria and a pulmonary outflow tract. Processing with a 50% count threshold should in general produce lower volume values than use of a 35% count threshold, which in the context of the current investigation may have produced computed volumes in closer agreement with phantom values. Other investigators have found that the optimal threshold value for volume calculations derived from SPECT data can depend on the source shape; King, et. al., found that the use of a 50% threshold to determine the location of the edge of cylindrical and spherical sources lead to a systematic, progressive underestimation of source volumes for ratios of diameter/FWHM < 6 . [13] That was the case in our experiments, and considering that the smallest RV dimensions of our phantom were 8 x 1.5 x 1.5 cm, partial volume effects undoubtedly were an important factor in our experiments. [14,15] Thus, it may well be that there is a need for using different thresholds for the RV compared to LV, given the different geometrical shape of the RV compared to LV. Consequently, more realistic cardiac phantoms are warranted to clarify some issues, along with further correlative clinical studies with other imaging modalities, such as cardiac MR and x-ray contrast angiography.

There were several limitations to the study. Using algorithms developed for use with clinical data in phantom experiments can only give an estimate of the accuracy of the algorithms. Inclusion of background activity, use of different count thresholds, and of different imaging parameters (e.g., different collimators, different image filters, 180° versus 360° reconstructions) all may influence GBP-SPECT volume computations. No corrections were applied for scatter or attenuation, which also may influence GBP-SPECT calculations. The phantom itself was a simplified model of both cardiac ventricles, without atrial or vascular structures, background counts, or non-cardiac scattering media. Identifying valve planes is an important part of processing GBP-SPECT data, but this aspect of data processing was not realistically tested by the phantom used for this study. Nevertheless, this is the first published report of the use of a dynamic physical phantom to evaluate the ability of GBP-SPECT approaches to assess the right ventricle, and as such demonstrates that GBP-SPECT algorithms can

indeed produce realistic values of both right ventricular volumes and ejection fractions.

CONCLUSION

We have demonstrated that the calculation of left and right ventricular ED and ES volumes of a dynamic cardiac phantom can be performed automatically by new GBP-SPECT algorithms. Use of dynamic physical phantoms can help define the advantages and limitations of new algorithms that seek to measure both left and right ventricular functional parameters.

Acknowledgements

The authors thank Stefaan De Mey and Tom Cottens for their assistance with the phantom model experiments. This investigation was supported in part by a grant from Siemens Medical Systems, Inc., Chicago, IL. Columbia University, Syntermed, Inc., and one of the authors (KN) stand to benefit from the sale of the software discussed in this paper.

REFERENCES

1. Bartlett ML, Srinivasan G, Barker WC, Kitsiou AN, Dilsizian V, Bacharach SL. Left ventricular ejection fraction: Comparison of results from planar and SPECT gated blood pool studies. *J Nucl Med.* 1996;37:1795-1799.
2. Faber TL, Stokely EM, Templeton GH, Akers MS, Parkey RW, Corbett JR. Quantification of three-dimensional left ventricular segmental wall motion and volumes from gated tomographic radionuclide ventriculograms. *J Nucl Med.* 1989;30:638-649.
3. Chin BB, Bloomgarden DC, Xia W, et al. Right and left ventricular volume and ejection fraction by tomographic gated blood-pool scintigraphy. *J Nucl Med.* 1997;38:942-948.
4. Van Krieking SD, Berman DS, Germano G. Automatic quantification of left ventricular ejection fraction from gated blood pool SPECT. *J Nucl Cardiol.* 1999;6:498-506.
5. Mariano-Goulart D, Piot C, Boudousq V, et al. Routine measurements of left and right ventricular output by gated blood pool emission tomography in comparison with thermodilution measurements: a preliminary study. *Eur J Nucl Med.* 2001;28:506-513.
6. Vanhove C, Franken PR, Defrise M, Momen A, Everaert H, Bossuyt A. Automatic determination of left ventricular ejection fraction from gated blood-pool tomography. *J Nucl Med.* 2001;42:401-407
7. Nichols K, Saouaf R, Ababneh AA, et al. Validation of SPECT equilibrium radionuclide angiographic right ventricular parameters by cardiac MRI. *J Nucl Card.* 2002;9:153-160.
8. Di Salvo TG, Mathier M, Semigran MJ, Dec GW. Preserved right ventricular ejection fraction predicts exercise capacity and survival in advanced heart failure. *J Am Coll Cardiol.* 1995;25:1143-1153.
9. De Groote P, Millaire A, Foucher-Hossein C, et al. Right ventricular ejection fraction is an independent predictor of survival in patients with moderate heart failure. *J Am Coll Cardiol.* 1998;32:948-954.

10. Nichols K, DePuey EG, Rozanski A. Automation of gated tomographic left ventricular ejection fraction. *J Nucl Card*. 1996;3:475-482.
11. Nichols K, Saouaf R, Bergmann SR. A Comparison of models for right ventricular parameters computed from gated blood pool SPECT data [abstract]. *J Nucl Card* 2001;8:S130.
12. De Bondt P, Vandenberghe S, De Mey S, et al. Validation of planar and tomographic radionuclide ventriculography by a dynamic ventricular phantom. *Nuc Med Comm*. In press.
13. King MA, Long DT, Brill AB. SPECT volume quantitation: influence of spatial resolution, source size and shape, and voxel size. *Med Phys*. 1991;18:1016-1024.
14. Hoffman EJ, Huang SC, Phelps ME. Quantitation in positron emission computed tomography: I. Effects of object size. *J Comput Assist Tomogr*. 1979;5:391-400.
15. Galt JR, Garcia EV, Robbins WL. Effects of myocardial wall thickness of SPECT quantification. *IEEE Trans Med Imaging*. 1990;9:144-150.

CHAPTER 5:

ACCURACY OF FOUR DIFFERENT ALGORITHMS FOR THE ANALYSIS OF TOMOGRAPHIC RADIONUCLIDE VENTRICULOGRAPHY USING A PHYSICAL DYNAMIC FOUR-CHAMBER CARDIAC PHANTOM

Pieter De Bondt ^{1,2}; Tom Claessens³; Bart Rys³; Olivier De Winter¹; Stijn Vandenberghe³; Patrick Segers³; Pascal Verdonck³ and Rudi Andre Dierckx¹

¹ Division of Nuclear Medicine, Ghent University Hospital, De Pintelaan 185, 9000 Ghent, Belgium

² Division of Nuclear Medicine, OLV Hospital, Moorselbaan 164, 9300 Aalst, Belgium

³ Hydraulics Laboratory, Ghent University, Sint-Pietersnieuwstraat 41, Gent, Belgium

J Nucl Med. 2005 Jan;46(1):165-71.

SUMMARY

Different automatic algorithms are now being developed to calculate left (LV) and right (RV) ventricular ejection fraction (EF) from tomographic radionuclide ventriculography (TRV). Four of these algorithms were tested on their performance in estimating LV and RV volume and EF using a dynamic four-chamber cardiac phantom. Methods: We developed a realistic physical dynamic four-chamber cardiac phantom and performed 25 TRV acquisitions within a wide range of end-diastolic (EDV), end-systolic (ESV) and stroke volumes. Four different algorithms (QBS, QUBE, 4DM-SPECT and BP-SPECT) were tested on their assessment to calculate left (LVV) and right ventricular volumes (RVV) and EF's. Results: For the LV, the correlations between reference and estimated volumes (0.93; 0.93; 0.96 and 0.93 respectively; all $P < 0.001$) and EF's (0.90; 0.93; 0.88 and 0.92; all $P < 0.001$) were good, although an underestimation for the volumes was seen for all algorithms (mean difference \pm 2SD from Bland-Altman analysis -39.83 ± 43.12 ; -33.39 ± 38.12 ; -33.29 ± 40.70 and -16.61 ± 39.64 mL respectively). QBS, QUBE, 4DM-SPECT showed also a growing underestimation for higher volumes. QBS, QUBE, and BP-SPECT could also be tested for the RV. Correlations were good for the volumes (0.93; 0.95 and 0.97; all $P < 0.001$). In terms of absolute volume estimation, mean difference \pm 2SD from Bland-Altman analysis was -41.28 ± 43.66 ; 11.13 ± 49.26 and -13.11 ± 28.20 mL. Calculation of RVEF correlated well with true values (0.84; 0.92 and 0.94; all $P < 0.001$), although an overestimation was seen for higher EF. Conclusion: TRV based calculation of LVEF and RVEF is accurate for all tested algorithms. All algorithms show an underestimation for the calculation of LVV, calculation of RVV seems more difficult with different results for each algorithm. The more irregular shape and inclusion of a relative hypokinetic right ventricular outflow tract in the right ventricle seems to be the cause that delineation of the right ventricle is more difficult, compared to the left side.

INTRODUCTION

The accurate estimation of right ventricular ejection fraction (RVEF) has been challenging for years. In nuclear medicine, different isotopes and injection techniques have been extensively studied [1-6]. The "first-pass technique" of a radioactive bolus

through the right heart circulation was often used but became unpopular because its success grossly depends on a perfect bolus injection, introducing operator dependency and limiting the application to experienced people. Planar radionuclide ventriculography (PRV) for the calculation of RVEF was not optimal because of the important overlap of atrial with ventricular activity with the camera in the left anterior oblique position. Tomographic radionuclide ventriculography (TRV) seems to overcome this problem by offering a three-dimensional image of the vascular structures of the heart. Initially, software was developed based on manual or semi-automatic contour detection [4;7] but these procedures were time-consuming, still needed experienced people to process the images and brought uncertainties about reproducibility. It has become clear that a good algorithm has to be accurate, automatic and fast. Nowadays, new automatic algorithms, like “QBS” [8], “QUBE” [9], “4D-MSPECT” [10] have become available. The validation of these programs is limited to a comparison of LVEF from PRV with LVEF from TRV. To our knowledge, validation studies for the calculation of left (LVV) and right ventricular volumes (RVV) and RVEF are lacking. There is only one program called “BP-SPECT” [11] with validation data for the right ventricle. The aim of this study was therefore to test these four algorithms, using a physical dynamic four-chamber cardiac phantom.

MATERIALS AND METHODS

Phantom Description

Our realistic cardiac phantom includes 2 ventricles and 2 atria (Figure. 1). The chamber walls are about 2 mm thick and are made of a silicone-elastomer (Wilsor Kunstharsen, Biddinghuizen, The Netherlands). The atrioventricular valve plane, however, is made of a membrane of 1-2 mm thick. Both ventricles are filled and emptied through the outflow tracts respectively. The atria are filled through tubes, connected at the base of the model. The atrioventricular valve plane itself is hung up in a PVC ring, which allows the cardiac model to move during the contraction in the long axis direction. The interventricular septum is constructed from a 15 mm thick synthetic spongy material. Both ventricles are covered with an external membrane, which makes it possible to achieve a septal thickening during end-systole. As the right ventricular outflow tract is relatively hypokinetic, it has been modelled with a stiff

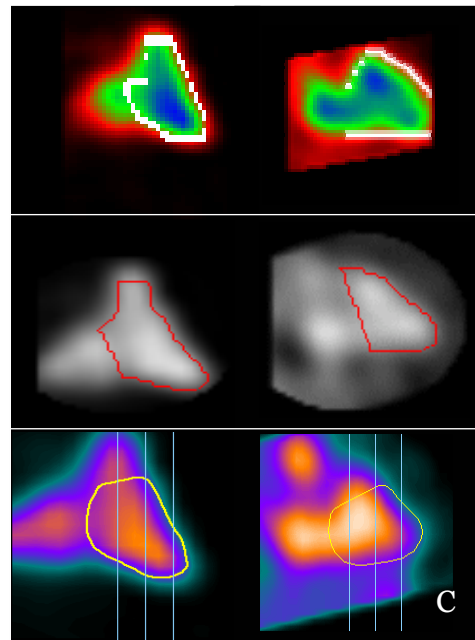
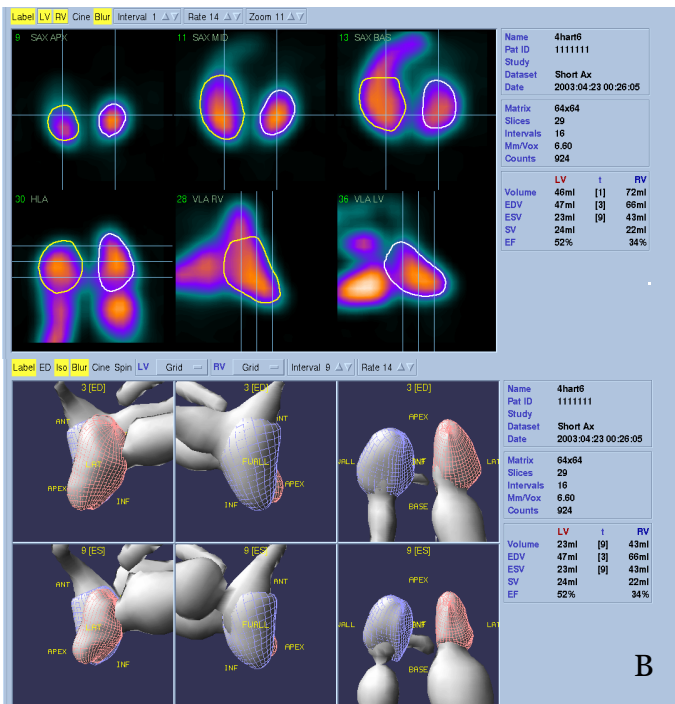
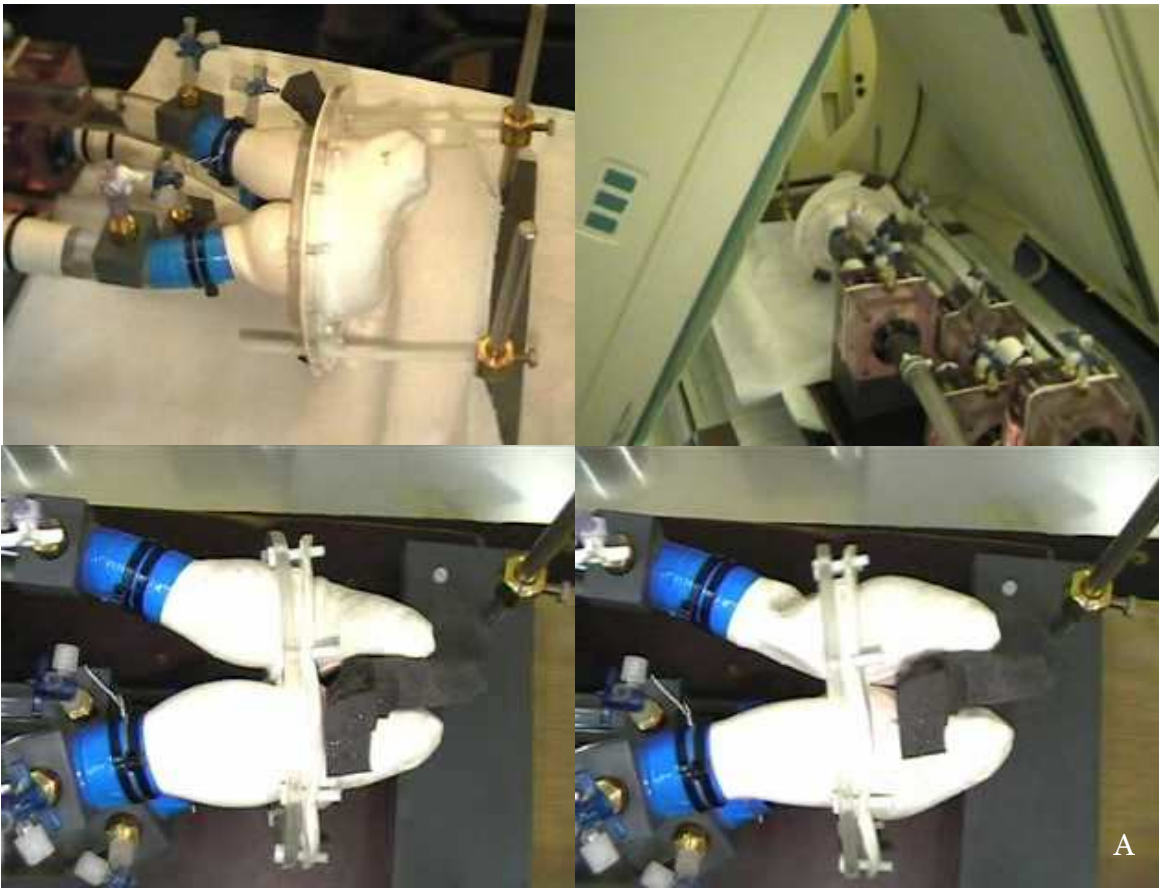


Figure 1

- A.** (top right) Four-chamber cardiac phantom
 (top left) Overview of the cardiac model, during the image acquisition
 (bottom left) End-systolic image (ventricles uncovered)
 (bottom right) End-diastolic image (ventricles uncovered)
- B.** At top are images of cardiac phantom, processed with QBS: horizontal long axis slice (down left), short axis slice (upper row) and vertical long axis slice (down right)
 At bottom are the 3D images of the cardiac phantom, processed with QBS: end-diastolic image (upper row) and end-systolic image (lower row) showing LV (red maze), RV (blue maze), atria and vascular structures (grey shaded)
- C.** Vertical long axis slice through the RV of the phantom after processing with BP-SPECT (top left), QUBE (middle left) and QBS (down left)
 Comparison with vertical long axis slice through the RV of a patient after processing with BP-SPECT (top right), QUBE (middle right) and QBS (down right)

PVC tube. The outflow tract of the RV is responsible for only 15% of the RV stroke volume [12] and it has also been shown that the amplitude of the right ventricular outflow tract on images of tomographic radionuclide angiography is very low [13], this was in a population of patients suffering from Wolff Parkinson White syndrome, where a delay in phase is known in this region but not necessarily a decrease in amplitude.

Two separate double acting piston pumps are connected to the cardiac phantom by means of reinforced perspex pipes and are used to supply the chamber with water and thereby simulating filling and emptying of the chambers. The ejection of both pumps supplied both ventricles, while the suctioning at the other side of the pistons in the pumps was used to empty both atria. In this way, during the opposite movement both ventricles were emptied and atria were filled, resulting in all four cardiac chambers having the same stroke volume. This stroke volume was easily adjustable, by changing the length of the piston (range 25.74 – 73.99 mL). An activity of 74 MBq/L (2 mCi/L) of ^{99m}Tc in water was used in the chambers, with no background activity. Volume variation in the phantom was sinusoidal.

To set the reference end-systolic volumes in each of the 4 chambers, the pistons were moved to their end-systolic positions. After that, the chamber was emptied and the predefined end-systolic volume was added through a tap on the connecting tubes between the phantom and the pumps. The ranges of volumes and ejection fractions used in this experiment were for LVEDV 51-196 mL, for LVESV 17-162 mL, for LVEF

17-70%, for RVEDV 60-209 mL, for RVESV 26-175 mL and for RVEF 16-70%.

Data Acquisition

Twenty-five experiments were performed. TRV data were acquired using a three-headed gamma camera (IRIX, Marconi-Phillips, Cleveland, Ohio) with low energy high-resolution collimators. Parameters of acquisition were as follows: 360° step-and-shoot rotation, 40 stops per head, 30 seconds per stop, 64 x 64 matrix, zoom 1.422 (pixel size 6.5 mm), and 16 time bins per R-R interval, the latter being fixed on 60 beats/min. An R-wave simulator synchronized with the pistons supplied R-wave triggers. Projection data were pre-filtered using a Butterworth filter (cutoff frequency: 0.5 cycles/cm; order: 5) and reconstructed by filtered backprojection using a ramp filter. Data were then reoriented into gated short axis tomograms. The resulting gated short axis data sets were then used as input for the four algorithms.

Processing

“QBS” [8] (Figure 1B)

This method is primarily a gradient-based method. A deformable ellipsoid is used to approximate the LV endocardium, followed by a sampling (not further clarified) to compute the endocardial surface for each gating interval. This sampling is used to generate a second surface to represent the RV endocardium. A correction is performed to locate the pulmonary valve. Separation of the RV from the pulmonary artery is achieved by truncating the RV surface with a plane. It is, however, not clear how this plane is being positioned during reconstruction.

“QUBE” [9]

The left ventricular cavity at end-diastole is delineated by segmentation using an iterative threshold technique. An optimal threshold is reached when the corresponding isocontour best fits the first derivative of the end-diastolic count distribution. This optimal threshold is then applied to delineate the left ventricular cavity on the other time bins. Left ventricular volumes are determined using a geometry-based method and are used to calculate the ejection fraction.

“4D-MSPECT” [10]

4D-MSPECT utilizes gradient and segmentation operators in conjunction with phase analysis to track the surface contours of the left ventricle through the cardiac cycle.

4D-MSPECT calculates only LVEF and LVV. Calculation of RV parameters is not yet available. There is up to now only one abstract available about the use of 4D-MSPECT in TRV.

“BP-SPECT” [11]

BP-SPECT is based on the use of threshold from % of maximum count in each cavity. After maximum activity in the RV is located, the algorithm automatically defines ventricular regions as those pixels with counts > 35% threshold of maximum ED counts over the entire cardiac volume. Bi-ventricular EF's are computed from systolic count changes within voxels inside identified ED and ES ventricular surfaces. All calculations are count-based, not geometric. For analyzing the right ventricle, the pulmonary valve plane is defined as high as necessary to include all structures for which counts are detected by the algorithms to increase in synchrony with LV count increases.

Statistical Analysis

χ^2 analysis was used to test whether data were normally distributed. Results were reported as mean values \pm 1 standard deviation (SD). Correlations between calculated and true (measured) values were expressed as the Pearson coefficient. Variability about the regression line was expressed as the standard error of the estimate (SEE). Bland-Altman analysis of differences between pairs of estimated and reference values was used to search for trends and systematic errors. Statistical significance was defined as $p < 0.05$.

RESULTS

Calculation Of Volumes

All values of both calculated and real EF and volume values were normally distributed. Correlation coefficients between the calculated and real volumes of the LV for QBS, QUBE, 4D-MSPECT and BP-SPECT were 0.93; 0.93; 0.96 and 0.93 respectively, all $P < 0.001$. (Figure 2).

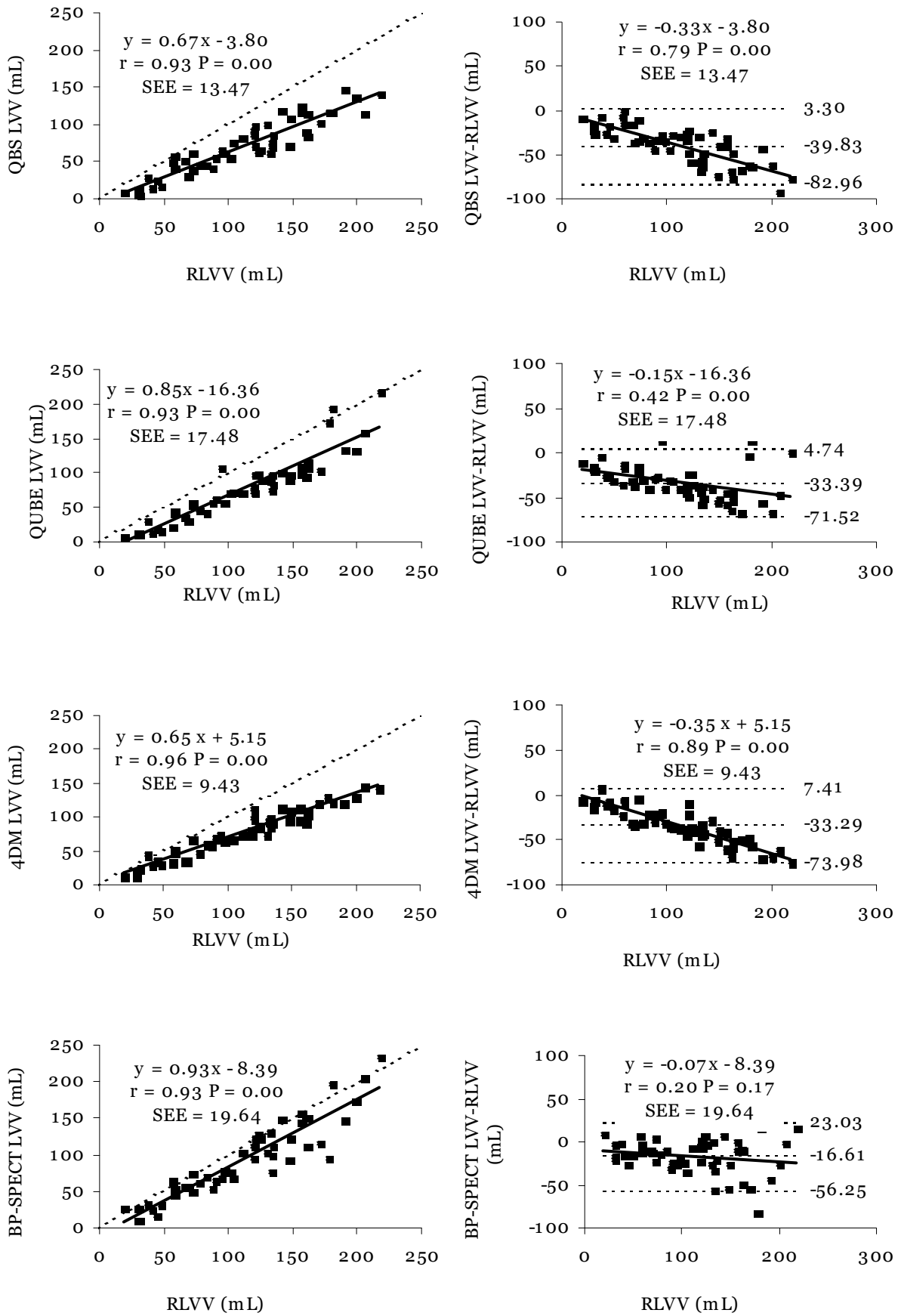


Figure 2 Linear regression and Bland-Altman analysis of left ventricular volume calculation (EDV and ESV) for the four methods (QBS, QUBE, 4DM and BP-SPECT)

There was a global underestimation for the calculated volumes (mean difference \pm 2SD: -39.83 ± 43.12 ; -33.39 ± 38.12 ; -33.29 ± 40.70 and -16.61 ± 39.64 mL respectively).and this underestimation was growing for higher volumes (slope of the regression line in the Bland-Altman was significantly different from zero for QBS, QUBE and 4D-MSPECT). QBS, QUBE, and BP-SPECT were also used to calculate RVV (Figure 3).

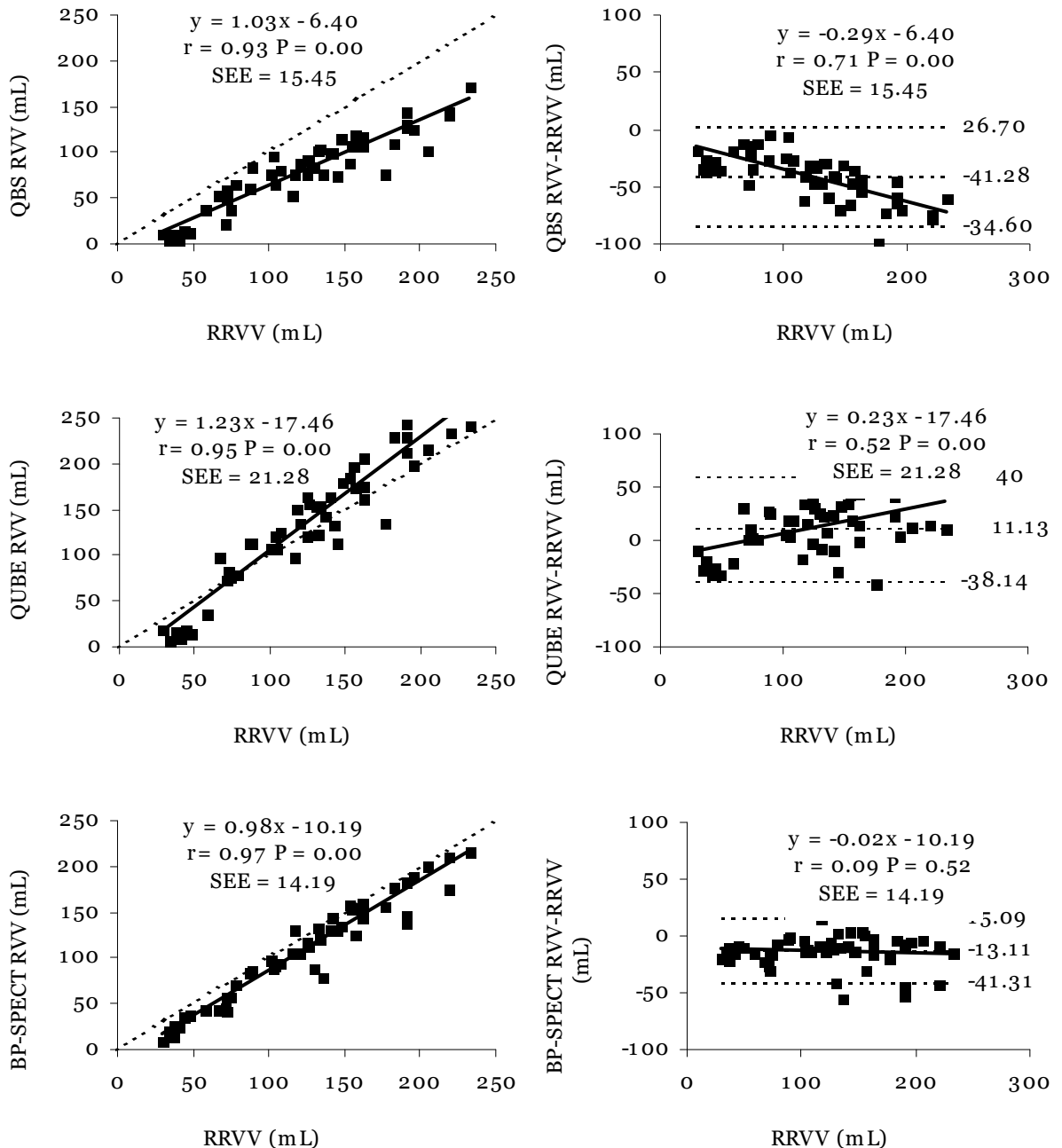


Figure 3 Linear regression and Bland-Altman analysis of right ventricular volume calculation (EDV and ESV) for the three methods (QBS, QUBE and BP-SPECT)

Correlation coefficients between reference and estimated RVV were within the same range as for the LV (0.93; 0.95 and 0.97 respectively; all $P < 0.001$). QBS and BP-SPECT showed a significant underestimation of RVV (mean difference \pm 2SD: -41.28 ± 43.66 and -13.11 ± 28.20 mL respectively), whereas QUBE showed a significant overestimation (mean difference \pm 2SD: 11.13 ± 49.26 mL respectively). The underestimation of RVV in QBS and the overestimation of RVV in QUBE increased with increasing EF.

Calculation Of Ejection Fractions

The correlation between the calculated and reference LVEF for the four programs was very acceptable (0.90; 0.93; 0.88 and 0.92 respectively; all $P < 0.001$) (Figure 4).

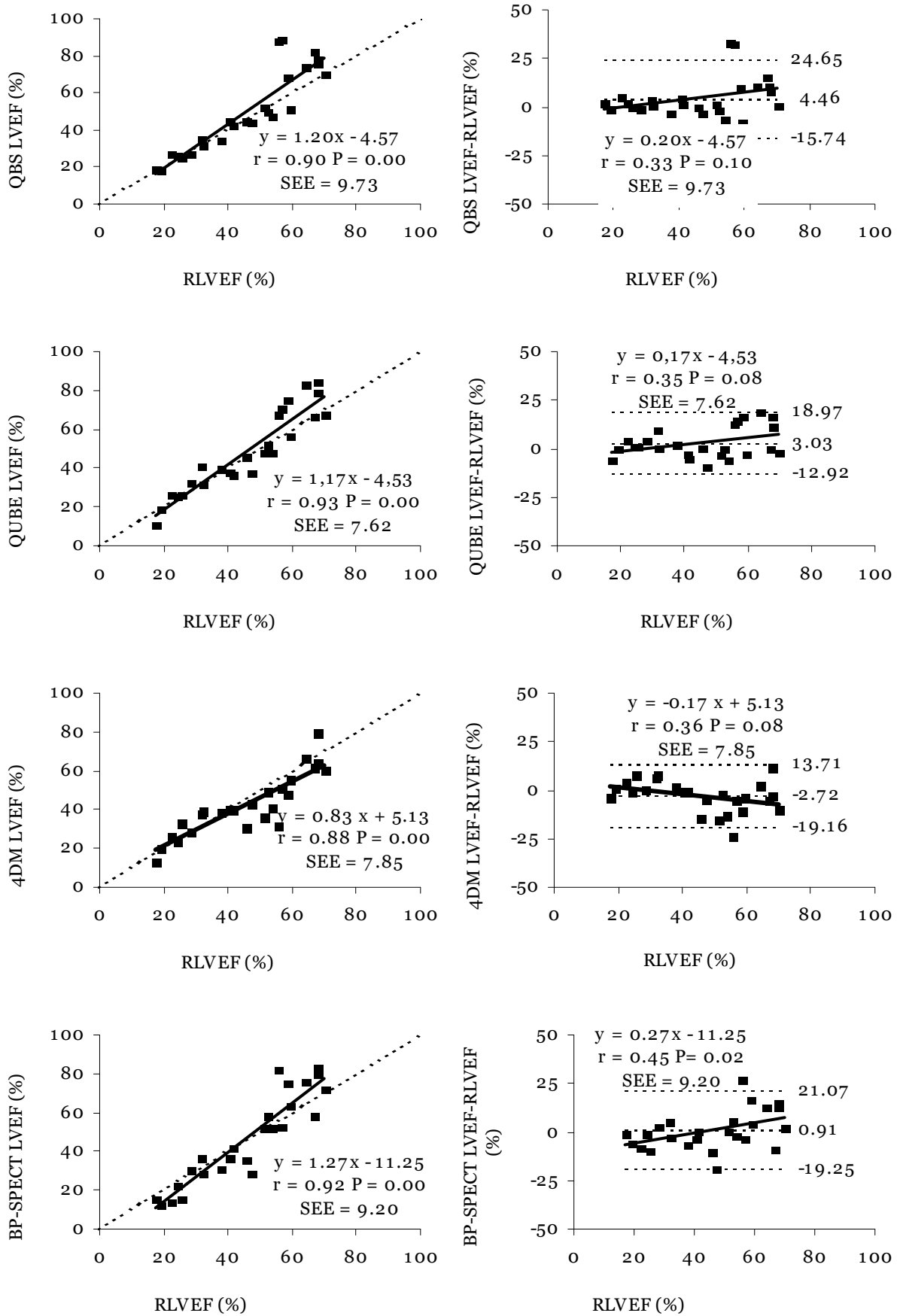


Figure 4 Linear regression and Bland-Altman analysis of left ventricular ejection fraction calculation for the four methods (QBS, QUBE, 4DM and BP-SPECT)

Mean differences \pm 2SD were 4.46 ± 20.19 ; 3.03 ± 15.94 ; -2.72 ± 16.44 and 0.91 ± 20.16 % respectively and only the BP-SPECT program showed a significant trend to overestimate the LVEF with increasing EF. For RVEF good correlations were seen for QUBE and BP-SPECT (0.92 and 0.94 respectively; all $P < 0.001$) with a slightly lower correlation coefficient for QBS (0.84; $P < 0.001$) (Figure 5).

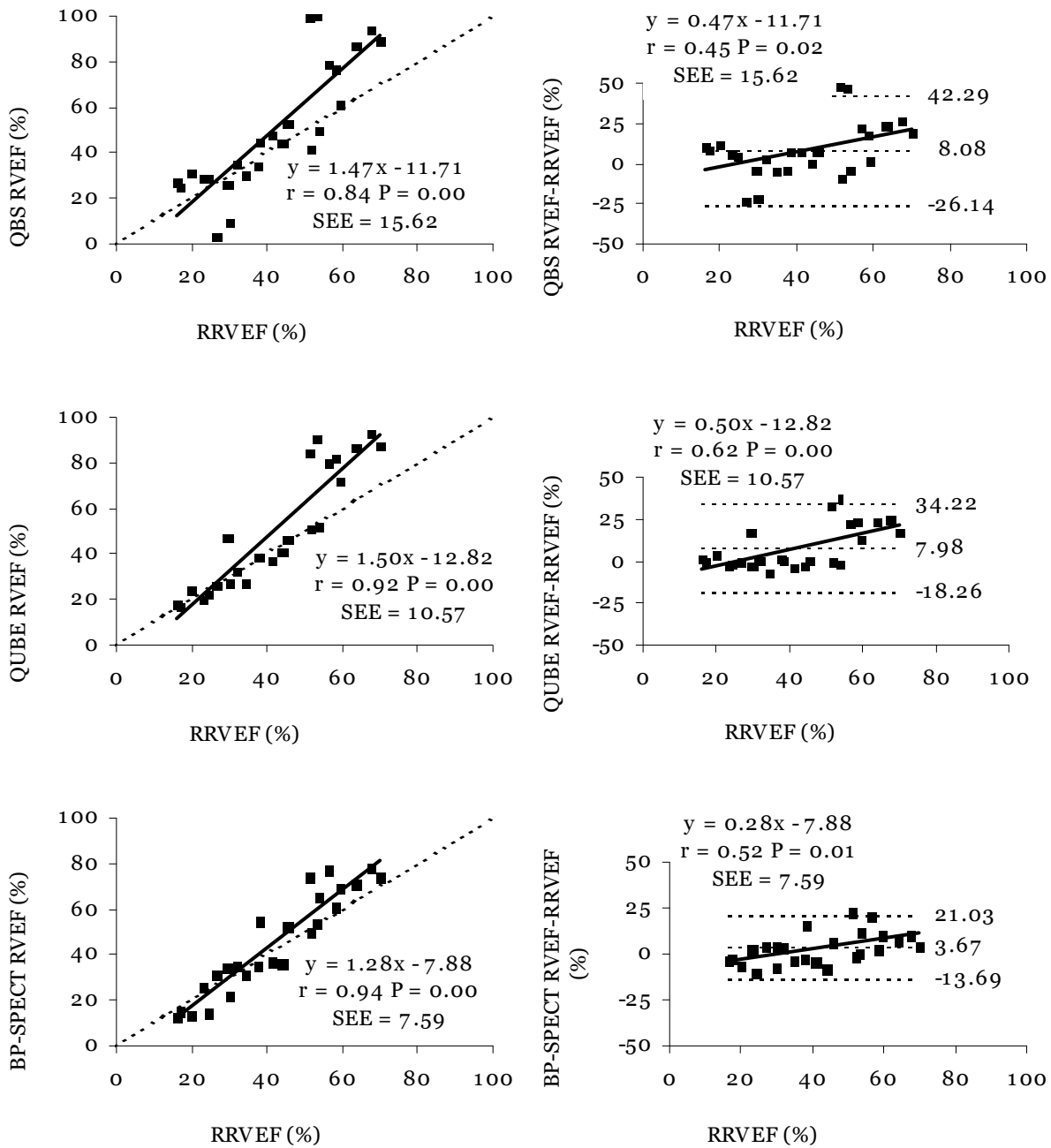


Figure 5 Linear regression and Bland-Altman analysis of right ventricular ejection fraction calculation for the three methods (QBS, QUBE and BP-SPECT)

QBS, QUBE and BP-SPECT overestimated RVEF (mean difference \pm 2SD: 8.08 ± 34.20 ; 7.98 ± 26.24 and 3.67 ± 17.36 %, respectively) and this overestimation increased with increasing EF for all three methods.

DISCUSSION

We have demonstrated that QBS, QUBE, 4D-MSPECT and BP-SPECT provide accurate calculations of left and right ventricular EF. For the LV volume calculation, all algorithms underestimated volumes, an observation for which we have no clear answer. A partial inclusion of atrial activity in the ventricular region could be an explanation, but this was not visually confirmed. On the contrary, we previously reported an overestimation of LV volume with BP-SPECT, calculating the LV volumes in a biventricular cardiac model [14]. In this model, however, the LV consisted of double concentric walls (inner and outer walls), mimicking the LV myocardium. For the measurement of the exact volume of the LV, the inner wall was suctioned through the entrance at the atrioventricular border, and this was not an ideal situation since the outer wall together with the inner one moved inside during this operation (space between the walls was kept constant) and no visual check could be made whether the LV was perfectly emptied. It is our experience, that this four-chamber model, provided with single ventricular walls and an improved pump experimental setup, causes fewer deviations in correct volume measurements. It is also our experience that making phantom models to measure absolute parameters (eg. volumes) is far more difficult than constructing phantoms to measure relative parameters (eg. EF). All four algorithms were developed to calculate volumes in human organs, taking into account the influence of attenuation and scatter of nearby structures. In this paper, as in the previous report, no background activity was used, no scatter and attenuation correction was performed and no thoracic phantom was used. Because we used an isolated heart phantom, the count threshold differed to that used in human examinations [14].

The potential added value of TRV over other routine cardiac imaging modalities is the accurate measurement of RVV and RVEF in a fast and simple way. The gold standard for these calculations is nowadays magnetic resonance imaging (MRI). Nevertheless, the MRI procedure and calculations are still time-consuming, operator-dependent and don't take into account the numerous trabeculae, which turn the endocardium of the RV into a very irregular surface. Unfortunately, our 4-chamber phantom contains

ferromagnetic material, and could not be tested in the MRI setting. An additional problem of calculating correct RV volumes with TRV is the difficult delineation of the RV outflow tract. This relatively hypokinetic structure contains a part of the volume of the RV but does not really participate in its contraction. Furthermore, the exact localization of the pulmonary valve is far more difficult than the aortic valve.

There is little literature on the validation of TRV for the calculation of RVV and RVEF. To our knowledge, of the four tested algorithms, validation studies have been done only for BP-SPECT [11]. Correlation values between MRI and BP-SPECT RVV and RVEF calculations were comparable to our results, and the underestimation of RVV found in our experiments were consistent with their results.

Our results indicate that, compared to QUBE and BP-SPECT, QBS yields slightly lower correlation coefficient for the calculation of RVEF and underestimates RVV. We believe that this is due to the fact that QBS locates the end of the outflow tract of the right ventricle more towards the apex of the RV (Figure. 1C). For QUBE and BP-SPECT, which yielded more accurate RVV calculations, a larger RVV is delineated including distal parts in the RV outflow tract. Therefore, we paid special attention in our model to manufacture the distal part of the RV outflow tract from non-compliant PVC tubes, in order to test if the software was able to find the exact border of the RV.

BP-SPECT is the only algorithm without a significant trend for its volume calculations, for LV as well as RV. The trend seen in the other algorithms is not only significant, but play a major role in dilated hearts. As cardiac volume measurements are important diagnostic and prognostic tools in the workup of cardiovascular disease, BP-SPECT is the method of choice, when reporting TRV with volume calculations.

CONCLUSION

We have shown, using a dynamic 4-chamber phantom model, that QBS, QUBE, 4D-MSPECT and BP-SPECT provide accurate estimates of RVEF and LVEF. When calculating RV volumes, the software codes need to take into account the relative hypokinetic RV outflow tract, which has to be included in the RVV. The more irregular shape and inclusion of a relative hypokinetic right ventricle outflow tract in the right ventricle seems to be the cause that delineation of the right ventricle is more difficult than the left ventricle.

Acknowledgements

We want to thank Edward Ficaró PhD, Assistant Research Scientist, University of Michigan Health System, Department of Radiology, Ann Arbor Medical Center, USA, for his kind cooperation to let us use his program (4D-MSPECT) and Philippe Briandet PhD, SEGAMI corporation, Columbia, USA, who made it possible to try the program QUBE. Special thanks to Ken Nichols PhD, Long Island Jewish Medical Center, Division of Nuclear Medicine, USA, who gave advice during the processing with BP-SPECT. Tom Claessens is funded by a specialization grant of the Institute for the Promotion of Innovation by Science and Technology in Flanders (IWT 021228)

REFERENCES

1. Franken PR, Delcourt E, Ham HR. Right ventricular ejection fraction: comparison of technetium-99m first pass technique and ECG-gated steady state krypton-81m angiocardigraphy. *Eur J Nucl Med.* 1986;12:365-368.
2. Gayed I, Boccalandro F, Fang B, Podoloff D. New method for calculating right ventricular ejection fraction using gated myocardial perfusion studies. *Clin Nucl Med.* 2002; 27:334-338.
3. Ham HR, Franken PR, Georges B, Delcourt E, Guillaume M, Piepsz A. Evaluation of the accuracy of steady-state krypton-81m method for calculating right ventricular ejection fraction. *J Nucl Med.* 1986; 27:593-601.
4. Mariano-Goulart D, Collet H, Kotzki PO, Zanca M, Rossi M. Semi-automatic segmentation of gated blood pool emission tomographic images by watersheds: application to the determination of right and left ejection fractions. *Eur J Nucl Med.* 1998;25:1300-1307.
5. Oliver RM, Fleming JS, Dawkins KD, Waller DG. Right ventricular function at rest and during submaximal exercise assessed by 81Krm equilibrium ventriculography in normal subjects. *Nucl Med Commun.* 1993;14:36-40.
6. Perings SM, Perings C, Kelm M, Strauer BE. Comparative evaluation of thermodilution and gated blood pool method for determination of right ventricular ejection fraction at rest and during exercise. *Cardiology.* 2001;95:161-163.
7. Groch MW, Marshall RC, Erwin WD, Schippers DJ, Barnett CA, Leidholdt EM, Jr. Quantitative gated blood pool SPECT for the assessment of coronary artery disease at rest. *J Nucl Cardiol.* 1998;5:567-573.
8. Van Krieking SD, Berman DS, Germano G. Automatic quantification of left ventricular ejection fraction from gated blood pool SPECT. *J Nucl Cardiol.* 1999;6:498-506.
9. Vanhove C, Franken PR, Defrise M, Momen A, Everaert H, Bossuyt A. Automatic determination of left ventricular ejection fraction from gated blood-pool tomography. *J Nucl Med.* 2001;42:401-407.

10. Ficaro EP, Quaife RF, Kritzman JN, Corbett JR. Validation of a New Fully Automatic Algorithm for Quantification of Gated Blood Pool SPECT: Correlations with Planar Gated Blood Pool and Perfusion SPECT. [abstract]. *J Nucl Med.* 2002;5:97P.
11. Nichols K, Saouaf R, Ababneh AA, Barst RJ, Rosenbaum MS, Groch MW et al. Validation of SPECT equilibrium radionuclide angiographic right ventricular parameters by cardiac magnetic resonance imaging. *J Nucl Cardiol.* 2002;9:153-160.
12. Geva T, Powell AJ, Crawford EC, Chung T, Colan SD. Evaluation of regional differences in right ventricular systolic function by acoustic quantification echocardiography and cine magnetic resonance imaging. *Circulation.* 1998;98:339-345.
13. Nakajima K, Bunko H, Tada A, Tonami N, Hisada K, Misaki T et al. Nuclear tomographic phase analysis: localization of accessory conduction pathway in patients with Wolff-Parkinson-White syndrome. *Am Heart J.* 1985;109:809-815.
14. De Bondt P, Nichols K, Vandenberghe S, et al. Validation of gated blood-pool SPECT cardiac measurements tested using a biventricular dynamic physical phantom. *J Nucl Med.* 2003;44:967-972.

Part 3: Gated Bloodpool SPECT, human experiments

CHAPTER 6:

**MODEL DEPENDENCE OF GATED BLOOD
POOL SPECT VENTRICULAR FUNCTION
MEASUREMENTS**

Kenneth Nichols¹, Naeem Humayun², Pieter De Bondt³, Stijn Vandenberghe⁴,
Olakunle O. Akinboboye⁵, Steven R. Bergmann²

¹ Division of Nuclear Medicine, Northwestern Memorial Hospital, Chicago, IL.

² Department of Cardiology, Columbia University, New York, NY.

³ Division of Nuclear Medicine, Ghent University Hospital, Ghent, Belgium

⁴ Hydraulics Laboratory, Ghent University, Ghent, Belgium

⁵ Division of Cardiology, St. Francis Hospital, Roslyn, NY

J Nucl Cardiol. 2004 May-Jun;11(3):282-92.

SUMMARY

Calculational differences between various gated blood pool SPECT (GBPS) algorithms may arise due to different modeling assumptions. Little information has been available yet regarding differences for right ventricular (RV) function calculations, for which GBPS may be uniquely well suited. Measurements of “QBS” (Cedars-Sinai Medical Center, Los Angeles, CA) and “BP-SPECT” (Columbia University, New York, NY) algorithms were evaluated. QBS and BP-SPECT left ventricular (LV) ejection fraction (EF) correlated strongly with conventional planar-GBP LV EF for 422 patients ($r=0.81$ versus $r=0.83$). QBS correlated significantly more strongly with BP-SPECT for LV EF than for RV EF ($r=0.80$ versus $r=0.41$). Both algorithms demonstrated significant gender differences for 31 normal subjects. BP-SPECT normal LV EF ($67\pm 9\%$) was significantly closer to the magnetic resonance imaging (MRI) literature ($68\pm 5\%$) than QBS ($58\pm 9\%$), but both algorithms underestimated normal RV EF ($52\pm 7\%$ and $50\pm 9\%$) compared to the MRI literature ($64\pm 9\%$). For 21 patients, QBS correlated similarly to MRI as BP-SPECT for LV EF ($r=0.80$ versus $r=0.85$), but RV EF correlation was significantly weaker ($r=0.47$ versus $r=0.81$). For 16 dynamic phantom simulations, QBS LV EF correlated similarly as BP-SPECT ($r=0.81$ versus $r=0.91$), but QBS RV EF correlation was significantly weaker ($r=0.62$ versus $r=0.82$). Volumes were lower by QBS than BP-SPECT for all data types. Both algorithms produced LV parameters that correlated strongly with all forms of image data, but all QBS RV relationships were significantly different from BP-SPECT RV relationships. Differences between the two algorithms were attributed to differences in their underlying ventricular modeling assumptions.

INTRODUCTION

Many imaging methods produce reliable left ventricular (LV) ejection fraction (EF) results, including x-ray contrast angiography, echocardiography, cardiac magnetic resonance imaging (MRI), planar gated blood pool (planar-GBP) imaging, and myocardial perfusion gated SPECT [29; 55]. Planar-GBP has long been considered the “gold standard” for LV EF, the extension of which to GBP-SPECT (GBPS) represents the next logical step, having the potential to provide complete regional LV EF and regional LV motion assessment [3-6], and a more direct means of measuring LV

volumes than by planar-GBP volume methods [7]. However, GBPS algorithms have become commercially available only recently [8,9], so that these approaches are only now beginning to be applied on a widespread basis. For any given imaging modality, dissimilar ventricular modeling assumptions can produce disparity in computed variables and in normal limits, as has been found in comparing different algorithms that analyze gated myocardial perfusion tomograms [1,2,10]. Therefore, it is timely to enquire whether different means of computing LV and right ventricular (RV) functional parameters from GBPS data yield different results.

Two distinctly different approaches have emerged for computing GBPS cardiac parameters, being primarily count-based methods [8,11,12], or primarily gradient-based methods [9].

Differences between separate models have been examined only recently, primarily for the left ventricle [11]. Modelling the right ventricle is considerably more difficult because of its eccentric shape even in normal individuals, yet GBPS may be uniquely well suited for analysis of RV size and function [5,12]. Little information has been available previously regarding comparisons among nuclear cardiology approaches to RV function computations [13,14]. Therefore the aim of this investigation was to evaluate relationships between calculations of two distinctly different GBPS approaches: QBS (Cedars-Sinai Medical Center, Los Angeles, Calif), based primarily on gradient searches [9], and BP-SPECT (Columbia University, New York, NY), based primarily on count thresholds [12]. The latter technique was designed specifically for RV analyses for patients with primary arterial hypertension (PAH) and tetralogy of Fallot (TOF), for whom right heart structures often are markedly abnormal. We sought to compare calculations of these methods, given the same common input of a wide spectrum of clinical and phantom data, and to determine whether observed differences could be understood on the basis of underlying assumptions of the two different approaches.

MATERIALS AND METHODS

Patient Population

Between 9/1/01 and 2/1/03, 486 patients (age = 52 ± 17 years, 61% male) were referred to Columbia University and St. Francis Medical Center for measurement of LV EF by conventional planar-GBP imaging. Of these, it was necessary to eliminate 64 studies for

technical reasons (given below), leaving 422 studies for subsequent analysis. Specifically, patients were referred for status evaluation following heart transplantation (28%), for congestive heart failure (27%), evaluation following the beginning of chemotherapy for cancer (26%), PAH (11%), benign hypertension (2%), cardiomyopathy (2%), or for “other” reasons (4%). GBPS data also were acquired for these same patients. All images and patient information collected at St. Francis Medical Center were transmitted to Columbia University for this investigation.

During that same time period, 31 patients (age = 54 ± 18 years, 58% male) also were evaluated by planar-GBP imaging and GBPS prior to beginning chemotherapy for cancer. None of the 31 patients in this group were among the 486 clinical cases described above. These patients had a low likelihood of coronary artery disease, and no history of cardiac disease. GBPS studies were analysed for these patients to provide a reasonable estimate of normal limits of RV and LV values for both GBPS algorithms, short of having data from normal volunteers. Height and weight information for these subjects were used to estimate body surface area for indexing of volume values, to permit comparisons to recent MRI literature of RV and LV functional parameters normal limits.

Planar-GBP Studies

Conventional planar-GBP was performed for all patients in the left anterior oblique projection that optimised septal separation of RV from LV counts. For adults, injected Tc-99m-pertechnetate activity was 925 MBq (25 mCi), following injection of 5 milligrams of pyrophosphate. For patients under 18 years of age whose body weight was less than 70 kg (n=24), these injections were scaled linearly downward for body weight. Clinical data were acquired at both institutions with the same commercially available gamma cameras (“Vertex,” ADAC Corporation, Milpitas, CA). As these were dual-detector gamma cameras, no caudal tilt was used in positioning patients for planar-GBP. A 20% energy window centered on 140 keV was used for data acquisition, with low energy general-purpose (LEGP) collimation. Images were acquired as 64x64 matrices at 3.0 mm/pixel, gated for 24 frames per R-R interval for 10 minutes.

Planar-GBP images were transmitted to a Pegasys computer system (Picker Corporation, Cleveland, OH), where processing was performed with commercially available software typical of processing used for planar-GBP data [16,17]. For LV EF assessment, observers drew initial LV outlines, primarily guided by their visual impression of the LV shape as seen at end-diastole (ED), aided by Fourier amplitude and phase maps [5]. For all time intervals of the complete planar-GBP study,

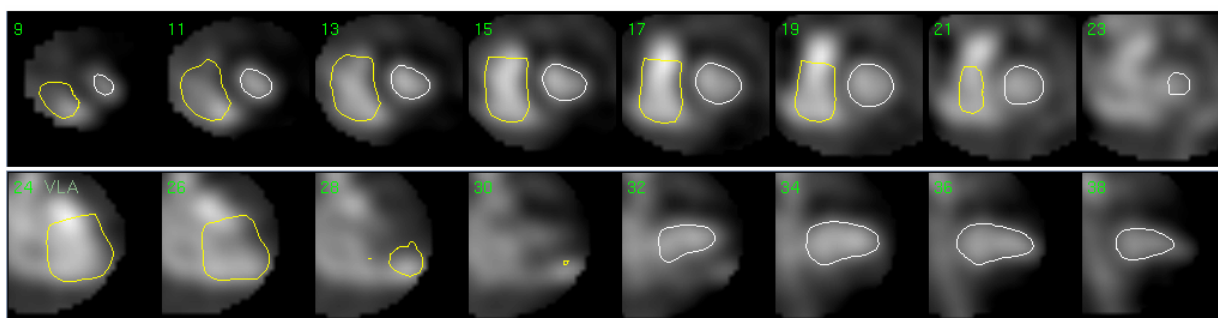


Figure 1

The RV and LV outlines generated by QBS algorithms are shown for a 45 year-old female patient with breast cancer evaluated following chemotherapy, for whom RV volumes were judged to be enlarged based on visual assessment of the GBPS images. The upper row displays end-diastolic short-axis tomographic sections from apex to base; the bottom row shows vertical long-axis sections from right posterior to left lateral walls. QBS calculations were: LV EF = 59%, LV EDV = 85 mL, LV ESV = 35mL; RV EF = 37%, RV EDV = 151 mL and RV ESV = 96 mL. Planar-GBP LVEF was 60%.

algorithms generated regions automatically based on the limiting ED region, which observers reviewed and modified as necessary. Planar-GBP algorithms have recently been shown to be highly accurate and reproducible, using dynamic physical phantom data [17].

GBPS Data Acquisition

Immediately following planar-GBP image collection, all patients then underwent gated blood pool SPECT. A dual detector gamma camera (“Vertex,” ADAC Corporation) was used to collect images at 64 projections over a 180° circular arc. 64x64 tomograms with a pixel size of 3.8 mm were acquired with LEGP collimators for 20 seconds per projection. Tomograms were acquired with patients at rest, at 8 frames per R-R interval, using a 100% R-wave window. The rationale for these data collection parameter choices was to guarantee collection of adequate tomographic count density per R-R interval, at the expense of limiting the spatial and temporal resolution of collected image data, as is done routinely in performing gated myocardial perfusion 3D quantitation.

All data sets from all sites were sent to Columbia University, where they were reviewed for any confounding imaging artifacts. Butterworth (cutoff = .45 of Nyquist frequency, power = 5.0) pre-filters were used for gated tomograms, followed by ramp filtering in

the transaxial plane. Images were reoriented into short axis sections using manual choices of approximate LV symmetry axes, using a commercially available computer system ("ICON," Siemens Medical Solutions, Inc., Chicago, IL).

QBS Methodology

The QBS approach was based primarily on gradient searches. An ellipsoidal coordinate system for the LV was found automatically and used to compute a static endocardial surface from relative counts and count density gradients. A dynamic endocardial surface was computed for each gating interval by way of temporal Fourier analysis of volumetric count density information. LV volumes were computed for each gating interval, with EF computed from end-diastolic and end-systolic volumes [9]. In this sense, QBS EF calculations were geometric, not count-based. It was observed that the pulmonary valve plane was defined in such a manner that it rarely extended more than 1-2 pixels above the anterior wall or below the inferior wall of the identified LV limits (see Figure 1).

There were 3 ways to run the Siemens Esoft implementation of QBS: (1) completely automatically, (2) semi-automatically, by first reselecting suggested mid-LV and mid-RV planes and reselecting apex-to-base heart limits, and (3) manually re-centering and re-sizing ellipses to define the LV as seen in mid-short axis and mid-horizontal long axis (HLA) planes to establish boundaries for searching for the LV (but not for the RV). All three methods were run for each data set, and measurements recorded for the one particular method for an individual data set for which observers perceived optimal agreement of computed outlines with their visual impression of both ventricles. The rationale for this experimental design was to emulate as realistically as possible the manner in which we believed QBS would actually be used in standard clinical practice, as it is inevitable that observers will use those regions that agree most closely with their visual impression of actual ventricular locations and limits. No means were provided by QBS to permit adjustments to outlines after the point at which computed outlines were displayed superimposed on tomographic sections (Figure 1).

BP-SPECT Methodology

BP-SPECT algorithms were based primarily on the use of % thresholds of maximum volumetric counts. Mid-ventricular locations were determined automatically by searching for maximum activity in likely RV locations in SA, HLA and vertical long-

axis (VLA) orientations. The algorithm automatically defined ventricular regions as corresponding to those contiguous regions that contained counts $\geq 35\%$ threshold of maximum ED counts over the entire cardiac volume. This particular 35% threshold value has been used by nuclear medicine investigators in defining endocardial and epicardial surfaces derived from myocardial perfusion images [18], and in methods applied to GBPS data [11]. ED volumes were computed from the number of voxels (i.e., 3D pixels) within these limits, while end-systolic (ES) volumes were computed by combining end-diastolic volume (EDV) with EF values. This convention had been found previously to yield the most accurate end-systolic volume (ESV) values [16]. Bi-ventricular EF's were computed from systolic count changes within voxels inside identified ED and ES ventricular surfaces. Thus, BP-SPECT EF calculations were count-based, not geometric. For analysing the right ventricle, the pulmonary valve plane was defined to extend as high as necessary to include all volumes for which counts were detected by the algorithms to increase in synchrony with LV count increases. No constraints were imposed on RV or LV stroke volumes. In cases in which automated algorithms failed to produce pulmonary valve planes sufficiently high by these criteria, users altered the included RV territories to reflect their visual perceptions.

There were three ways to influence the size and shape of regions used to segment ventricles: (1) re-selecting mid-chamber planes, (2) manually redrawing valve planes in mid-RV and mid-LV planes, or (3) editing ED and ES individual regions for any and all HLA slices, as deemed necessary (Figure 2).

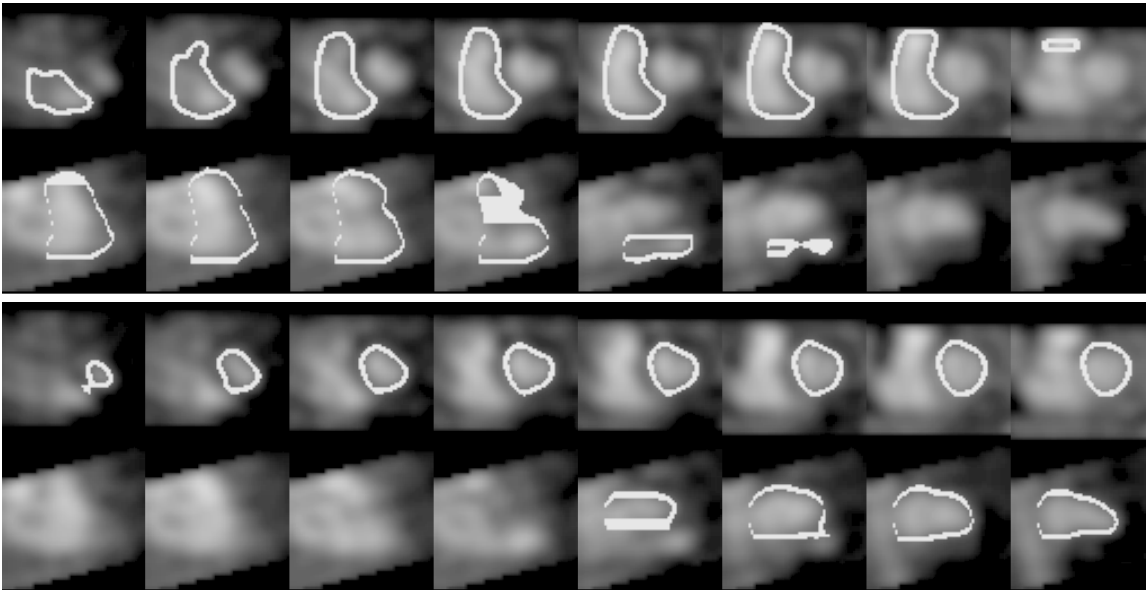


Figure 2

Ventricular outlines generated by BP-SPECT algorithms are shown for the same patient as in Figure 1, for the same tomographic sections. RV outlines are shown in the upper two rows and LV outlines in the lower 2 rows. BP-SPECT calculations were: LV EF = 64%, LV EDV = 123 mL, LV ESV = 44 mL; RV EF = 48%, RV EDV = 194 mL and RV ESV = 101 mL. Note that the RV outlines reach down further to the inferior wall and higher towards the pulmonary valve plane than do the QBS RV outlines.

This combination of software “tools” meant that it was always possible for observers to produce RV and LV outlines that agreed with their visual impression of actual ventricular edges.

Correlative MRI Studies

To date, there have been no published reports comparing QBS calculations to MRI data. To gain some insight as to absolute accuracy of the two algorithms when presented with the same input data, QBS algorithms also were applied to clinical GBPS images for 28 patients with PAH or TOF who also had correlative MRI evaluations, for which RV calculations of BP-SPECT algorithms have been previously reported [12]. None of the 28 patients in this group were among the 486 clinical cases described above.

Cardiac gated gradient-echo cine MRI evaluations were acquired using a 1.5 Tesla scanner using a “Spoiled Gradient Recall” non-breath-hold technique (TR Min TE 13,

FA 30, Matrix 256 x 128, FOV 30-41, NEX 1, Sl Thickness 8, gap 0) or a breath-hold technique (TR Min TE min full, FA 15, Matrix 256 x 128, FOV 30-41, NEX 1, Sl thickness 8, gap 0). 8-mm-thick tomographic sections were acquired for 16-20 intervals/R-R. Further details regarding the MRI acquisitions are provided in reference 12.

Dynamic Phantom Experiments

To date, there have been no published reports comparing QBS calculations to phantom data. To help understand the implications of methodological differences between the two algorithms, QBS algorithms also were run on bi-ventricular dynamic phantom data for 20 phantom simulations, for which results of BP-SPECT calculations have been reported previously [19]. For these phantom data, it was necessary to run the QBS algorithms by manually setting all regions and limits, as described above.

Statistical Analysis

All results are reported as mean values \pm 1 standard deviation. Differences among EF values are reported in absolute EF units, not as percentages of EF's. Paired t-tests were used to assess whether means of calculations were different between two methods. Unpaired t-tests were used to determine whether values found by the two GBPS algorithms for low likelihood subjects differed from those reported in the MRI literature. Linear regression analyses were used to compare calculations of ventricular volumes and EF's between QBS and BP-SPECT, to compute the standard error of the estimate (SEE) values indicative of the "spread" of values to be expected for each method given the results of the other, and in conjunction with Bland-Altman plots of differences versus means to search for trends and systematic errors. Statistical significance of differences between pairs of different regression analyses was assessed by the Fisher z-test. For all tests $p < 0.05$ was considered statistically significant.

RESULTS

Software Region Generation

For clinical data, 64 of 486 patients (13%) showed obvious evidence of serious ventricular tracking problems for QBS, regardless of the manner in which algorithms were run (see above). This was consistent with previously reported QBS automation

success rates of 70%-85% [9]. To permit a fair and realistic comparison between the two algorithms for clinical images the questionable cases were eliminated, leaving 422 clinical studies, thereby censoring studies in the same fashion used by previous investigator [9]. Reasons for censoring data due to QBS algorithm failure were: failure for unknown reasons to identify the LV (15% of discarded cases) or RV (18%) or both LV and RV (7%), pericardial effusion resulting in LV's at ES being obviously much too small (30%), misidentification of spleen, liver or aortal counts as ventricular counts (24%), and incorrect tracking of high background counts (6%).

For MRI correlative studies previously reported for BP-SPECT [12], QBS outlines were considered to be usable for 21 of 28 subjects with PAH or TOF, so that a comparable success rate of 75% was found in applying QBS to MRI data, as had been reported previously by other investigators for clinical data [9]. The major factor causing failure of QBS region generation was unusually large and/or unusually eccentric RV's, sometimes causing QBS to produce LV regions that intruded substantially into RV regions. Of 20 dynamic phantoms for which BP-SPECT calculations previously were reported [19], QBS algorithms were able to process 16 data sets, yielding a success rate of QBS algorithms of 75%, again similar to success rates reported by previous investigators [9].

Clinical Data

Linear regression least-squares fitted curves comparing QBS against BP-SPECT values are shown in Figures 3 and 4.

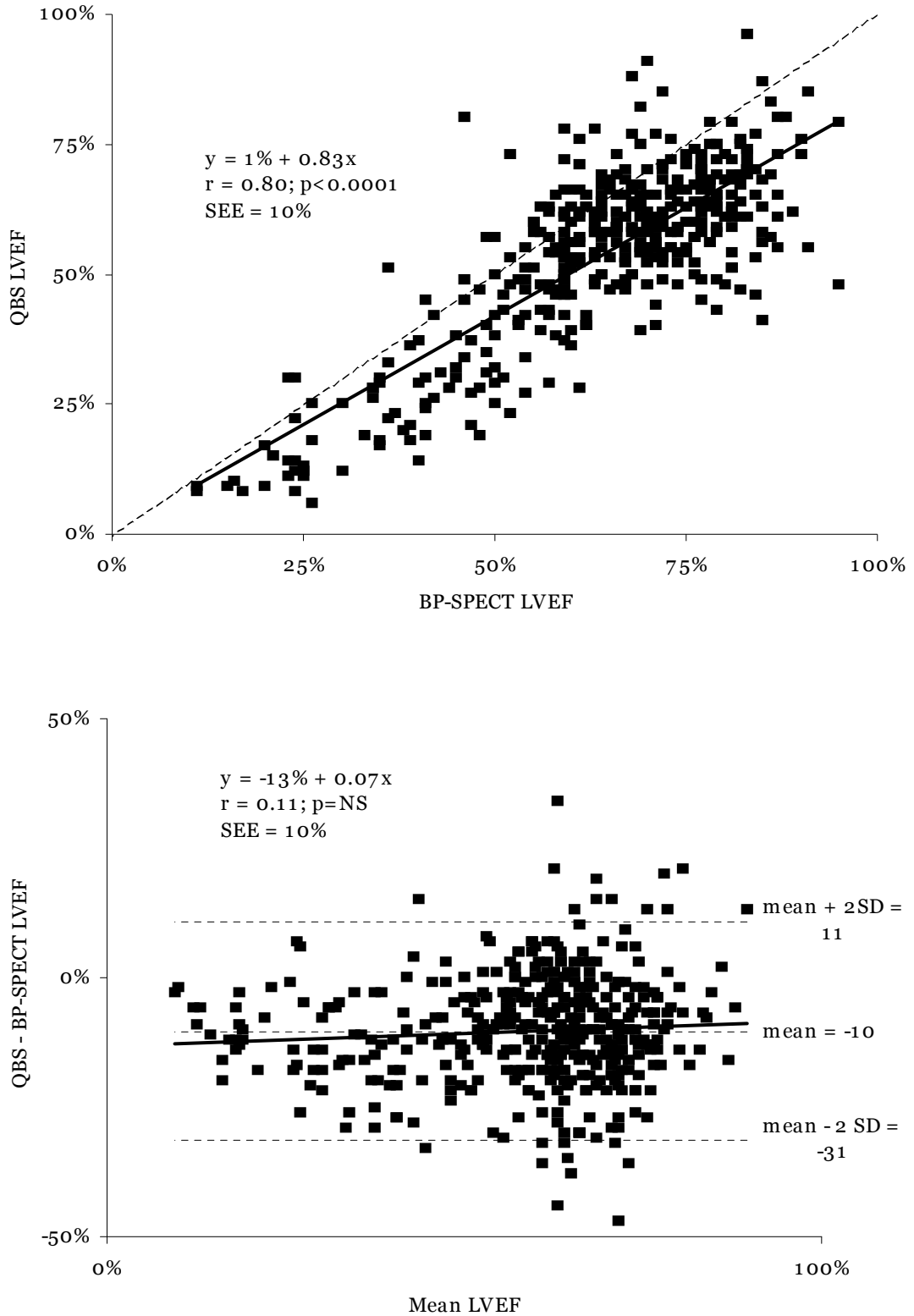


Figure 3
 Linear regression curves for QBS versus BP-SPECT left ventricular (LV) ejection fraction (EF) (top), and Bland-Altman curves of differences versus means of LV EF for both methods (bottom).

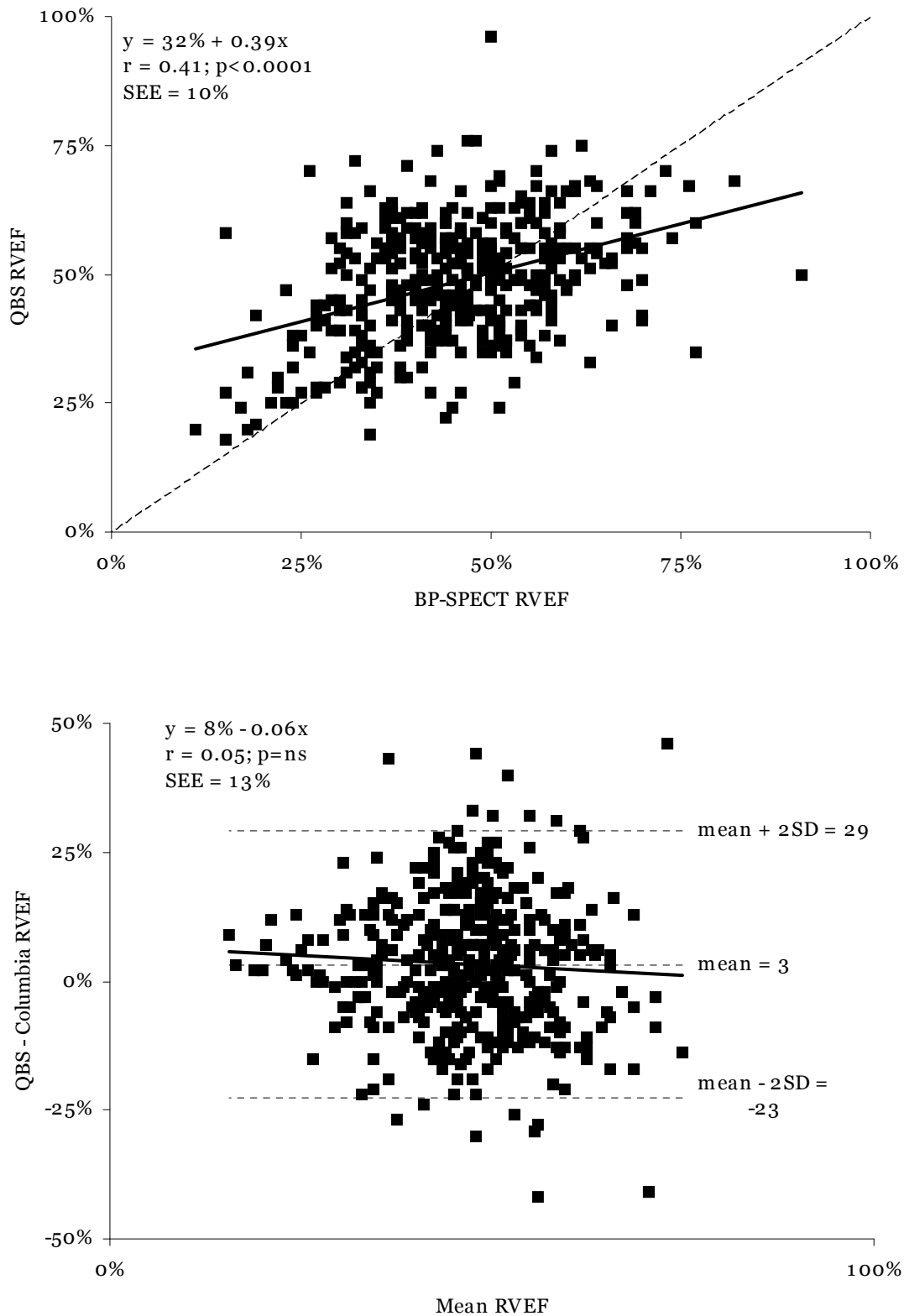


Figure 4

Linear regression curves for QBS versus BP-SPECT right ventricular (RV) ejection fraction (EF) (top), and Bland-Altman curves of differences versus means of RV EF for both methods (bottom).

Linear regression least squares fitted curves comparing QBS against BP-SPECT values are shown in Figures 3 and 4. For these clinical data, all QBS parameters for both ventricles were significantly correlated with BPSPECT values, although correlation for each LV relationship was significantly stronger ($P = .05$) than for each corresponding RV relationship. QBS LVEDV values were significantly lower than BP-SPECT LVEDV values (regression analysis: $y = -13 \text{ mL} + 0.90x$, $r = 0.85$, $P < .0001$, $\text{SEE} = 33 \text{ mL}$; Bland-Altman analysis: $y = -31 \text{ mL} + 0.06x$, $r = 0.11$, $P = \text{not significant}$), but LVESVs were not different (regression analysis: $y = 1 \text{ mL} + 1.04x$, $r = 0.89$, $P < .0001$, $\text{SEE} = 26 \text{ mL}$; Bland-Altman analysis: $y = -6 \text{ mL} + 0.19x$, $r = 0.41$, $P < .0001$, $\text{SEE} = 24 \text{ mL}$), resulting in QBS LVEF being significantly lower by 11% than BP-SPECT LVEF values (Table 1).

	LV EDV	LV ESV	LV EF	RV EDV	RV ESV	RV EF
QBS	96±68 mL*	52±62 mL	53±17%*#	112±46 mL*	61±38 mL*	49±11%*
BP-SPECT	122±60 mL	49±51 mL	64±17%#	144±60 mL	78±47 mL	45±12%
Planar-GBP	-	-	59±14%	-	-	-

Table 1

Paired T-test results for clinical data for 422 patients.

* = $p < 0.05$ for QBS versus BP-SPECT

= $p < 0.05$ versus planar-GBP LV EF

Because 90% of LV ESV values were $< 100 \text{ mL}$, a sub-analysis was performed for LV ESV's $< 100 \text{ mL}$, demonstrating statistically significant but significantly weaker correlation ($r=0.65$; $y = 8 \text{ mL} + 0.81x$; $\text{SEE} = 19 \text{ mL}$) than $r=0.89$, probably due to a smaller range of ESV values.

For the right ventricle, linear regression analysis findings for QBS versus BP-SPECT EDV were as follows: $y = 31 \text{ mL} + 0.52x$, $r = 0.74$, $P < .0001$, $\text{SEE} = 30 \text{ mL}$; and for RVESV, findings were as follows: $y = 19 \text{ mL} + 0.49x$, $r = 0.66$, $P < .0001$, $\text{SEE} = 26 \text{ mL}$. Bland-Altman analyses demonstrated that QBS RV volumes had a strong tendency to underestimate BP-SPECT RV volumes, to a greater extent as mean volume increased (RVEDV: $y = 10 \text{ mL} - 0.39x$, $r = 0.46$, $P < .0001$, $\text{SEE} = 37 \text{ mL}$; RVESV: $y = -1 \text{ mL} + 0.25x$, $r = 0.27$, $P < .0001$, $\text{SEE} = 34 \text{ mL}$), the net result of which was to produce QBS RVEF values significantly higher by 5% than BP-SPECT values for this patient population (Table 1). QBS correlated significantly more strongly with BP-

SPECT values for LVEF ($r = 0.80$) (Figure 3) than for RVEF ($r = 0.41$) (Figure 4).

For the 422 clinical studies, both QBS and BP-SPECT correlated significantly with planar-GBP LV EF ($r=0.81$ versus $r=0.83$) (Figures 5 and 6),

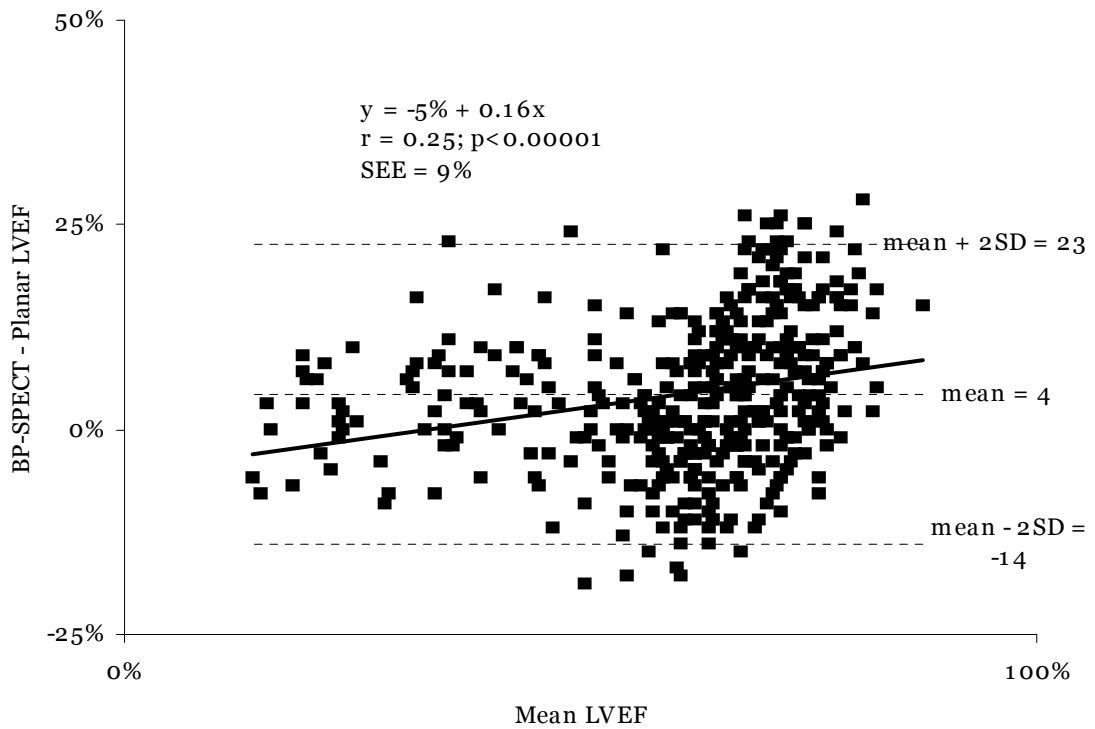
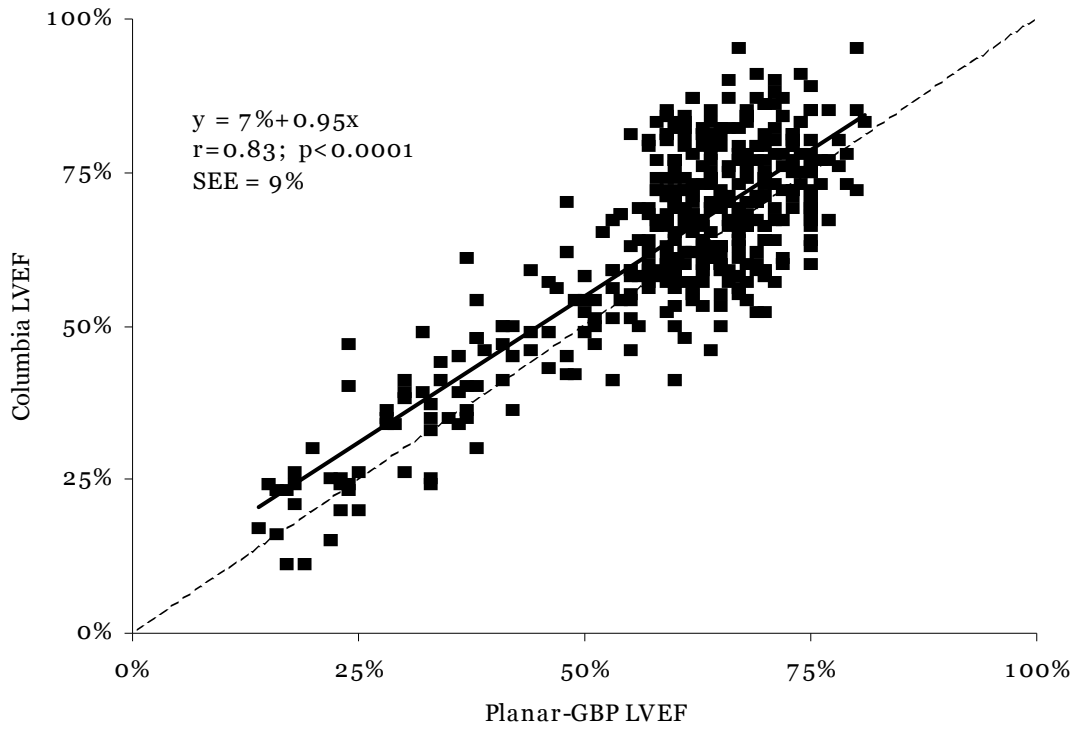


Figure 5

Linear regression curves for QBS versus conventional planar gated blood pool (GBP) LV EF (top), and Bland-Altman curves of differences versus means of LV EF for both methods (bottom).

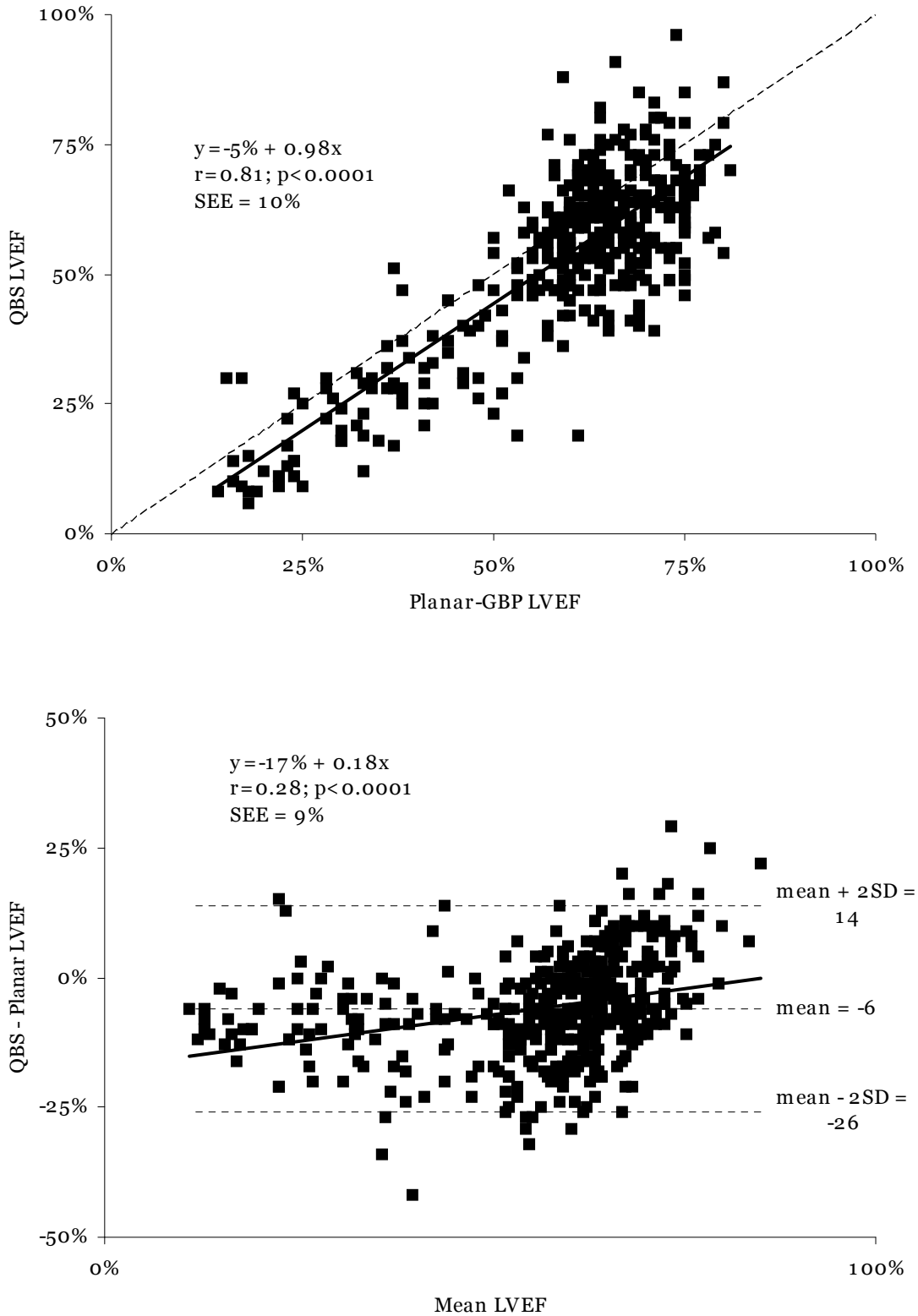


Figure 6

Linear regression curves for BP-SPECT versus conventional planar gated blood pool (GBP) LV EF (top), and Bland-Altman curves of differences versus means of LV EF for both methods (bottom).

with no difference in strengths of association. Mean QBS LV EF was significantly lower by 6% than mean planar-GBP LV EF ($59\pm 14\%$), and mean BP-SPECT LV EF was significantly higher by 5% than planar-GBP LV EF values (Table 1).

Low likelihood subjects

Overall, these same methodological trends and differences were reflected in values found for the 31 low likelihood subjects (Table 2),

	QBS All	BP-SPECT All	QBS Males	BP-SPECT Males	QBS Females	BP-SPECT Females
LVEDV	91 ± 35 mL*	117 ± 39 mL	106 ± 33 mL*	135 ± 35 mL	71 ± 28 mL*	92 ± 29 mL
LVESV	41 ± 22 mL	39 ± 25 mL	50 ± 21 mL	48 ± 28 mL	29 ± 18 mL	27 ± 12 mL
LVEF	$58\pm 9\%$ *	$67\pm 9\%$	$54\pm 10\%$ *	$66\pm 11\%$	$62\pm 10\%$ *	$71\pm 7\%$
RVEDV	109 ± 29 mL*	129 ± 29 mL	120 ± 28 mL*	136 ± 32 mL	93 ± 26 mL*	120 ± 23 mL
RVESV	55 ± 20 mL	61 ± 18 mL	64 ± 21 mL	66 ± 17 mL	44 ± 13 mL	53 ± 16 mL
RVEF	$50\pm 9\%$ *	$53\pm 8\%$	$48\pm 10\%$ *	$51\pm 6\%$	$53\pm 6\%$ *	$56\pm 9\%$

Table 2

Left ventricular functional parameters for subjects at low likelihood for coronary artery disease.

* = $p < 0.05$ for QBS versus BP-SPECT

with all QBS volume values significantly smaller than BP-SPECT volumes, and QBS LV EF values significantly lower by 9%. The only exception to the relationships observed between the two methods in the 422 clinical studies was that RV EF was not different, probably because RV EF values were predominantly between 40%-60% for these normal subjects, in which range the least RV EF differences between the two methods were observed (Figure 6). For both methods, all volume values were significantly larger, and EF values lower, for males than for females (Table 2), reflecting gender differences found previously in analysing myocardial perfusion gated SPECT data.”

Although all linear correlations between QBS and BP-SPECT measurements were statistically significant, they were significantly weaker for the 31 low likelihood patients than for the 422 clinical studies ($r = 0.61$, slope = 0.64; $r = 0.61$, slope = 0.55; and $r = 0.75$, slope = 0.67 for LV EF, EDV and ESV, respectively, and $r = 0.22$, slope = 0.25; $r = 0.73$, slope = 0.73; and $r = 0.62$, slope = 0.71 for RV EF, EDV and ESV). This was likely due to the considerably smaller sample size and much smaller ranges of

EF's and volume values being compared.

Functional parameters for the low likelihood subjects were compared to the most recent normal limits reported in the cardiac MRI literature.

	MRI literature	QBS	BP-SPECT
LV EDVi	72 mL/m ²	57 mL/m ² *#	75 mL/m ² #
LV ESVi	31 mL/m ²	32 mL/m ²	35 mL/m ²
LV EF	58%	40% *#	50%
RV EDVi	84 mL/m ²	60 mL/m ² *#	70 mL/m ² #
RV ESVi	41 mL/m ²	33 mL/m ²	36 mL/m ²
RV EF	46%	32% #	39% #

Table 3

Lower limits of ejection fraction and upper limits of volumes indexed to body surface area for subjects at low likelihood for coronary artery disease.

* = $p < 0.05$ for QBS versus BP-SPECT by paired t-test

= $p < 0.05$ versus MRI literature by unpaired t-test

The patients studied for our investigation were reasonably similar to those cited in this MRI literature, as those subjects (N=36; 50% males) were between the ages of 22-74 (mean age = 44 ± 16 years) and were composed of normotensive volunteers with no history of cardiac disease. BP-SPECT EDV values indexed to body surface area (45 ± 15 mL/m²) were significantly closer to the MRI literature (58 ± 12 mL/m²) than were QBS values (35 ± 11 mL/m²). Both QBS and BP-SPECT yielded EDV-indexed values lower than for MRI for the RV (42 ± 9 mL/m² and 50 ± 10 mL/m² versus 60 ± 12 mL/m²). However, both QBS and BP-SPECT produced similar ESV-indexed values as MRI for the LV (16 ± 8 mL/m² and 15 ± 10 mL/m² versus 19 ± 6 mL/m²) and for the RV (21 ± 6 mL/m² and 25 ± 6 mL/m² versus 23 ± 9 mL/m²). Consequently, BP-SPECT normal LV EF ($67 \pm 9\%$) was significantly closer to the MRI literature ($68 \pm 5\%$) than QBS ($58 \pm 9\%$), and both algorithms underestimated normal RV EF ($52 \pm 7\%$ and $50 \pm 9\%$) compared to MRI literature ($64 \pm 9\%$). The lower limits for normal EF and the upper limits for normal volumes for all methods are provided in Table 3. That the lower limit for normal LVEF was 40% for QBS and 50% for BP-SPECT is a reflection of the finding described above for the 422 clinical studies of significantly lower QBS LV EF values.

Patients with MRI Validations

For the separate group of 21 patients with MRI validations, BP-SPECT measurements reported in reference 12 were compared to QBS and to MRI measurements. Mean BP-SPECT values were not significantly different from MRI values, but for QBS LV EF and LV EDV were significantly lower than MRI values and BP-SPECT values (Table 4).

	LV EDV	LV ESV	LV EF	RV EDV	RV ESV	RV EF
QBS	83±68 mL*#	45±43 mL	50±16%*#	129±53 mL	73±44 mL	47±16%
BP-SPECT	107±59 mL	42±41 mL	65±13%	148±75 mL	84±49 mL	44±10%
MRI	101±64 mL	42±41 mL	62±12%	133±56 mL	79±37 mL	41±10%

Table 4

Paired T-test results for data for 21 patients with correlative MRI validations.

* = p<0.05 for QBS versus BP-SPECT

= p<0.05 versus MRI

Correlations of QBS to MRI for LV EF and volumes were quite similar to those of BP-SPECT versus MRI, but all QBS RV correlations were significantly weaker (Table 5).

	QBS versus MRI	BP-SPECT versus MRI
LV EDV	r=0.84; y=-8mL+0.90x; SEE=39mL	r=0.89; y=24mL+0.82x; SEE=28mL
LV ESV	r=0.89; y=6mL+0.92x; SEE=12mL	r=0.95; y=3mL+0.94x; SEE=14mL
LV EF	r=0.80; y=-8%+0.94x; SEE=12%	r=0.85; y=9%+0.91x; SEE=7%
RV EDV	r=0.71*; y=40mL+0.68x; SEE=39mL	r=0.83; y=-2mL+1.13x; SEE=43mL
RV ESV	r=0.66*; y=11mL+0.79x; SEE=34mL	r=0.78; y=2mL+1.04x; SEE=32mL
RV EF	r=0.47*; y=16%+0.74x; SEE=13%	r=0.81; y=12%+0.78x; SEE=6%

Table 5

Linear regression results for data for 21 patients with TOF or PAH with MRI validations

* = p<0.05 for strength

Thus, these findings for clinical MRI data confirmed the same trends found in comparing results for normal subjects to the MRI literature, namely that QBS LV EF's and volumes were lower than MRI values, while BP-SPECT LV measurements were closer to MRI results (Table 3).

Bi-ventricular Physical Phantoms

In the 16 phantom simulations, QBS measurements were compared to true phantom values and BP-SPECT values. For LV EF QBS, BP-SPECT and true phantom measurements were similar, but QBS LV volumes were significantly lower than BP-SPECT or phantom LV volumes; BP-SPECT overestimated LV phantom volumes (Table 6). All QBS RV measurements were significantly different from BP-SPECT and phantom RV values, while all BP-SPECT RV measurements were similar to phantom RV values (Table 6).

	LV EDV	LV ESV	LV EF	RV EDV	RV ESV	RV EF
QBS	42±22 mL*#	25±16 mL*#	44±14%	69±25 mL*#	39±32 mL*#	54±22%*#
BP-SPECT	122±20 mL#	77±23 mL#	44±13%	167±44 mL	111±49 mL	40±16%
Phantoms	88±22 mL	51±22 mL	44±14%	153±39 mL	103±47 mL	35±13%

Table 6

Paired T-test results for data for 16 physical phantoms.

* = $p < 0.05$ for QBS versus BP-SPECT

= $p < 0.05$ versus phantoms

Linear regression analysis showed that all QBS and BP-SPECT LV measurements correlated significantly, and similarly, with true phantom LV values (Table 7), but all QBS RV measurements correlated significantly less strongly with phantom RV values than did the BP-SPECT RV values. All QBS RV correlations were weaker than QBS LV correlations (Table 7).

	QBS versus Phantoms	BP-SPECT versus Phantoms
LV EDV	$r=0.84; y=-8\text{mL}+0.90x; \text{SEE}=39\text{mL}$	$r=0.89; y=24\text{mL}+0.82x; \text{SEE}=28\text{mL}$
LV ESV	$r=0.89; y=6\text{mL}+0.92x; \text{SEE}=12\text{mL}$	$r=0.95; y=3\text{mL}+0.94x; \text{SEE}=14\text{mL}$
LV EF	$r=0.81; y=10\%+0.77x; \text{SEE}=8\%$	$r=0.91; y=6\%+0.85x; \text{SEE}=6\%$
RV EDV	$r=0.10^*; y=60\text{mL}+0.07x; \text{SEE}=26\text{mL}$	$r=0.89; y=16\text{mL}+0.99x; \text{SEE}=21\text{mL}$
RV ESV	$r=0.29^*; y=19\text{mL}+0.20x; \text{SEE}=32\text{mL}$	$r=0.93; y=12\text{mL}+0.95x; \text{SEE}=18\text{mL}$
RV EF	$r=0.62^*; y=19\%+1.02x; \text{SEE}=18\%$	$r=0.82; y=4\%+1.04x; \text{SEE}=10\%$

Table 7

Linear regression results for data for 16 physical phantoms.

* = $p < 0.05$ for strength of association of QBS versus phantoms compared to BP-SPECT versus phantoms

DISCUSSION

For clinical data, normal subjects, MRI and phantom data, QBS and BP-SPECT LV parameters correlated strongly with one another, but all QBS RV relationships were significantly weaker than all QBS LV relationships. QBS algorithm region generation success rates also were quite similar for all data types. Another finding in common across all data types was that QBS LV EF's and LV EDV's were significantly lower than BP-SPECT values and the other imaging modalities' LV values.

The latter finding was consistent with the result that QBS normal limits were significantly lower than BP-SPECT or MRI normal limits. The relevance of this clinically is that it would be necessary to apply different normal limits to MRI than to scintigraphic images [15] as well as separate normal limits to QBS or BP-SPECT calculations, in interpreting measurements. This is comparable to the documented necessity of applying different normal limits for different myocardial perfusion gated SPECT algorithms [10]. The fact that the standard error for MRI LV EF is smaller (5%) than for our patient population (9%) for normal limits may be due to differences in populations studied [15] as well as the fact that it is unlikely that scintigraphic methods can be as precise or reproducible as MRI measurements.

Differences between QBS and BP-SPECT are most striking for RV measurements. QBS volumes may have systematically underestimated both BP-SPECT and MRI volumes because it was observed that QBS often included considerably less of the RV toward the pulmonary outflow tract and toward the RV apex (compare Figure 1 to Figure 2). That is predictable, since QBS is a gradient method, but at ED there is rarely any identifiable pulmonary valve plane. Rather, RV and pulmonary artery counts can

appear to be continuous at ED, whereas observing the evolution of counts as ventricular chambers contract in these questionable territories distinguishes RV counts from those of the pulmonary artery. In addition, QBS was more prone to miss perceived apical RV counts when the RV was narrow. Partial volume effects undoubtedly reduced observed radioactivity concentrations under those conditions, which would compromise calculations of both gradient and count-threshold approaches.

With regard to QBS for the LV, the mitral valve plane occasionally was placed further forward than as perceived by observers, causing computed LV EDV's to be smaller than expected. The BP-SPECT methodology was by no means perfect, either. When inadequate, the first attempt was to reselect planes and make no other changes. If insufficient, observers then redrew outlines on VLA ED, VLA ES and SA ED images, and if still inadequate, then observers modified individual HLA ED and ES outlines for any and all slice levels. Consequently, whereas observers could not alter QBS outlines to better match perceived chamber limits, BP-SPECT calculations had the disadvantage of likely introducing interobserver errors. It is likely that the ability to manually alter regions to reflect users' perceptions of actual ventricular volumes was an important difference between QBS and BP-SPECT algorithms. The reproducibility of QBS has only recently been explored and reported [24].

Study Limitations

It would have been preferable to use more direct "gold standards," such as the animal cast studies that have been performed to validate MRI RV measurements [25]. Drawbacks of the correlative studies that were available for this investigation included: that planar-GBP is compromised by overlap of cardiac structures; that more realistic dynamic phantoms would have been preferable; and that the clinical MRI studies were performed on patients likely to have very enlarged RV volumes and/or very depressed RV EF's.

Data were collected in a manner intended to maximize the likelihood of collecting adequate counts in all clinical studies, at the expense of sacrificing temporal and spatial resolution, just as is done routinely in performing gated myocardial perfusion studies. GBPS distributes counts over 8-10 tomographic sections compared to planar-GBP, reducing count densities by 1/8th to 1/10th per slice, potentially presenting a challenge to algorithms, especially in patients with significant attenuation due to

enlarged hearts or large body habitus. It would be preferable to collect at least 16 frames per R-R cycle so as to obtain additional information regarding ventricular filling and emptying parameters, but only if sufficient counts can be acquired routinely for this purpose. The optimal GBPS acquisition parameters have not yet been studied systematically and are not known at this time, nor is it known whether attenuation corrections or improved tomographic reconstruction techniques would produce more accurate GBPS measurements.

It is likely that QBS underestimated all phantom volumes because the phantom included no background counts [19]. However, it should be noted that neither QBS nor BP-SPECT algorithms were designed to process phantom data. Instead, both algorithms expected to find left and right atria, neighbouring lung counts and pulmonary outflow tracts. It is likely that both QBS and BP-SPECT GBPS algorithms will produce values closer in agreement with actual phantom parameters when presented with more realistic physical simulations. In this regard, the phantom data used in this investigation provided valuable insights into how the algorithms respond to clinical data for patients with small atria and/or unusually low neighbouring tissue cross talk counts, such as occurs with pericardial effusion and excess pericardial fat.

Normal limits used for this investigation were obtained for patients with cancer but no known cardiac disease. It is possible that values obtained for age-matched normal volunteers could be different. Future studies will be needed to document ventricular function parameters generated by GBPS algorithms in various distinct subgroups, such as normal volunteers and patients with CHF and/or CAD, who also have direct correlative cardiac MRI studies. This will be necessary in order to determine the actual limits of accuracy in specific groups, and to provide information required to improve the agreement of algorithms with other imaging modalities.

CONCLUSION

Both QBS and BP-SPECT produced LV volume and EF values that correlated strongly with planar-GBP, cardiac MRI and phantom values. However, all LV parameters correlated more strongly than did the corresponding RV values, and all BP-SPECT RV measurements correlated significantly more strongly with MRI and phantom data than did QBS values. Overall, QBS gradient-method RV measurements were substantially different from values obtained by the BP-SPECT count-threshold

method.

Acknowledgment

This study was supported in part by grants from Siemens Medical Solutions, Inc. Some of the authors (K Nichols) stand to benefit from sale of software proceeds through marketing arrangements with Syntermed, Inc., related to the research described in this article. The terms of this arrangement have been reviewed and approved by Columbia University in accordance with its conflict-of-interest practice.

REFERENCES

1. Germano G, Kiat H, Kavanagh PB, Mariel M, Mazzanti M, Su HT, et al. Automatic quantification of ejection fraction from gated myocardial perfusion SPECT. *J Nucl Med* 1995;36:2138-47.
2. Faber TL, Cooke DC, Folks RD, Vansant JP, Nichols KJ, DePuey EG, et al. Left ventricular function from gated SPECT perfusion images: An integrated method. *J Nucl Med* 1999;40:650-9.
3. Faber TL, Stokely EM, Templeton GH, Akers MS, Parkey RW, Corbett JR. Quantification of three-dimensional left ventricular segmental wall motion and volumes from gated tomographic radionuclide ventriculograms. *J Nucl Med* 1989;30:638-49.
4. Bartlett ML, Srinivasan G, Barker WC, Kitsiou AN, Dilsizian V, Bacharach SL. Left ventricular ejection fraction: Comparison of results from planar and SPECT gated blood-pool studies. *J Nucl Med* 1996;37:1795-9.
5. Chin BB, Bloomgarden DC, Xia W, Kim HJ, Fayadz ZA, Ferrari VA, et al. Right and left ventricular volume and ejection fraction by tomographic gated blood-pool scintigraphy. *J Nucl Med* 1997; 38:942-8.
6. Vanhove C, Franken PR, Defrise M, Momen A, Everaert H, Bossuyt A. Automatic determination of left ventricular ejection fraction from gated blood-pool tomography. *J Nucl Med* 2001;42:401-7
7. Links JM, Becker LC, Shindlecker JG, et al. Measurement of absolute left ventricular volume from gated blood-pool studies. *Circulation* 1982;65: 82-92.
8. Groch MW, Marshall RC, Erwin WD, Schippers DJ, Barnett CA, Leidholt EM Jr. Quantitative gated blood pool SPECT for the assessment of coronary artery disease at rest. *J Nucl Cardiol* 1998;5:567-73.
9. Van Krieking SD, Berman DS, Germano G. Automatic quantification of left ventricular ejection fraction from gated blood pool SPECT. *J Nucl Cardiol* 1999;6:498-506.

10. Nichols K, Santana CA, Folks R, Krawczynska E, Cooke CD, Faber TL, et al. Comparison between “ECTb” and “QGS” for assessment of left ventricular function from gated myocardial perfusion SPECT. *J Nucl Card* 2002;9:285-93.
11. Daou D, Harel F, Helal BO, Fourme T, Colin P, Lebtahi R, et al. Electrocardiographically gated blood-pool SPECT and left ventricular function: comparative value of 3 methods for ejection fraction and volume estimation. *J Nucl Med* 2001;42:1043-9.
12. Nichols K, Saouaf R, Ababneh AA, Barst RJ, Rosenbaum MS, Groch MW, et al. Validation of SPECT equilibrium radionuclide angiographic right ventricular parameters by cardiac MRI. *J Nucl Card* 2002;9:153-60.
13. Daou D, Haidar M, Vilain D, Lebtahi R, Parent F, Sitbon O, et al. Automatic calculation of right ventricular ejection fraction with gated blood pool SPECT: A clinical validation study [abstract]. *J Nucl Med* 2002;43:97P.
14. Daou D, Coaguila C, Lebtahi R, Colin P, Fourme T, Razzouk M, et al. Right ventricular (RV) function quantification with ECGogated radionuclide blood pool SPECT (RNA SPECT): Validation of the “4-cavity echocardiography-like” method in patients with coronary artery disease (CAD) [abstract]. *J Nucl Med* 2003;44:55P.
15. Sandstede J, Lipke C, Beer M, Hofmann S, Pabst T, Kenn W, et al. Age- and gender-specific differences in left and right ventricular cardiac function and mass determined by cine magnetic resonance imaging. *Eur Radiol* 2000;10:438-42.
16. De Bondt P, Vandenberghe S, De Mey S, Segers P, De Winter O, De Sutter J, et al. Validation of planar and tomographic radionuclide ventriculography by a dynamic ventricular phantom. *Nuc Med Comm.* 2003, 24(7):771-7.
17. Nichols K, DePuey EG, Rozanski A. Automation of gated tomographic left ventricular ejection fraction. *J Nucl Cardiol* 1996;3:475-82.
18. Nichols K, Shoyeb AH, Shazhad A, De Bondt P, Vandenberghe S, Bergmann SR. Accuracy of gated blood pool SPECT hybrid model: Phantom validation [abstract]. *J Nucl Cardiol* 2002;9:S11.
19. De Bondt P, Nichols K, Vandenberghe S, Segers P, De Winter O, Van de Wiele C, et al. Validation of gated blood pool SPECT cardiac measurements tested using a biventricular dynamic physical phantom. *J Nucl Med* 2003;44:967-72.

20. Sharir T, Germano G , Kavanagh PB, Lai S, Cohen I, Lewin HC, et al. Incremental prognostic value of post-stress left ventricular ejection fraction and volume by gated myocardial perfusion single photon emission computed tomography. *Circulation*. 1999;100:1035-42.
21. Rozanski A, Nichols K, Yao SS, Malhotra S, Cohen R, DePuey EG. Development and Application of normal limits for left ventricular ejection fraction and volume measurements from tc-99m sestamibi myocardial perfusion gated SPECT. *J Nucl Med* 2000;41:1445-50.
22. Ababneh AA, Sciacca RR, Kim B, Bergmann SR. Normal limits for left ventricular ejection fraction and volumes estimated with gated myocardial perfusion imaging in subjects with normal exercise tests: Influence of tracer, gender and acquisition camera. *J Nucl Cardiol* 2000;7:661-8.
23. Galt JR, Garcia EV, Robbins WL. Effects of myocardial wall thickness of SPECT quantification. *IEEE Trans Med Imaging* 1990;9:144-50.
24. Wright GA, Thackray S, Howey S, Cleland JG. Left ventricular ejection fraction and volumes from gated blood-pool SPECT: Comparison with planar gated blood-pool imaging and assessment of repeatability in patients with heart failure. *J Nucl Med* 2003;44:494-8.
25. Jauhiainen T, Jarvinen VM, Hekali PE, Poutanen VP, Penttila A, Kupari M. MR gradient echo volumetric analysis of human cardiac casts: focus of the right ventricle. *J Comp Assist Tomogr* 1998; 22: 899-903.

CHAPTER 7:

AGREEMENT BETWEEN FOUR AVAILABLE ALGORITHMS TO EVALUATE GLOBAL SYSTOLIC LEFT AND RIGHT VENTRICULAR FUNCTION FROM TOMOGRAPHIC RADIONUCLIDE VENTRICULOGRAPHY AND COMPARISON WITH PLANAR IMAGING.

Pieter De Bondt ^{1,2} , Olivier De Winter ¹ , Johan De Sutter ³ , Rudi Andre Dierckx¹

¹ Division of Nuclear Medicine, Ghent University Hospital, Ghent, Belgium

² Division of Nuclear Medicine, OLV Hospital, Aalst, Belgium

³ The Division of Cardiology, Ghent University Hospital, Ghent, Belgium

Nucl Med Commun. 2005 Apr;26(4):351-9.

SUMMARY

Left and right ventricular ejection fractions (LVEF and RVEF) and end-diastolic and end-systolic volumes (LVEDV, RVEDV, LVESV and RVESV) can be calculated from tomographic radionuclide ventriculography (TRV). We wanted to validate and compare these parameters from four different TRV software's (QBS, QUBE, 4D-MSPECT and BP-SPECT). We compared LVEF from planar radionuclide ventriculography (PRV) with LVEF from TRV from the four different software's in 166 patients. Furthermore, ventricular volumes from TRV (QBS, QUBE and 4D-MSPECT) were compared with those from BP-SPECT, the latter being the only method with a validation of ventricular volumes in literature. Correlation for LVEF between PRV and TRV was good for all methods, being 0.81 for QBS, 0.79 for QUBE, 0.71 for 4D-MSPECT and 0.79 for BP-SPECT. Mean difference \pm standard deviation (SD) was 3.16 ± 9.88 , 10.72 ± 10.92 , 3.43 ± 11.79 and 2.91 ± 10.39 respectively. Correlation for RVEF between BP-SPECT and QUBE and QBS was poor, being 0.33 and 0.38 respectively. LV volumes calculated from QBS, QUBE and 4D-MSPECT correlated well with those from BP-SPECT (0.98, 0.90 and 0.98 respectively) with mean difference \pm SD being 7.31 ± 42.94 , -22.09 ± 36.07 , -40.55 ± 39.36 respectively, whereas RV volumes correlated worse between QBS and BP-SPECT and between QUBE and BP-SPECT (0.82 and 0.57 respectively).

LVEF calculated from TRV correlates well with those from PRV but is not interchangeable with values from PRV. Volume calculations, for LV and RV, and RVEF need further validation before it can be used in clinical practice.

INTRODUCTION

Recently, different programs are being developed to process tomographic radionuclide ventriculography (TRV) [1-4]. These programs are fast, provide left (LVV) and right ventricular volume (RVV) and ejection fractions (EF), but the validation of these parameters, mostly of the RV, remains scarce. We therefore wanted to compare LVEF calculated from planar radionuclide ventriculography (PRV) with values from TRV, calculated by four different programs, QBS [2], QUBE [3], 4D-MSPECT [4] and BP-SPECT[1]. For LVV and RVV calculations, we compared values from QBS, QUBE and

4D-MSPECT with those of BP-SPECT, the latter being the only algorithm with MRI-validation of volumetric parameters in literature[1,5]. For the algorithm 4D-MSPECT, only parameters of the LV were available. Furthermore, we wanted to compare LV and RV stroke volumes, calculated from TRV from QBS, QUBE and BP-SPECT, as a method of validation of LV and RV volumetric parameters.

MATERIALS AND METHODS

Data acquisition

All images were acquired on two three-headed gamma camera's (IRIX and Prism 3000, Marconi-Philips, Cleveland, Ohio) equipped with low energy high-resolution collimators. PRV data were acquired over a 5 minute period, in 16 electrocardiographic gated frames, 64 x 64 matrix, zoom 1.333 (pixel size 7 mm) and with a beat acceptance window at 20 % of the average R-R interval calculated just before the acquisition was started. The gamma camera was positioned in left anterior oblique projection in order to obtain the best "septal view". Parameters of TRV acquisition were as follows: 360° step-and-shoot rotation, 40 stops per head, 30 seconds per stop, 64 x 64 matrix, zoom 1.422 (pixel size 6.5 mm), and 16 time bins per R-R interval, with a beat acceptance window at 20% of the average R-R interval. Projection data were pre-filtered using a Butterworth filter (cutoff frequency: 0.5 cycles/cm; order: 5) and reconstructed by filtered backprojection using an x-plane ramp filter. Data were then reoriented into gated short axis tomograms. The resulting gated short axis data sets were then used as input for the four algorithms.

From a database of 203 patients, who underwent PRV and TRV between 2001 and 2004, 37 patients were excluded because the best septal view in left anterior oblique position was not reached during PRV, and these were all patients after heart transplantation. None of the patients had proven intracardiac or intrapulmonary shunting.

From the remaining 166 patients (100 men, 66 women) clinical indications were pre-chemotherapy (55, 33%), post-chemotherapy (67, 40%), heart failure (8, 5%), acute myocardial infarction (7, 4%), pulmonary hypertension (3, 2%), congenital heart diseases (2, 1%) and other (24, 14%).

Processing

For the processing of the images, we used four software's: QBS (Quantitative Bloodpool SPECT software from Cedars-Sinai Medical Center, Los Angeles, USA), QUBE (Free University of Brussels, Brussels, Belgium), 4D-MSPECT (University of Michigan Medical Center in Ann Arbor, Michigan, USA) BP-SPECT (algorithms from Columbia University, New York, USA).

For the validation of LVEF, we used PRV as the gold standard. PRV was processed with Multi-Gated Analysis, version march 2001, on an Odyssey workstation, Philips Medical Systems, The Netherlands. For the comparison of LVV and RVV, we compared data from QBS, QUBE and 4D-MSPECT with BP-SPECT, since this program is the only one available with validation of volumetric parameters.

Statistical Analysis

Results were reported as mean values \pm 1 standard deviation (SD). Correlations (r) between the different methods to calculate LVEF, LVV, RVEF and RVV were expressed as the Pearson coefficient. Variability about the regression line was expressed as the standard error of the estimate (SEE). Bland-Altman analysis of differences versus means of paired values was used to search for trends and systematic errors. Statistical significance was defined as $p < 0.05$. Histograms and Box and whisker diagrams were used to show the distribution of the stroke volume index for the different techniques.

RESULTS

Global results

All gated short axis tomograms were processed on a pc, Pentium 4, 1.8 GHz, 512 Mb RAM.

Mean processing times were 105 sec, 18 sec, 19 sec and 15 sec for QBS, QUBE, 4D-MSPECT and BP-SPECT respectively.

The automatic option for all programs was first performed, followed by a visual inspection of the delineation of both ventricles. This was done by reviewing the dynamic images, slices into short, horizontal long and vertical long axis images with the calculated outlines of both ventricles superimposed on it.

QBS could successfully process the images automatically in 130 patients. From the

other 36 patients, only 6 could be corrected by the manual option. The manual option for QBS is defining a ROI around the LV. After trying the automatic and manual option, in 3 patients there could be no satisfactory delineation of the LV and in 16 cases for the RV. For 11 patients, no result could be calculated at all.

For QUBE, 114 patients were correctly processed by the automatic option. The manual intervention included masking, defining RV limit, condense number of gates or define septum and this revealed a good LV and RV delineation in 51 patients. Only in 1 patient, no result could be achieved for both ventricles.

Seventy-one patients could be processed correctly with the automatic program of 4D-MSPECT, in 85 patients, the atrioventricular border has to be adjusted manually, or a ROI around the LV had to be drawn. In 10 patients, no result could be calculated. No results for the RV were available.

BP-SPECT could process the images completely automatic in 99 patients, whereas in the other 67 scans a satisfactory result could be achieved by drawing an end-diastolic and an end-systolic ROI in the vertical long axis slice through the RV and LV together with one ROI through the short axis of both chambers.

Validation of LVEF

Mean \pm SD for LVEF from PRV and TRV are displayed in Table 1.

	PRV		TRV		
		QBS	QUBE	4D-MSPECT	BP-SPECT
LVEF	51.95 \pm 15.81	55.87 \pm 16.53*	62.87 \pm 17.40*	55.47 \pm 15.14*	54.86 \pm 16.01*
LVEDV		129.55 \pm 81.43**	114.92 \pm 72.95**	88.10 \pm 63.16**	141.53 \pm 77.66
LVESV		65.20 \pm 72.65	50.28 \pm 67.40**	44.12 \pm 55.74**	70.40 \pm 71.82
RVEF		51.35 \pm 11.87**	47.47 \pm 13.51**		55.57 \pm 12.71
RVEDV		133.96 \pm 40.92	141.81 \pm 55.39**		138.23 \pm 47.65
RVESV		66.06 \pm 28.86	76.33 \pm 41.09**		62.85 \pm 32.44

Table 1

Mean \pm SD for PRV and TRV for all programs with paired T-test results for TRV compared to PRV.

*: significant (p<0.05) difference compared to PRV

** : significant (p<0.05) difference compared to BP-SPECT

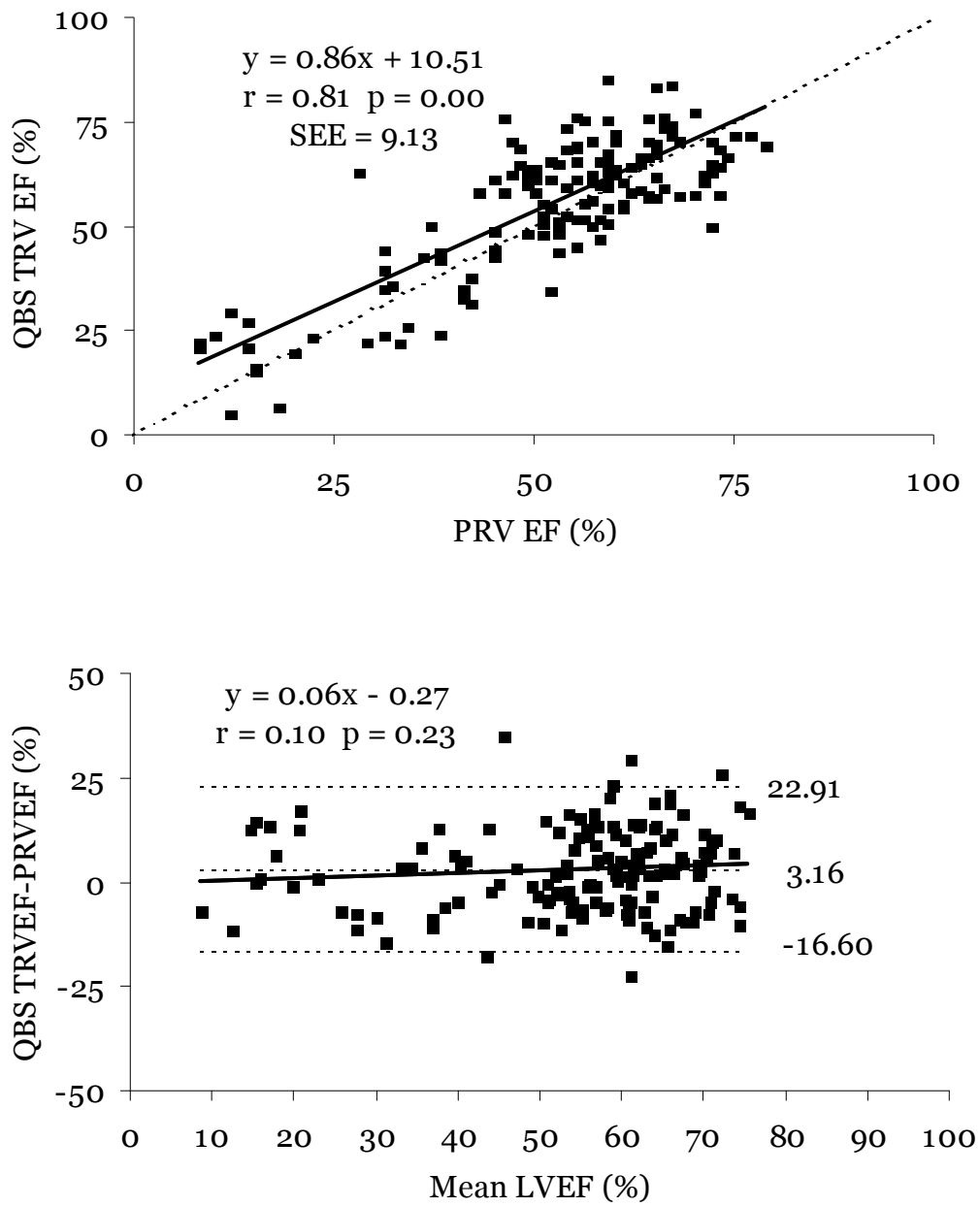


Figure 1
 Linear regression and Bland-Altman analysis of left ventricular ejection fraction calculation
 QBS compared with LVEF from PRV.

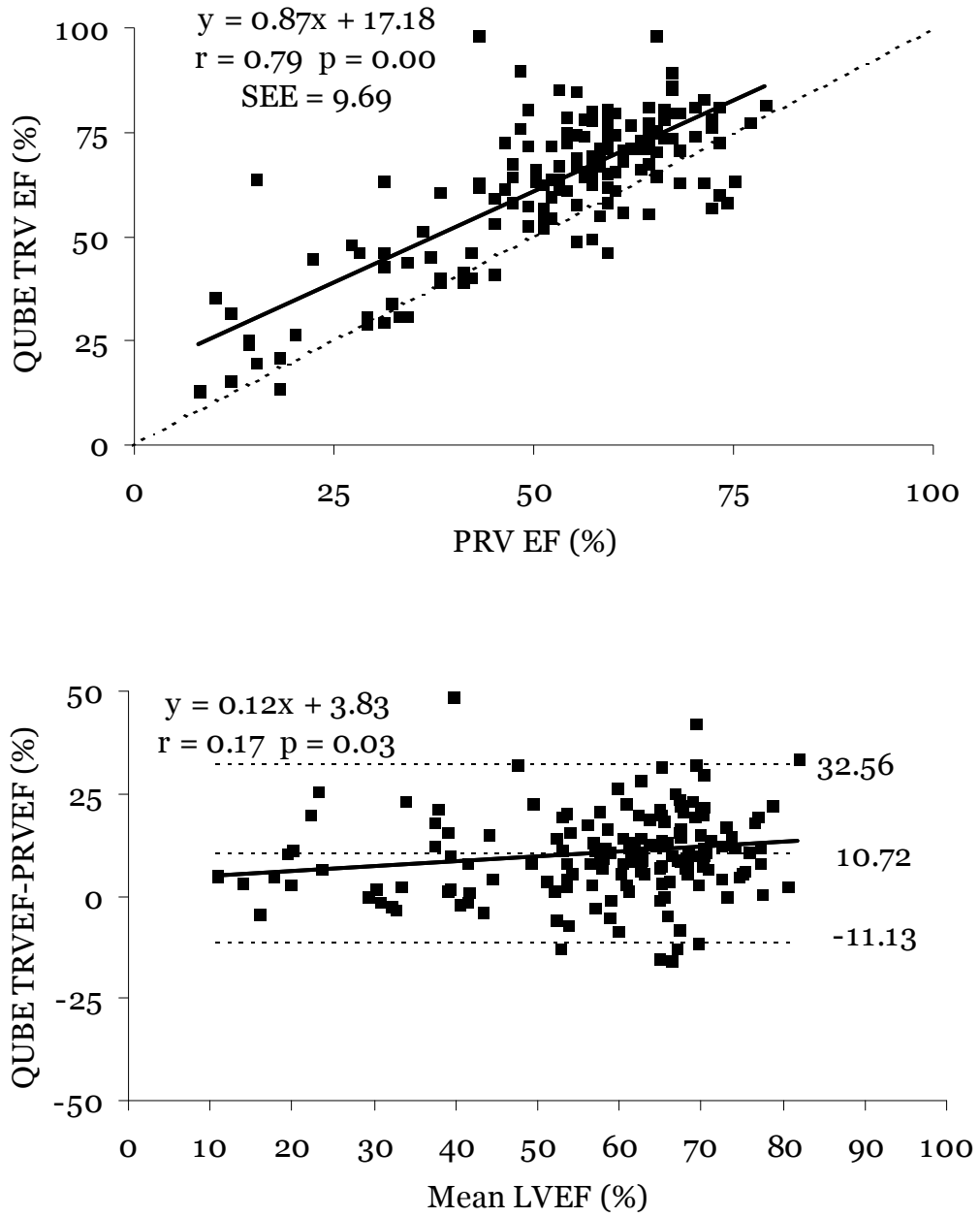


Figure 2
 Linear regression and Bland-Altman analysis of left ventricular ejection fraction calculation
 QUBE compared with LVEF from PRV.

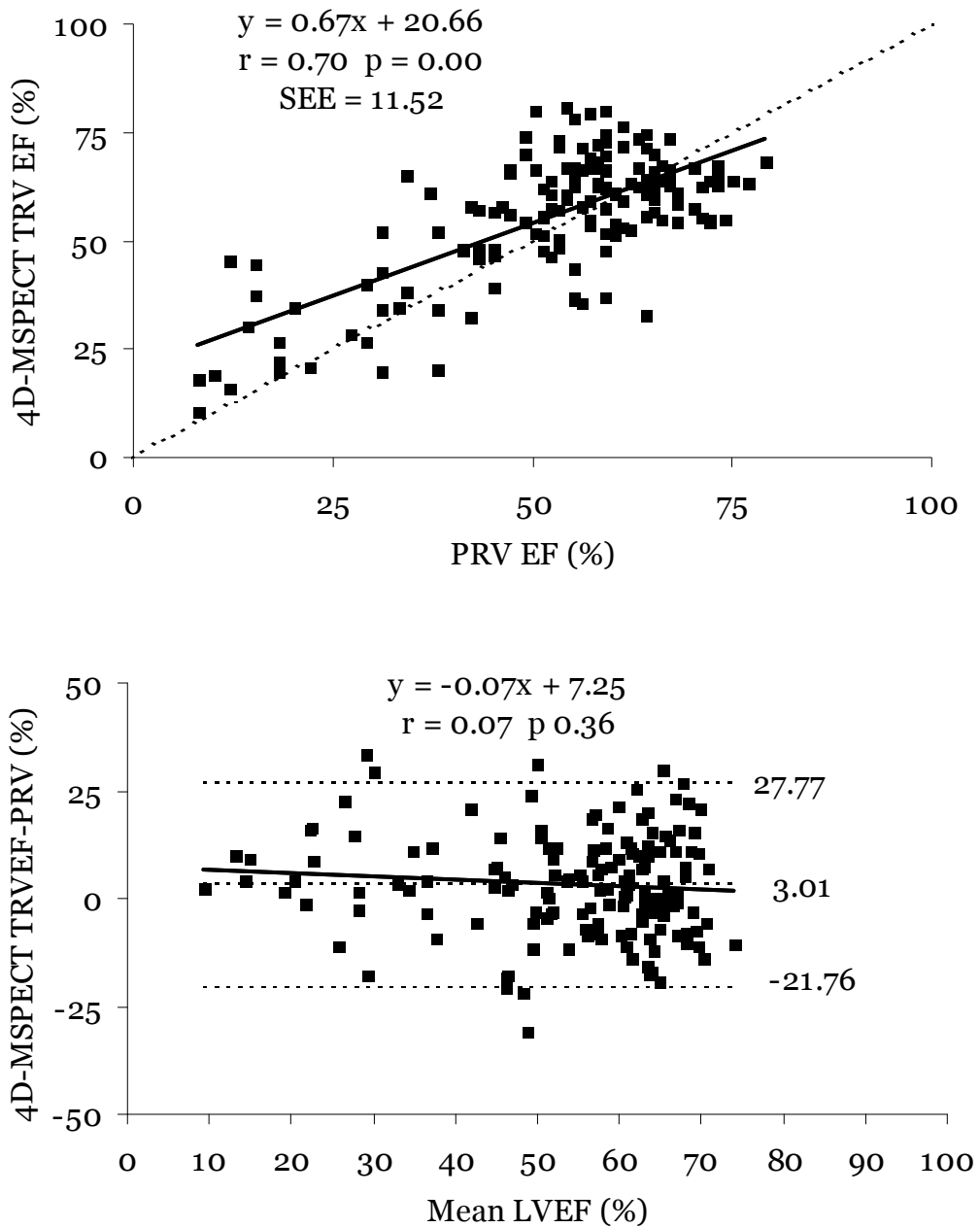


Figure 3
 Linear regression and Bland-Altman analysis of left ventricular ejection fraction calculation QUBE compared with LVEF from PRV.

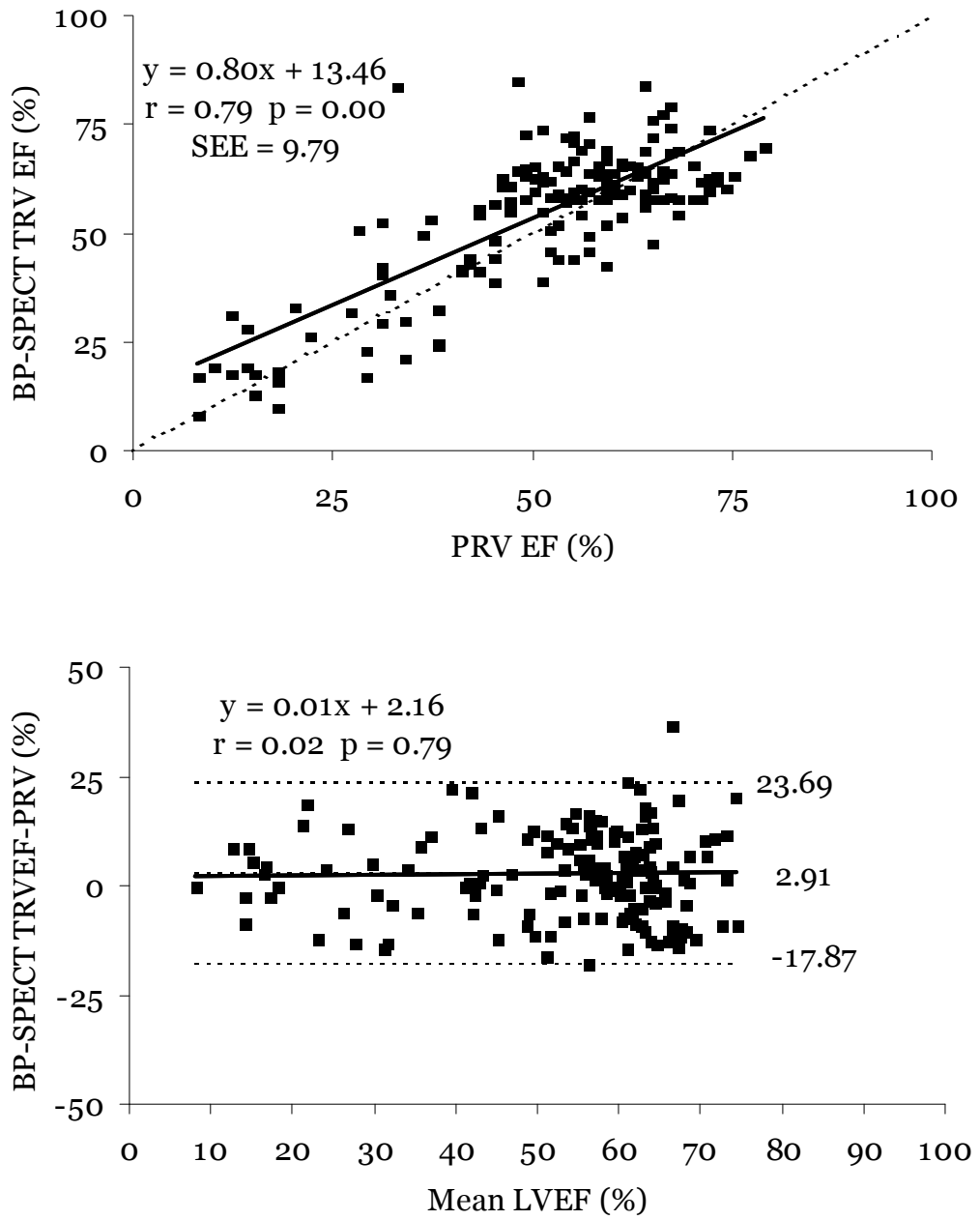


Figure 4

Linear regression and Bland-Altman analysis of left ventricular ejection fraction calculation BP-SPECT compared with LVEF from PRV.

Values of LVEF from all the methods to process TRV were significantly higher ($P < 0.001$) compared to PRV. Furthermore, LVEF from QUBE was significantly higher ($P < 0.001$) compared to the other methods of TRV. Regression and Bland-Altman analysis were performed for LVEF calculated with the four methods, compared to PRV (Figure 1-4).

Correlation between PRV and TRV was good for all methods, being 0.81 for QBS, 0.79 for QUBE, 0.71 for 4D-MSPECT and 0.79 for BP-SPECT. The standard error of the estimate (SEE) was smallest for QBS (9.86) and BP-SPECT (9.79), somewhat larger for QUBE (10.79) and for 4D-MSPECT (12.18). From Bland-Altman analysis, no significant trend was seen for all methods across the range of LVEF.

Validation and comparison of LVV, RVV and RVEF

Mean \pm SD for LVEDV, LVESV, RVEDV and RVESV from TRV are displayed in Table 1. Regression and Bland-Altman analysis were performed for LVV calculated with QBS, QUBE and 4D-MSPECT, compared to LVV from BP-SPECT (Figure 5-7). LVV calculations from QBS, QUBE and 4D-MSPECT correlated well (0.98, 0.90 and 0.98) with values from BP-SPECT. All calculations of LVV, LVEDV and LVESV, showed the smallest values with 4D-MSPECT and largest with BP-SPECT. The values of LVEDV and LVESV from all the software's differed significantly ($P < 0.001$) with every other technique, except LVESV from QBS compared to BP-SPECT. In the Bland-Altman analysis, no significant trend was observed between LVV calculated by QBS and BP-SPECT, but there was between QUBE and BP-SPECT and even more obvious between 4DM-SPECT and BP-SPECT, with a growing underestimation of LVV for QUBE and 4D-MSPECT for larger volumes. Furthermore, a lot of outliers were observed, especially between 4D-MSPECT and BP-SPECT and especially for larger volumes, and the variation of all methods depended strongly on the magnitude of measurements, by means that for large volumes difference between the two methods is often lying outside the 95% confidence interval (Figure 2).

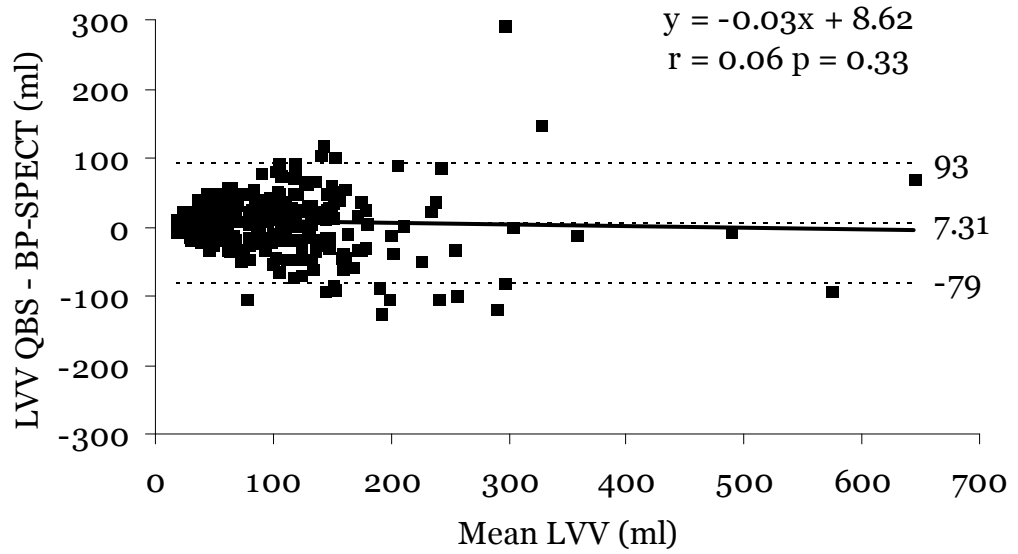
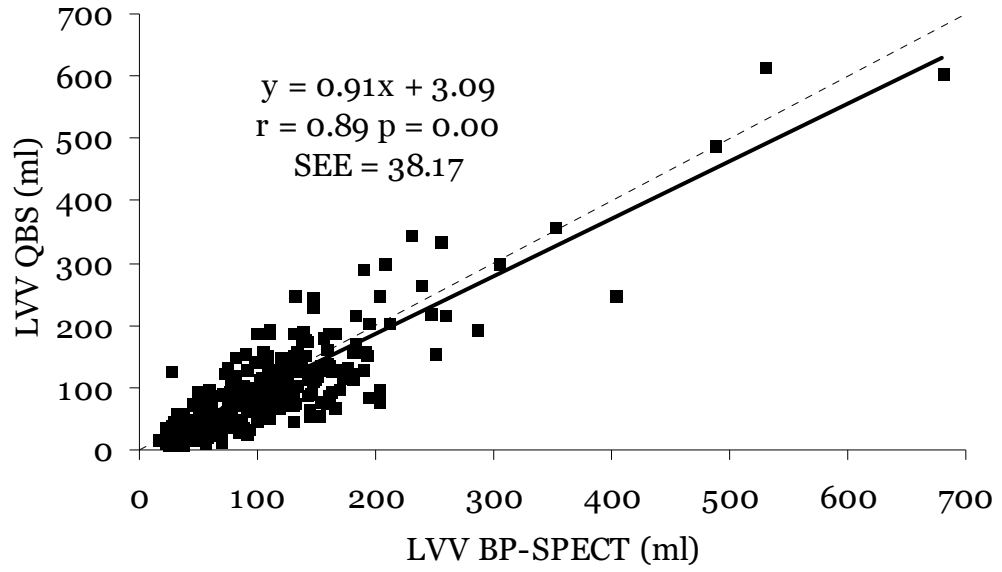


Figure 5
 Linear regression and Bland-Altman analysis of left ventricular volume calculation with QBS compared with LVV from BP-SPECT.

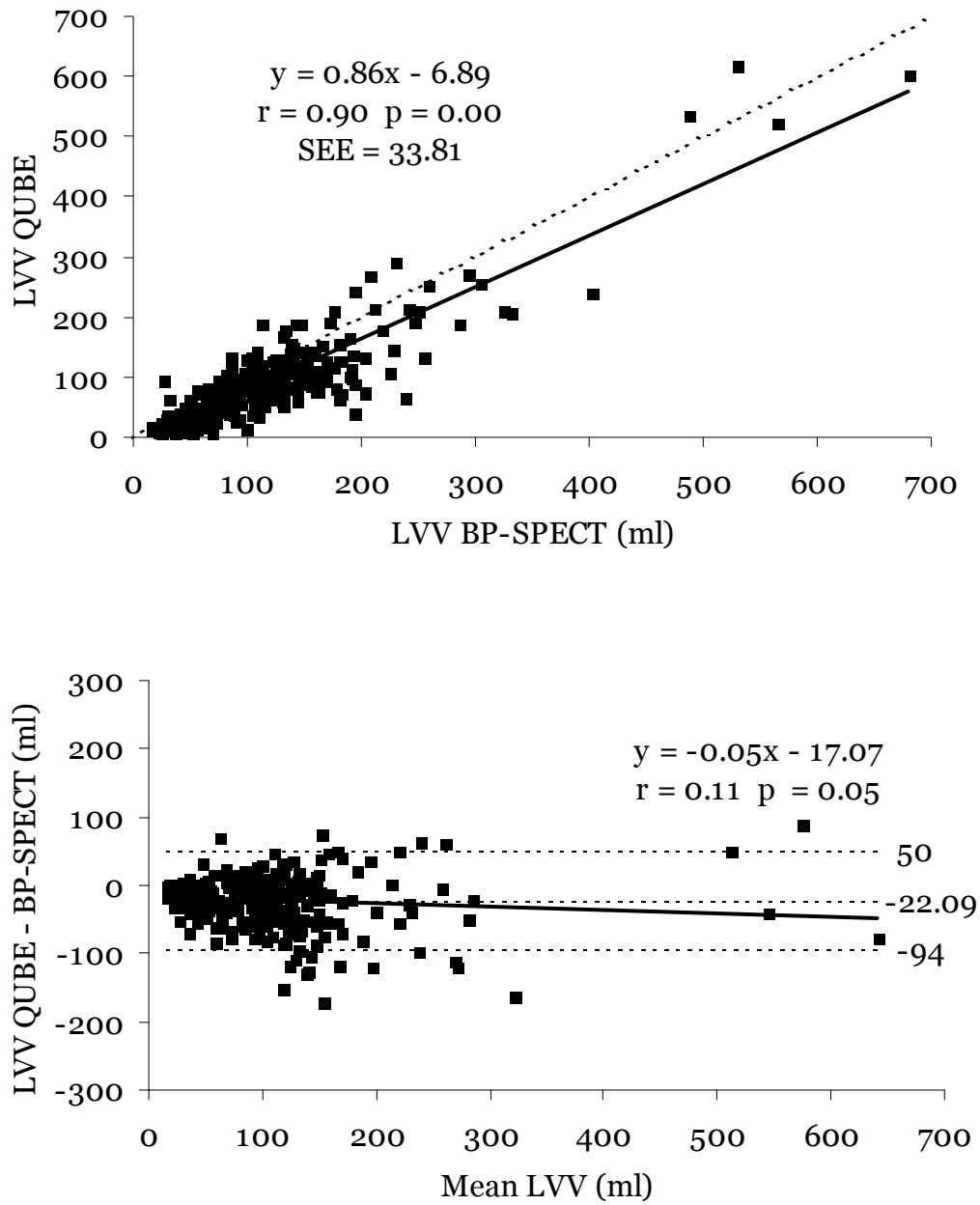


Figure 6

Linear regression and Bland-Altman analysis of left ventricular volume calculation with QUBE compared with LVV from BP-SPECT.

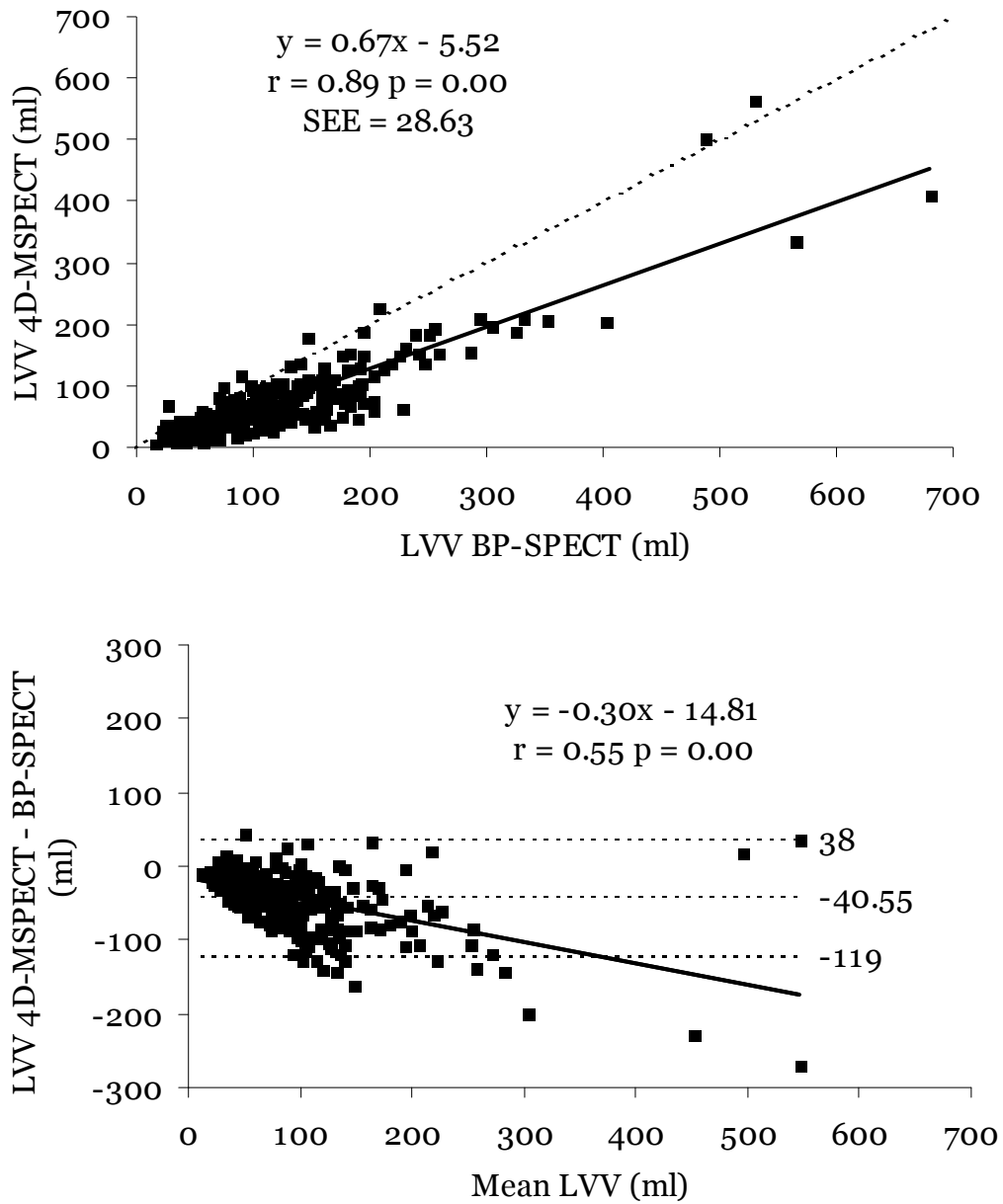


Figure 7

Linear regression and Bland-Altman analysis of left ventricular volume calculation with 4D-MSPECT compared with LVV from BP-SPECT.

For RVV, correlation was slightly lower for QBS (0.82), but with an acceptable mean difference and confidence interval on Bland-Altman plot, and much lower for QUBE (0.57) compared to the values found by BP-SPECT (Figure 8-9). When considering RVEDV, no significant difference was found between QBS, QUBE and BP-SPECT, whereas for RVESV, only significant higher values were found for QUBE, compared to QBS and BP-SPECT, and not between values of QBS and BP-SPECT.

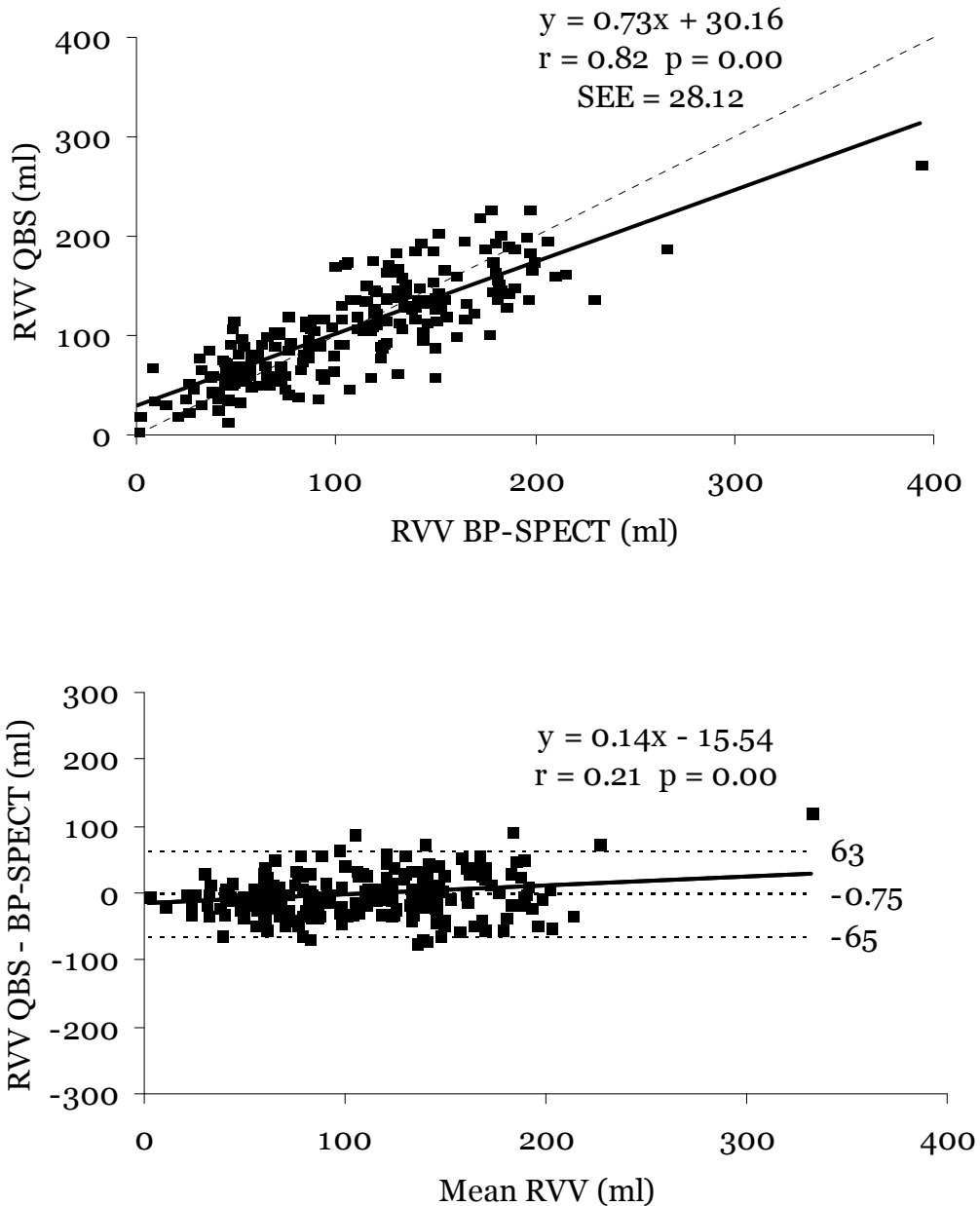


Figure 8

Linear regression and Bland-Altman analysis of right ventricular volume calculation with QBS compared with RVV from BP-SPECT.

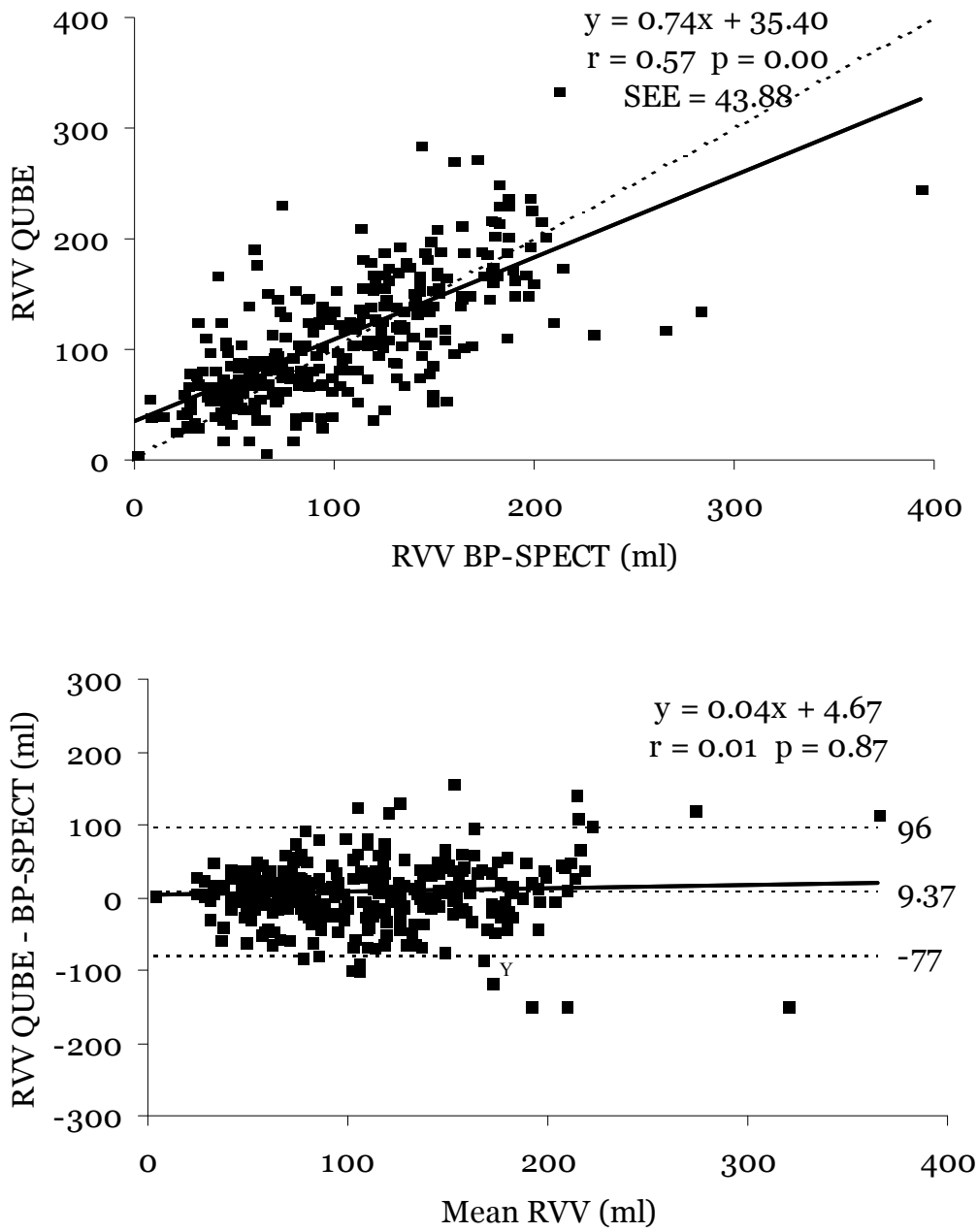


Figure 9

Linear regression and Bland-Altman analysis of right ventricular volume calculation with QUBE compared with RVV from BP-SPECT.

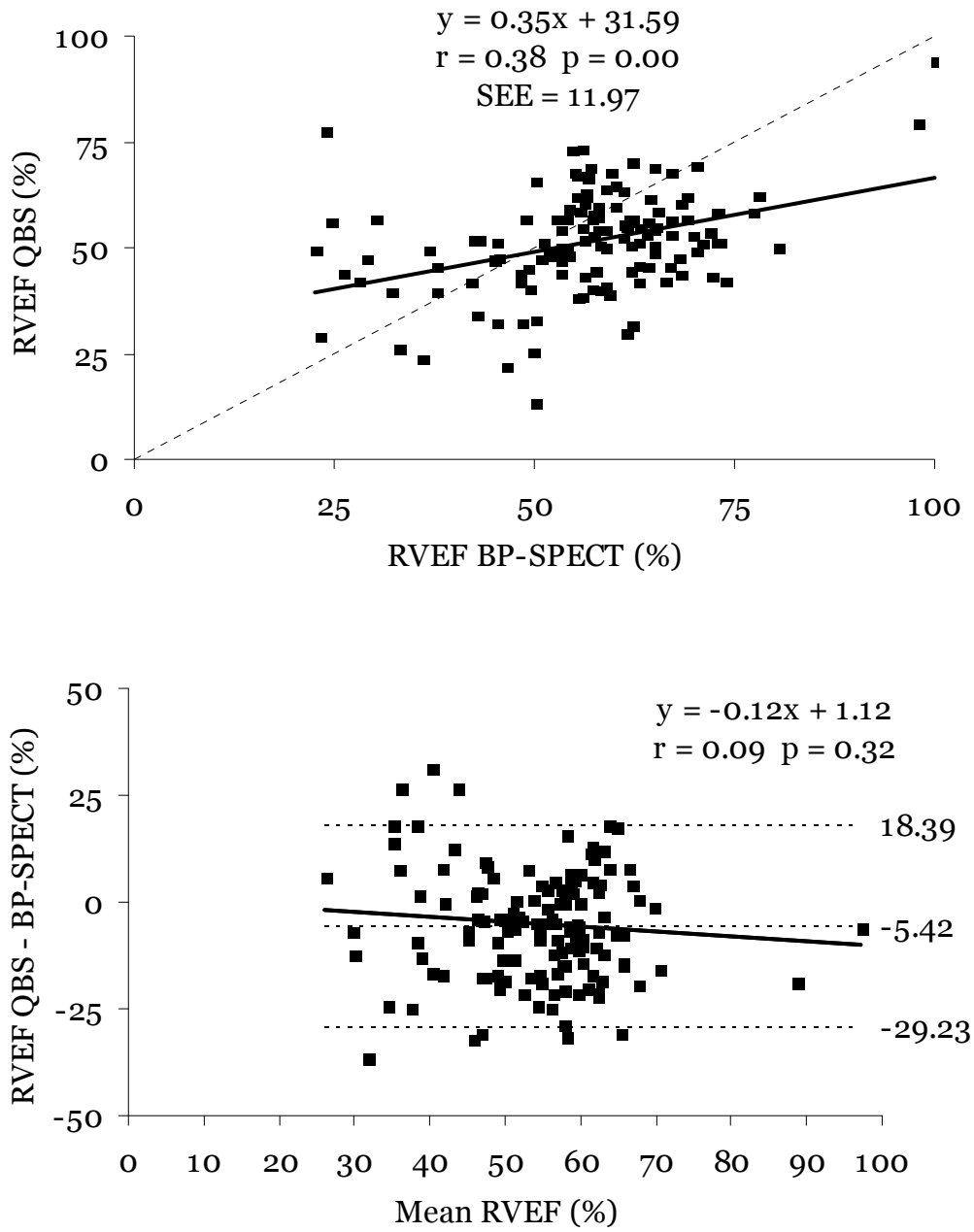


Figure 10

Linear regression and Bland-Altman analysis of right ventricular ejection fraction calculation with QBS compared with RVEF from BP-SPECT.

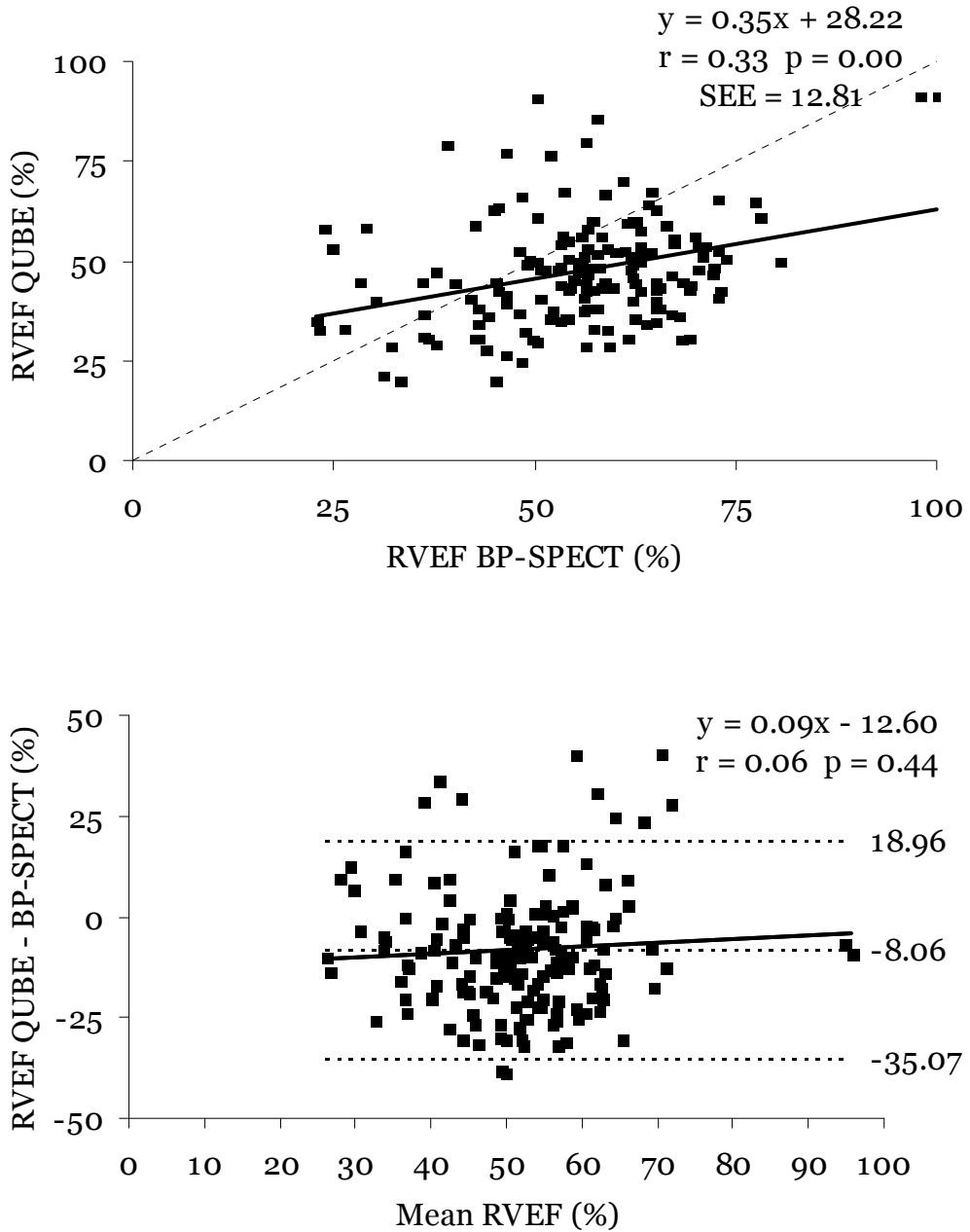


Figure 11

Linear regression and Bland-Altman analysis of right ventricular ejection fraction calculation with QBS compared with RVEF from BP-SPECT.

and between QUBE and BP-SPECT and a poor correlation was found, 0.38 and 0.33 respectively (Figure 10-11).

Since the stroke volume (SV) is equal in LV and RV, proportion of stroke volumes (stroke volume index, SVI) has to be ideally 1. Histogram and Box and whisker diagrams with the distribution of the SVI for the different techniques are shown in Figure 12. Mean SVI \pm SD for BP-SPECT, QBS and QUBE were 1.01 ± 0.43 , 0.99 ± 0.38 and 1.11 ± 0.51 respectively. Half of the patients show a difference between LVSV and RVSV more than 40% for BP-SPECT, 39% for QBS and 54% for QUBE.

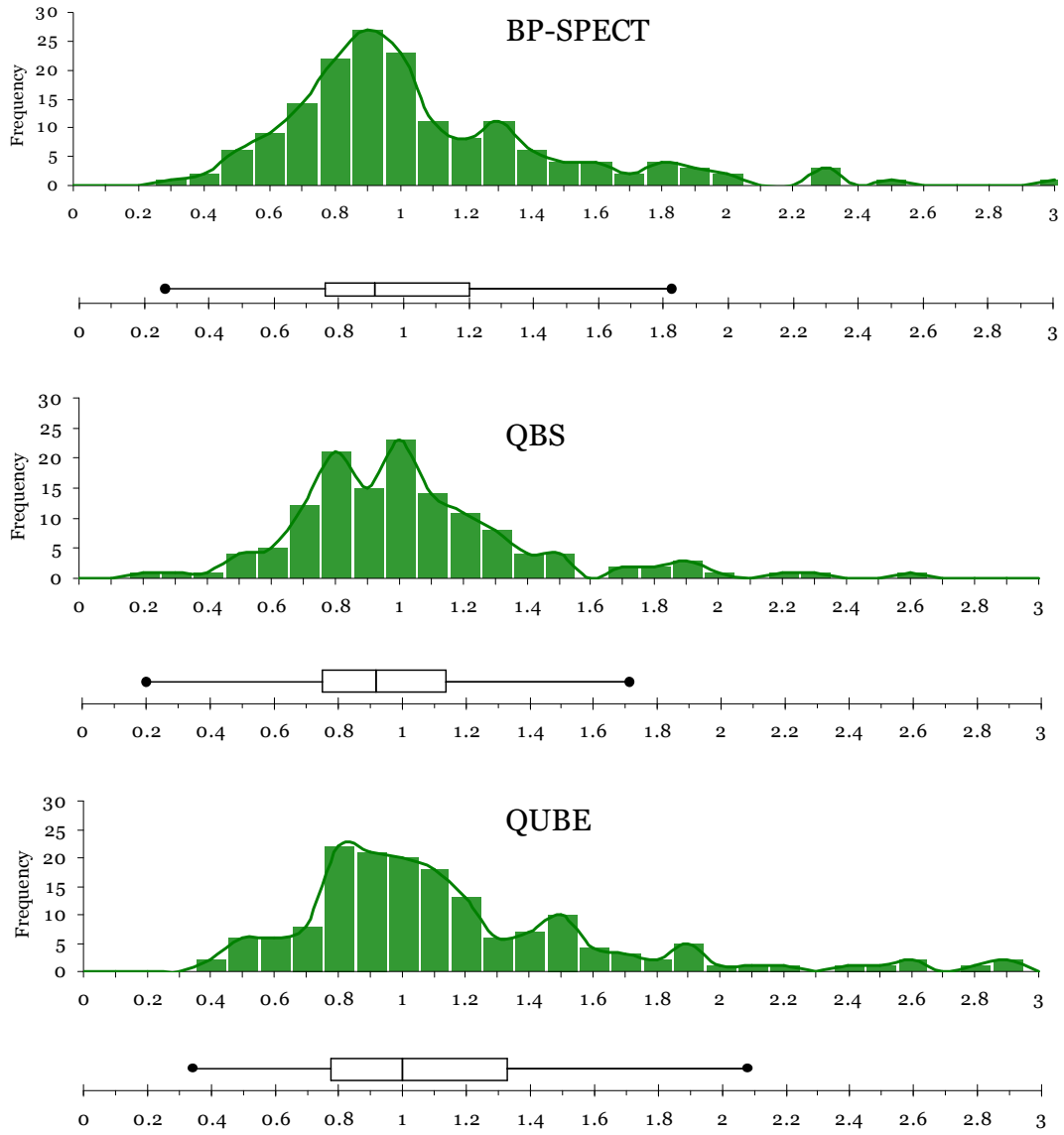


Figure 12

DISCUSSION

QBS is a very straightforward program but with only very limited possible manual intervention. After automatic processing, the visual interpretation of the delineation of the ventricles is not optimal in 22% of the patients, this is mostly the case in the lateral wall of the left ventricle and in the inferior wall of both ventricles. Another error seen was the inclusion of atrial structures in the LV or RV. Only in 17% of these cases, the manual option (defining LV in short axis, horizontal long axis and vertical long axis) resulted in a satisfactory result, mostly for the LV. Nevertheless, this program is easy to use and the result page is visually attractive, with display of bull's eye analysis of wall motion, similar to the well-known gated myocardial perfusion analysis software, QGS [6].

QUBE is more validated [3,7-9] and is nowadays distributed by Segami corporation. The reconstruction software is directly linked to the software itself, with the obvious advantage of easily making corrections in realignment of the short axis images, zooming, masking and condensing 16 time frames into 8. The manual options gave satisfactory results in nearly all the cases, for LV as well as for RV. Additional results are presented like 3D phase analysis and RV fraction shortening, but these items remain unvalidated.

4D-MSPECT is known for its analysis of gated myocardial perfusion [10], and it also includes a possibility to process TRV. At the moment of analysis, only the option of processing LV was available. The manual intervention is very fast and accurate in most of the cases, and the program is very flexible and open, which makes it possible to create own databases of normal patients and to export every parameter to a text-file to create an extensive and quantitative report. Wall motion is not only directly calculated in a predefined bull's eye (3, 5, 9, 13, 17, 19 or 20 segment polar map), but can be scored as well as normal, mild hypokinesis, moderate hypokinesis, severe hypokinesis, akinesis or dyskinesis by predefined cut-offs. Only, there is a subjective impression that wall motion in the apex is relatively underestimated, compared to visual analysis of the images. Most of the scans needed manual intervention (51%), but this was easily done by adjusting the valve plane in end-diastolic and end-systolic position. The way these programs define the valve plane is a critical point and influences volume calculations extensively. The method used to detect the valve plane is not described by the manufacturers and can be completely automatically in one program and not adjustable (e.g. QBS), and visually less accurate and easily adjustable in another

program (e.g. 4D-MSPECT).

BP-SPECT is the only software with validation of LVV and RVV [1,5] which is absolutely necessary for this kind of software. During processing, RV results are first calculated and when these are accepted, LV delineation is done. Drawing ROI's in end-diastolic and end-systolic images for RV as well as LV, was successful in all clinical cases where the automatic program couldn't define the ventricular outline properly.

For the calculation of LVEF, all programs supply good results with correlation coefficients between 0.71 and 0.81. These values are lower than those mentioned in other publications about comparison of LVEF between PRV and TRV (Table 2.), although consistent with the finding that LVEF from TRV is higher compared to LVEF from PRV, probably because of atrial overlap with LV in PRV [11].

	year	N° pts	Software	Corr	Linear Regression $y = TRV; x = PRV$	Highest value	SEE	Ref.
Our results			QBS	0.81	$y = 0.86x + 10.51$	TRV	9.1	
		166	QUBE	0.79	$y = 0.87x + 17.18$	TRV	9.7	
			4D-MSPECT	0.71	$y = 0.67x + 20.66$	TRV	11.5	
			BP-SPECT	0.79	$y = 0.80x + 13.46$	TRV	9.8	
Nichols	2004	422	QBS	0.81	$y = 0.98x + 5$	PRV	10	[25]
			BP-SPECT	0.83	$y = 0.95x + 7$	TRV	9	
Slart	2004	22	NuSMUGA (M)	0.90		TRV		[15]
			NuSMUGA (A)	0.88		PRV		
Wright	2003	50	QBS	0.80		-		[16]
Ficaro	2002	56	4D-MSPECT	0.97	$y = 1.06x - 1.58$	-	-	[10]
			QBS	0.99	$y = 0.92x$	TRV	6.8	
Daou	2001	29	TMUGA	0.98	$y = 0.82x$	TRV	8.1	[17]
			M	0.98	$y = 0.84x$	TRV	8.4	
Groch	2001	178	NuSMUGA	0.92	$y = 1.04x + 6.1$	TRV	5.4	[18]
Vanhove	2001	53	QUBE	0.78	$y = 0.94x + 6.33$	TRV (for EF > 50%)	8.8	[3]
Vanhove	2001	92	QUBE	0.82	$y = 1.04x - 4.75$	TRV	8.8	[8]
			QBS	0.80	$y = 0.98x + 4.42$	PRV	9.4	
Daou	2004	29	QBS	0.62		TRV		[19]
Van Kriekinge	1999	89	QBS	0.89	$y = 1.01x + 2.00$	TRV		[2]
Chin	1997	18	M	0.96		TRV	6.7	[20]
Bartlett	1996	23	Reprojection image	0.89	$y = 1.4x - 8$	TRV	8	[11]
Mariano- Goulart	1998	30	TMUGA	0.93	$y = 0.99x + 4.17$	TRV	5.9	[13]

Table 2
Comparison of LVEF from PRV with TRV in literature

A larger correlation is mainly found in papers with smaller patient groups, which makes it less representative for a large group of clinical patients or is found with a relative manual or semi-automatic technique, like the programs NuSMUGA [12] and TMUGA [13]. Like NuSMUGA, drawing LV ROI's is all short axis slices in every time bin can derive accurate volume measurements when using an optimal cutoff, but you need an experienced user and it is clear that such a way of processing is very time-consuming and will not be popular in clinical practice. Moreover, there is to our knowledge no possibility to process the RV with NuSMUGA in contrast to TMUGA, with even a comparison of LV and RV cardiac output measurements from TRV compared with the thermodilution method [13]. The more the software is automatic (and reproducible), the more errors it produces and on the contrary, the more manual, the more time-consuming it is.

For LVV calculations, the difference between the program with smallest values (4D-MSPECT) and largest values (BP-SPECT) is almost double. The difference between 4D-MSPECT and BP-SPECT in volume calculation was also shown in a four-chamber cardiac phantom experiment (submitted) whereas BP-SPECT overestimated LVV in another biventricular cardiac phantom experiment [14].

The discussion about what technique gives the exact EF is inferior to the fact that TRV gives additional information, like each tomographic examination gives more information than a planar one. In this view it is also important to stress that, when describing a TRV, visual analysis of global and regional kinetic function of both ventricles should be included, even before delineation of ventricular volumes, without the influence of any (computerized) calculation. There were patients included in this study with a lower LVEF on PRV who showed a good contractility on TRV, and this is probably the cause of the "overestimation" of LVEF on TRV compared to PRV, but analysis of the gated reconstructed short axis slices showed a perfect contractility.

Limitations

Using PRV as gold standard for LVEF is acceptable but validation of TRV, a technique that can produce volumes and EF of both ventricles, is better done by MRI, but this was not available in our database of patients.

The relatively limited number of patients with impaired LV function (73% were cancer patients studies pre- and post chemotherapy) should also be stressed.

CONCLUSION

LVEF calculated from TRV with the four described methods correlate well with those from PRV and can be applied in clinical practice, although the values are not interchangeable with other techniques and even not within the same technique with other types of software.

Volume calculations from TRV, especially from the RV, need further validation, mainly with other techniques, such as MRI, before they can be applied in clinical practice

REFERENCES

1. Nichols K, Saouaf R, Ababneh AA, Barst RJ, Rosenbaum MS, Groch MW, Shoyeb AH, Bergmann SR. Validation of SPECT equilibrium radionuclide angiographic right ventricular parameters by cardiac magnetic resonance imaging. *J Nucl Cardiol* 2002; 9:153-160
2. Van Krieking SD, Berman DS, Germano G. Automatic quantification of left ventricular ejection fraction from gated blood pool SPECT. *J Nucl Cardiol* 1999; 6:498-506
3. Vanhove C, Franken PR, Defrise M, Momen A, Everaert H, Bossuyt A. Automatic determination of left ventricular ejection fraction from gated blood-pool tomography. *J Nucl Med* 2001; 42:401-407
4. Ficaro EP, Quaife RF, Kritzman JN, Corbett JR. Validation of a New Fully Automatic Algorithm for Quantification of Gated Blood Pool SPECT: Correlations with Planar Gated Blood Pool and Perfusion SPECT. *J.Nucl.Med.* 2002; 5: 97P(Abstract)
5. Nichols K, Humayun N, De Bondt P, Vandenberghe S, Akinboboye OO, Bergmann SR. Model dependence of gated blood pool SPECT ventricular function measurements. *J Nucl Cardiol* 2004; 11:282-292
6. Germano G, Kiat H, Kavanagh PB, Moriel M, Mazzanti M, Su HT, Van Train KF, Berman DS. Automatic quantification of ejection fraction from gated myocardial perfusion SPECT. *J Nucl Med* 1995; 36:2138-2147
7. Vanhove C, Walgraeve N, De Geeter F, Franken PR. Gated myocardial perfusion tomography versus gated blood pool tomography for the calculation of left ventricular volumes and ejection fraction. *Eur J Nucl Med Mol Imaging* 2002; 29:735-741
8. Vanhove C, Franken PR. Left ventricular ejection fraction and volumes from gated blood pool tomography: comparison between two automatic algorithms that work in three-dimensional space. *J Nucl Cardiol* 2001; 8:466-471
9. Vanhove C, Franken PR, Defrise M, Bossuyt A. Comparison of 180 degrees and 360 degrees data acquisition for determination of left ventricular function from

- gated myocardial perfusion tomography and gated blood pool tomography. *Eur J Nucl Med Mol Imaging* 2003; 30:1498-1504
10. Ficaro EP, Quaife RF, Kritzman JN, Corbett JR. Accuracy and reproducibility of 4D-MSPECT for estimating left ventricular ejection fraction in patients with severe perfusion abnormalities. *Circulation* 2004; 100: I-26(Abstract)
 11. Bartlett ML, Srinivasan G, Barker WC, Kitsiou AN, Dilsizian V, Bacharach SL. Left ventricular ejection fraction: comparison of results from planar and SPECT gated blood-pool studies. *J Nucl Med* 1996; 37:1795-1799
 12. Groch MW, Marshall RC, Erwin WD, Schippers DJ, Barnett CA, Leidholdt EM, Jr. Quantitative gated blood pool SPECT for the assessment of coronary artery disease at rest. *J Nucl Cardiol* 1998; 5:567-573
 13. Mariano-Goulart D, Collet H, Kotzki PO, Zanca M, Rossi M. Semi-automatic segmentation of gated blood pool emission tomographic images by watersheds: application to the determination of right and left ejection fractions. *Eur J Nucl Med* 1998; 25:1300-1307
 14. De Bondt P, Nichols K, Vandenberghe S, Segers P, De Winter O, Van de WC, Verdonck P, Shazad A, Shoyeb AH, De Sutter J. Validation of gated blood-pool SPECT cardiac measurements tested using a biventricular dynamic physical phantom. *J Nucl Med* 2003; 44:967-972
 15. Slart RH, Poot L, Piers DA, van Veldhuisen DJ, Nichols K, Jager PL. Gated blood-pool SPECT automated versus manual left ventricular function calculations. *Nucl Med Commun* 2004; 25:75-80
 16. Wright GA, Thackray S, Howey S, Cleland JG. Left ventricular ejection fraction and volumes from gated blood-pool SPECT: comparison with planar gated blood-pool imaging and assessment of repeatability in patients with heart failure. *J Nucl Med* 2003; 44:494-498
 17. Daou D, Harel F, Helal BO, Fourme T, Colin P, Lebtahi R, Mariano-Goulart D, Faraggi M, Slama M, Le Guludec D. Electrocardiographically gated blood-pool SPECT and left ventricular function: comparative value of 3 methods for ejection fraction and volume estimation. *J Nucl Med* 2001; 42:1043-1049
 18. Groch MW, Depuey EG, Belzberg AC, Erwin WD, Kamran M, Barnett CA, Hendel RC, Spies SM, Ali A, Marshall RC. Planar imaging versus gated blood-

pool SPECT for the assessment of ventricular performance: a multicenter study.
J Nucl Med 2001; 42:1773-1779

19. Daou D, Coaguila C, Benada A, Razzouk M, Haidar M, Colin P, Lebtahi R, Slama M, Guludec DL. The value of a completely automatic ECG gated blood pool SPECT processing method for the estimation of global systolic left ventricular function. Nucl Med Commun 2004; 25:271-276
20. Chin BB, Bloomgarden DC, Xia W, Kim HJ, Fayad ZA, Ferrari VA, Berlin JA, Axel L, Alavi A. Right and left ventricular volume and ejection fraction by tomographic gated blood-pool scintigraphy. J Nucl Med 1997; 38:942-948

CHAPTER 8:
COMPARISON OF “QUBE” AND “4D-
MSPECT” TOMOGRAPHIC
RADIONUCLIDE VENTRICULOGRAPHY
CALCULATIONS TO MAGNETIC
RESONANCE IMAGING

Pieter De Bondt¹, Kenneth Nichols², Rola Saouaf³, Olivier De Winter¹, Johan De
Sutter⁴, Rudi Andre Dierckx⁵, Steven R. Bergmann⁶

¹ Division of Nuclear Medicine, Ghent University Hospital, Ghent, Belgium

² Division of Nuclear Medicine, Long Island Jewish Medical Center, New Hyde Park,
NY.

³ Department of Radiology, UCLA Medical Center, Los Angeles, CA

⁴ Division of Cardiology, Ghent University Hospital, Ghent, Belgium

⁵ PET-centrum - Nuclear Medicine, GUMC, Groningen, The Netherlands

⁶ Division of Cardiology, Beth-Israel Medical Center, New York, NY.

Submitted to J Nucl Med

SUMMARY

Background: Different algorithms are now being distributed to process tomographic radionuclide ventriculographic (TRV) data, but for some of them there is little literature regarding validations. Therefore, we compared left ventricular (LV) and right ventricular (RV) volumes and ejection fraction (EF's) computed by two different unvalidated TRV algorithms (QUBE and 4D-MSPECT) that use a surface-gradient approach against magnetic resonance imaging (MRI), the gold standard for ventricular volumes, and against two other TRV algorithms for which MRI validations have previously been reported (QBS, another surface-gradient approach, and BP-SPECT, a count-threshold approach).

Methods and Results: Twenty-eight patients with primary arterial hypertension (PAH) or tetralogy of Fallot (TOF) were evaluated with planar radionuclide ventriculography (PRV), tomographic radionuclide ventriculography (TRV) and MRI. LV volumes were compared between MRI, QUBE, 4D-MSPECT, QBS and BP-SPECT, while LVEF was compared among those methods and PRV. RV volumes were compared among MRI, QUBE, QBS and BP-SPECT methods, while RVEF was compared among those methods and PRV. By ANOVA, there were significant differences among LVEF and RVEF values, with values being significantly lower than MRI LVEF's for QBS and PRV, and significantly higher for QUBE. An underestimation was found for LVV calculations from QBS, QUBE and 4DM-SPECT compared to MRI. PRV significantly underestimated RVEF compared to MRI. An underestimation of RVV calculations was seen for QBS, whereas QUBE overestimated RVV.

Conclusions: TRV surface-gradient methods that computed volumes, and that derived EF's from volumes, were found to be sub-optimal, compared to the BP-SPECT count-threshold method.

INTRODUCTION

Currently, several different algorithms are commercially distributed to analyze tomographic radionuclide tomographic (TRV) data. Among these, three surface-gradient method (QBS [1], QUBE [2], 4D-MSPECT [3]) and one count-threshold method (BP-SPECT [4]) were recently described with validation studies against planar radionuclide ventriculography (PRV) [1;2], gated myocardial perfusion SPECT [3] and/or cardiac phantom studies [5;6]. Of the various computational methods, only the QBS and BP-SPECT algorithms have been validated against magnetic resonance imaging (MRI) data, for both the left ventricle (LV) and for the right ventricle (RV) [4;7]. Those validation studies were performed for 28 patients with primary arterial hypertension (PAH) or tetralogy of Fallot, for whom RV EF was expected to be abnormally low and/or RV volumes abnormally large so that only MRI validations were considered to be the only reliable method of comparison. The aim of this study was to use QUBE and 4D-MSPECT to process these data for the same 28 patients, as QUBE and 4D-MSPECT have not previously been validated against MRI data, and to compare RV and LV measurements among all TRV methods, PRV and MRI.

MATERIALS AND METHODS

The patient data were collected between 1st September 2001 and 1st February 2003, at Columbia University. There were 16 men and 12 women, mean age \pm standard deviation (SD) was 28 ± 14 years. 15 patients suffered from PAH and 13 from TOF. All nuclear and MR imaging procedures were performed within 1 month of one another (mean interval = 10 ± 10 days). No patient experienced any significant cardiac event between studies, and none had changes in medical or surgical therapy.

Magnetic Resonance Imaging

A 1.5 Tesla scanner ("LX" or "Signa Horizon," General Electric Medical Systems, Inc., Milwaukee, WI) with a body phased array surface coil was used for cardiac gated gradient-echo cine MRI data acquisitions. The cine images were acquired using a "Spoiled Gradient Recall" (SPGR) non-breath-hold technique (n=8) (TR Min TE 13, FA 30, Matrix 256 x 128, FOV 30-41, NEX 1, Sl Thickness 8, gap 0) or a breath-hold technique (n=20) (TR Min TE min full, FA 15, Matrix 256 x 128, FOV 30-41, NEX 1, Sl thickness 8, gap 0). Data were acquired gated at 16-20 frames/R-R

interval. Gated short axis slices spanned the entire heart, from beneath the apex to above the AV valves.

Semi-automated algorithms ("Cardiac Analysis" software from General Electric Medical Systems, Inc., Milwaukee, WI) were used for the segmentation of left and right ventricles for all short axis sections at ED and ES. Automatically-generated outlines were visually reviewed and manually altered as necessary, to conform to the observer's visual impression of endocardium. Trabeculation were manually excluded. EV and ES volumes were obtained by summing short axis slices by Simpson's rule.

PRV Studies

Conventional PRV was performed for all patients in the left anterior oblique projection that optimized septal separation of the RV from the LV. For adults, injected Tc-99m-pertechnetate activity was 925 MBq (25 mCi), following injection of 5 milligrams of pyrophosphate. For patients under 18 years of age whose body weight was less than 70 kg, these injections were scaled linearly downward for body weight. Clinical data were acquired at both institutions with the same commercially available gamma cameras ("Vertex," ADAC Corporation, Milpitas, CA). As these were dual-detector gamma cameras, no caudal tilt was used in positioning patients for PRV. A 20% energy window centered on 140 keV was used for data acquisition, with low energy general-purpose (LEGP) collimation. Data were acquired as 64x64 matrices, gated for 24 frames per R-R interval for 10 minutes.

TRV Data Acquisition

Immediately following PRV data collection, all patients then underwent TRV data acquisition. A dual detector gamma camera ("Vertex," ADAC Corporation Milpitas, CA, USA) was used to collect images at 64 projections over a 180° circular arc. 64x64 tomograms with a pixel size of 3.8 mm were acquired with LEGP collimators for 20 seconds per projection. Tomograms were acquired with patients at rest, at 8 frames per R-R interval, using a 100% R-wave window. Eight frames per R-R interval were used, as opposed to a larger number, to guarantee routine collection of sufficient tomographic counts per R-R interval.

All data sets were reviewed for any confounding imaging artifacts. Butterworth pre-filters (cutoff = .45 of Nyquist frequency, power = 5.0) were used for gated tomograms, followed by ramp filtering in the transaxial plane. Images were reoriented into short axis sections using manual choices of approximate LV symmetry axes, using

a commercially available computer system ("ICON," Siemens Medical Solutions, Inc., Chicago, IL).

TRV Data Processing

Data processing with QBS and BP-SPECT were performed at Columbia University and with algorithms QUBE and 4D-MSPECT at Ghent University Hospital. The version of QBS distributed by Siemens Medical Systems, Inc., was executed on a Siemens Esoft computer, while BP-SPECT was run on a Siemens "ICON" computer. QUBE and 4D-MSPECT were run on a conventional laptop PC running the Windows XP operating systems (Microsoft Corp., Redmond, WA, USA). All algorithms used gated short axis images for import in DICOM format. A description of the modelling assumptions and modes of operation of the algorithms is given at length elsewhere [6], but briefly, QBS, QUBE and 4D-MSPECT are primarily based on a surface-gradient approach [1], [2], [3], whereas BP-SPECT is primarily a count-threshold method [4]. All 4 TRV methods computed LVEF, LVEDV and LVESV values. QUBE, QBS and BP-SPECT also computed RVEF, RVEDV and RVESV values, but 4D-MSPECT did not. In the process of running these algorithms on the TRV data, it was impossible to get QBS to process data for the patient with the largest LVEDV (with an MRI value of 344 mL). All other algorithms were able to process that data, and all other data.

TRV regional wall motion assessment

Both QUBE and 4D-MSPECT provide displays of parameters relevant to regional wall motion. In the case of QUBE, this program uses several views of the LV to display regional EF, using a 10% color bar scale, whereas 4D-MSPECT displays wall motion in units of mm on a polar map. Neither QBS nor BP-SPECT displayed information in this fashion. To assess the degree to which QUBE and 4D-MSPECT calculations reflect visual observations, an expert observer (PDB) graded his impression of wall motion on a 5-point scale (0: Normal, 1: Mild Hypokinesis, 2: Moderate Hypokinesis, 3: Severe Hypokinesis, 4: Akinesis, 5: Dyskinesis) as perceived by the observer when reviewing TRV endless cine loops. To simplify the process of performing these comparisons, only apical visual scores were compared to QUBE regional EF and 4D-MSPECT wall motion values.

Statistical Analysis

All statistical analyses were performed by "SPSS 13.0" statistical software (SPSS, Inc., Chicago, IL, USA). χ^2 analyses were used to test whether data were normally

distributed. Results are reported below as mean values \pm 1 standard deviation. ANOVA was used to test for differences among all values considered together, and Bonferoni post hoc tests were performed to identify differences between pairs of values. Correlations between TRV and MRI values were expressed as the Pearson correlation coefficient (r). Variability about the regression line was expressed as the standard error of the estimate (SEE). Bland-Altman analyses of differences between pairs of estimated and reference values were used to search for trends and systematic errors. Rank correlation was used to computed Spearman's rho coefficient for QUBE LV and RV apical regional EF values and 4D-MSPECT LV regional wall motion values versus visual motion scores. Differences between strengths of correlation were assessed by the F-test. Statistical significance was defined as $p < 0.05$ for all tests but ANOVA, for which $p < 0.05/(v-1)$ was considered significant.

RESULTS

All results for LV and RV were normally distributed and summarized in table 1. Figures 1 – 6 display linear regression and Bland-Altman curves for LVEF, LVEDV, LVESV, RVEF, RVEDV and RVESV.

Left Ventricle

ANOVA showed significant differences among methods for LVEF ($p = 0.000$) and LVEDV ($p = 0.000$) and for LVESV ($p = 0.000$). LVEF values were significantly lower than MRI for QBS and PRV, and significantly higher for QUBE (Table 1).

	LV EDV (mL)	LV ESV (mL)	LV EF (%)	RV EDV (mL)	RV ESV (mL)	RV EF (%)
MRI	92 \pm 36	36 \pm 23	63 \pm 12	143 \pm 94	87 \pm 63	41 \pm 10
QUBE	76 \pm 32 #	21 \pm 15 #	73 \pm 17 #	189 \pm 119 #	102 \pm 77	48 \pm 17 #
4D-MSPECT	62 \pm 28 #	24 \pm 13 #	61 \pm 11			
QBS	80 \pm 46	50 \pm 41	43 \pm 20 #	143 \pm 81	86 \pm 66	44 \pm 16
BP-SPECT	101 \pm 34	86 \pm 66	64 \pm 13	163 \pm 107 #	96 \pm 74	44 \pm 11
PRV			57 \pm 13 #			34 \pm 12 #

Table 1

= $p < 0.05$ versus MRI

QBS LVEF values were significantly lower than MRI ($p = 0.004$), QUBE ($p = 0.000$), 4D-MSPECT ($p = 0.011$) and BP-SPECT ($p = 0.002$), but not for PRV ($p = 0.110$). QUBE, on the contrary, produced significantly higher LVEF values than QBS ($p = 0.000$) and PRV ($p = 0.009$).

By the F-test, LVEF correlations versus MRI were not significantly different ($p=0.09$) for PRV ($r=0.72$; $p=0.00$), BP-SPECT ($r=0.77$; $p = 0.00$), QUBE ($r=0.50$; $p = 0.01$), 4D-MSPECT LVEF ($r=0.48$; $p = 0.01$) or QBS LVEF ($r=0.40$; $p = 0.02$). The underestimation of QBS and overestimation of QUBE was such that their mean differences were -20% and $+10\%$, respectively. The standard error of the estimate (SEE) was lower for BP-SPECT and 4D-MSPECT (8% and 13%) and higher for QUBE and QBS (18% and 26%). Bland-Altman analysis demonstrated a significant trend only for 4D-MSPECT ($p = 0.01$), with an overestimation for lower values of LVEF and an underestimation for higher values of LVEF (Figure 1).

LVEDV and LVESV values were significantly lower than MRI for QUBE and 4D-MSPECT (Table 1). Among TRV methods, only BP-SPECT and 4D-MSPECT LVEDV values differed from one another ($p= 0.001$). For LVESV, the calculations from QUBE and 4D-MSPECT were significantly lower than any other methods of processing TRV.

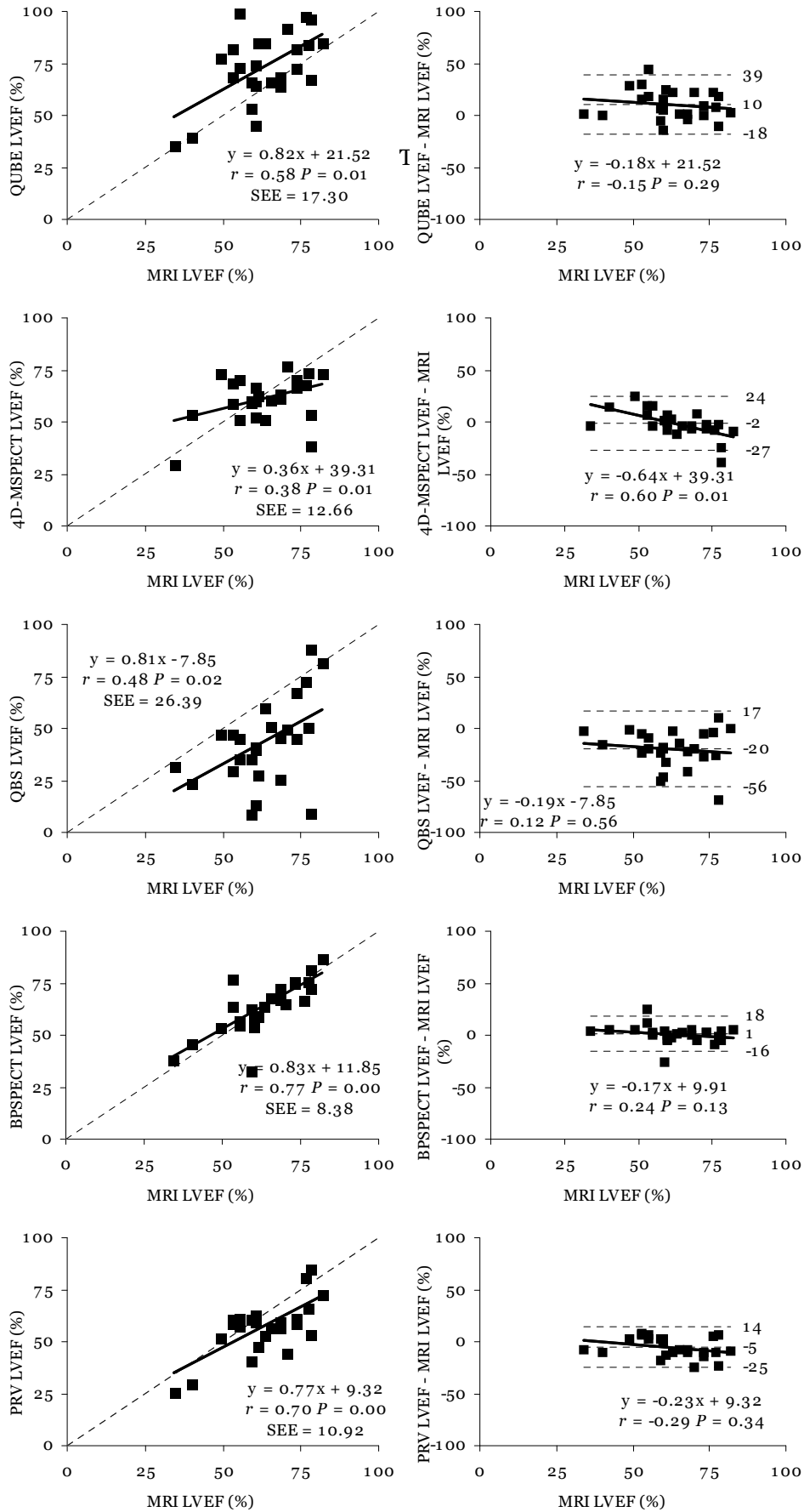


Figure 1 Comparison of PRV LVEF and TRV LVEF with MRI

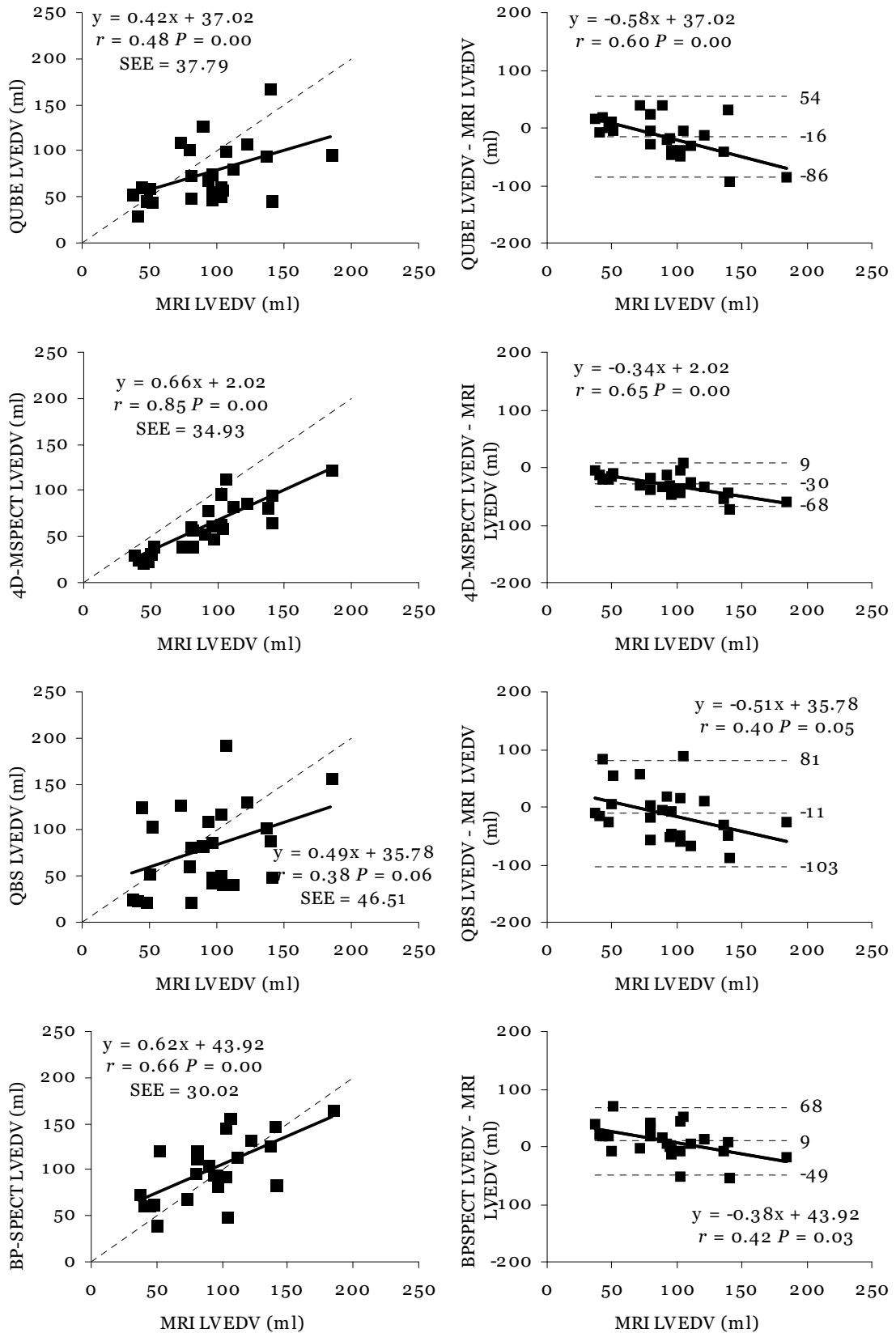


Figure 2 Comparison of TRV LVEDV with MRI LVEDV

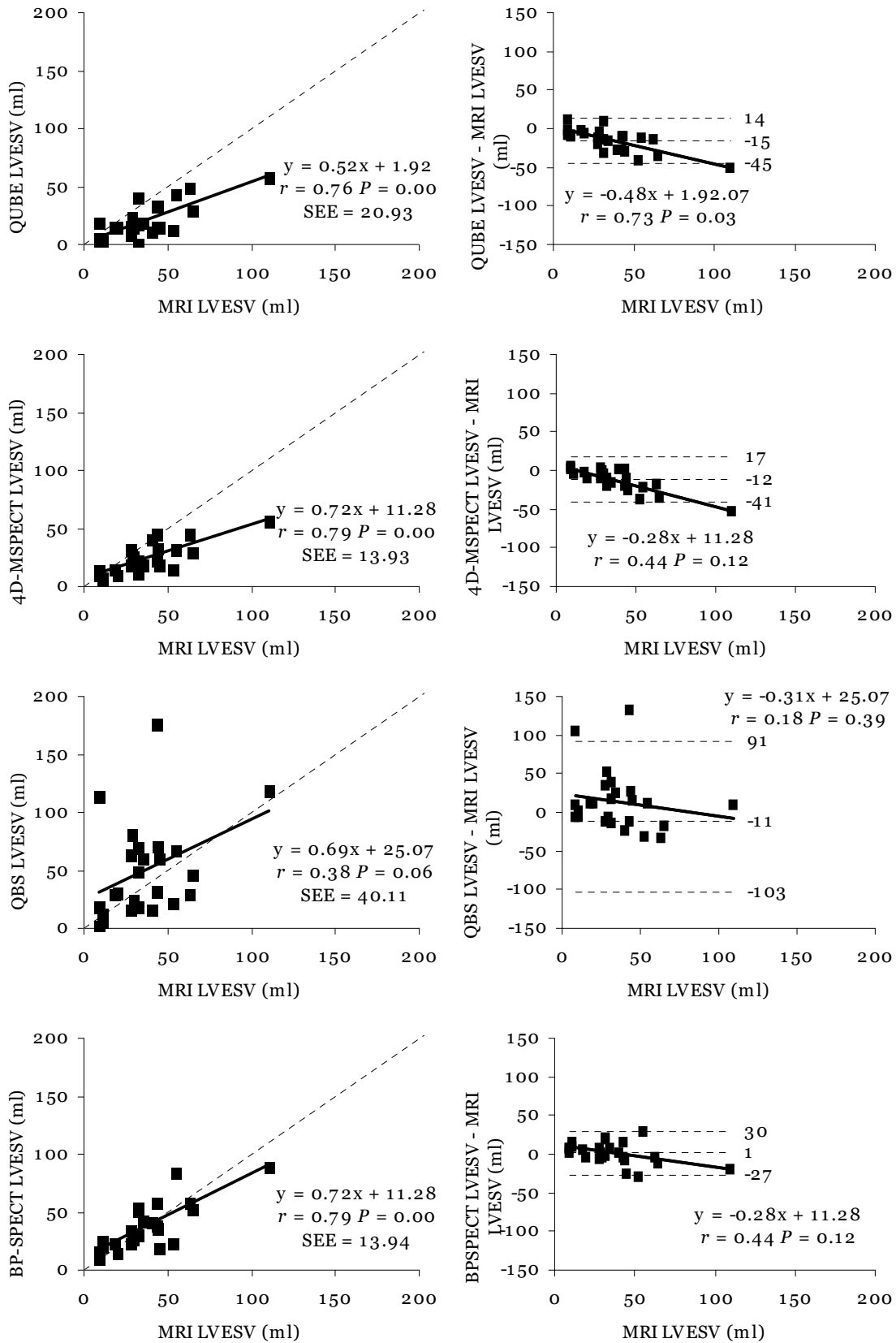


Figure 3 Comparison of TRV LVESV with MRI LVESV

QBS LVEDV and LVESV values were not significantly correlated to MRI values ($r=0.38$; $p = 0.06$ and $r=0.38$; $p = 0.06$ respectively) (Figures 2-3). Also, LVEDV and LVESV linear correlations were significantly weaker ($p<0.02$) versus MRI for QBS than for 4D-MSPECT (0.85 ; $p = 0.00$ and 0.79 , $p = 0.00$) and BP-SPECT (0.66 ; $p = 0.00$ and 0.79 ; $p = 0.00$). A significant trend toward a greater degree of underestimation for higher values of LVEDV was found for QUBE ($p = 0.00$), 4D-MSPECT ($p = 0.00$), QBS ($p = 0.05$) and BP-SPECT ($p = 0.03$) (Figures 2-3). For LVESV, this trend was seen only for QUBE ($p = 0.03$).

Right ventricle

ANOVA found significant differences among methods for RVEF ($p = 0.023$), but not for RVEDV ($p = 0.457$) or RVESV ($p = 0.848$). Among the radionuclide methods that computed RV parameters, PRV RVEF was significantly lower only compared to QUBE RVEF ($p = 0.040$). RVEF was significantly lower than MRI measurements only for PRV (Table 1).

For RVEF, the lowest correlation versus MRI was found for QBS (0.44 ; $p = 0.03$), which was significantly weaker ($p=0.04$) than BP-SPECT ($r=0.79$; $p = 0.00$), but not lower than QUBE ($r=0.60$; $p = 0.00$). The RVEF correlation between PRV and MRI was $r=0.77$, $p = 0.00$. No significant Bland-Altman RVEF trends were found for any of the techniques (Figure 4).

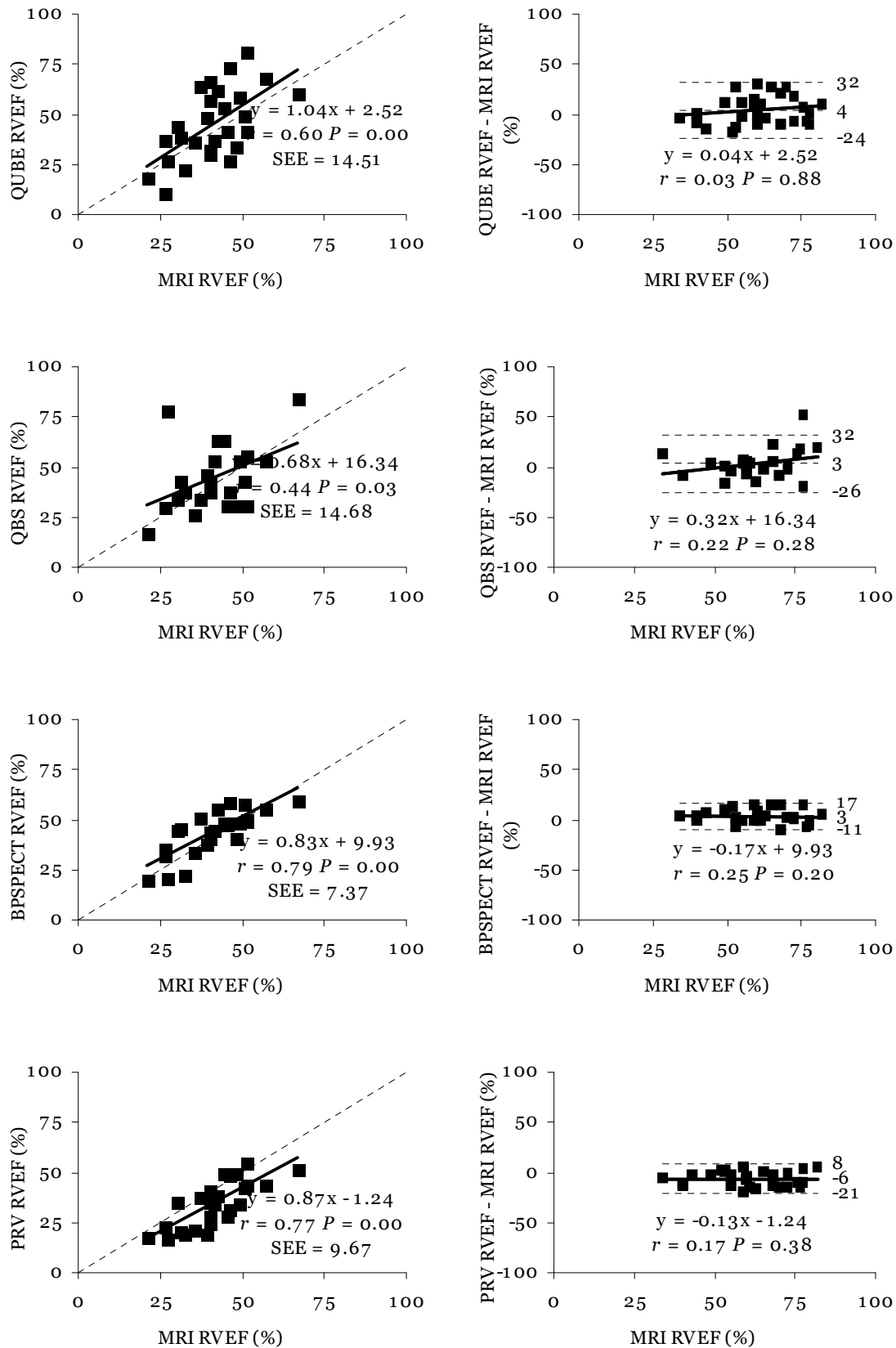


Figure 4
 Comparison of PRV and TRV (QBS, QUBE and BP-SPECT) RVEF to MRI RVEF.

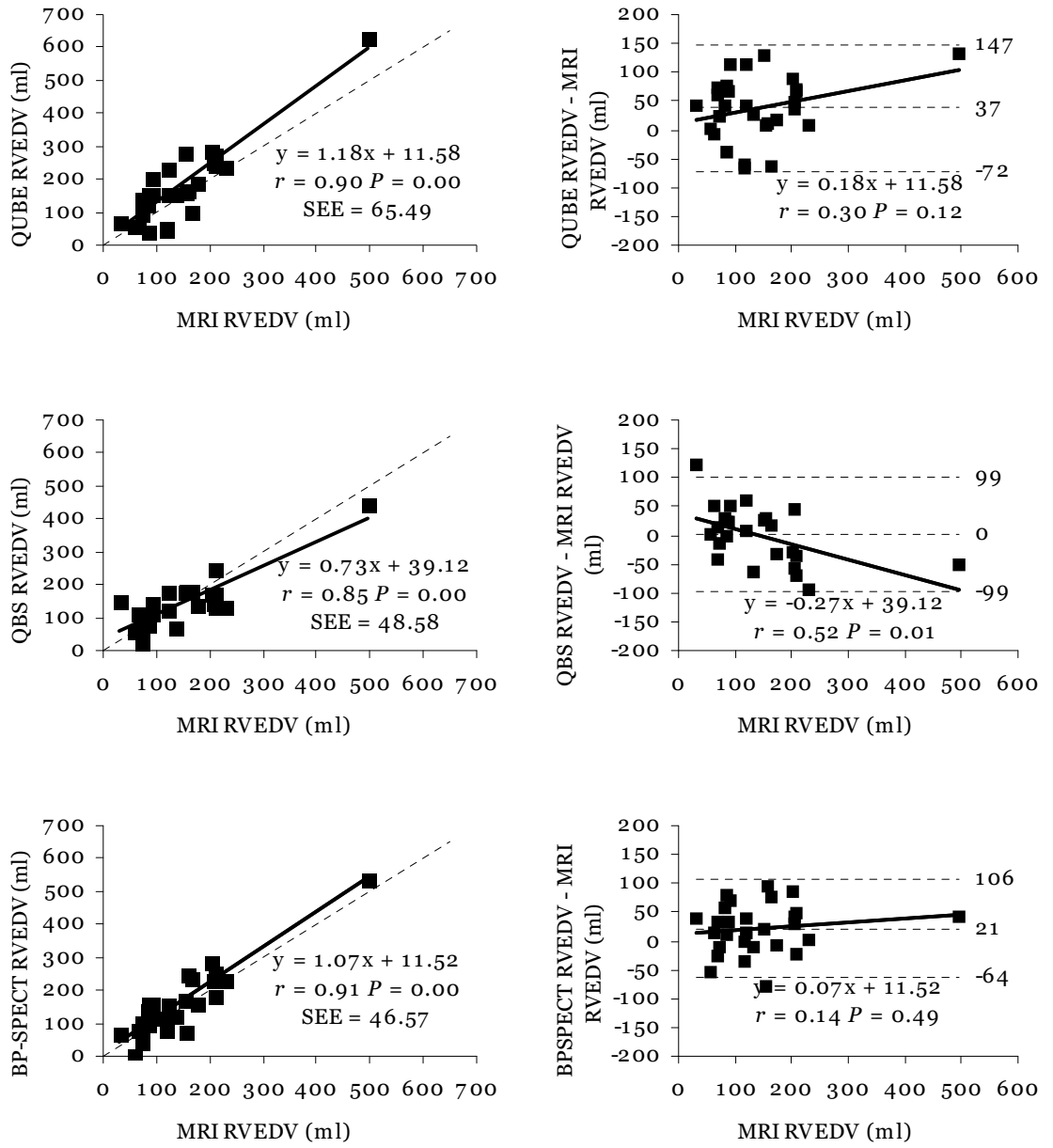


Figure 5
Comparison of TRV (QBS, QUBE and BP-SPECT) RVEDV to MRI RVEDV

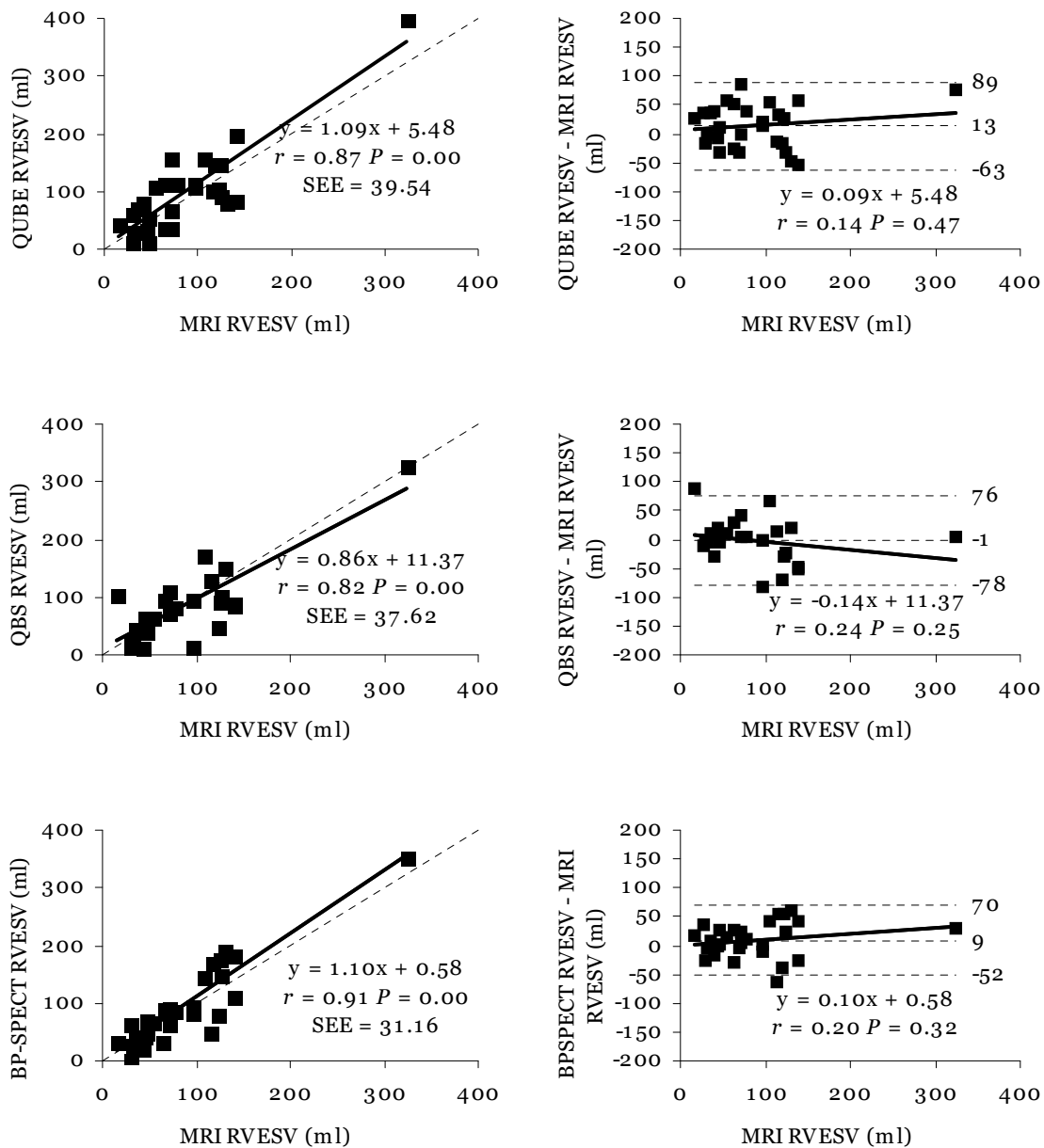


Figure 6
Comparison of TRV (QBS, QUBE and BP-SPECT) RVESV to MRI RVESV.

Linear regression correlations for RVEDV and RVESV were 0.85 and 0.82 for QBS, 0.90 and 0.87 for QUBE, and 0.91 and 0.91 for BP-SPECT (Figures 5-6). A significant trend of underestimation at higher RVEDV volume values was found only for QBS ($r = 0.52$, $p = 0.01$). No significant trends were found for RVESV for any of the 3 TRV algorithms.

Visual score LV	Patients n	QUBE RLVEF (%)	4D-MSPECT wall motion (mm)
0	18	56.7	9.5
1	6	50.8	9.1
2	1	35.0	5.6
3	1	15.0	3.8
4	1	5.0	1.5
5	1	-10.0	2.4

Table 2

Mean regional LVEF calculated by QUBE and mean wall motion calculated by 4D-MSPECT in the LV apex, compared with visual analysis.

Visual score (0: Normal, 1: Mild Hypokinesis, 2: Moderate Hypokinesis, 3: Severe Hypokinesis, 4: Akinesis, 5: Dyskinesis)

TRV regional wall motion assessment

In table 2 are tabulated regional kinetic information of the LV apex derived from visual analysis as compared to values of regional EF from QUBE and 4D-MSPECT for patients grouped according to visual wall motion scores. By rank correlation analysis, QUBE regional EF correlated to visual scores as $r = -0.494$, $P = 0.010$, while 4D-MSPECT correlated to visual scores as $r = -0.237$, $P = 0.219$. In the group of normal ventricular function (i.e., those with a score of “0”) 9/20 (45%) patients showed a regional ejection fraction of less than 50% (QUBE), but all patients who were scored visually as “1” in the LV apex (mild hypokinesis) had wall motion values equal or higher than 8 mm (4D-MSPECT), which is considered to be a normal value in the apex [8]. Thus, the apical wall motion of the LV was often underestimated by QUBE and overestimated by 4D-MSPECT.

Visual score RV	Patients n	QUBE RRVEF (%)
0	6	80.8
1	1	100.0
2	2	40.0
3	10	53.0
4	3	21.7
5	6	23.0

Table 3

Mean regional RVEF calculated by QUBE in the LV apex, compared with visual analysis.

Visual score (0: Normal, 1: Mild Hypokinesis, 2: Moderate Hypokinesis, 3: Severe Hypokinesis, 4: Akinesis, 5: Dyskinesis)

Table 3 displays apical regional RV EF from QUBE for patients grouped according to visual wall motion scores. By rank correlation analysis, QUBE regional RVEF correlated to visual scores as $r = -0.790$, $P = 0.000$. In the RV, overestimation of regional kinetic information was found to be most pronounced in hypokinetic apical regions. That is, 5/10 (50%) patients who were scored visually as exhibiting severe hypokinesis were reported by QUBE to have regional RVEF values exceeding 50%.

DISCUSSION

Conventional planar radionuclide ventriculography values of LVEF correlated significantly with MRI values, but PRV significant underestimated LVEF. It is likely that for the patient population, characterized by impaired RV function, dilated right ventricles overlapped other cardiac structures to some extent, including the LV. This would give rise to misinterpretation of LV and RV outlines in the left anterior oblique projection, as some RV counts would be expected to “shine through” the LV under those imaging conditions [9]. Given this likelihood, PRV performed well for LVEF, and surprisingly well for RVEF.

QUBE and 4D-MSPECT demonstrated an underestimation for the calculation of LVV to the greatest degree of all of the algorithms, particularly at end-diastole. Regression and Bland-Altman graphs of LVV were similar to those reported by us [6], in that previously we found for dynamic 4-chamber phantom experiments the same degree of underestimation of LVV compared to true values, with mean difference values

between -16.61 mL for BP-SPECT and -39.83 mL for QBS. The reason for this underestimation is not entirely clear. It is possible that a sub-optimal percentage of gradient threshold definition for ventricular segmentation could contribute to this finding for QBS and 4D-MSPECT. Use of a fixed threshold value, either for a count-threshold method or for a gradient-surface method, may necessarily produce errors for both smaller and larger volumes than for average-sized volume values [10].

For larger RV's, QBS underestimated RVV compared to MRI, consistent our with previous phantom experiments for the algorithms QBS and BP-SPECT [6], while QUBE overestimated RVV. These findings strengthen the impression, stated previously [7], that QBS has some difficulty in defining the correct plane of the RV outflow tract in clinical data, resulting in RV volume underestimation. QUBE RV volume overestimation could be due to the fact that QUBE places the pulmonary valve and the tricuspid valve in a single plane, as we have observed in some cases as seen on the vertical long axis trough the RV (arrow in Figure 7.)

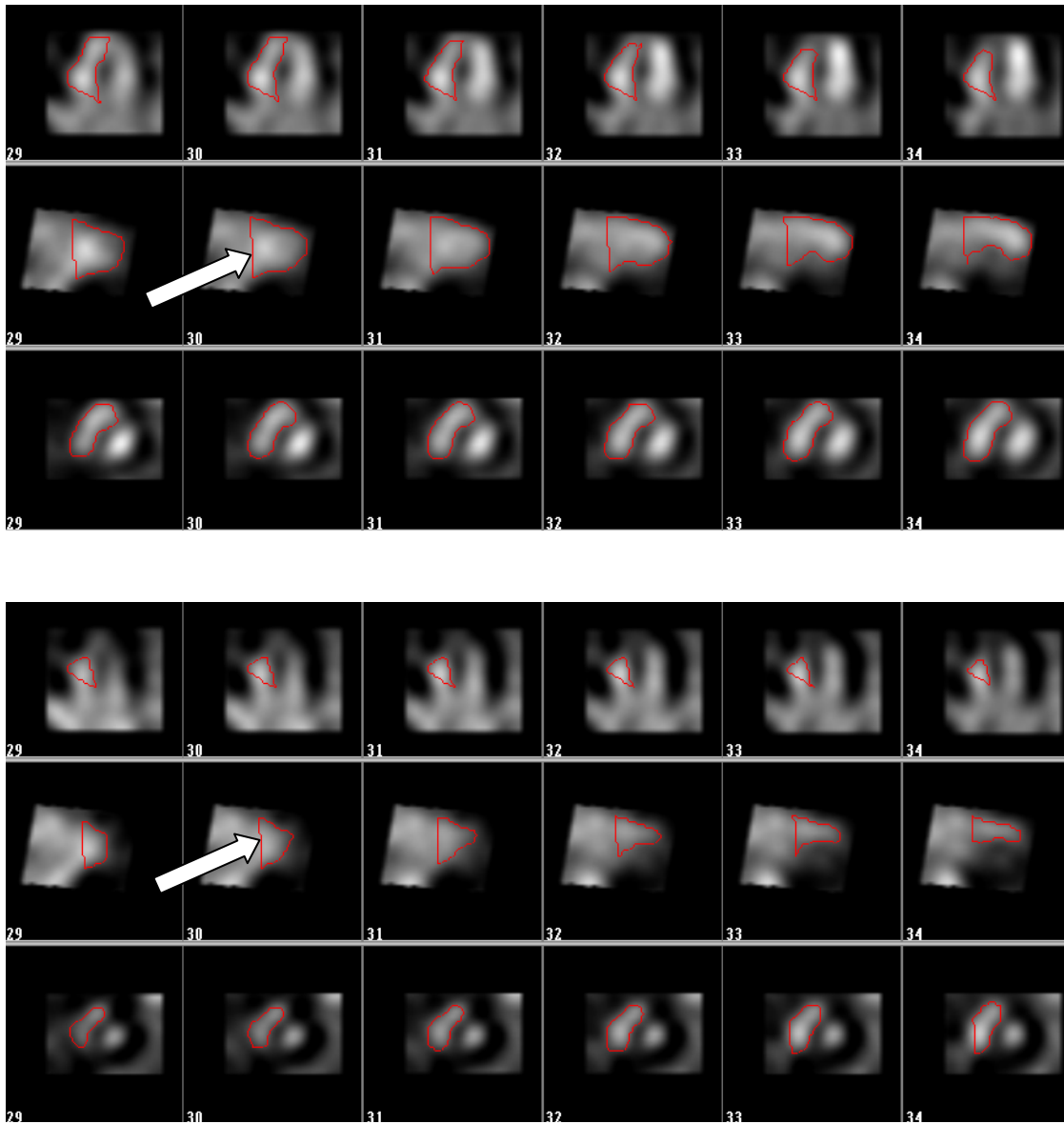


Figure 7

Upper: RV outline in horizontal long axis (upper row), vertical long axis (middle row) and short axis (lower row) in end-diastolic position
 Lower: RV outline in horizontal long axis (upper row), vertical long axis (middle row) and short axis (lower row) in end-systolic position

Limitations

For the LVV calculations, QBS had the lowest correlation. This finding was influenced by the fact that for the scan with largest LVEDV on MRI (344 mL), the data could not be processed by QBS, which instead resulted in an error message, thereby yielding a smaller range of volume values, for which r-values are consequently lower [11]. Also, the patient population used for this investigation is unusual, in that primary pulmonary arterial hypertension is a very rare condition, as is tetralogy of Fallot. Further experience in comparing TRV to MRI calculations in a wider variety of patients, particularly those with CHF and those with no known cardiac disease, would be very helpful in clarifying methodological differences for more typical clinical settings.

CONCLUSION

TRV has the potential to evaluate biventricular kinetic information, regional wall motion, and volumetric parameters in addition to global ejection fraction. However, careful review of computed endocardial walls, and visual comparison to actual perceived wall locations, is essential in interpreting volume calculations for the different algorithms, considering that most TRV algorithms underestimate LVV but overestimate RVV. Therefore, it is our opinion that ventricular volume calculation necessitates a critical review of the underlying mechanisms of the TRV algorithms. Based on the overall higher correlation of BP-SPECT to MRI RV and LV values, smaller SEE values, and closer agreement to mean MRI values, BP-SPECT currently represents the method of choice when reporting TRV volume calculations in conjunction with reporting RV and LV ejection fractions.

REFERENCES

1. Van Kriekinge SD, Berman DS, Germano G. Automatic quantification of left ventricular ejection fraction from gated blood pool SPECT. *J Nucl Cardiol* 1999; 6(5):498-506.
2. Vanhove C, Franken PR, Defrise M, Momen A, Everaert H, Bossuyt A. Automatic determination of left ventricular ejection fraction from gated blood-pool tomography. *J Nucl Med* 2001; 42(3):401-407.
3. Ficaro EP, Quaife RF, Kritzman JN, Corbett JR. Validation of a New Fully Automatic Algorithm for Quantification of Gated Blood Pool SPECT: Correlations with Planar Gated Blood Pool and Perfusion SPECT. *J.Nucl.Med.* 5, 97P. 2002. Abstract
4. Nichols K, Saouaf R, Ababneh AA, Barst RJ, Rosenbaum MS, Groch MW et al. Validation of SPECT equilibrium radionuclide angiographic right ventricular parameters by cardiac magnetic resonance imaging. *J Nucl Cardiol* 2002; 9(2):153-160.
5. De Bondt P, Nichols K, Vandenberghe S, Segers P, De Winter O, Van de WC et al. Validation of gated blood-pool SPECT cardiac measurements tested using a biventricular dynamic physical phantom. *J Nucl Med* 2003; 44(6):967-972.
6. De Bondt P, Claessens T, Rys B, De Winter O, Vandenberghe S, Segers P et al. Accuracy of 4 different algorithms for the analysis of tomographic radionuclide ventriculography using a physical, dynamic 4-chamber cardiac phantom. *J Nucl Med* 2005; 46(1):165-171.
7. Nichols K, Humayun N, De Bondt P, Vandenberghe S, Akinboboye OO, Bergmann SR. Model dependence of gated blood pool SPECT ventricular function measurements. *J Nucl Cardiol* 2004; 11(3):282-292.
8. Cain P, Baglin T, Khoury V, Case C, Marwick TH. Automated regional myocardial displacement for facilitating the interpretation of dobutamine echocardiography. *Am J Cardiol* 2002; 89(12):1347-1353.
9. Bartlett ML, Srinivasan G, Barker WC, Kitsiou AN, Dilsizian V, Bacharach SL. Left ventricular ejection fraction: comparison of results from planar and SPECT gated blood-pool studies. *J Nucl Med* 1996; 37(11):1795-1799.

10. King MA, Long DT, Brill AB. SPECT volume quantitation: influence of spatial resolution, source size and shape, and voxel size. *Med Phys* 1991; 18(5):1016-1024.
11. Bland JM, Altman DG. Statistical methods for assessing agreement between two methods of clinical measurement. *Lancet* 1986; 1(8476):307-310.

CHAPTER 9:

NORMAL VALUES FOR LEFT AND RIGHT VENTRICULAR EJECTION FRACTION AND VOLUMES FROM TOMOGRAPHIC RADIONUCLIDE VENTRICULOGRAPHY

Pieter De Bondt^{1,2}, Olivier De Winter¹, Johan De Sutter³, Rudi Andre Dierckx¹

¹ Division of Nuclear Medicine, Ghent University Hospital, Ghent, Belgium,

² Division of Nuclear Medicine, OLV Hospital, Aalst, Belgium,

³ Department of Cardiology, Ghent University Hospital, Ghent, Belgium

Submitted to Nucl Med Commun

SUMMARY

Background: Different algorithms are developed to process tomographic (T) radionuclide ventriculographic (RV) studies. The aim of the study was to determine gender-related normal values for left ventricular (LV) ejection fraction (EF), right ventricular (RV) EF and LV and RV end-diastolic volumes (EDV) and end-systolic volumes (ESV) in a prospective normal database.

Methods and Results: 51 healthy volunteers (29 men and 22 women) were prospectively studied. All subjects had a normal electrocardiogram, a normal echocardiographic examination and underwent a planar RV and TRV acquisition. Four different algorithms were used to process the TRV: QBS, QUBE, 4D-MSPECT and BP-SPECT. Higher values of LVEF were found in TRV, compared to PRV. No significant differences were found in calculating LVEF and RVEF between men and women. Most of the software packages however could demonstrate significant higher ventricular volumes in men, compared to women. Most of the volume differences could not be eliminated after correction for Body surface area (BSA). Normal LV and RV EF and volumes were comparable with other cardiac imaging techniques.

Conclusions: Gender-specific normative values for LV and RV EF and volumes are important when evaluating cardiac function with TRV. Men show higher ventricular volumes compared to women. Higher LVEF was found with TRV, compared to PRV.

INTRODUCTION

Gender-related differences in normal left ventricular (LV) ejection fraction (EF), right ventricular (RV) EF and LV and RV end-diastolic volumes (EDV) and end-systolic volumes (ESV) have proven to be useful and are described for several cardiac imaging techniques (1-10). Different software programs have been developed to calculate LVEF, RVEF and LV and RV EDV and ESV from tomographic radionuclide ventriculography (TRV) [1; 2; 3; 4]. We wanted to set up a prospective normal database, from healthy volunteers, with left and right volumetric values for men and women separately and compare these values with other techniques in literature.

MATERIALS AND METHODS

51 healthy volunteers (29 men and 22 women) were prospectively studied. All individuals had no previous history of cardiovascular disease, hypertension or diabetes. All individuals had a normal electrocardiogram, a normal echocardiographic examination and were in sinus rhythm. Informed consent was signed by all volunteers.

Acquisition of tomographic radionuclide scintigraphy

All images were acquired on two three-headed gamma camera's (IRIX and Prism 3000, Marconi-Philips, Cleveland, Ohio) equipped with low energy high-resolution collimators. PRV data were acquired over a 5 minute period, in 16 electrocardiographic gated frames, 64 x 64 matrix, zoom 1.333 (pixel size 7 mm) and with a beat acceptance window at 20 % of the average R-R interval calculated just before the acquisition was started. The gamma camera was positioned in left anterior oblique projection in order to obtain the best "septal view". Parameters of TRV acquisition were as follows: 360° step-and-shoot rotation, 40 stops per head, 30 seconds per stop, 64 x 64 matrix, zoom 1.422 (pixel size 6.5 mm), and 16 time bins per R-R interval, with a beat acceptance window at 20% of the average R-R interval. Projection data were pre-filtered using a Butterworth filter (cutoff frequency: 0.5 cycles/cm; order: 5) and reconstructed by filtered backprojection using an x-plane ramp filter. Data were then reoriented into gated short axis tomograms. The resulting gated short axis data sets were then used as input for the four algorithms.

Processing of tomographic radionuclide scintigraphy

For the processing of the images, we used four software's: QBS (Quantitative Bloodpool SPECT® software from Cedars-Sinai Medical Center, Los Angeles, USA), QUBE (Free University of Brussels, Brussels, Belgium), 4D-MSPECT (University of Michigan Medical Center in Ann Arbor, Michigan, USA) and BP-SPECT (algorithms from Columbia University, New York, USA). The development and validation of these algorithms are being described elsewhere. [3; 5; 2; 6; 7; 8; 9; 1]

Statistical Analysis

Results were reported as mean values \pm 1 standard deviation (SD). Comparison between men and women was performed using Student's t-test for paired observations. Analysis of variance (ANOVA) with Bonferoni post hoc tests was performed to identify differences between groups. A value of $p < 0.05$ was considered statistically significant.

RESULTS

Demographic findings of the group of volunteers is described in table1.

	Overall group (n=51)	Men (n=29)	Women (n=22)
Age (years)	49.6 \pm 16.0	48.7 \pm 16.6	50.7 \pm 15.5
BMI (g/m ²)	24.5 \pm 3.8	25.3 \pm 3.3	23.6 \pm 4.3
BSA	1.9 \pm 0.2	2.0 \pm 0.2	1.7 \pm 0.2

Table 1

Results for ventricular EF, ventricular volumes and ventricular volumes corrected for BSA for the different techniques are listed in table 2.

	PRV		TRV: QBS		TRV: QUBE		TRV: 4D-MSPECT		TRV: BP-SPECT	
	Men	Women	Men	Women	Men	Women	Men	Women	Men	Women
LVEF	62 ± 8	60 ± 6	64 ± 8	65 ± 9 *	72 ± 7 *	72 ± 9 *	62 ± 6	65 ± 7	66 ± 7 *	65 ± 7 *
LVSV	-	-	82 ± 20 #	60 ± 16	70 ± 18	66 ± 16	53 ± 13 #	41 ± 13	83 ± 23 #	65 ± 24
LVEDV	-	-	130 ± 33 #	96 ± 31	97 ± 25	93 ± 23	85 ± 21 #	62 ± 17	127 ± 34 #	100 ± 30
LVESV	-	-	48 ± 19 #	35 ± 18	27 ± 13	27 ± 13	33 ± 10 #	22 ± 6	44 ± 16 #	35 ± 10
LVEDVi	-	-	66 ± 16 #	56 ± 16	49 ± 12	55 ± 11	44 ± 12 #	36 ± 8	65 ± 17	59 ± 18
LVESVi	-	-	24 ± 9	20 ± 9	14 ± 6	16 ± 7	17 ± 6 #	13 ± 4	23 ± 8	21 ± 7
RVEF	-	-	50 ± 10	52 ± 12	45 ± 7	48 ± 13	-	-	62 ± 6	63 ± 9
RVSV	-	-	78 ± 21 #	63 ± 20	73 ± 19 #	60 ± 14	-	-	101 ± 24 #	77 ± 25
RVEDV	-	-	159 ± 35 #	122 ± 32	161 ± 38 #	130 ± 31	-	-	165 ± 30 #	122 ± 33
RVESV	-	-	81 ± 16 #	59 ± 23	88 ± 26 #	75 ± 36	-	-	64 ± 20 #	45 ± 14
RVEDVi	-	-	66 ± 16 #	70 ± 15	82 ± 20	77 ± 19	-	-	85 ± 22 #	72 ± 19
RVESVi	-	-	24 ± 9	34 ± 13	45 ± 14	44 ± 21	-	-	33 ± 10 #	27 ± 9

Table 2

Differences between men and women

(* P < 0.05 for TRV versus PRV; # P < 0.05 for men versus women)

	ANOVA sign. Between groups	Bonferoni Post Hoc Tests					
		QBS - QUBE	QBS - 4D-MSPECT	QBS - BP-SPECT	QUBE - 4D- MSPECT	QUBE - BP-SPECT	BP-SPECT - 4D- MSPECT
LVEF	0.000	0.000	NS	NS	0.000	0.003	NS
LVSV	0.000	NS	0.000	NS	0.004	0.034	0.000
LVEDV	0.000	0.000	0.000	NS	NS	0.000	0.000
LVESV	0.000	0.000	0.001	NS	NS	0.000	0.017
LVEDVi	0.000	0.000	0.000	NS	NS	0.000	0.000
LVESVi	0.000	0.000	0.001	NS	NS	0.000	0.020
RVEF	0.000	NS	-	0.000	-	0.000	-
RVSV	0.000	NS	-	0.000	-	0.000	-
RVEDV	NS	NS	-	NS	-	NS	-
RVESV	0.002	NS	-	0.040	-	0.002	-
RVEDVi	NS	NS	-	NS	-	NS	-
RVESVi	0.002	NS	-	0.041	-	0.002	-

Table 3

Anova and Bonferoni post hoc tests of calculated values in men between different algorithms to process TRV

The lowest LVEF were found in PRV, for men as well as women. The higher LVEF from TRV were significant for QBS in women, and for QUBE and BP-SPECT in both sexes.

No significant difference was found between men and women, in calculating LVEF or RVEF from PRV or TRV. For QBS, all ventricular volume calculations had higher values in men, except for LV and RVESVi. For QUBE, LVV showed no significant difference between men and women. On the contrary, for the RV, higher non-corrected volumes were calculated. In the case of 4D-MSPECT, all LV volumes were significant higher in men compared to women. This was also the case in BP-SPECT, for LV as well as RV, except for corrected LV volumes.

Differences between different algorithms to process TRV (table 3 and 4)

LVV measurements in men were significant smaller with QUBE and 4D-MSPECT compared to QBS and BP-SPECT (table 3). This resulted in a significant high LVEF

	ANOVA sign. Between groups	Bonferoni Post Hoc Tests					
		QBS - QUBE	QBS - 4D- MSPECT	QBS - BP- SPECT	QUBE - 4D- MSPECT	QUBE - BP- SPECT	BP-SPECT - 4D- MSPECT
LVEF	0.007	0.034	NS	NS	0.026	0.022	NS
LVSV	0.000	NS	0.003	NS	0.000	NS	0.000
LVEDV	0.000	NS	0.000	NS	0.001	NS	0.000
LVESV	0.001	NS	0.005	NS	NS	NS	0.004
LVEDVi	0.000	NS	0.000	NS	0.000	NS	0.000
LVESVi	0.001	NS	0.005	NS	NS	NS	0.001
RVEF	0.000	NS	-	0.012	-	0.000	-
RVSV	0.017	NS	-	NS	-	0.022	-
RVEDV	NS	NS	-	NS	-	NS	-
RVESV	0.002	NS	-	NS	-	0.001	-
RVEDVi	NS	NS	-	NS	-	NS	-
RVESVi	0.003	NS	-	NS	-	0.002	-

Table 4

Anova and Bonferoni post hoc tests of calculated values in women between different algorithms to process TRV

(mean 72%) in men with QUBE compared to the three other methods. For 4D-MSPECT, a significant low LVSV (mean 53 mL) resulted in a mean LVEF (62%), comparable with the values from QBS and BP-SPECT. For women, LVV calculations were significant smaller in 4D-MSPECT, compared to QBS, QUBE and BP-SPECT (table 4). No significant difference was found in the LVV measurements from QBS compared with BP-SPECT, for both sexes.

Normal RVEF had significant higher values with BP-SPECT (mean for men 62%, for women 63%) compared to QBS (50% and 52 % respectively) and QUBE (45% and 48% respectively). This was clearly the result of a significant lower RVESV (and a higher RVSV) with BP-SPECT compared to the other two algorithms. No significant differences were found in RVEDV calculations between the three algorithms.

DISCUSSION

Most of the LVEF calculated by TRV was significant higher compared to PRV, which is

in agreement with other papers [12]. Only 4D-MSPECT didn't show higher values of LVEF, due to relatively small, and probably underestimated LVEDV, and this is also demonstrated by a validation study of TRV with MRI (submitted). Additionally, 4D-MSPECT shows small ventricular volumes, compared to other techniques (Figure 4). All mean values of LVEF of all techniques range from 59% (lowest) to 72 % (largest), a range that doesn't permit to exchange values from one technique to another, this is also consistent with other findings in literature [7]. The relatively large SD found in this series, however, can cause problems when defining patient examinations as normal or abnormal. It is not unlikely that a few patients would be categorized as normal, when they are not.

Values of normal RVEF are scarce in literature, especially gender-specific values. Only recently some papers have published results for MRI [4-6]. Our results for BP-SPECT, with higher values of RVEF compared to the other three algorithms seems to be more in relation to these MRI papers. The relatively large RVEDV and small RVESV are responsible for the high RVEF processed with BP-SPECT. On the contrary, high values for RVESV found with QUBE, are responsible for low RVEF, for men as well as for women. With larger volumes for the RV and a fixed stroke volume for the LV and RV, a slightly lower RVEF is very likely, but mean values < 50% are not found in literature for other techniques, so our results for QBS and QUBE seems to underestimate the real normal RVEF.

Nuclear techniques, like GSPECT and TRV, seem to result in smaller values for LVV compared to MRI. The underestimation of LVV was also demonstrated in other papers [10]. The partial volume effect and subsequently underestimated LVESV, like demonstrated in small hearts especially in women in gated perfusion SPECT, could be also play a major role why small LVESV is found with TRV, compared with other cardiac imaging techniques. For the RVV on the contrary, mean values of different techniques were much more comparable. Nevertheless, the higher values of RVV found with QUBE and BP-SPECT are consistent with a dynamic phantom study [18]. One of the differences between QUBE and BP-SPECT is the calculation of RVESV, which is much larger with QUBE, compared to BP-SPECT.

Normal values of LVEF in men and women for TRV are higher compared to gated perfusion SPECT but more in relation to other papers with other techniques. It is nevertheless very important to determine normal values for each technique separately. Not only can normal LVEF or LVV from MRI not be compared to normal values from TRV, even within one single technique, values from one type of software (or

department) cannot be interchanged by another software. This implies that different nuclear cardiology laboratories need to set up their own normal values, and this for each technique they use.

For the RVEF, we found in men and women $62 \pm 6 \%$ and $63 \pm 9 \%$ respectively, calculated with TRV and processed with BP-SPECT. These values are the lowest values for RVEF, compared with other imaging techniques, but in a correct proportion to the LV, since larger volumes in the RV and an identical stroke volume, result in a lower RVEF, compared to the LVEF. Especially RVEDV seems to be higher compared with MRI values for RVEDV. Gated perfusion SPECT is not suitable to calculate RV volumes, processing RV parameters from planar ventriculography is far from ideal [19] and measuring RV diameters from echocardiography is even more questionable. MRI is the only technique which is suitable to compare with. And even then, TRV and MRI are suffering from disadvantages to calculate accurate RV volumes, e.g. very irregular endocardial surface (trabeculae), relatively low contraction amplitude in inflow and especially outflow tract, and the relatively large tricuspid ring, making it hard to separate correctly right atrium from RV. Calculating volumes and ejection fraction of the RV is since years a challenging item and is has even recently proven to be of clinically important [20]. Although, finding the exact borders of the RV remains a challenging item and will be a topic of research and discussion for years.

About normalization for body surface area (BSA), which could eliminate the different body habitus between men and women, results from different papers are conflicting. BSA normalization for ventricular volumes eliminated gender differences in one study [6], whereas in the other paper [21] BSA normalization didn't remove the gender differences but normalization for weight did. One author [22] is even suggesting that correction for BSA of LV volumes could make it possible to use one (corrected) normal volume range for men and women together, and even to make volume ranges from one technique comparable with another technique, something we could not demonstrate.

Limitations

The relatively large SD found in this series can cause problems when defining patient examinations as normal or abnormal. Probably a higher number of patients is needed to refine these limits of agreement.

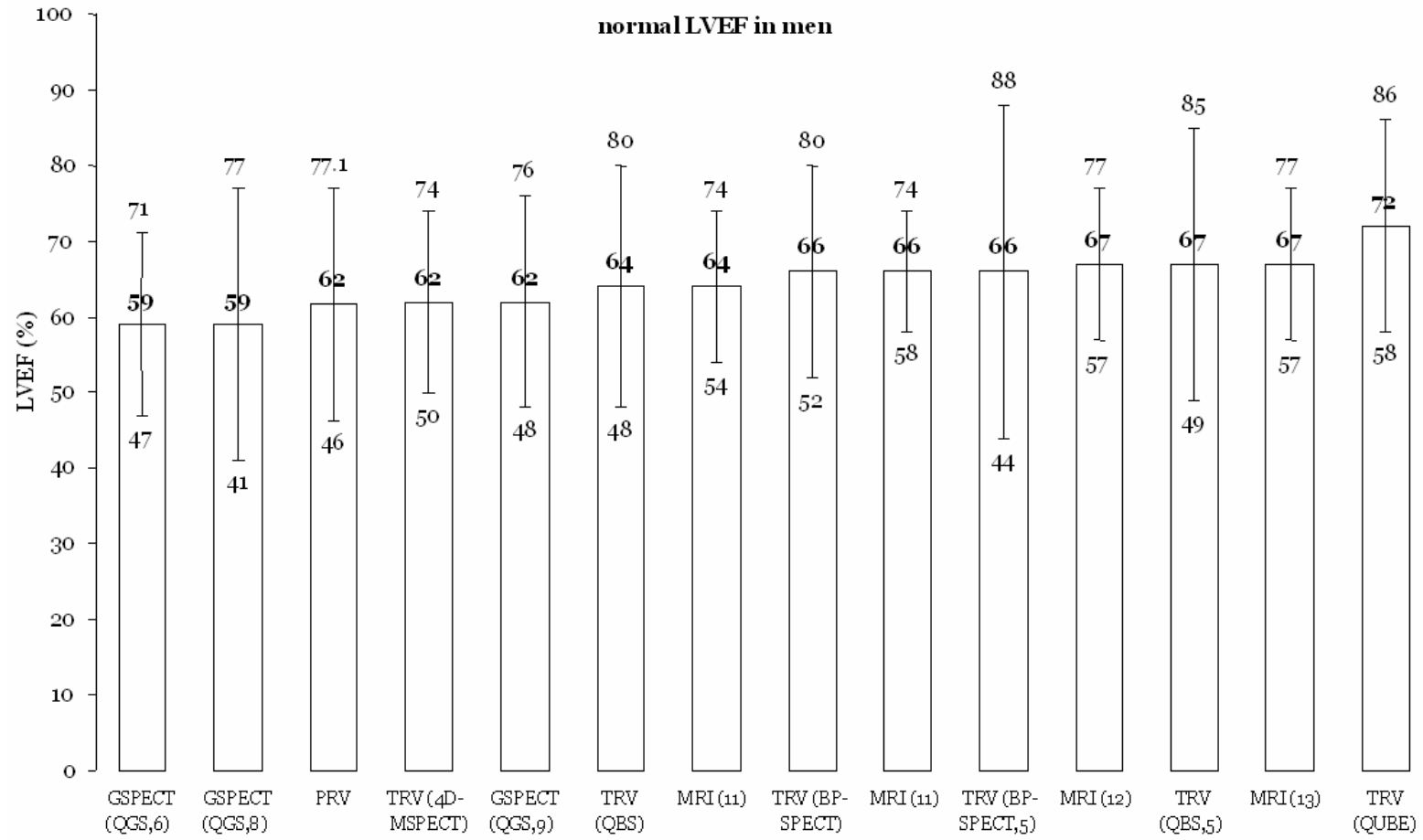


Figure 1

Normal LVEF in men, derived with different techniques. (bold: mean values, other: $\pm 2SD$)

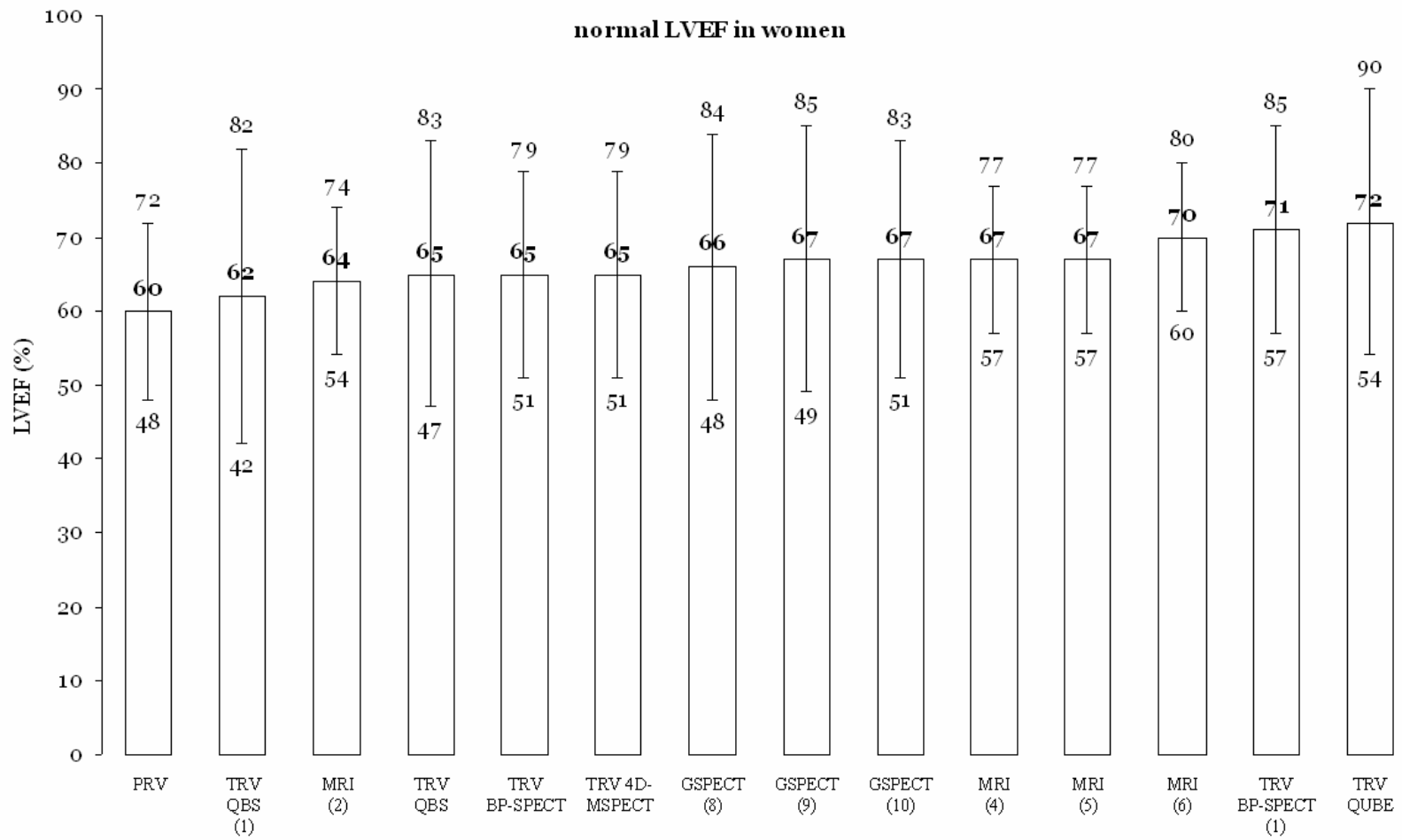


Figure 2
Normal LVEF in women, derived with different techniques. (bold: mean values, other: \pm 2SD)

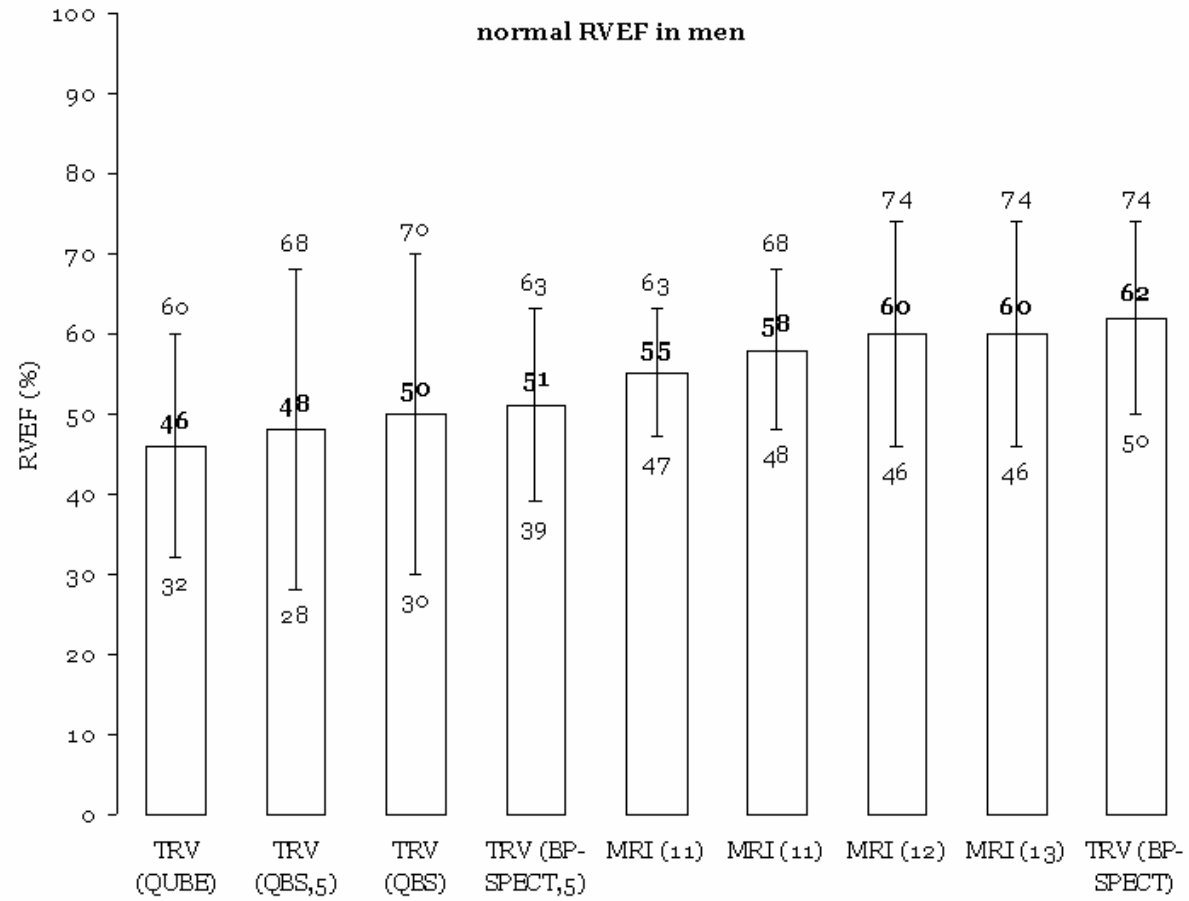


Figure 3a

Normal RVEF in men, derived with different techniques. (bold: mean values, other: $\pm 2SD$)

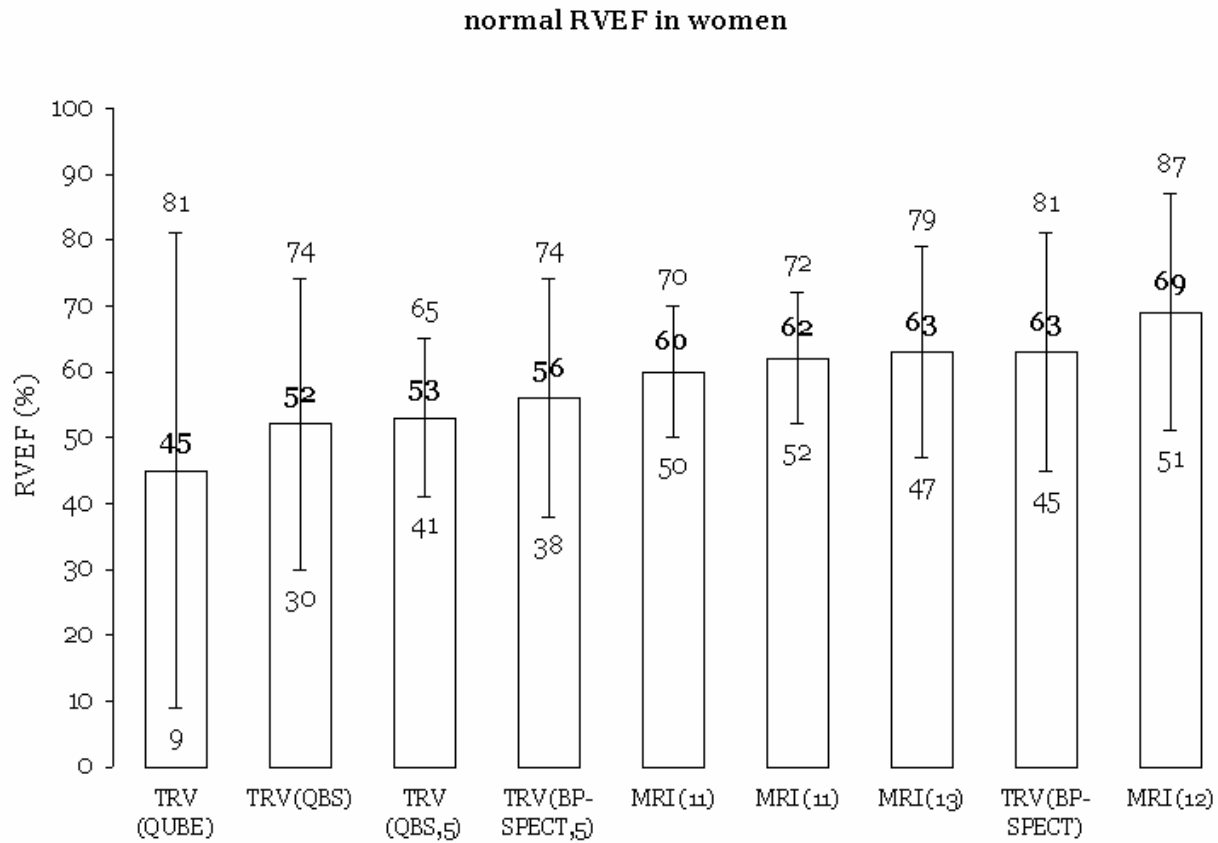


Figure 3b
Normal RVEF in women, derived with different techniques. (bold: mean values, other: $\pm 2SD$)

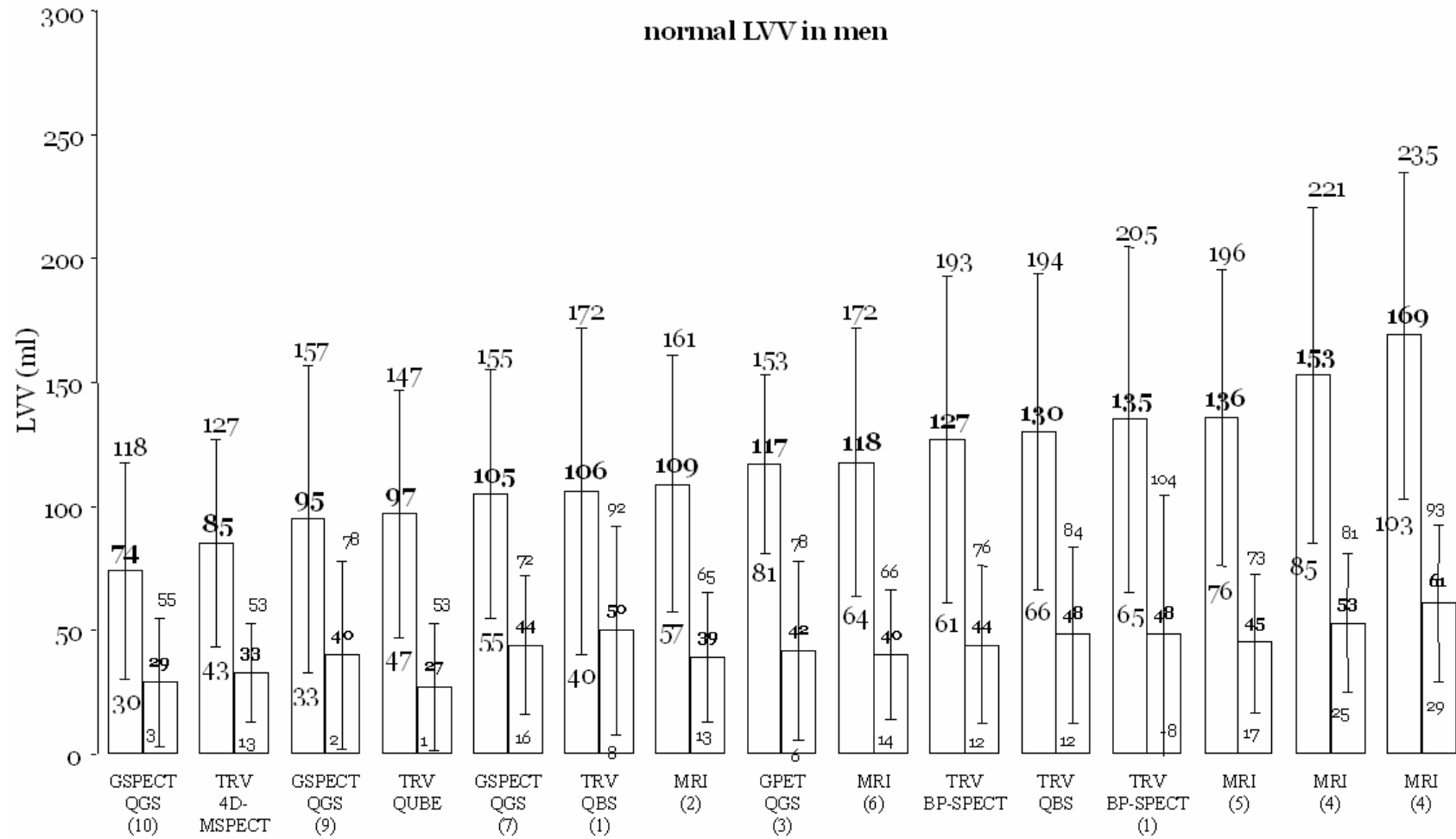


Figure 4

Normal LVV in men, derived with different techniques. (solid line: EDV, dashed line: ESV, bold: mean values, other: $\pm 2SD$)

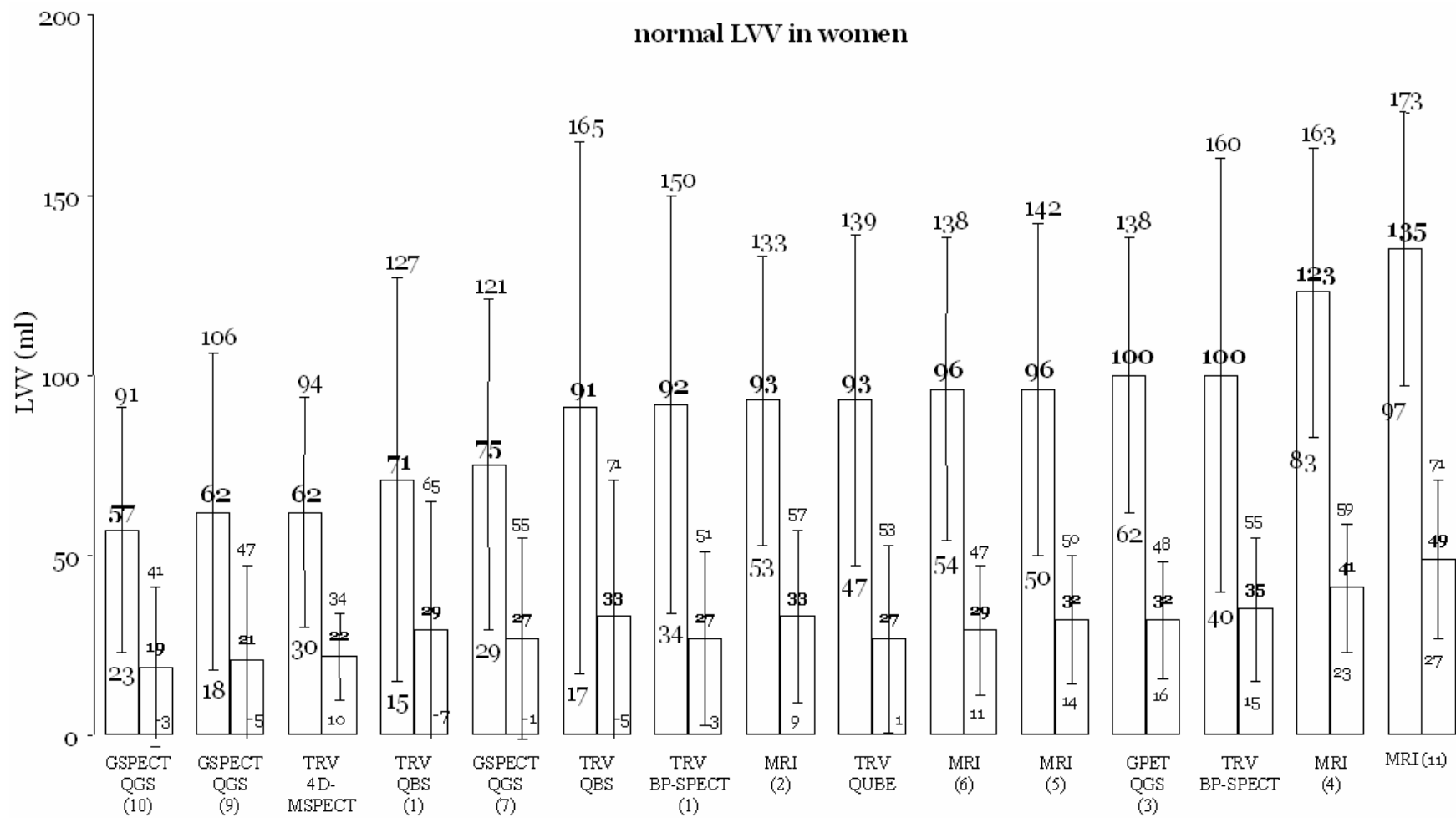


Figure 5

Normal LVV in women, derived with different techniques. (solid line: EDV, dashed line: ESV, bold: mean values, other: $\pm 2SD$)

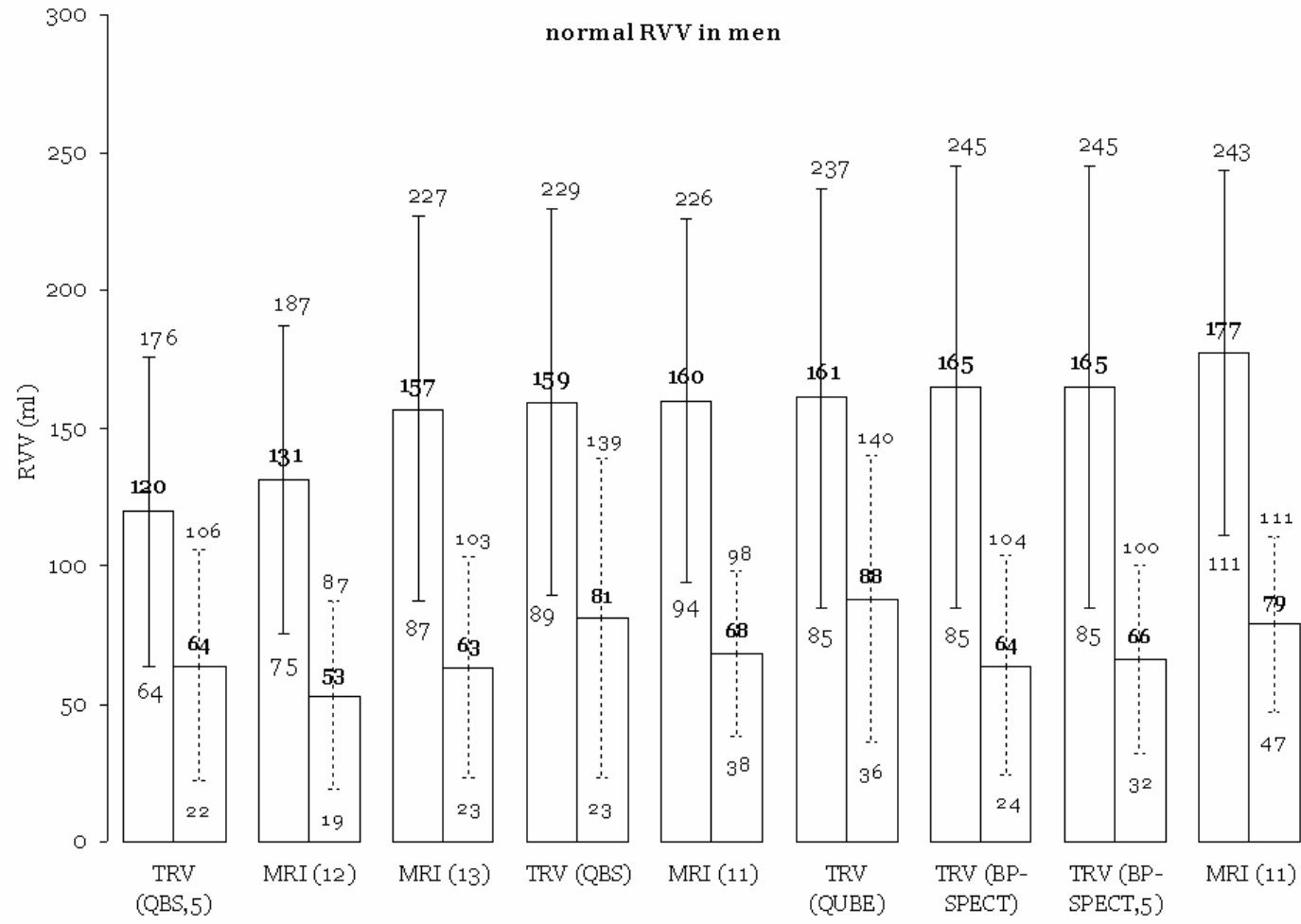


Figure 6

Normal RVV in men, derived with different techniques. (solid line: EDV, dashed line: ESV, bold: mean values,

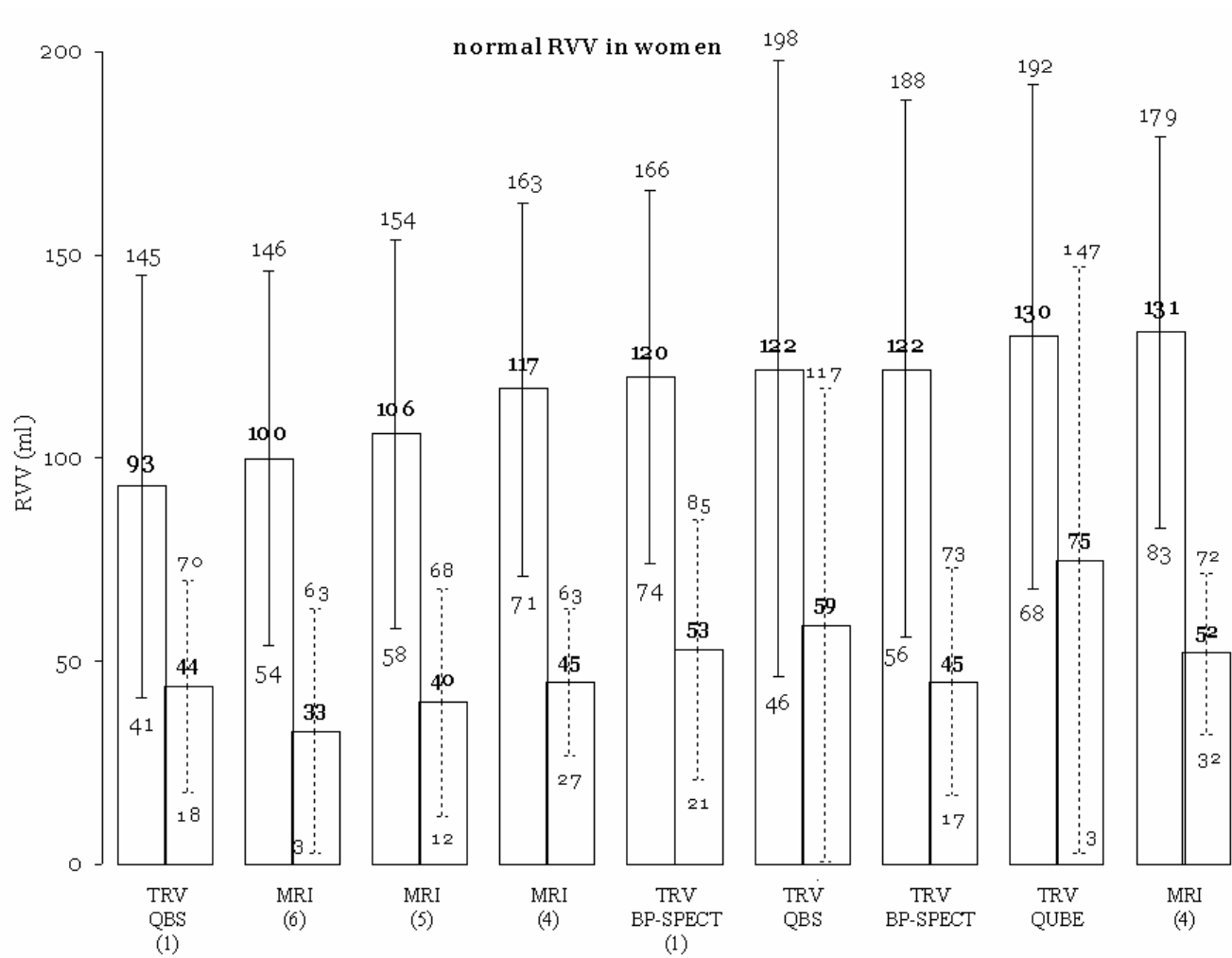


Figure 7 Normal RVV in women, derived with different techniques. (solid line: EDV, dashed line: ESV, bold: mean values, other: $\pm 2SD$)

CONCLUSION

We calculated gender-specific normative values of LVEF, LVEDV, LVESV, RVEF, RVEDV and RVESV for four algorithms processing TRV. LVEF calculated from TRV reveals higher values than calculated with PRV. There are statistically differences between the four algorithms studied, and these has to be further clarified in other validation studies in larger populations.

Acknowledgement

We want to thank Edward Ficaró PhD, Assistant Research Scientist, University of Michigan Health System, Department of Radiology, Ann Arbor Medical Center, USA, for his kind cooperation to let us use his program (4D-MSPECT) and Philippe Briandet PhD, SEGAMI corporation, Columbia, USA, who made it possible to try the program QUBE. Special thanks to Ken Nichols PhD, Long Island Jewish Medical Center, Division of Nuclear Medicine, USA, who gave advise during the processing with BP-SPECT. Johan De Sutter is a senior clinical investigator of the Fund for Scientific Research – Flanders (Belgium) (FWO – Vlaanderen).

REFERENCES

1. Nichols K, Humayun N, De Bondt P, Vandenberghe S, Akinboboye OO, Bergmann SR. Model dependence of gated blood pool SPECT ventricular function measurements. *J Nucl Cardiol* 2004; 11(3):282-292.
2. Nikitin N, De silva R, Witte K, Lowe A, Lukaschuk E, Clark A et al. Normal age- and sex-related values of left ventricular volumes, myocardial mass and ejection fraction obtained with cardiac magnetic resonance using FIESTA imaging. *J Magn Reson. Imaging* . 2004. Ref Type: Abstract
3. Boyd HL, Rosen SD, Rimoldi O, Cunningham VJ, Camici PG. Normal values for left ventricular volumes obtained using gated PET. *G Ital Cardiol* 1998; 28(11):1207-1214.
4. Alfakih K, Plein S, Thiele H, Jones T, Ridgway JP, Sivananthan MU. Normal human left and right ventricular dimensions for MRI as assessed by turbo gradient echo and steady-state free precession imaging sequences. *J Magn Reson Imaging* 2003; 17(3):323-329.
5. Lorenz CH, Walker ES, Morgan VL, Klein SS, Graham TP, Jr. Normal human right and left ventricular mass, systolic function, and gender differences by cine magnetic resonance imaging. *J Cardiovasc Magn Reson* 1999; 1(1):7-21.
6. Sandstede J, Lipke C, Beer M, Hofmann S, Pabst T, Kenn W et al. Age- and gender-specific differences in left and right ventricular cardiac function and mass determined by cine magnetic resonance imaging. *Eur Radiol* 2000; 10(3):438-442.
7. De Bondt P, Van De WC, De Sutter J, De Winter F, De Backer G, Dierckx RA. Age- and gender-specific differences in left ventricular cardiac function and volumes determined by gated SPECT. *Eur J Nucl Med* 2001; 28(5):620-624.
8. De Bondt P, Van de WC, De Sutter J, De Winter F, De Backer G, Dierckx RA. Age- and gender-specific differences in left ventricular cardiac function and volumes determined by gated SPECT. *Eur J Nucl Med* 2001; 28(5):620-624.
9. Rozanski A, Nichols K, Yao SS, Malholtra S, Cohen R, Depuey EG. Development and application of normal limits for left ventricular ejection fraction and

- volume measurements from ^{99m}Tc-sestamibi myocardial perfusion gates SPECT. *J Nucl Med* 2000; 41(9):1445-1450.
10. Ababneh AA, Sciacca RR, Kim B, Bergmann SR. Normal limits for left ventricular ejection fraction and volumes estimated with gated myocardial perfusion imaging in patients with normal exercise test results: influence of tracer, gender, and acquisition camera. *J Nucl Cardiol* 2000; 7(6):661-668.
 11. Nichols K, Saouaf R, Ababneh AA, Barst RJ, Rosenbaum MS, Groch MW et al. Validation of SPECT equilibrium radionuclide angiographic right ventricular parameters by cardiac magnetic resonance imaging. *J Nucl Cardiol* 2002; 9(2):153-160.
 12. Van Krieking SD, Berman DS, Germano G. Automatic quantification of left ventricular ejection fraction from gated blood pool SPECT. *J Nucl Cardiol* 1999; 6(5):498-506.
 13. Vanhove C, Franken PR, Defrise M, Momen A, Everaert H, Bossuyt A. Automatic determination of left ventricular ejection fraction from gated blood-pool tomography. *J Nucl Med* 2001; 42(3):401-407.
 14. Ficaro EP, Quaife RF, Kritzman JN, Corbett JR. Validation of a New Fully Automatic Algorithm for Quantification of Gated Blood Pool SPECT: Correlations with Planar Gated Blood Pool and Perfusion SPECT. *J.Nucl.Med.* 5, 97P. 2002. Ref Type: Abstract
 15. Vanhove C, Franken PR. Left ventricular ejection fraction and volumes from gated blood pool tomography: comparison between two automatic algorithms that work in three-dimensional space. *J Nucl Cardiol* 2001; 8(4):466-471.
 16. Daou D, Van Krieking SD, Coaguila C, Lebtahi R, Fourme T, Sitbon O et al. Automatic quantification of right ventricular function with gated blood pool SPECT. *J Nucl Cardiol* 2004; 11(3):293-304.
 17. De Bondt P, Nichols K, Vandenberghe S, Segers P, De Winter O, Van de WC et al. Validation of gated blood-pool SPECT cardiac measurements tested using a biventricular dynamic physical phantom. *J Nucl Med* 2003; 44(6):967-972.
 18. De Bondt P, Claessens T, Rys B, De Winter O, Vandenberghe S, Segers P et al. Accuracy of 4 different algorithms for the analysis of tomographic radionuclide ventriculography using a physical, dynamic 4-chamber cardiac phantom. *J Nucl Med* 2005; 46(1):165-171

19. Klocke, F. J., Baird, M. G., Lorell, B. H., Bateman, T. M., Messer, J. V., Berman, D. S., O'Gara, P. T., Carabello, B. A., Russell, R. O., Jr., Cerqueira, M. D., John Sutton, M. G., DeMaria, A. N., Udelson, J. E., Kennedy, J. W., Verani, M. S., Williams, K. A., Antman, E. M., Smith, S. C., Jr., Alpert, J. S., Gregoratos, G., Anderson, J. L., Hiratzka, L. F., Faxon, D. P., Hunt, S. A., Fuster, V., Jacobs, A. K., Gibbons, R. J., and Russell, R. O. ACC/AHA/ASNC guidelines for the clinical use of cardiac radionuclide imaging--executive summary: a report of the American College of Cardiology/American Heart Association Task Force on Practice Guidelines (ACC/AHA/ASNC Committee to Revise the 1995 Guidelines for the Clinical Use of Cardiac Radionuclide Imaging). *J.Am.Coll.Cardiol.* 42[7], 1318-1333. 1-10-2003.
20. Redington, A. N. Right ventricular function. *Cardiol.Clin.* 20[3], 341-9, v. 2002.
21. Lorenz, C. H., Walker, E. S., Morgan, V. L., Klein, S. S., and Graham, T. P., Jr. Normal human right and left ventricular mass, systolic function, and gender differences by cine magnetic resonance imaging. *J Cardiovasc.Magn Reson.* 1[1], 7-21. 1999.
22. Salton, C. J., Chuang, M. L., O'Donnell, C. J., Kupka, M. J., Larson, M. G., Kissinger, K. V., Edelman, R. R., Levy, D., and Manning, W. J. Gender differences and normal left ventricular anatomy in an adult population free of hypertension. A cardiovascular magnetic resonance study of the Framingham Heart Study Offspring cohort. *J.Am.Coll.Cardiol.* 39[6], 1055-1060. 20-3-2002.

General Discussion

Phantom experiments for tomographic radionuclide ventriculography (TRV): why?

GSPECT has undergone a profound scientific validation before it was used in clinical practice, an evaluation what is still ongoing. This is different with the TRV technique. Although the technique of performing tomography during a ventriculography study exist since many years, it is only recently that automatic software programs to calculate LV and RV volumes and EF. Most of them underwent a validation of LVEF, but there was a lack of validation of volumes, especially of the RV. When observing these programs, several questions could be asked:

1. Are these programs capable to correctly define the ventricular volume?

The left ventricular phantom was designed.

2. Are these programs capable to correctly separate left from right ventricle?

The biventricular phantom was designed.

3. Are these programs capable to correctly define the atrioventricular valve plane in each ventricle?

The 4-chamber cardiac phantom was designed.

Left ventricular heart phantom.

We developed the first physical dynamic heart phantom that could be used to study planar and tomographic ventriculography. We could demonstrate that an ejection fraction, calculated from (end-diastolic and end-systolic) volumes was more accurate than an ejection fraction, calculated from (end-diastolic and end-systolic) counts. In this model we included background-activity, which was not possible anymore in the following heart model, due to physical restrictions. The ventricle was “activated” through volume changes in the surrounding tank.

This phantom was also used to compare different available algorithms to process planar ventriculography studies and they closely correlated to the “real” ejection fraction, measured directly from the heart phantom.

Left and right ventricular heart phantom

BP-SPECT was used to calculate with success volumes and ejection fractions from the

left and right ventricle in our biventricular heart model. Not only accuracy of volume determination was studied, also inter- and intraobserver variability was studied. Here, the program was able to detect the ventricular boundaries and to correctly separate left from right ventricle. In this model, left and right heart was filled and emptied through the atrioventricular border, while these were directly connected to filling and emptying tubes. The model itself was constructed so that the volume of the septal wall was kept constant and systolic thickening was simulated.

Dynamic four-chamber heart phantom

We developed a more realistic shape of the RV in our dynamic four-chamber heart phantom. The main goal of this study was to evaluate if the programs, QBS, QUBE, 4D-MSPECT and BP-SPECT, and see if they were able to correctly separate ventricular from atrial counts, in order to measure correct volumes in both ventricles. All programs provided accurate estimates of LV and RV EF, but in the calculation of RV volumes, a large difference was found between the several programs and a trend together with an underestimation or overestimation was seen. Most of the programs need to reconsider the analysis of the RV.

Normal values for LV and RV function determined by gated perfusion SPECT and gated bloodpool SPECT.

We found for normal LVEF in men and women $62 \pm 8 \%$ and $60 \pm 6 \%$ for planar ventriculography[1], $59 \pm 6 \%$ and $66 \pm 9 \%$ for gated myocardial perfusion SPECT [2] and $66 \pm 7 \%$ and $65 \pm 7 \%$ for gated bloodpool SPECT, processed with BP-SPECT. Especially the low LVEF in men, found with gated perfusion SPECT is remarkable and is the lowest values of LVEF in normal adults, found in literature. A reason for this, is that in our population of patients with a low likelihood of coronary artery disease (CAD), there were a certain amount of unknown cases with decreased LV function. In our last paper (chapter 9), we used a population of normal volunteers, who underwent all normal physical examination, electrocardiography and echocardiography, all supervised by an experienced cardiologist.

Normal values of LVEF in men and women for gated bloodpool SPECT are higher compared to gated perfusion SPECT but more in relation to other papers with other techniques. It is nevertheless very important to determine normal values for each technique separately. Not only can normal LVEF or LVV from MRI not be compared

to normal values from Gated bloodpool SPECT, even within one single technique, values from one type of software (or department) cannot be interchanged by another software. This implies that different nuclear cardiology laboratories need to set up their own normal values, and this for each technique they use.

For the RVEF, we found in men and women $62 \pm 6 \%$ and $63 \pm 9 \%$ respectively, calculated with gated bloodpool SPECT and processed with BP-SPECT [1]. These values are the lowest values for RVEF, compared with other imaging techniques, but in a correct proportion to the LV, since larger volumes in the RV and an identical stroke volume, result in a lower RVEF, compared to the LVEF [3]. Especially RVEDV seems to be higher compared with MRI values for RVEDV. Gated perfusion SPECT is not suitable to calculate RV volumes, processing RV parameters from planar ventriculography is far from ideal [4] and measuring RV diameters from echocardiography is even more questionable. MRI is the only technique which is suitable to compare with. And even then, gated bloodpool SPECT and MRI are suffering from disadvantages to calculate accurate RV volumes, e.g. very irregular endocardial surface (trabeculae), relatively low contraction amplitude in inflow and especially outflow tract, and the relatively large tricuspid ring, making it hard to separate correctly right atrium from RV. Calculating volumes and ejection fraction of the RV is since years a challenging item and is has even recently proven to be of clinically important [3]. Although, finding the exact borders of the RV remains a challenging item and will be a topic of research and discussion for years.

Influence of gender

Our normal values for LVV were higher in men compared to women, for GSPECT as well as for TRV. For LVEF, only a significant higher value could be found in women compared to men with GSPECT, not with TRV. It is possible that there were certain men in our GSPECT population with unknown decreased LV function. Nevertheless, there are some papers using GSPECT [5; 6] that found higher LVEF in women compared to men, due to lower LVV. This gender-difference of volumes and EF is in agreement with other papers, who used MRI to quantify LV function [7-9]. It is possible that morphologic parameters (like volumes) can show differences between genders, whereas functional parameters (like EF) could be more independent from age and gender [7-9]. Wong et al found that LVEDV and LVESV were $> 25\%$ greater in men than in women using echocardiography, a value which we could detect in our TRV-study as well.

About normalization for body surface area (BSA), which could eliminate the different body habitus between men and women, results from different papers are conflicting. In our GSPECT study, volume differences still existed after BSA correction, in our TRV study, values of LV and RV in men were still higher in men after correction, but not anymore significant. The latter is obvious, since the same relative difference between two absolute numbers has lower chance to be significant if the absolute value of the numbers is low (like BSA-corrected volumes). BSA normalization for ventricular volumes eliminated gender differences in one study [7], whereas in the other paper [9] BSA normalization didn't remove the gender differences but normalization for weight did. One author [8] is even suggesting that correction for BSA of LV volumes could make it possible to use one (corrected) normal volume range for men and women together, and even to make volume ranges from one technique comparable with another technique, something we could not demonstrate. Very important when comparing different studies in this matter is each definition of "normalcy", the latter is varying from "low likelihood for coronary artery disease" [2;5], "no history of cardiac disease" [7;9], "free of overt cardiovascular disease and no hypertension" [8], "a normal Bruce stress test" [6] to "no history of cardiovascular disease, no hypertension, no diabetes, normal ECG and normal echocardiogram" [1]. Since the prevalence of cardio-vascular disease is remarkable in a symptom-free population, some of the differences between several studies could also be explained by this factor.

Differences in ventricular volumes between genders are also described for the RV [1;7], there is no reason why ventricular volume differences between men and women should be different for the LV and the RV, but since these papers are scarce, more investigation is needed from techniques with an accurate RV volume assessment.

Influence of age

Only our first paper with GSPECT is dealing with the influence of age on volumetric parameters. We found, using analysis of variance, lower LVV and higher LVEF in the group of women > 65 years, compared to the 2 younger groups. Using correlation analysis, we found significant negative correlation between LV volumes and age in men and women, and significant positive correlation between LVEF and age in women. An important point in this discussion is the underestimation of small volumes by GSPECT. Nakajima [10] has nicely shown that this underestimation is growing increasingly with smaller volumes, which were calculated as 15% underestimation in a 101 ml model, 25 % in a 52 ml model, 50% in a 37 ml model and even 93% in a 14 ml

model. It is clear that with this varying influence, effect on LVESV will be much larger than on LVEDV, resulting in an increase in LVEF for small volumes. This partial volume effect is also seen in the software QBS to process TRV, and mentioned in their own validation paper [11]. When getting more and more experienced in processing and evaluating TRV, it is not uncommon to calculate LVEF and RVEF's close to 100% with undetectable activity or even no activity at ES, which is of course not physiological. So this underestimation seems to be an inherent negative point of GSPECT as well as TRV, so the difference between EF of 55% or 65% or 75% or even higher has probably no physiologic implication and is due to a technical shortcoming of GSPECT and TRV. I should therefore recommend that all values of EF > 55% are normal (it makes no sense that an EF of 75% is more "normal" than 60%) and that with calculated volumes < 20 ml one would be extremely cautious when this value is used in the calculation of other parameters, like EF.

Age itself has its effect on myocardial morphology and function, only data for this point is conflicting again. Most of the age-related papers have used other techniques than these from nuclear cardiology. The reason for this is that age causes a complex series of modifications, morphologic as well as functional. A lot of papers give a prominent role to change of myocardial mass in the elderly heart. Although some nuclear cardiology studies could quantify myocardial mass, the method they use is questionable and most studies on the effect of age are performed with echocardiography or MRI. Together with the relation between LV mass and increased risk in cardiovascular events [12], there was a positive relation between LV volumes and fractional shortening (systolic function) with age in women [13]. Together with an increase in atrial natriuretic factor and a decrease in plasma renin activity, this would suggest plasma volume expansion, increase in cardiac preload and this may contribute to the increase in LV mass in older women [13]. This may contribute to the partial loss of cardiovascular protection among older women. Others found no relation between LVV, LVEF and age in healthy subjects [14]. An increase in wall thickness is described [7;15] together with a decrease of diastolic function in the elderly [15]. The effect of this on LV volumes and LVEF is not clear.

Pro's and contra's of different algorithms to process gated bloodpool SPECT

	QBS	QUBE	4D-MSPECT	BP-SPECT
Ease of use	3	4	4	3
Speed	3	3	4	3
Value of references in literature	2	2	2	4
Automaticity	4	4	4	3
Manual intervention possibilities	0	4	3	4
Pure manual processing possibilities	NA	4	NA	NA
Supplementary processing options	NA	4	NA	NA
Accuracy for LV parameters (compared with MRI)	1	2	2	3
Accuracy for RV parameters (compared with MRI)	1	2	NA	3

Table 1

Subjective impression of software to process gated bloodpool SPECT, scored (0 = very poor, 1 = poor, 2 = moderate, 3 = good, 4 = excellent)

QBS [1;11;16-21]

(<http://www.cedars-sinai.edu/5854.html>)

QBS is a very straightforward program developed by Cedars-Sinai Medical Center, who developed very popular software to process gated perfusion SPECT (QGS and QPS). QBS uses gated short axis images, processed by standard nuclear medicine software. Mostly, QBS is being sold separately from this standard processing-software. The layout of QBS is very similar to this of QGS. The processing time is acceptable (mostly below 30 sec.) and the display is easily changed between 3D volumes with or without isocontour, dynamic slices and results. Results are displayed in bulls eyes, comparable to the bulls eyes generated with gated perfusion SPECT. They give the wall motion of LV and RV, expressed in millimeters, displayed in a circle and half a circle respectively. The latter describing wall motion of the anterior, free lateral, apical and inferior wall of the RV, since the authors don't believe it is useful to display results for the septal wall, since these are displayed on the left side of the LV bulls eye. We are not convinced of this, since septal wall thickens during contraction and shows different motion, seen from the left or the right side of the heart. LV and RV values of EF, EDV and ESV are always simultaneous given. Most errors in the delineation of both

ventricles were seen in the basal and inferior part of the LV and in the inferior region of the RV. Manual processing is possible, but only the LV can be positioned during this option. We experienced no satisfactory result after manual processing, nor for LV nor for RV. If the user want additional masking, zooming or reorienting, this has to be done back in the standard nuclear medicine software and is not incorporated into the program itself. The overall accuracy of LV and especially RV values, compared to MRI values, is relatively low.

QUBE [1 ;17 ;20 ;22-24]

(<http://www.segamicorp.com/>)

QUBE is developed by the Free University of Brussels (Belgium), and is now being incorporated in the Segami software. For this research, a full working demo version of the software was made available from this company. The package is not a stand-alone package and both raw gated bloodpool SPECT data as well as reconstructed short axis bloodpool SPECT data can be the input files of the program. Before automatic detection of ventricular cavities, the program asks the ventricle to be zoomed and reoriented properly. The direction of reorientation is indicated and this is easily done. The zooming can be chosen freely, but in our experience, has to be rather small, otherwise the program fails to detect the proper border of LV and RV. If the automatic processing give no satisfactory results, and this can as an experienced reader easily be evaluated on the dynamic slices with the ventricular delineation superimposed, several options can be chosen: condensing the heart cycle (in our case from 16 to 8 heart beats/cycle), to position septum, to point the RV outflow tract and to mask every disturbing activity around the myocardium. These supplementary options were considered as very useful in some conditions.

Recently, a manual option is added to the more automatic “QUBE” processing, based on the watershed algorithm, developed by Dr Mariano-Goulart [84; 85] from the University of Montpellier. This option could however not be tested anymore to our four chamber cardiac phantom and our patient data. However, in our laboratory we had only limited experience with this program (with the dynamic left ventricle phantom) and this program seems to have a lot of possibilities but is semi-automatic (and not fully automatic) and time-consuming. The way of defining ventricular cavities, and even atria, based on this watershed algorithm is nevertheless a very valuable tool to define volumes on the relatively low count slices of a gated bloodpool SPECT scan. The program performs a segmentation of all the separate time bins

SPECT slices, so in our studies this was done on 16 different SPECT data. All these segmentations has to be reviewed very carefully and adjusted if one segmented slice has assigned a region to another volume, based on the colours in the successive slices.

4D-MSPECT [27-29]

(<http://www.4dmspect.com/>)

The 4D-MSPECT software application was developed at the University of Michigan Medical Center under the direction of James Corbett and Edward Ficaro. The software development and support is now being done by a new company, CF Imaging Solutions LLC, a spin-off company of the University. It was Dr Ficaro's effort that also this software was installed on our pc and could be used freely for research purposes. This software handles both gated and non-gated myocardial perfusion data and bloodpool SPECT data in a single package. The users manual is extensive, very clear and comprehensible and contains references to (own) validation data. The software is very flexible, in that way that all parameters can be adjusted to the own requirements of the laboratory or hospital. Own normal databases are easily configured and stored. Automatic scoring system is provided and cut-offs for values (normal, equivocal, hypokinetic, akinetic and dyskinetic) can be adjusted if necessary. The software provides to create a report and contains the option to export all values of wall motion values (in mm) and wall motion scores (0 to 4) to a text file, which can then be exported to other software. Multiple patients can be selected at one time and the speed of processing is very acceptable and is the best, compared with all other packages. At the time of processing, no option of calculating right ventricle volumes and ejection fraction was available.

BP-SPECT [1;20;21;30-33]

(<http://www.syntermed.com/gatedblood.htm>)

This program is being developed by Ken Nichols, while he was working at the Columbia University, NY. It is now being distributed by Syntermed, Inc. This program has the strongest validation data, which shows the best correlation with phantom data and MRI data, for left ventricle as well as for right ventricle. BP-SPECT was developed using Research Systems, Inc. (RSI) Interactive Data language® (IDL). BP-SPECT was made available onsite by Dr Nichols. The program is fast and performs an analysis of the right ventricle first. The automatic processing can be accepted or rejected when visual inspection is not satisfactory. The latter is easy when you are an experience gated bloodpool SPECT data reader, but this is the case in all programs processing

gated bloodpool SPECT. When the automatic processing is rejected, manual processing is performed and several supplementary options can be chosen like reorienting, masking, smoothing... if necessary.

Should we use gated bloodpool SPECT (TRV) in clinical routine or not?

With the fast computers nowadays, the big capacity hard drives, no special hardware needed (like camera) and no supplementary radiation of the patient, I think there is little argument not to do it. A little learning curve is needed before reporting and only giving “an estimation” of ventricular volumes is preferred when they are visually correctly identified by the software used. The visual interpretation of “the ventricle seems enlarged” or “there is an impression of moderate hypokinesis in the inferolateral wall” is better than giving absolute contents of the ventricles in mL, and not knowing the exact accuracy of that measurement. In other words, nuclear medicine is (still) in the majority of cases based on visual interpretation, and even nowadays, the gold standard in many papers, despite sophisticated and fast software, is still the visual scoring or interpretation.

Future in nuclear cardiology

All these chapters are mainly based on technical optimisation of existing techniques within nuclear cardiology. It is my opinion however, that the real future in nuclear medicine is the radiopharmacy. Unfortunately, it is remarkable that during the last 10 years, almost no new molecules are introduced into the nuclear cardiology laboratories, although the developments in radiopharmaceuticals are the cornerstone of nuclear medicine. Most of the papers and abstracts recently published and presented are dealing with the use of SPECT and PET in prediction and prognosis, in certain subgroups of patients (like diabetes), special procedures (stem cells), advances in software (like bloodpool SPECT) or some technical or hardware advances (PET/CT). This evolution is ongoing and contributes to the non-invasive diagnosis of functional and morphological changes in the human heart.

I think with the gated myocardial SPECT and gated bloodpool SPECT, we have two techniques we can use in clinical practice to give insight in some of the aspects of perfusion and function of the heart. A little “upgrade” from PRV to TRV gives a lot more of information, if it is interpreted with caution.

REFERENCES

1. De Bondt P. Normal values for left and right ventricular ejection fraction and volumes from tomographic radionuclide ventriculography. submitted .
2. De Bondt P, Van de Wiele C, De Sutter J, De Winter F, De Backer G, Dierckx RA. Age- and gender-specific differences in left ventricular cardiac function and volumes determined by gated SPET. *Eur J Nucl Med* 2001; 28(5):620-624.
3. Redington AN. Right ventricular function. *Cardiol Clin* 2002; 20(3):341-9, v.
4. Klocke FJ, Baird MG, Lorell BH, Bateman TM, Messer JV, Berman DS et al. ACC/AHA/ASNC guidelines for the clinical use of cardiac radionuclide imaging--executive summary: a report of the American College of Cardiology/American Heart Association Task Force on Practice Guidelines (ACC/AHA/ASNC Committee to Revise the 1995 Guidelines for the Clinical Use of Cardiac Radionuclide Imaging). *J Am Coll Cardiol* 2003; 42(7):1318-1333.
5. Rozanski A, Nichols K, Yao SS, Malholtra S, Cohen R, Depuey EG. Development and application of normal limits for left ventricular ejection fraction and volume measurements from 99mTc-sestamibi myocardial perfusion gates SPECT. *J Nucl Med* 2000; 41(9):1445-1450.
6. Ababneh AA, Sciacca RR, Kim B, Bergmann SR. Normal limits for left ventricular ejection fraction and volumes estimated with gated myocardial perfusion imaging in patients with normal exercise test results: influence of tracer, gender, and acquisition camera. *J Nucl Cardiol* 2000; 7(6):661-668.
7. Sandstede J, Lipke C, Beer M, Hofmann S, Pabst T, Kenn W et al. Age- and gender-specific differences in left and right ventricular cardiac function and mass determined by cine magnetic resonance imaging. *Eur Radiol* 2000; 10(3):438-442.
8. Salton CJ, Chuang ML, O'Donnell CJ, Kupka MJ, Larson MG, Kissinger KV et al. Gender differences and normal left ventricular anatomy in an adult population free of hypertension. A cardiovascular magnetic resonance study of the Framingham Heart Study Offspring cohort. *J Am Coll Cardiol* 2002; 39(6):1055-1060.

9. Lorenz CH, Walker ES, Morgan VL, Klein SS, Graham TP, Jr. Normal human right and left ventricular mass, systolic function, and gender differences by cine magnetic resonance imaging. *J Cardiovasc Magn Reson* 1999; 1(1):7-21.
10. Nakajima K, Taki J, Higuchi T, Kawano M, Taniguchi M, Maruhashi K et al. Gated SPET quantification of small hearts: mathematical simulation and clinical application. *Eur J Nucl Med* 2000; 27(9):1372-1379.
11. Van Kriekinge SD, Berman DS, Germano G. Automatic quantification of left ventricular ejection fraction from gated blood pool SPECT. *J Nucl Cardiol* 1999; 6(5):498-506.
12. Dannenberg AL, Levy D, Garrison RJ. Impact of age on echocardiographic left ventricular mass in a healthy population (the Framingham Study). *Am J Cardiol* 1989; 64(16):1066-1068.
13. de Simone G, Devereux RB, Roman MJ, Ganau A, Chien S, Alderman MH et al. Gender differences in left ventricular anatomy, blood viscosity and volume regulatory hormones in normal adults. *Am J Cardiol* 1991; 68(17):1704-1708.
14. Merino A, Alegria E, Castello R, Martinez-Caro D. Influence of age on left ventricular contractility. *Am J Cardiol* 1988; 62(16):1103-1108.
15. Pearson AC, Gudipati CV, Labovitz AJ. Effects of aging on left ventricular structure and function. *Am Heart J* 1991; 121(3 Pt 1):871-875.
16. Daou D, Van Kriekinge SD, Coaguila C, Lebtahi R, Fourme T, Sitbon O et al. Automatic quantification of right ventricular function with gated blood pool SPECT. *J Nucl Cardiol* 2004; 11(3):293-304.
17. Vanhove C, Franken PR. Left ventricular ejection fraction and volumes from gated blood pool tomography: comparison between two automatic algorithms that work in three-dimensional space. *J Nucl Cardiol* 2001; 8(4):466-471.
18. Higuchi T, Taki J, Nakajima K, Kinuya S, Ikeda M, Namura M et al. Evaluation of left and right ventricular functional parameters with automatic edge detection program of ECG gated blood SPET. *Nucl Med Commun* 2003; 24(5):559-563.
19. Wright GA, Thackray S, Howey S, Cleland JG. Left ventricular ejection fraction and volumes from gated blood-pool SPECT: comparison with planar gated

- blood-pool imaging and assessment of repeatability in patients with heart failure. *J Nucl Med* 2003; 44(4):494-498.
20. De Bondt P, Claessens T, Rys B, De Winter O, Vandenberghe S, Segers P et al. Accuracy of 4 different algorithms for the analysis of tomographic radionuclide ventriculography using a physical, dynamic 4-chamber cardiac phantom. *J Nucl Med* 2005; 46(1):165-171.
 21. Nichols K, Humayun N, De Bondt P, Vandenberghe S, Akinboboye OO, Bergmann SR. Model dependence of gated blood pool SPECT ventricular function measurements. *J Nucl Cardiol* 2004; 11(3):282-292.
 22. Vanhove C, Franken PR, Defrise M, Momen A, Everaert H, Bossuyt A. Automatic determination of left ventricular ejection fraction from gated blood-pool tomography. *J Nucl Med* 2001; 42(3):401-407.
 23. Vanhove C, Franken PR, Defrise M, Bossuyt A. Comparison of 180 degrees and 360 degrees data acquisition for determination of left ventricular function from gated myocardial perfusion tomography and gated blood pool tomography. *Eur J Nucl Med Mol Imaging* 2003; 30(11):1498-1504.
 24. Vanhove C, Walgraeve N, De Geeter F, Franken PR. Gated myocardial perfusion tomography versus gated blood pool tomography for the calculation of left ventricular volumes and ejection fraction. *Eur J Nucl Med Mol Imaging* 2002; 29(6):735-741.
 25. Mariano-Goulart D, Piot C, Boudousq V, Raczka F, Comte F, Eberle MC et al. Routine measurements of left and right ventricular output by gated blood pool emission tomography in comparison with thermodilution measurements: a preliminary study. *Eur J Nucl Med* 2001; 28(4):506-513.
 26. Mariano-Goulart D, Collet H, Kotzki PO, Zanca M, Rossi M. Semi-automatic segmentation of gated blood pool emission tomographic images by watersheds: application to the determination of right and left ejection fractions. *Eur J Nucl Med* 1998; 25(9):1300-1307.
 27. Ficaro EP, Quaife RF, Kritzman JN, Corbett JR. Validation of a New Fully Automatic Algorithm for Quantification of Gated Blood Pool SPECT: Correlations with Planar Gated Blood Pool and Perfusion SPECT. *J.Nucl.Med.* 5, 97P. 2002.

28. Ficaro EP, Quaipe RF, Kritzman JN, Corbett JR. Accuracy and reproducibility of 4D-MSPECT for estimating left ventricular ejection fraction in patients with severe perfusion abnormalities. *Circulation* 100, I-26. 2004.
29. Schaefer WM, Lipke CS, Nowak B, Kaiser HJ, Reinartz P, Buecker A et al. Validation of QGS and 4D-MSPECT for quantification of left ventricular volumes and ejection fraction from gated 18F-FDG PET: comparison with cardiac MRI. *J Nucl Med* 2004; 45(1):74-79.
30. De Bondt P, Nichols K, Vandenberghe S, Segers P, De Winter O, Van de Wiele C. et al. Validation of gated blood-pool SPECT cardiac measurements tested using a biventricular dynamic physical phantom. *J Nucl Med* 2003; 44(6):967-972.
31. Nichols K, Saouaf R, Ababneh AA, Barst RJ, Rosenbaum MS, Groch MW et al. Validation of SPECT equilibrium radionuclide angiographic right ventricular parameters by cardiac magnetic resonance imaging. *J Nucl Cardiol* 2002; 9(2):153-160.
32. Nichols K, Depuey EG, Rozanski A. Automation of gated tomographic left ventricular ejection fraction. *J Nucl Cardiol* 1996; 3(6 Pt 1):475-482.
33. Slart RH, Poot L, Piers DA, van Veldhuisen DJ, Nichols K, Jager PL. Gated blood-pool SPECT automated versus manual left ventricular function calculations. *Nucl Med Commun* 2004; 25(1):75-80.

Conclusion

Normal values for left ventricle (LV) and right ventricle (RV) ejection fraction (EF) and end-diastolic and end-systolic volumes (EDV and ESV) are not interchangeable between different techniques (nuclear cardiology, MRI, echocardiography, angiography) and even not within one technique processed with different software packages.

Normal values for LV and RV EF, EDV and ESV has to be gender- and (probably) age-specific. It has clinically no sense to produce values in a gender-mixed population. Men have larger ventricular volumes compared to women. Women have smaller ventricles, especially at older age. LVEF can be higher in women, probably due to smaller ventricles at ES.

We have developed a dynamic heart phantom with 1, 2 and 4 chambers, which can be used to develop software, perform quality controls and organize software audits.

It is possible to calculate absolute volumes from single photon emission tomography (SPECT) reconstructed slices. Without background, we found an optimal cut-off for region growing of 50%.

Phantom experiments show that ejection fraction calculation with three-dimensional volumes is more accurate than with two-dimensional counts.

The programs to process Tomographic radionuclide ventriculography (TRV) have the capability to correctly define the interventricular septum and the atrioventricular valve plane.

The RV has a very complex shape: triangular, irregular surface (many trabeculae) and a relative hypokinetic outflow tract, which makes it difficult to exactly measure the exact volume. TRV or bloodpool SPECT could have advantage over other imaging modalities since the ventricular counts are directly proportionate to the exact volume and no endocardial surface has to be traced. Nevertheless, even TRV has some possibilities to exactly delineate ventricular surface, but refinements and adjustments are needed of the different software packages.

Besluit

Normaalwaarden van linker (LV) en rechter ventrikel (RV) ejectie fractie (EF) en van eind-diastolische (EDV) en eind-systolische volumina (ESV) zijn niet uitwisselbaar tussen verschillende technieken (nucleaire cardiologie, NMR, echocardiografie, angiografie) en zelfs niet binnen dezelfde techniek met verschillende methoden (software) gemeten.

Normaalwaarden van LV en RV EDV en ESV moeten geslacht-specifiek zijn, het heeft klinisch gezien geen zin om normaalwaarden te bepalen in een gemengde populatie. Mannen hebben grotere ventrikels in vergelijking met vrouwen. Vrouwen hebben kleinere ventrikels, vooral op hogere leeftijd. LVEF kan hoger zijn bij vrouwen, door kleinere ventrikels in eind-systole.

Wij hebben een dynamisch hart fantoom ontworpen met 1, 2 en 4 kamers. Deze kan worden gebruikt in het ontwikkelen van software, om kwaliteits-audits uit te voeren en om software audits te organiseren.

Het is mogelijk om van de single photon emission tomography (SPECT) gereconstrueerde beelden, volumes te kwantificeren. Zonder background vonden we een optimale cut-off van 50% bij “region growing”.

Fantoom experimenten hebben aangetoond dat LVEF accurater zijn wanneer ze drie-dimensionaal berekend zijn, in vergelijking met de twee-dimensionale berekening.

Software om TRV te berekenen kunnen het interventriculair septum en de atrioventriculaire overgang in fantoomexperimenten goed definiëren.

Verschillende software programma's zijn nu op de markt om bloodpool SPECT te verwerken, ze hebben alle hun voor en hun nadelen en de meeste van hen hebben nog een kritische bijsturing nodig, voornamelijk voor de analyse van het RV. De RV heeft een zeer complexe vorm en oppervlak, wat ze moeilijk maakt bij berekening van ventriculaire volumes. TRV heeft het voordeel dat ze met counts werken en dat deze counts rechtvaardig zijn met het echte volume in het ventrikel, er moet geen endocardiale aflijning worden getraceerd of getekend.

Dankwoord

Rudi, bedankt, jij bent absoluut de aanzet geweest van mijn onderzoek. Jouw aanstekelijk enthousiasme voor het wetenschappelijk werk heeft zeker vruchten afgeleverd. Waar ik nu sta in de wereld van de Nucleaire Geneeskunde, heb ik voor een groot stuk aan jou te danken.

Johan en Christophe, bedankt dat jullie mij vijf jaar geleden hebben laten proeven van de nucleaire cardiologie. Het werk dat jullie hebben opgestart, is van onschatbare waarde voor het UZ Gent. De microbe van het wetenschappelijk onderzoek op de P7 sloeg al snel op mij over en daar is dan ook het onderwerp van mijn thesis ontstaan. Ik vond het een fantastische tijd op P7.

In die periode werkte ik ook vaak samen met Frederic. Hij is er niet meer en er gaan weinig dagen voorbij dat ik niet aan hem denk.

De vele avond- en nachturen die we doorbrachten op P7 experimenterend met de siliconen hartmodellen zijn memorabel. Stefaan, Stijn, Bart, Tom, Patrick en Pascal, we hebben een uniek hartmodel. Zonder jullie hulp was het absoluut onmogelijk geweest.

Luc, bedankt voor onze trip naar Parijs, ter kennismaking met de dienst Nucleaire van Dominique Le Guludec.

My very special thanks goes to Ken Nichols: the way you helped me from the first day I met you in Toronto, is amazing. You believed in our heart model and what I admire most in you is your very high scientific level. I hope I can continue in collaborating on the field of bloodpool tomography and other topics in nuclear medicine. Even until now, our collaboration is fruitful since you are thinking of incorporating our normal database into your software.

Alle mensen van P7 wil ik van harte bedanken; in het bijzonder Norbert, Michel, Jean, Andy, Werner, Charlotte, Filip, Erik, Martine, Hamphrey en niet in het minste Sonja en Denise. In jullie ploeg werkte ik echt graag.

Dankjewel aan de vele mensen die steeds weer enthousiast informeerden hoe ver ik stond met mijn thesis.

Griet, je was er. Jouw interesse en drijfveer hebben mee deze thesis gerealiseerd. Jij was al even enthousiast over mijn nachtelijke experimenten als ikzelf. Dikwijls bleef je nog laat op om toch maar te weten hoe het geweest was. Dit was voor mij een enorme stimulans. Ook toen het wat minder vlotte, hielp je me een planning op te stellen waarna

ik weer met volle kracht vooruit kon gaan. Ik hoop oprecht dat ik je evenveel kan steunen in jouw verwezelijkingen.

Lieve Lotte, Corneel en Marie, papa zijn “boek” is eindelijk af!

Nu werk ik in Aalst. Hugo en Paul, bedankt voor het vertrouwen dat jullie in mij hebben gesteld. De dienst Nucleaire ligt nog geen 100 meter van de plaats waar mijn vader een praktijk had en waar ik opgegroeid ben. De cirkel is terug rond. Mam, ik denk dat ik nog meer gemeen had met papa dan ik ooit kon vermoeden. Meer dan 20 jaar is hij er al niet meer en soms komen mensen mij nu nog vertellen dat ze heel wat gelijkenissen zien tussen hem en mij. Pap, ik hoop dat je fier op me bent.

